Nucleolar roles of the PI3K pathway in cancer and differentiation

Fatemeh Mazloumi Gavgani

Thesis for the degree of Philosophiae Doctor (PhD)
University of Bergen, Norway
2017

UNIVERSITY OF BERGEN

Nucleolar roles of the PI3K pathway in cancer and differentiation

Fatemeh Mazloumi Gavgani

Thesis for the degree of philosophiae doctor (PhD)
at the University of Bergen

2017

Date of defence: 18.12.2017

Year: 2017

Title: Nucleolar roles of the PI3K pathway in cancer and differentiation

Name: Fatemeh Mazloumi Gavgani

Print: Skipnes Kommunikasjon / University of Bergen

Scientific environment

The work in this thesis was performed at the research group led by Associate professor Aurélia E. Lewis as part of the NUCREG (Mechanisms of gene regulation and molecular interactions) program at the Department of Molecular Biology, Faculty of Mathematics and Natural Sciences at the University of Bergen. A short part of the research was performed at The Laboratory of Eukaryotic Molecular Biology (LBME) which is part of CBI (Center for Integrative Biology of Toulouse) at the Université de Toulouse-Paul Sabatier, France during a three weeks stay funded by a ERASMUS mobility grant. This project was funded by the University of Bergen, the Norwegian Cancer Society, the Western Norway Regional Health Authority (project #911682) as well as from the Meltzer Research Fund (L. Meltzer Høyskolefond).

Acknowledgements

I would first like to thank my supervisors, Associate professor Aurélia E. Lewis and Professor Rein Aasland; I could not have asked for better supervision. Aurélia, I feel very fortunate to have been able to pursue my PhD under your supervision. Your door has always been open for my questions and you have been very supportive of my ideas. Thank you for being there for me both scientifically and emotionally. Rein, I have really enjoyed our discussions and meetings together. You welcomed me into the department and encouraged me at all times.

I am grateful to the members of NucReg, both past and present. It has been amazing working with every single one of you. I would also like to give special thanks to my coauthors and those who contributed to the papers in this thesis. You have been a great team and all your hard work is very much appreciated.

I am also grateful to the administrative and teaching staff at the Department of Molecular Biology (MBI) for their continuous help over these past four years. I would like to thank all the people at MBI for creating a great and friendly work environment. I thank all my friends for all the support that they have given me and all the fun times we have had together.

I am forever very thankful for my parents, even though they are no longer physically present, they have always been with me every step of the way. I am grateful for my supportive family and amazing siblings who provided me with encouragement and reassurance along the way. And I am thankful for my little nephews that have brought so much joy into my life.

Last but not least, I would like to dedicate this thesis to my husband and best friend, Jake. Thank you for always being there for me, for supporting me and making my life more meaningful.

Fatemeh Mazloumi Gavgani
October 2017

Abstract

The phosphoinositide 3-kinase (PI3K) pathway is essential for many cellular functions including; proliferation, cell survival, differentiation and metabolism. Although this pathway has been well studied in the cytoplasm, the role of PI3Ks in the nucleus has also been emerging as essential determinants of cell function. Previous work from our group has mapped the class I PI3K p110β and its product PtdIns(3,4,5)P_3 to the nucleus and nucleolus in a breast cancer cell line. Here, we aimed to understand and characterize the role of this kinase and its lipid product in the nucleus during tumorigenesis and adipocyte differentiation. We first found that the PI3K is active in the nucleus of differentiating 3T3-L1 and endometrial cancer cells and identified an active form of Akt in the nucleoli of endometrial cancer cell lines. Using subcellular fractionation, mass spectrometry and different staining methods, we confirmed the nucleolar localization of PtdIns(3,4,5)*P*3 in several cell types but at different levels. In adipocytes, the levels of p110β were low in the nucleus and nucleoli upon differentiation. In contrast, endometrial cancer cell lines had high amounts of nuclear p110β and PtdIns(3,4,5)P_3. The nucleolus is the sub nuclear site where ribosomal RNA (rRNA) transcription and processing occurs and interestingly we found that inhibition of p110β reduced the level of transcription of this RNA species. In addition, endometrial cancer cell lines with high amounts of nuclear p110β and PtdIns(3,4,5)P_3 showed significant elevations in pre-rRNA transcription.

To gain further insights of the nuclear roles of PtdIns(3,4,5)P_3, we used a quantitative interactomics approach and identified 219 PtdIns(3,4,5)P_3 interacting proteins that were highly enriched in cytokinesis, RNA processing and DNA repair functions. PARP1 (Poly (ADP-ribose) polymerase 1), a DNA repair protein abundant in the nucleoli, was one of the identified proteins which was then validated to interact with phosphoinositides directly, including PtdIns(3,4,5)P_3. The nucleolar presence and co-localization of PARP1 with PtdIns(3,4,5)P_3 was dependent on active rRNA transcription. Altogether the results from this thesis suggests an active role of the class I PI3K p110β and its product PtdIns(3,4,5)P_3 in the nucleolus of differentiating adipocytes and endometrial cancer cells but with distinct regulation.

List of publications

Paper I **Nuclear upregulation of PI3K p110β correlates with increased rRNA transcription in endometrial cancer cells**

Fatemeh Mazloumi Gavgani[*], Thomas Karlsson[*], Victoria Smith Arnesen, Ole Horvli, Pamela Pollock, Ingvild L Tangen, Camilla Krakstad, and Aurélia E Lewis (manuscript)

Paper II **Nuclear phosphatidylinositol 3,4,5-triphosphate interactome**

Fatemeh Mazloumi Gavgani, Diana C. Turcu, Julie Guillermet-Guibert, Rein Aasland, Clive D'Santos and Aurélia E. Lewis
(manuscript)

Paper III **Synthesis of phosphatidylinositol 3,4-P_2 and phosphatidylinositol 3,4,5-P_3 in distinct nuclear sites upon adipocyte differentiation**

Rhîan G. Jacobsen[*], Marianne Goris[*], **Fatemeh Mazloumi Gavgani**[*], Vandana Ardawatia, Thomas Karlsson and Aurélia E. Lewis
(manuscript)

***** Shared first author

Publication not included in the thesis:

Jacobsen RM, **Mazloumi Gavgani F**, Mellgren G and AE Lewis (2016). DNA Topoisomerase IIα contributes to the early steps of adipogenesis in 3T3-L1 cells. Cellular Signalling. 28:1593-1603.

Contents

List of selected abbreviations

EC	Endometrial cancer
K/R	Lysine/Arginine
MTM	Myotubularin
mTOR	Mammalian target of rapamycin
NORs	nucleolar organizer regions
NPM	Nucleophosmin
PARP	Poly (ADP-ribose) polymerase
PDK1	3-phosphoinositide-dependent protein kinase 1
PH	Pleckstrin homology
PI	Phosphoinositide
PI3K	Phosphoinositide 3-kinase
PPIn	Polyphosphoinositides
IPMK	Inositol Polyphosphate multikinase
IRS-1	Insulin Receptor Substrate 1
PKB	Protein kinase B
PtdIns	Phosphatidylinositol
PTEN	Phosphatase and tensin homolog
RNP	Ribonucleoprotein
SHIP	Src homology 2-domain-containing inositol phosphatase
TAG	Triacylglycerol
TopoIIα	Topoisomerase IIα
UBF	Upstream binding factor

1. Introduction

1.1 General aspects of Polyphosphoinositides

Polyphosphoinositides (PPIn) are derived from the phosphorylation of phosphatidylinositol (PtdIns). PtdIns is a glycerophospholipid which consists of two hydrophobic acyl chains attached to the glycerol backbone, which is itself coupled to an inositol head group via a phosphodiester bond with the 1′ OH group (Figure 1) [1]. The inositol ring can be phosphorylated at the 3′, 4′, or 5′ positions resulting in several combinations and a total of seven variants, one tri-phosphorylated (PtdIns(3,4,5)P_3), three di-phosphorylated (PtdIns(3,4)P_2, PtdIns(3,5)P_2, PtdIns(4,5)P_2) and three mono-phosphorylated PPIn (PtdIns3*P*, PtdIns4*P*, PtdIns5*P*) (Table-1). They are called PPIn and have unique functions in the cell [1-3]. These low-abundance phospholipids comprise less than 1% of the total lipid content of the cell with the highest amounts of PPIns accounting for PtdIns(4)*P* and PtdIns(4,5)P_2 [4]. The most dominant type of fatty acyl chain found in mammalian phosphoinositides are stearoyl and arachidonoyl represented as C18:0/C20:4 or summed as 38:4 (total number of carbons: total double bonds count in fatty acids) [5]. The hydrophobic acyl tails allow them to be anchored in cellular membranes and through their inositol head group, exposed to the aqueous milieu, they bind specific PPIn-binding domains on target proteins [6]. As summarized in table-1, PPIn localize in different cellular membranes. For example among other cellular compartments PtdIns(3)*P* and PtdIns(3,5)P_2 localize at the membrane of early or late endosomes and PtdIns(4)*P* to the Golgi, PtdIns5*P* to the endoplasmic reticulum and PtdIns(4,5)P_2, to the plasma membrane [7, 8].

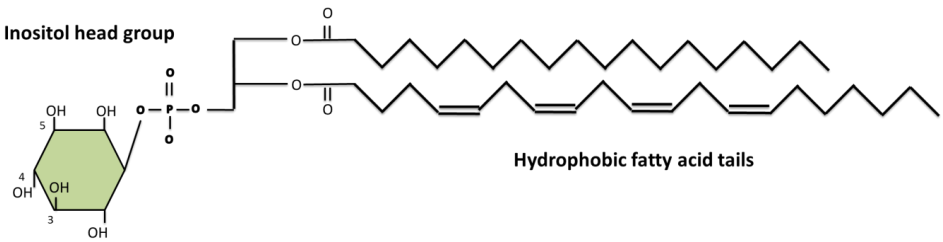

Figure 1. Chemical structure diagram of phosphatidylinositol (PtdIns). The inositol head group can be phosphorylated at the 3′, 4′, or 5′ OH to generate different variants of polyphosphoinositides (PPIn). The hydrophobic fatty acid chains (here shown as C18:0/C20:4) are attached to the glycerol backbone which is linked to the inositol head group by a phosphodiester bond [1, 5].

These lipids act as signaling molecules and their levels are tightly regulated. Their synthesis and metabolism is catalyzed by a series of lipid kinases and phosphatases which can convert these PPIns to each other [1] (see Table 1).

Table-1. Properties of the seven polyphosphoinositides lipid species. The red circles represent the phosphate group on the inositol ring shown here in green. The acyl chains are shortened due to space constraints. The phosphatases using the indicated PPIn as substrate and the kinases producing them are listed. Phosphatases are indicated in bold. PtdIns: phosphatidylinositol. MTM: myotubularins. PI3K: phosphoinositide 3-kinase. PTEN: phosphatase and tensin homolog. SHIP: Src homology 2-domain-containing inositol phosphatase. The abundances are a percentage of the total amount of phosphoinositides. This table is modified and updated from the tables in the following references: [4, 9].

PPIn	Localization	Kinase/Phosphatase	Abundance	Reference
PtdIns3*P* 	Endosomes, Nuclear envelope, Nucleolus, smooth endoplasmic reticulum, Golgi	PI3K class II and III **MTMs**	Low Less than 2%	[1, 4, 10-12]
PtdIns4*P* 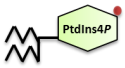	Golgi, Nucleoplasm	PI4 kinases (Type II and III)	High about 10%	[4, 13-16]
PtdIns5*P* 	Cytoplasm Nucleus, Golgi, Endoplasmic reticulum	PIKfyve (PI5K)	Low Less than 1%	[1, 4, 8, 17-22]
PtdIns(3,4)*P2* 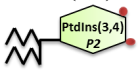	plasma membrane Nuclear envelope	PI3K class II **PtdIns-3,4-P_2 4 phosphatase type I and II**	Low Less than 1%	[1, 4, 23, 24]
PtdIns(3,5)*P2* 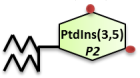	Endosomes	PIKfyve (PIP5K) **MTMs**	Low Less than 1%	[1, 4, 22, 25]
PtdIns(4,5)*P2* 	plasma membrane Nuclear speckles, Nucleolus	PIP4 Kinases PIP5 Kinases **5-phosphatases PtdIns-4,5-P_2 4 phosphatase type I and II**	High about 10%	[1, 4, 24, 26, 27]
PtdIns(3,4,5)*P3* 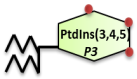	plasma membrane Nuclear matrix Nucleolus	PI3K class I, PIP5 Kinase **PTEN** (acts on 3'OH) **SHIP1/2** (acts on 5'OH)	Low Less than 1%	[1, 4, 28, 29]

PPIn can either act directly as second messengers or as precursors to other second messengers to regulate a wide range of cellular processes [3, 4, 30, 31]. The levels of some

PPIn can change rapidly upon cellular stimulation. A perfect example for this is PtdIns(3,4,5)P_3 (also known and referred to as PIP3), which has low levels in resting cells and is increased rapidly upon various stimuli [1]. The best known target for PtdIns(3,4,5)P_3 binding is a basic amino acid lining pocket of proteins containing the pleckstrin homology (PH) domain in several of its effector proteins [32-34].

1.2 The Phosphoinositide3-Kinase family

The PI3K enzymes consist of a family of lipid kinases that phosphorylate the 3'OH on the inositol ring of PPIn or PtdIns and generate the lipid second messengers; PtdIns(3)*P*, PtdIns(3,4)P_2, and PtdIns(3,4,5)P_3 [35-37]. Based on their structure and substrate specificity, the PI3K family is organised into 3 main classes, class I, II and class III [38]. Class I PI3Ks are heterodimers that consist of a catalytic subunit of either p110α, β, δ or γ associated with a regulatory subunit of p85α, p85β, p55 or p101, p87 [2, 39]. Class II PI3Ks are monomers and mammalian cells have three isoforms of this class; PI3K-C2α, PI3K-C2β, and PI3K-C2γ [40]. The preferred substrate of class II PI3Ks is PtdIns both *in vitro* and *in vivo* and they generate PtdIns(3)*P*[40]. Class II enzymes can also generate PtdIns(3,4)P_2 *in vitro* and have been reported to generate it also *in vivo* [41]. Vps34 (vacuolar protein sorting 34) is the only member of the class III PI3K bound to its adaptor Vps15 and it generates PtdIns3*P* [12, 42]. The protein and gene names of the catalytic and regulatory subunits of the PI3K pathway are listed in table 2.

Table 2. The PI3K family gene names and protein products. Table was adapted and modified from the following reference: **[43]**.

PI3K	Regulatory subunit		Catalytic subunit	
	Gene	**Protein**	**Gene**	**Protein**
Class IA	*PIK3R1* *PIK3R2* *PIK3R3*	p85α, p55α, p50α p85β p55γ	*PIK3CA* *PIK3CB* *PIK3CD*	p110α p110β p110δ
Class IB	*PIK3R5* *PIK3R6*	p101 p84 (also known as p87)	*PIK3CG*	P110γ
Class II	No known regulatory subunit		*PIK3C2A* *PIK3C2B* *PIK3C2G*	C2α C2β C2γ
Class III	*PIKCR4*	VPS15	*PIK3C3*	VPS34

1.2.1 Class I PI3K signaling

The *in vivo* substrate for this class of PI3Ks is PtdIns(4,5)P_2 which results in the generation of PtdIns(3,4,5)P_3 [2, 44]. The p85 subunit interacts with the p110 catalytic subunit and has a negative regulatory effect on p110 activity [45-47]. Upon activation by the receptors the inhibition of p110 by p85 is blocked and p110 can then generate PtdIns(3,4,5)P_3 by phosphorylating PtdIns(4,5)P_2 [48]. It is well known that the binding of PtdIns(3,4,5)P_3 to some of its target proteins are through the PH domain [33, 34]. Akt, a protein kinase, is a downstream signaling molecule of the PI3K pathway and binds to PtdIns(3,4,5)P_3 through its PH domain and then localizes to the plasma membrane for further activation [49-51]. Prior lysine residue deacetylation of the PH domain by SIRT1 deacetylase is crucial for PtdIns(3,4,5)P_3 binding [52]. Akt is then subsequently activated by the PtdIns(3,4,5)P_3 binding protein phosphoinositide-dependent protein kinase 1(PDK1) and mammalian target of rapamycin (mTOR) complex 2 by phosphorylation at Thr308 and Ser473 respectively (Figure-1) [53, 54]. Since PPIn lipids act as signalling molecules in a wide range of cellular processes, the cells have a mechanism to precisely control and regulate their levels and localizations in the cell. As a result of lipid phosphatases activity the levels of PtdIns(3,4,5)P_3 can be regulated. The tumor suppressor phosphatase and tensin homolog (PTEN) is an antagonist of the actions of class I PI3Ks, by dephosphorylating PtdIns(3,4,5)P_3 to PtdIns(4,5)P_2, thereby negatively regulating this pathway [55]. Other regulators of PtdIns(3,4,5)P_3 levels are SH2 (Src homology 2)-domain-containing inositol phosphatase (SHIP) 1 and 2 polyphosphate 5-phosphatases that can dephosphorylate PtdIns(3,4,5)P_3 to PtdIns(3,4)P_2 [56, 57].

The Class I PI3Ksare activated through either tyrosine kinase receptors (for p110α, p110β and p110δ) or the G protein coupled receptors (for p110β, and p110γ) [2, 58]. RAS proteins (family of small GTPase's) can directly bind to p110α, p110δ and p110γ isoforms and activate them, while the p110β is activated by RAC1 and CDC42 (RHO family of GTPases) [59-62]. While the expression of both p110δ and p110γ is restricted to immune cells, both p110α and β are ubiquitously expressed [35]. As mentioned earlier, they both target PtdIns(4,5)P2 and produce PtdIns(3,4,5)P_3, have very similar catalytic and regulatory domains, share the same mode of activation and embryonically lethal when knocked out [63, 64]. Although it may seem that p110α and p110β may possess redundant roles in the cell each of these isoforms has somehow distinct properties and functions. As an example, while

both isoforms have essential roles in metabolism and insulin signaling, only p110α is necessary for vascular endothelial growth factor (VEGF) signaling [63-69]. One feature that may explain their different cellular roles is that they localise in specific cellular compartments. More precisely, while both isoforms are present in the cytoplasm, only p110β is found in the nucleus in chromatin enriched fractions and the nucleoli [28, 70].

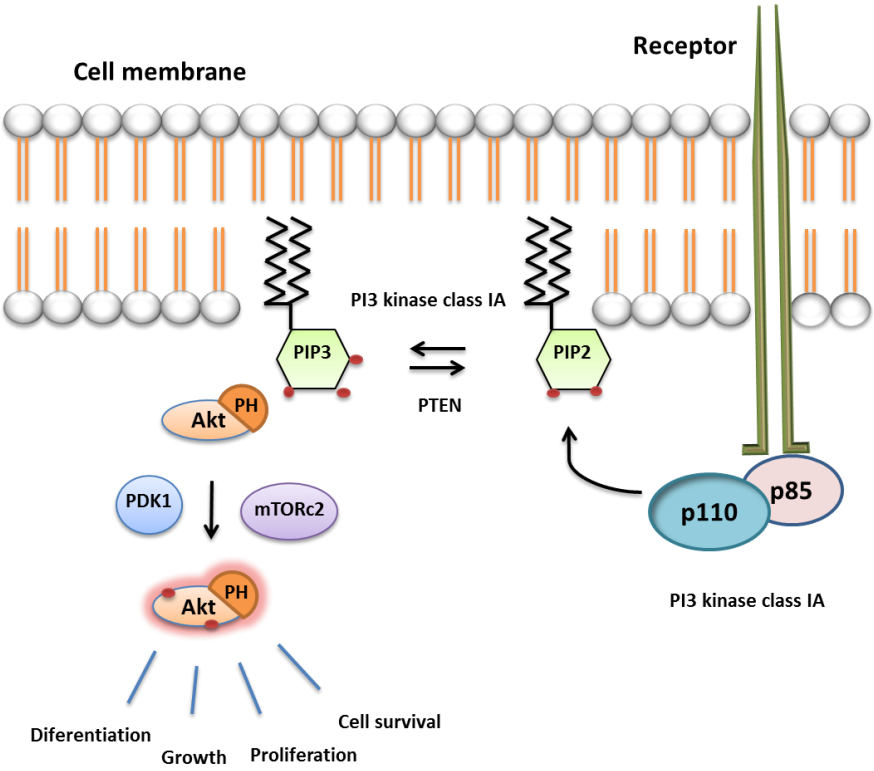

Figure 2. Diagram of class IA PI3K activation at the cell membrane. Upon ligand binding and stimulation of the receptor tyrosine kinases or the G-protein-coupled receptors, class IA PI3Ks are activated and they phosphorylate phosphatidylinositol (4,5)-bisphosphate (PIP2) and generate phosphatidylinositol (3,4,5)-triphosphate (PIP3). The generated PIP3 then interacts with the pleckstrin homology (PH) domain containing proteins such as Akt and targets them to the plasma membrane which leads to their activation and triggers a signaling cascade leading to many cellular functions. For its activation, AKT contains critical residues (Thr^{308} and Ser^{473}) that need to be phosphorylated (phosphate groups are shown as red circles) by PDK1 and mTORC2 respectively. PTEN function as antagonists of the PI3K activity by converting PIP3 to PIP2 [71]. This diagram is based on information from the figures in the following references: [51, 72].

1.2.2 Nuclear PPIn

Although the actions of PPIn are mostly known at the plasma membrane, several studies have shown their presence together with PPIn kinases and phosphatases in the nucleus and there is a growing appreciation to the important roles they play in the nucleus [73, 74] (Table-3). In the early 1980s the nuclear presence of PPIns and their metabolizing enzymes were discovered to be restricted to the nuclear membrane [75]. Later on, it was shown, by Cocco and colleagues in 1987, that when the nuclear membrane was depleted from mouse erythroleukemia nuclei using detergents, these isolated nuclei still contained PPIns which was followed by more studied showing the PPIn signalling and metabolism in the nucleus [76-80]. The chemical structure of these lipids is suitable for the hydrophobic environment of the membrane but as to how the acyl chains of these lipids are kept away from the aqueous environment of the nucleus is still a matter of debate. There are suggestions that by interaction with proteins these acyl chains are shielded in structured pockets [16, 73]. An example for this is the binding of the nuclear receptor Steroidogenic Factor-1 (SF-1) to PtdIns(4,5)P_2 which shielded the acyl chains of the lipid in its hydrophobic ligand binding pocket, while allowing the inositol head group to be accessible for phosphorylation by lipid signaling enzymes [81, 82].

Proteins with basic residues that can attract the negatively charged inositol head group are expected to be good targets for nuclear phosphoinositide binding. Examples of such proteins are histones that can have up to 35% of basic amino acids in their structure and they have been shown to bind PPIns [83]. Consistent with this are studies that have shown the interaction of PtdIns(4,5)P_2 to histone H1 that can regulate RNA polymerase transcription [84]. A list of the nuclear proteins discovered to bind to PPIns and of their functions is given in Table 3. Furthermore, by enriching for nuclear PPIn-binding proteins using neomycin displacement and subsequently PtdIns(4,5)P_2 pull down, a number of nuclear PtdIns(4,5)P_2 binding proteins have been identified [31]. Most of the identified pool of proteins contained at least one the following polybasic motif, K/R-(X (n= 3-7)-K-X-K/R-K/R rich in lysine and arginine residues (56%) but not structured domains [31].

Table-3. Nuclear PPIns and their interacting proteins; ALY (THO complex subunit 4), BAF (BRG1-associated factors), BASP1 (brain acid soluble protein 1), EBP1 (ErbB3-binding protein 1), ING2 (inhibitor of growth protein 2), LRH-1 (liver receptor homolog-1), NPM (nucleophosmin), PDZ (Postsynaptic density protein, Disc large, Zona occludens), Pf1 (PHD Factor 1), PIKE (PI3-Kinase Enhancer), PIP3-BP (PtdIns(3,4,5)P_3-binding protein), SAP30 (Sin3A-associated protein 30), SAP30L (human SAP30-like protein), SF-1 (steroidogenic factor-1), Star-PAP (speckle targeted PIP5KIα regulated poly (A) polymerase), TAF3 (Transcription initiation factor TFIID subunit 3), Topo IIα (DNA Topoisomerase IIα), UHRF1 (Ubiquitin-like with PHD and Ring finger domains 1). Table updated and modified from the following reference [85].

PPIn	Nuclear localization	Interacting proteins	Possible Function	Reference
PtdIns(3,4,5)P_3	Nuclear matrix, Nucleolus	PIP3-BP, NPM, ALY, PIKE, AKT, SF-1, LRH-1, EBP1	Cell survival, Proliferation, Transcriptional regulation, mRNA export	[28, 29, 82, 86-94]
PtdIns(4,5)P_2	Nuclear speckles, Nucleolus	Star-PAP, Topo IIα, BAF complex, ALY, SF-1, LRH-1, BASP, Histone H1, PDZ protein syntenin-2	mRNA expression, DNA topology, Chromatin remodeling, proliferation, Nuclear receptor transcriptional activity, RNA pol I transcription, pre-mRNA processing	[15, 27, 29, 31, 82, 84, 94-100]
PtdIns(3,4)P_2	Nuclear membrane	unknown	unknown	[23]
PtdIns5*P*	Nuclear foci	Pf1, SAP30/SAP30L, ING2, TAF3, UHRF1	Transcriptional regulation, Tumor suppressor, Regulation of DNA methylation, DNA damage response	[101-106]
PtdIns4*P*	Nucleoplasm, Nucleoplasmic foci	Pf1, SAP30/SAP30L	Transcriptional regulation	[15, 101, 102]
PtdIns3*P*	Nuclear envelope, Nucleolus	Pf1, SAP30/SAP30L	Transcriptional regulation	[11, 15, 101, 102]

1.2.3 Nuclear PtdIns(3,4,5)P_3 and PI3Ks

Several studies have demonstrated that members of the PI3K pathway are localized in different sub-nuclear compartments and can have distinct functions [107-109]. The levels of the PPIns in the nucleus are regulated by the PPIn kinases and phosphatases present also in the nucleus with both class I and class II PI3Ks showing nuclear localizations. Among the PtdIns(3,4,5)P_3 generating enzymes, the class I PI3K p110β but also IPMK (Inositol polyphosphate multikinase) localize to the nucleus [110, 111].The nuclear p110β isoform

has been shown to have a nuclear localization signals (NLS) and is involved in multiple important cellular functions such as DNA replication, cell cycle progression and DNA double strand break (DSB) repair [70, 111-113]. Nuclear IPMK was shown to phosphorylate PtdIns(4,5)P_2 when bound to SF-1 and generates the SF-1/ PtdIns(3,4,5)P3 complex, which becomes activated and can induce transcription [82]. In addition IPMK is involved in the nuclear mRNA export of transcripts that are enriched in DNA repair functions [89]. The class II PI3K-C2α also contains an NLS at the C2 domain and it localizes to the nuclear speckles. [114]. Nuclear speckles are enriched in pre-mRNA splicing machinery components and are hence site of pre-mRNA-processing [115]. PtdIns(4,5)P_2 has been identified to also localize in the nuclear speckles [26, 96]. PtdIns(3,4,5)P_3 is found in the nucleoplasm around speckles where its precursor PtdIns(4,5)P_2 localizes [26, 86]. Importantly, production of PtdIns(3,4,5)P_3 in the nucleoplasm was blocked by wortmannin (a pan PI3K inhibitor), suggesting that this pool is made by PI3Ks [86]. However as mentioned earlier the kinase activity of IPMK can also generate the nuclear PtdIns(3,4,5)P_3 and can therefore contribute in the synthesis of nuclear PtdIns(3,4,5)P_3 [110]. Our group has more recently reported the presence of PtdIns(3,4,5)P_3 in the nucleoplasm and the nucleolus in of a breast cancer cell line [28]. The presence of PtdIns(3,4,5)P_3 in the nucleolus was also greatly decreased following PI3K inhibition [28]. The downstream signaling molecule of the PI3K pathway, Akt, also localizes to the nucleus and can be either translocated in its active form to the nucleus or activated there [116, 117]. The PTEN and SHIP2 phosphatases are also present in the nucleus [118]. However, the activities of PTEN in the nucleus are suggested to be phosphatase independent in several studies [119-121]. One study on the other hand showed that nuclear PTEN impacts the level of PtdIns(3,4,5)P_3 [87].

There are only a few PtdIns(3,4,5)P_3-binding proteins that have so far been identified in the nucleus (see Table 3). These include the PtdIns(3,4,5)P_3-binding protein (PIP3-BP) found in the brain [93]. PIKE (L-isoform of PI3K enhancer) is also a nuclear PtdIns(3,4,5)P_3 binding protein which when mutated at its binding site it translocates to the cytoplasm [92]. Another nuclear PtdIns(3,4,5)P_3 interactor is the mRNA export protein, ALY (THO complex subunit 4) which its binding to PtdIns(3,4,5)P_3 is thought to mediate the selective transport of certain mRNA transcripts enriched in DNA repair functions from the nucleus [89]. The association of the nucleolar protein, Nucleophosmin with PtdIns(3,4,5)P_3 has also been reported [88]. In addition recently, PtdIns(3,4,5)P_3 was found to interact with the EBP1

protein in the nucleolus where the nucleolar localization of EBP1 was lost when it was mutated at the PPIn-binding motifs [28].

1.2.4 PI3K in the nucleolus

During interphase the nucleus is divided into different sub-compartments which are referred to as the nuclear bodies where specific nuclear processes occur. The nucleolus is among one of these microenvironments and is the largest sub-nuclear structure [122, 123]. The nucleolus is the territory where ribosomal DNA regions are co-organised, transcribed and where ribosomes are assembled [122, 124]. Ribosomes are composed of four ribosomal RNAs (rRNAs) and many different ribosomal proteins. In humans, nucleolar organizer regions (NORs) are mainly tandem repeats of ribosomal genes (18S, 5.8S, and 28S rRNA genes) located on acrocentric chromosomes (chromosomes 13, 14, 15, 21 and 22) with intergenic spacer regions [122, 125-128]. First, the 47S rRNA precursor is transcribed and after several processing steps, the 18S, 5.8S, and 28S rRNAs are generated which then together with 5S (made outside of the nucleolus) and the ribosomal proteins will form the 40S and 60S subunits [124, 129-131]. The transcriptional state of rDNA is determined by the epigenetic markers on the DNA and the presence of the transcription factor UBF (upstream binding factor) [132]. The nucleoli of mammalian cells are divided into 3 different regions (Figure-3); the fibrillar centers, dense fibrillar component and the granular component [122]. The fibrillar center contains the ribosomal DNA and the border with the dense fibrillar component is where the rRNAs are transcribed and start their maturation. In the granular component the ribosomal subunits assemble and get prepared to be exported to the cytosol [122, 133-135]. A heterochromatin shell surrounds the nucleolus that contains mostly silent DNA, although genes encoding for tRNA and 5S RNA have also been reported to localize in these perinucleolar heterochromatin areas [136, 137]. On the other hand associated with the surface of the nucleolus is the perinucleolar compartment (PNC) which was first described when the polypyrimidine tract-binding (PTB) protein was characterized and detected as intense foci in this area [138] (Figure-3). This compartment contains many RNA binding proteins and also RNA polymerase III transcripts [139].

Over the years the presence of some of the PPIns and their metabolizing enzymes has also been reported in the nucleolus. The PPIns and their metabolizing enzymes identified in the nucleolus to date are listed in table 4. Our group has recently mapped p110β and

PtdIns(3,4,5)P_3 to nucleoli in AU565 cells [28]. This may be relevant to a previous study showing the interaction of the nucleolar protein NPM to PtdIns(3,4,5)P_3 [88].

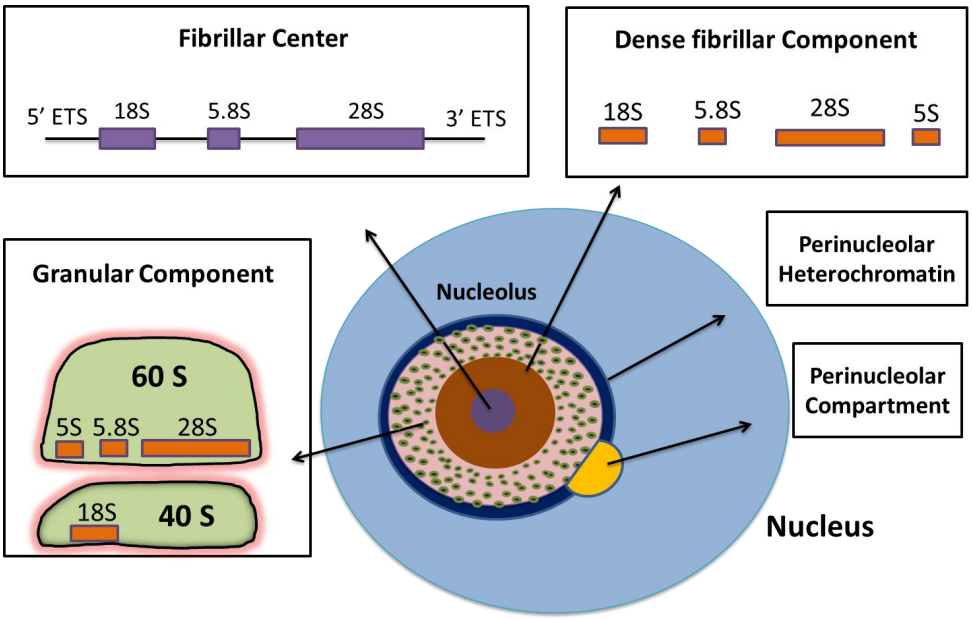

Figure 2. Diagram of the compartments in and around the nucleolus. At the boundary of the fibrillar center (FC) and dense fibrillar component (DFC) the transcription of rDNA by RNA polymerase I occur. The pre-RNA is cleaved and modified to 18S, 5.8S and 28S ribosomal RNAs in the DFC. The Granular component (GC) is where these rRNAs go through their final maturation and assemble to form the 40S and 60S ribosome subunits [122]. Together with the ribosomal proteins and the 5S rRNA a functional ribosome is formed and exported to the cytoplasm. The nucleolus is surrounded by a heterochromatin shell which mostly contains silent DNA known as the perinucleolar heterochromatin [136, 137]. The perinucleolar compartment is also associated with the nucleolar surface which is rich in RNA binding proteins and transcripts of RNA polymerase III [139].

Multiple proteins that play essential roles in regulating rRNA transcription and synthesis are affected and regulated either directly by PPIns or other members of the PI3K pathway. UBF and transcription initiation factor-I (TIF-I) are two examples of essential nucleolar factors that are influenced by this pathway [27, 140]. A minor pool of PtdIns(4,5)P_2 has been reported to be localized in nucleoli and to be involved in the regulation of RNA polymerase I transcription by binding to UBF [27, 141]. A study in 2004

showed that insulin receptor substrate 1(IRS-1) can translocate to the nucleolus and stimulate the phosphorylation of UBF by a PI3K p110 isoform (likely p110β) and therefore result in the activation of the rDNA promotor [142]. Akt is involved in activating and stabilizing TIF-I and therefore enhancing rRNA transcription [140]. A recent study on Drosophila S2R+ cells showed that inhibition of PI3K or TOR (using LY294002 or rapamycin) decreases the expression of rRNA [143].

Table-4. Known nucleolar PPIns and PPIns metabolizing enzymes.

PPIns or enzymes	Nucleolar function	Reference
PtdIns(3,4,5)P_3	unknown function	[28]
PtdIns(4,5)P_2	Promotes Pol I transcription	[27, 96, 141]
p110β	unknown function	[28]
PTEN	Regulation of ribosome biogenesis	[144]
SHIP1	unknown function	[145]
PI4K230/IIIα	Possibly produces PtdIns4P (precursor of PtdIns(4,5)P_2)	[146, 147]
PIP5KIα	rDNA silencing	[148]

1.3 Selected functions of the PI3K pathway in health and disease

This pathway is essential for cell survival and plays major roles in many aspects of cell biology [51]. Upon PI3K activation multiple downstream pathways can be triggered simultaneously which can explain the participation of PI3K in a wide range of cellular processes. The balance between PI3K isoform specific signalling is critical and the development of the immune system is a perfect example of its importance as not only changes in certain PI3K genes can lead to immunodeficiency but also inhibition of certain PI3K isoforms can increase the efficiency of immune cells against tumour cells [149, 150].

The PI3K-mTOR and Akt signalling pathway is among the most mutated pathways in human cancers [151, 152]. Even though inactivation and loss of the *PTEN* tumor suppressor is the most common alteration in the PI3K pathway leading to cancer [153], abnormalities in the different isoforms of PI3K can also lead to multiple diseases. Activating mutations in the PIK3CD gene (that encodes PI3Kδ) have been associated with diseases related to the

respiratory and immune system [154]. In 2004, the PI3K genes in different human cancers were sequenced by Samuel *et al* [155]. The mutations discovered in the *PIK3CA* gene (encodes p110α) were mostly located at the helical and kinase domains and were found at later stages of tumorigenesis. Mutations in other p110 isoforms are not very common in cancer cells. However, PTEN deficient cancer cells have been shown to be dependent upon the product of the *PIK3CB* gene, p110β, in tumorigenesis in some cancers, including breast and prostate cancers [68, 156-158]. It has been shown that overexpression of the non-alpha p110 isoforms (β, δ or γ subunits) can trigger oncogenic phenotypes in their wildtype state [159]. mTOR is a member of PIKK (phosphoinositide 3-kinase -related protein kinases) family and it comprises the catalytic subunit of mTORC1 and mTORC2 complexes [160]. The mTOR complexes mediate the PI3K pathway signaling and activating mutations of Akt and mTOR occur occasionally in cancer cells [152, 161, 162]. PDK1, that activates Akt by phosphorylation, was found to accumulate in the nucleus in a PI3K signaling dependent manner and it appeared to be involved in tumorigenesis to a higher extend than the cytoplasmic PDK1 [163, 164].

1.3.1 PI3K in endometrial cancer

Among the gynecological and female reproductive system cancers, endometrial cancer is the most prevalent in developed countries and the incidence of this cancer is increasing [165-167]. Endometrial cancer (EC) is the tumor of the inner lining of the uterus and can occur in women both before and after menopause and due to abnormal symptoms this type of cancer is normally diagnosed at early stages [168-170]. Endometrial carcinomas have long been divided into two subtypes; type I and type II [171]. Type I accounts for up to 70% of endometrial cancers with low grade tumors that associate with obesity, positive for hormone-receptors and have good prognosis [171, 172]. Types II, on the other hand, are less common and high grade, hormone receptor negative endometrial cancers that result in poor outcomes [171, 172]. Some of the mutations that can be seen frequently in type I tumors are in the *PTEN*, *PIK3CA, KRAS and PIK3R1* genes [173-176]. One of the clinical problems in the treatment of this cancer is the heterogeneity and the different molecular subgroups that the endometrial cancer comprises. This has effected the risk assessments and the treatments that the patients are receiving which results in either under or over treatments [177]. Therefore in order to select an appropriate therapy, knowing the molecular mechanisms underlying each endometrial tumor subgroup is critical.

PI3K/AKT/mTOR pathway mutations in endometrial cancers were reported to be among the highest compared to any other tumor type in The Cancer Genome Atlas with *PIK3CA* and *PTEN* being among the most frequently mutated genes [174]. *PTEN* mutations are most frequent in early lesions as compared to *PIK3CA* mutations that are more frequently seen in invasive tumors [178, 179]. In addition, an increased PI3K signaling was also correlated with an aggressive phenotype of endometrial cancer [180]. Mutations in *PIK3CB* are rare in comparison with the *PIK3CA* gene, however mutations in p110β, was also discovered in an endometrial lesion [181]. Mostly, the mRNA levels of *PIK3CB* has been reported to increase in some endometrial cancer specimens [182] and more extensively in a study from our group [183]. The aforementioned study has indeed shown an increase in *PIK3CB* mRNA levels early in cancer progression, *i.e.* from complex atypical hyperplasia to grade 1 lesions. The mRNA levels remained high in grades 2 and 3 as well as in non-endometrioid and metastatic lesions.

Because of the high number of mutations in the PI3K pathway that occur in endometrial cancers multiple inhibitors that target this pathway have been used in clinical trials including Pilaralisib (a pan PI3K inhibitor), GDC-0980 (PI3K/mTOR inhibitor) and MK-2206 (an Akt inhibitor) [184-186]. Increased sensitivity of endometrial cancer cells to chemotherapeutic drugs have been observed upon downregulation of the Akt isoforms [187]. The use of a pan PI3K inhibitor, BKM-120, on patient derived endometrial xenografts showed a decrease in tumor volume [188]. Because endometrial cancer harbor frequent *PTEN* mutations, a recent clinical trial using a selective p110β inhibitor has been carried out on patients with advanced cancers with *PTEN* loss including 3 patients with endometrial cancer [189]. Some beneficial effects were observed due to the treatment in some patients. This study is encouraging as it demonstrates the possible therapeutic benefit of inhibiting p110β in PTEN-deficient tumors and hence rationalizes further research efforts in better understanding the underlying molecular mechanism of action of p110β.

1.3.2. PI3K and adipogenesis

Adipocytes are the main cells of the adipose tissue and store the excess fatty acids obtained from the diet as triacylglycerol (TAG) in form of lipid droplets and by doing this they have a high impact on cell metabolism [190, 191] . There are two well studied types of adipocytes; white and brown adipocytes as well as the emerging beige adipocytes. White adipocytes involved in the storage of fat and have high lipid content however the brown

adipocytes are involved in thermogenesis [191, 192]. Adipogenesis occurs in a multi-step process involving first the differentiation of mesenchymal cells to pre-adipocytes followed by several processes leading to a mature adipocyte [193, 194]. In order to accumulate the maximum amount of fat, the nucleus of adipocytes moves towards the plasma membrane while the morphology of cells are changing to a spherical shape as they become more mature adipocytes [190]. 3T3-L1 cells are mouse fibroblast cells that have the potential to differentiate in to adipocytes and have been frequently used in studies of adipogenesis [195, 196]. The differentiation of the 3T3-L1 cells into adipocytes is initiated by a cocktail of insulin, dexamethasone and 3-isobutyl-1-methylxanthine [197].

Signaling through insulin results in the uptake of glucose and the storage of fatty acids as TAGs in adipocytes [198]. The insulin receptor (IR), which is a tyrosine kinase receptor undergoes auto phosphorylation upon insulin binding and initiates downstream signaling [199-201]. Insulin is able to regulate glucose uptake by shifting the glucose transporter GLUT4 from cytosolic vesicles to the plasma membrane [202, 203]. Inhibition of the PI3K pathway in 3T3-L1 cells prevents the translocation of GLUT4 indicating an essential role of PI3K in insulin signaling [204, 205]. The involvement of Akt in GLUT4 transfer is well established as expression of active mutant of Akt has a positive and stimulated impact on in GLUT4 translocation in adipocytes whereas inhibition of Akt plays a negative role in this process [206, 207]. For the expression of specific genes that will result in the adipocyte phenotype, transcription factors are tightly regulated during adipogenesis and they come in two waves of activation. The expression of the key transcription factors in adipogenesis, PPARγ (peroxisome proliferator-activated receptor γ) and C/EBPα (CCAAT/enhancer-binding protein) are induced during the second wave of this cascade [208, 209].

There are several specific substrates that transfer signals from the insulin receptor and the link to the PI3K pathway downstream of IR is through the Insulin Receptor Substrate (IRS)-1 [210]. Through the SH2 domain, the regulatory subunit p85 of class I PI3K binds to IRS which subsequently initiates the production of PtdIns(3,4,5)P_3 [210]. Inhibition of PI3K signaling can have major effects on cells; among them is the effect on cell differentiation [211]. Inhibitor of the PI3Ks has shown to impair the differentiation of 3T3-L1 (pre-adipocytes) cells into adipocytes [212]. It has also been shown that the levels of p110β increases during adipocyte differentiation but the expression of the p110α does not change

[213]. In contrast, an increase in the levels of p110α has also been reported during adipocyte differentiation [214]. Using selective inhibitors of p110α, p110β and p110δ, our group and others have further shown that p110α plays a dominant role in adipogenesis, while p110β and p110δ also contribute to this process [215-217]. How these three isoforms act and whether they regulate different processes in adipogenesis is still however unclear. Insulin also activates the class II PI3KC2α in adipocytes. The increase in activity of PI3KC2α upon insulin stimulation in 3T3-L1 adipocytes was shown to be independent of IRS-1 and the insulin receptor [218]. However, the molecular mechanisms of action of PI3KC2α are poorly understood.

2. Aims of the study

Many cellular processes are dependent on the PI3K pathway as its members have central roles and play important functional aspects for living cells. The malfunctions in PI3K signalling can contribute to multiple different diseases. The PI3K is involved in regulating metabolism and cell growth and its hyper activation in many cancer types due to genetic alterations of components of the pathway has been reported [39, 51, 151, 219].

This pathway is orchestrated by several isoforms but our understanding of the exact contribution of each of these isoforms in the different cellular processes still lags behind. Furthermore, the complexity of this pathway increases due to the different subcellular localisations of these isoforms and their lipid products (see tables 1, 2 and 3 for summary). PtdIns(3,4,5)P_3 is an important second messenger in this pathway and its function has been well studied in the cytoplasm. Recent studies have mapped the class I PI3K p110β and its product PtdIns(3,4,5)P_3 to the nucleus but the functional role of PtdIns(3,4,5)P_3 in the nucleus is still poorly understood. In this thesis we aimed to study the significance of PtdIns(3,4,5)P_3 and p110β in the nucleus and how this links to cell differentiation and increase in cell proliferation (leading to cancer). This was performed by the means of the following aims:

1. To determine the levels of p110β and PtdIns(3,4,5)P_3 in the nucleus and to define their mode of action in tumorigenesis
2. To characterize the role of nuclear PtdIns(3,4,5)P_3 by identifying its interacting partners in the nucleus
3. To determine the involvement of nuclear PI3Ks in adipocyte differentiation

3. Summary of results

Elevated nuclear p110β and PtdIns(3,4,5)P_3 levels correlate with higher grade of endometrial cancer and increase in rRNA transcription

In a recent study, our group has shown that the p110β, but not p110α, protein levels were consistently elevated in endometrial cancer (EC) cells. In addition, *PIK3CB* mRNA levels were increased in grade 1 endometrioid endometrial lesions compared to complex hyperplasias [183]. While p110α and p110β both depict cytoplasmic localizations, p110β is also found in the nucleoplasm and in the chromatin rich fractions [70, 113]. Moreover, our laboratory has reported for the first time the presence of p110β and its product PtdIns(3,4,5)P_3 in the nucleolus in addition to the nucleoplasm [28]. In this thesis, we have shown that all EC cell lines showed an increase in nuclear p110β levels when compared to non-tumour endometrial cells (EM). When primary endometrial tumours were immunohistochemically stained for p110β, high nuclear to cytoplasmic ratios correlated with a higher tumour grade. In EC cells, active p-S473-Akt was also increased in the nucleus, indicating the presence of an active PI3K pathway in the nuclei of these cells. Moreover, the presence of p110β in the nucleus correlated with elevated levels of PtdIns(3,4,5)P_3 in particular in PTEN-deficient EC cells. Treatment with a p110β selective inhibitor reduced the nuclear levels of p-S473-Akt and PtdIns(3,4,5)P_3 suggesting that the p110β may be responsible for the production, at least partly, of the nuclear pool of PtdIns(3,4,5)P_3 in these cells. Immunofluorescence staining of EC cells showed the nucleolar localization of p110β, consistent with the previous report from our group [28]. PtdIns(3,4,5)P_3 was also detected in the nucleoli of multiple EC cell lines using immunofluorescence staining. We chose the RL952 endometrial cancer cells that contain the highest levels of nuclear PtdIns(3,4,5)P_3 to study its chemical composition in the nucleoli. Nucleolar PtdIns(3,4,5)P_3 measurements by LC-MS/MS detected the PtdIns(3,4,5)P_3 (38:4) species. Ribosomal RNA transcription levels of different EC cells were measured by real-time RT-qPCR. The PTEN-deficient RL95-2 cells with very high p110β and PtdIns(3,4,5)P_3 levels in nucleus/nucleolus showed an increase in the pre-rRNA transcription levels.

The identified nuclear PtdIns(3,4,5)P3 binding proteins were enriched in DNA repair and RNA processing factors

Mapping of p110β by immunostaining and cellular fractionation showed the presence of this kinase and its lipid product PtdIns(3,4,5)P_3 in the nucleoplasm and strongly in nucleoli of HeLa cells. In particular, we showed that p110β and PtdIns(3,4,5)P_3 appeared in the nucleolus following the exit from mitosis, as the nucleoli reformed. Importantly, the appearance of nucleolar PtdIns(3,4,5)P_3 was due to the p110β activity, as shown in murine embryonic fibroblast with WT versus kinase inactive p110β. Considering that by binding to proteins via specific domains or motifs PPIn elicit signaling responses, we pursued to systematically identify PtdIns(3,4,5)P_3 effector proteins in the nucleus. To this end, we have adapted a quantitative proteomics-based approach that our group has previously employed to identify PtdIns(4,5)P_2 nuclear interacting proteins [31]. This method uses the polybasic aminoglycoside neomycin to displace and enrich for PPIn-binding nuclear proteins in combination with a lipid pull down assay. Neomycin would therefore compete for PPIn-protein interaction through electrostatic forces and displace the proteins. PtdIns(3,4,5)P_3 versus control beads lipid pull downs were performed from neomycin-displaced proteins collected from stable isotope labeled ($^{13}C/^{15}N$) and non-labeled HeLa S3 nuclei respectively. Quantitative and statistical analyses revealed the identification of a total of 219 proteins as potential PtdIns(3,4,5)P_3 binders. Gene ontology analysis of these proteins showed an enrichment of multiple biological processes including the top following categories; RNA splicing, cytokinesis, mRNA processing and DNA repair. So far, we have chosen to focus on Poly [ADP-ribose] polymerase 1 (PARP1), one of the proteins within the DNA repair group, as it has previously been clearly detected in the nucleolus [220, 221] and to bind to NPM [220]. Among the DNA repair proteins, PARP1 was identified to co-localize with PtdIns(3,4,5)P_3 in nucleoli, which suggests the possible involvement of this PPIn in nucleolar response to rDNA damage. Furthermore, the presence of both PARP1and PtdIns(3,4,5)P_3 in the nucleoli were reorganized upon inhibition of RNA polymerase I, and no longer co-localized at the same foci. During the nucleolar rearrangement however PtdIns(3,4,5)P_3 co-localized with UBF in the perinucleolar caps. p110β was also translocated to the periphery of the nucleoli however it no longer colocalize with RNA polymerase I upon inhibition of rRNA transcription. Interestingly, preliminary data showed that the selective inhibition of p110β induced a decrease in rRNA transcription in HeLa cells.

Nuclear PI3K pathway is involved in the differentiation of 3T3-L1 cells into adipocytes

We have previously shown that p110α, β and δ catalytic isoforms of class I PI3K are expressed in the 3T3-L1 cells and that p110α contributes to TAG storage to a higher degree than the p110 β and δ isoforms [215]. Here, we show that during the differentiation of 3T3-L1 cells into adipocytes, the PI3K enzymes PI3KC2α and p110β are found in the same sub-nuclear compartments as their lipid products PtdIns(3,4)P_2 and PtdIns(3,4,5)P_3. Immunofluorescence staining and cellular fractionations showed the presence of p110β in the cytoplasm and the nucleoli whereas PI3KC2α was detected in the nucleoplasm with weak detection in the cytoplasm. The PI3K-Akt pathway was found to be active in the nucleus during differentiation and p-S473-Akt was detected 30 min after inducing the differentiation in 3T3-L1 cells. Nuclear lipid extracts from different stages of the differentiation showed an increase in both PtdIns(3,4)P_2 and PtdIns(3,4,5)P_3 upon insulin stimulation. PtdIns(3,4,5)P_3 could also be detected in the nucleoli of stimulated 3T3-L1 cells. Potential PPIn interacting proteins were extracted by neomycin at day1 following stimulation and DNA Topoisomerase IIα (Topo IIα) was detected as a potential binding partner for both PtdIns(3,4)P_2 and PtdIns(3,4,5)P_3 and nucleolin as an effector protein of just PtdIns(3,4,5)P_3.

4. General discussion

The PI3K pathway regulates many fundamental cellular processes such as metabolism, cell survival, proliferation and growth [51, 222]. In this thesis we emphasised on the role of nuclear PI3K/Akt signalling in the context of metabolism and tumorigenesis.

An increase in lipid synthesis is required to satisfy the needs of proliferating cancer cells for producing membranes and mediating signal transduction [223]. Cells are dependent on lipids to perform many of their functions and among the many alterations that occur in cancer cells are the deregulation in lipid biosynthesis [224, 225]. Lipids are not only key structural components of membranes but are also signaling molecules themselves of which their mechanisms of regulation can be altered, hence contributing to tumorigenesis [225]. In our study, we have particularly focused on lipid signaling in the nucleus. In paper I, we show that the levels of PtdIns(3,4,5)P_3 are elevated in the nuclei of endometrial cancer cells. We also show that the PI3K pathway is active in the nucleus of these cells as they exhibit increased phosphorylated Akt levels, particularly in PTEN deficient endometrial cancer cells compared to non-tumour endometrial (EM) cells. This is in line with existing knowledge that in human cancers Akt is frequently activated which can block apoptosis and result in abolishing the checkpoints of the cell cycle [226]. The lipid phosphatase PTEN is one of the most mutated proteins in endometrial cancers [174] and PTEN deficiency potentially implicates higher levels of PtdIns(3,4,5)P_3. Indeed, PTEN is well known to control the levels of PtdIns(3,4,5)P_3 particularly on plasma membranes [86, 227, 228]. PTEN is also found in the nucleus but was shown not to control the levels of the nuclear PtdIns(3,4,5)P_3 pool [86, 229, 230]. The other phosphatase that uses PtdIns(3,4,5)P_3 as a substrate is TPIP (TPTE and PTEN homologous inositol lipid phosphatase) but this was found to localize on the endoplasmic reticulum [231]. Instead, the nuclear pool of PtdIns(3,4,5)P_3 could possibly be controlled by 5-phosphatases. For example, SHIP2 was identified in the nuclear speckles and could hence regulate at least part of the nuclear pool of PtdIns(3,4,5)P_3 [232]. However, its nuclear substrate was suggested to be PtdIns(4,5)P_2 as it can be highly detected in this sub-nuclear site [232]. Furthermore, we found that p110β is overexpressed in endometrial cancer (EC) cells. This would suggest that the levels of this kinase needs to be tightly regulated and overexpression could lead to high PtdIns(3,4,5)P_3 levels hence contributing to tumorigenesis. This kinase is indeed tumorigenic in its WT state when overexpressed [159]. Since p110β was found with increased levels not only in the cytoplasmic but also in the

nuclear fractions of EC cells (paper I), we would suggest that the tumour-promoting properties of p110β could be due to its action from both of the locations. At least, a previous report showed that selective inhibition of p110β decreased cell proliferation in PTEN-negative EC cells [183] but whether the cytoplasmic, nuclear or even the combined fractions of p110β contributes is not known at present.

We found PtdIns(3,4,5)P_3 and its kinase p110β to localize to the nucleolus of different types of cell lines that we have studied, including 3T3-L1 cells (paper III), endometrial cancer cells (paper I), and HeLa cells (paper II). Importantly, we have shown that the appearance of PtdIns(3,4,5)P_3 in the nucleus of EC cells (paper I) and in the nucleolus of MEF cells (paper II) is dependent upon p110β activity. As the increase in nuclear p110β levels correlated with higher grade of endometrial tumours, this suggests a role for p110β to contribute to tumour development in a nucleolar dependent manner. The nucleolus is the site of ribosome production, involving rRNA synthesis, processing and assembly with ribosomal proteins [122, 124]. Growing evidence suggests that upregulation of nucleolar functions correlate with cancer progression [233-235]. More than 50 years ago, it was discovered that the size of the nucleolus was larger in malignant tumor cells when compared to normal cells [236]. Recently a link between elevated levels of nucleolar activity and ribosome biogenesis with an increased risk of cancer development has been uncovered [237]. There is a high demand for protein synthesis in highly dividing and proliferating cancer cells and since protein synthesis is reliant on ribosomes, an increase in nucleolar activity would be required to reach these demands. We found that the transcription of rRNA is elevated in endometrial cancer cells that have the highest nuclear levels of PtdIns(3,4,5)P_3 and p110β. These results correlate well with a study by Drakas *et al* that suggested that a p110 isoform (potentially the β isoform) can activate rDNA transcription by interacting with and phosphorylating the transcription factor UBF [142]. This study did not however explore the lipid kinase activity of p110 (β). Our results also confirm the study in 1965 showing that phospholipids tend to occupy active chromatin rather than repressed chromatin [238]. Furthermore, our preliminary results showing a reduction in rRNA synthesis upon p110β inhibition (paper II) adds additional support for the role of PtdIns(3,4,5)P_3 and p110β in rRNA transcription. The exact mechanism of action of nucleolar p110β regulating rDNA transcription is still unknown but may be linked to the following findings. The activity of the p53 tumor suppressor protein is regulated by ribosome biogenesis [239] which is thought to be due to the inhibition of MDM2 (a p53 degrading protein) by a complex composed of

ribosomal proteins such as RPL11 and RPL5 with the 5S rRNA [240]. Therefore, an upregulation of ribosome biogenesis correlates with decreased p53 activity levels as the MDM2 inhibition increases [241]. Furthermore, NPM which is a key player in ribosome biogenesis has previously been shown to bind to PtdIns(3,4,5)P_3 and to have an anti-apoptotic activity [88]. NPM also prevents the inhibition of MDM2 by keeping p14ARF (an antagonist of MDM2) in the nucleolus and therefore promoting p53 stability and activation [242]. NPM can be phosphorylated by Akt which prevents its effect on the nucleolar accumulation of p14ARF hence leading to opposite effect on p53 [243]. Considering that PtdIns(3,4,5)P_3 binds NPM, this interaction could play a role in regulating NPM-mediated p14ARF nucleolar sequestration. Also, PtdIns(3,4,5)P_3 could also possibly activate Akt locally in the nucleolus and induce Akt-mediated phosphorylation of NPM. In line with this, Kwon *et al* have shown that PtdIns(3,4,5)P_3 can compete for its interaction with NPM and Akt in the nucleus [87]. It is also possible that increased nucleolar p110β and PtdIns(3,4,5)P_3 levels in endometrial cancer cells can contribute to tumor progression by orchestrating the regulation of p53 activity by PtdIns(3,4,5)P_3 interaction with NPM. The tumor suppressor PTEN is also found in the nucleolus and interestingly reduction in the levels of PTEN was correlated with increased biogenesis of ribosomes [144]. PTEN deficient endometrial cancer cells can potentially have higher nucleolar PtdIns(3,4,5)P_3 levels with less phosphatase activity and hence promote tumorigenesis.

The nucleolus is primarily known as the site where rRNA is transcribed and processed but it is also associated with major roles in other cellular processes such as cell cycle regulation [234]. During the cell cycle the transition of cells from the G1 phase to S phase is dependent on the amount of ribosome synthesis [244]. When we synchronized HeLa cells with nocodazole treatment followed by mitotic shake-off, we observed the appearance of p110β in the nucleolus within 3 hours after replating which was about the same time as the appearance of RNA polymerase I in the nucleoli (paper II). However, PtdIns(3,4,5)P_3 did not appear in the nucleolus until 2 h later, perhaps due to the delayed activation of p110β. At least, using the same method in WT and kinase inactive p110β MEFs, PtdIns(3,4,5)P_3 was apparent in nucleoli 4 h post-plating and was dependent on p110β activity. We speculate that the co-appearance of RNA polymerase I and p110β may indicate a role of this kinase in rRNA transcription, which again supports our findings that correlated rRNA transcription to increased levels of p110β in endometrial cancer cells.

In paper II, we have shown that the nuclear interacting partners of PtdIns(3,4,5)P_3, are enriched to function in RNA processing and DNA repair mechanisms. Interestingly, p110β has already been shown to sense DNA damage and to regulate DNA repair and knock down of p110β results in the impairment of the DNA repair pathway [111]. In addition, it is also shown that PtdIns(3,4,5)P_3 localises to sites of DNA repair in the nucleus [111]. Our interactomics data (paper II) shows nuclear PtdIns(3,4,5)P_3 interacting proteins have a 6 fold enrichment in DNA repair mechanisms, hence adding further support to these existing studies. Some of the DNA repair proteins identified have been previously shown to localize in the nucleolus and even shown to have dual functions with roles in ribosome biogenesis, such as APEX1 (apurinic/apyrimidinic endodeoxyribonuclease 1), NPM and PARP1 [221, 245, 246]. DNA damage response is highly important and is an active process in the early stages of cancer cells in order to detect the DNA lesions caused by the replication stress [247]. Since cancer cells are dependent on the repair of DNA breaks, many cancer drugs are targeted to the DNA damage signaling molecules such as PARP1 inhibitors [248]. PARP1 is a critical protein involved in DNA repair with the ability to bind to the DNA damage sites and promote the accumulation of DNA repair proteins on those sites [249]. The boundaries of the dense fibrillar component (DFC) and the fibrillar center of the nucleolus is where rRNA transcription occurs and the PARP protein has been shown to localize in the DFC [250]. Upon DNA damage the activation of PARP1 is dependent on DNA-dependent protein kinase (DNA-PK) to inhibit the synthesis of rRNA [251]. We have identified DNA-PK in addition to PARP1 in our list of potential PtdIns(3,4,5)P_3 interacting proteins. In addition, we have determined the direct interaction of PARP1 with PPIn including PtdIns(3,4,5)P_3 *in vitro* and observed a co-localization of PARP1 with PtdIns(3,4,5)P_3 in the nucleoli by immunofluorescence staining. When rDNA is damaged, RNA polymerase I is inhibited and this causes the translocation of the rDNA to the perinucleolar heterochromatin caps where the DNA repair machinery will then accumulate to have easier access to damaged sites [252]. Similar to other research groups we show in paper II that in response to the RNA polymerase I inhibition by actinomycine D treatment, PARP1 leaves the nucleolar interior and translocates to the surrounding area [220]. However, our findings demonstrate that PtdIns(3,4,5)P_3 no longer co-localizes with PARP1 upon treatment and remains together with UBF where it is known to co-localize with other rRNA transcriptional machinery components in the perinucleolar caps [253]. On the other hand, the function of PARP1 in the nucleolus is not restricted to DNA repair and it impacts ribosome biogenesis as well [221]. Being highly abundant in the nucleolus, PARP1 interacts with key nucleolar proteins

such as nucleolin, NPM and fibrillarin [220, 221, 254]. In addition studies in *Drosophila* show that PARP1 generates poly(ADP-ribose) which acts as a matrix to keep the nucleolar proteins together [221]. Since NPM is known to interact with the DNA binding domain of PARP1 [220], it is possible that there is a potential crosstalk between PtdIns(3,4,5)P_3 and these proteins to regulate ribosome biogenesis.

Our findings demonstrate that mRNA processing and splicing factors were enriched over 12 fold in PtdIns(3,4,5)P_3 interacting proteins which adds to findings from our lab and others that show the presence of several other PPIns and their kinases in RNA rich compartments (also referred to as ribonucleoprotein (RNP) bodies) such as nuclear speckles and the nucleoli [26-28, 255]. They are membrane-less and they are abundant in proteins and RNA [256]. While the acyl chains of PPIn have been shown to be potentially shielded in ligand binding pockets of nuclear receptors [81, 82, 90] it is uncertain why and how the negatively charged PPIn can reside in close proximity of negatively charged phosphate groups of RNAs. We can speculate that PPIn can bind to RNA effector proteins and while their acyl chains are shielded, they perhaps compete with RNA for their interaction with the effector protein. This regulation can be assumed to be through a repelling effect to disrupt the protein –RNA interaction. On the other hand the nucleoli have been shown to have a condensed liquid phase behavior which seems to be a common characteristic of the membrane-less ribonucleoprotein rich organelles [257, 258]. Whether the presence of PPIn in these organelles can drive the phase transitions and change the biophysical properties of these environments still remains to be uncovered.

The PI3K pathway is complex due to the multiplicity of its isoforms and the variety of functions that they each perform in different subcellular compartments. One of the key findings in this thesis is that the PI3K signalling is active in the nucleus of 3T3-L1 cells during differentiation into adipocytes (paper III). The levels of phosphorylated Akt and its interacting PPIn; PtdIns(3,4,5)P_3 and PtdIns(3,4)P_2 are increased following the induction of adipocyte differentiation. Class I and II PI3K isoforms, which produce these PPIn, were found to be present in the nucleus of differentiating 3T3-L1 cells. PI3KC2α that potentially makes PtdIns(3,4)P_2 localizes to the nucleoplasm while p110β that produces PtdIns(3,4,5)P_3 localizes to the nucleolus. Consistent with our studies on HeLa cells (paper II) and EC cell lines (paper I), as well as a previous study in breast cancer cells [28], PtdIns(3,4,5)P_3 localizes in the nucleolus together with p110β in 3T3-L1 cells, albeit at low levels. Because

of seemingly low levels observed by immunofluorescence microscopy, p110β was not detectable by Western immunoblotting of nuclear fractions under the conditions used. Immunofluorescent stainings also showed that the levels of p110β in the nucleoplasm of differentiating 3T3-L1 cells to be low as compared to its lipid product PtdIns(3,4,5)P_3 where it is localised diffusely. This suggests that the PtdIns(3,4,5)P_3 present in the nucleoplasm may be the product of the kinase activity of another kinase, *i.e.* IPMK (Inositol polyphosphate kinase). While the nucleoleolar pool can be produced by p110β [110]. The p110β levels in the nucleoli of differentiating 3T3-L1 were not as high as we had observed in the endometrial cancer cell lines or HeLa cells. Even though a rapid proliferation stage occurs in the growth arrested 3T3-L1 preadipocytes upon induction of differentiation, these cells will again become growth arrested and then commit to differentiate to adipocytes [193, 259]. Therefore, differentiating 3T3-L1 cells do not require high nucleolar activity since the rate of rRNA transcription is linked to the growth status of the cell [260, 261]. Using the same approach as in paper II, *i.e.* by incubating nuclei with neomycin to enrich for and collect potential PPIn binding proteins, we have identified nucleolin and TopoIIα by mass spectrometry, as neomycin-displaced proteins from nuclei obtained 24 h after inducing adipogenesis. Interestingly, inhibition of the p110β isoform showed an increase in the levels of nucleolin and TopoIIα displaced by neomycin, indicating that a pool of these proteins are no longer retained by nuclear PtdIns(3,4,5)P_3, but rather by other mechanisms. Thus neomycin could then displace these proteins by competing with either other PPIn or nucleic acids that they may bind to TopoIIα. Notably, nucleolin is one of the most abundant proteins in the nucleolus and it plays many different functions such as rRNA synthesis, cell cycle regulation and cell proliferation which add additional support for the importance of the presence of PtdIns(3,4,5)P_3 in the nucleolus [262, 263]. Topo IIα was identified to bind both PtdIns(3,4,5)P_3 and PtdIns(3,4)P_2 in a current project in our laboratory and since the levels of both these lipids increase upon inducing differentiation, these results support and validates our previous finding that the Topo IIα levels increase in the early stages of adipogenesis in a PI3K dependent manner [215]. Although there are still uncertainties about the exact function that these kinases and PPIn play in the process of differentiation, they are novel nuclear factors that seem to be required to initiate the early stages of 3T3-L1 cell adipogenesis.

5. Conclusions

We show in this thesis that the molecular landscape of interactions that the PI3K pathway has in the nucleus is as complex as in the cytosol. The components of the PI3K pathway localize in distinct compartments of the nucleus with tendency to RNA rich bodies. Indeed in the nucleus they are contributing in the regulation of a variety of processes including differentiation and tumorigenesis. The localization of PtdIns(3,4,5)P_3 in the nucleoli and its interaction with nucleolar proteins such as NPM and PARP1 suggests that this signaling lipid is involved in regulating nucleolar activity. Since we find p110β localizing with PtdIns(3,4,5)P_3 in the nucleolus we conclude that this lipid is locally produced in the nucleolar compartment. The nuclear/nucleolar levels of both p110β and PtdIns(3,4,5)P_3 are high in cancer cells which demand higher levels of ribosome biogenesis in contrast to differentiating cells that require less. All together the results from this thesis provide evidence for novel nuclear functions for members of the PI3K pathway and suggest that nucleolar p110β/PtdIns(3,4,5)P_3 may be central in sensing the different metabolic requirements upon differentiation and proliferation.

References

1. Maffucci, T., *An introduction to phosphoinositides.* Curr Top Microbiol Immunol, 2012. **362**: p. 1-42.
2. Vanhaesebroeck, B. and M.D. Waterfield, *Signaling by distinct classes of phosphoinositide 3-kinases.* Exp Cell Res, 1999. **253**(1): p. 239-54.
3. Martelli, A.M., et al., *Nuclear phosphoinositides and their roles in cell biology and disease.* Crit Rev Biochem Mol Biol, 2011. **46**(5): p. 436-57.
4. Viaud, J., et al., *Phosphoinositides: Important lipids in the coordination of cell dynamics.* Biochimie, 2016. **125**: p. 250-8.
5. Traynor-Kaplan, A., et al., *Fatty-acyl chain profiles of cellular phosphoinositides.* Biochim Biophys Acta, 2017. **1862**(5): p. 513-522.
6. Lemmon, M.A. and K.M. Ferguson, *Signal-dependent membrane targeting by pleckstrin homology (PH) domains.* Biochemical Journal, 2000. **350**(Pt 1): p. 1-18.
7. Cullen, P.J. and J.G. Carlton, *Phosphoinositides in the Mammalian Endo-lysosomal Network*, in *Phosphoinositides II: The Diverse Biological Functions*, T. Balla, M. Wymann, and J.D. York, Editors. 2012, Springer Netherlands: Dordrecht. p. 65-110.
8. Sarkes, D. and L.E. Rameh, *A Novel HPLC-Based Approach Makes Possible the Spatial Characterization of Cellular PtdIns5P and Other Phosphoinositides.* The Biochemical journal, 2010. **428**(3): p. 375-384.
9. Rusten, T.E. and H. Stenmark, *Analyzing phosphoinositides and their interacting proteins.* Nat Methods, 2006. **3**(4): p. 251-8.
10. Falasca, M. and T. Maffucci, *Regulation and cellular functions of class II phosphoinositide 3-kinases.* Biochem J, 2012. **443**(3): p. 587-601.
11. Gillooly, D.J., et al., *Localization of phosphatidylinositol 3-phosphate in yeast and mammalian cells.* Embo j, 2000. **19**(17): p. 4577-88.
12. Backer, J.M., *The regulation and function of Class III PI3Ks: novel roles for Vps34.* Biochem J, 2008. **410**(1): p. 1-17.
13. Balla, A. and T. Balla, *Phosphatidylinositol 4-kinases: old enzymes with emerging functions.* Trends Cell Biol, 2006. **16**(7): p. 351-61.
14. Wang, Y.J., et al., *Phosphatidylinositol 4 phosphate regulates targeting of clathrin adaptor AP-1 complexes to the Golgi.* Cell, 2003. **114**(3): p. 299-310.
15. Kalasova, I., et al., *Tools for visualization of phosphoinositides in the cell nucleus.* Histochem Cell Biol, 2016. **145**(4): p. 485-96.
16. Keune, W., et al., *Phosphoinositide signalling in the nucleus.* Adv Enzyme Regul, 2011. **51**(1): p. 91-9.
17. Tronchere, H., et al., *Production of phosphatidylinositol 5-phosphate by the phosphoinositide 3-phosphatase myotubularin in mammalian cells.* J Biol Chem, 2004. **279**(8): p. 7304-12.
18. Shisheva, A., *PIKfyve: Partners, significance, debates and paradoxes.* Cell Biol Int, 2008. **32**(6): p. 591-604.
19. Jones, D.R., et al., *Nuclear PtdIns5P as a transducer of stress signaling: an in vivo role for PIP4Kbeta.* Mol Cell, 2006. **23**(5): p. 685-95.
20. Backer, J.M., *New methods for capturing the mystery lipid, PtdIns5P.* Biochem J, 2010. **428**(3): p. e1-2.
21. Ungewickell, A., et al., *The identification and characterization of two phosphatidylinositol-4,5-bisphosphate 4-phosphatases.* Proc Natl Acad Sci U S A, 2005. **102**(52): p. 18854-9.

22. Sbrissa, D., O.C. Ikonomov, and A. Shisheva, *PIKfyve, a mammalian ortholog of yeast Fab1p lipid kinase, synthesizes 5-phosphoinositides. Effect of insulin.* J Biol Chem, 1999. **274**(31): p. 21589-97.
23. Yokogawa, T., et al., *Evidence that 3'-phosphorylated polyphosphoinositides are generated at the nuclear surface: use of immunostaining technique with monoclonal antibodies specific for PI 3,4-P(2).* FEBS Lett, 2000. **473**(2): p. 222-6.
24. Balla, T., *Phosphoinositides: tiny lipids with giant impact on cell regulation.* Physiol Rev, 2013. **93**(3): p. 1019-137.
25. Michell, R.H., et al., *Phosphatidylinositol 3,5-bisphosphate: metabolism and cellular functions.* Trends Biochem Sci, 2006. **31**(1): p. 52-63.
26. Boronenkov, I.V., et al., *Phosphoinositide signaling pathways in nuclei are associated with nuclear speckles containing pre-mRNA processing factors.* Mol Biol Cell, 1998. **9**(12): p. 3547-60.
27. Yildirim, S., et al., *Involvement of phosphatidylinositol 4,5-bisphosphate in RNA polymerase I transcription.* J Cell Sci, 2013. **126**(Pt 12): p. 2730-9.
28. Karlsson, T., et al., *A polybasic motif in ErbB3-binding protein 1 (EBP1) has key functions in nucleolar localization and polyphosphoinositide interaction.* Biochem J, 2016. **473**(14): p. 2033-47.
29. Okada, M., S.W. Jang, and K. Ye, *Akt phosphorylation and nuclear phosphoinositide association mediate mRNA export and cell proliferation activities by ALY.* Proc Natl Acad Sci U S A, 2008. **105**(25): p. 8649-54.
30. Balla, T., Z. Szentpetery, and Y.J. Kim, *Phosphoinositide signaling: new tools and insights.* Physiology (Bethesda), 2009. **24**: p. 231-44.
31. Lewis, A.E., et al., *Identification of nuclear phosphatidylinositol 4,5-bisphosphate-interacting proteins by neomycin extraction.* Mol Cell Proteomics, 2011. **10**(2): p. M110.003376.
32. Rosen, S.A., et al., *Understanding the relative affinity and specificity of the pleckstrin homology domain of protein kinase B for inositol phosphates.* Phys Chem Chem Phys, 2012. **14**(2): p. 929-36.
33. Park, W.S., et al., *Comprehensive identification of PIP3-regulated PH domains from C. elegans to H. sapiens by model prediction and live imaging.* Mol Cell, 2008. **30**(3): p. 381-92.
34. Lietzke, S.E., et al., *Structural basis of 3-phosphoinositide recognition by pleckstrin homology domains.* Mol Cell, 2000. **6**(2): p. 385-94.
35. Sasaki, T., et al., *Mammalian phosphoinositide kinases and phosphatases.* Prog Lipid Res, 2009. **48**(6): p. 307-43.
36. Auger, K.R., et al., *PDGF-dependent tyrosine phosphorylation stimulates production of novel polyphosphoinositides in intact cells.* Cell, 1989. **57**(1): p. 167-75.
37. Whitman, M., et al., *Type I phosphatidylinositol kinase makes a novel inositol phospholipid, phosphatidylinositol-3-phosphate.* Nature, 1988. **332**(6165): p. 644-6.
38. Vanhaesebroeck, B., et al., *Phosphoinositide 3-kinases: a conserved family of signal transducers.* Trends Biochem Sci, 1997. **22**(7): p. 267-72.
39. Thorpe, L.M., H. Yuzugullu, and J.J. Zhao, *PI3K in cancer: divergent roles of isoforms, modes of activation and therapeutic targeting.* Nat Rev Cancer, 2015. **15**(1): p. 7-24.
40. Falasca, M. and T. Maffucci, *Role of class II phosphoinositide 3-kinase in cell signalling.* Biochem Soc Trans, 2007. **35**(Pt 2): p. 211-4.
41. Posor, Y., et al., *Spatiotemporal control of endocytosis by phosphatidylinositol-3,4-bisphosphate.* Nature, 2013. **499**(7457): p. 233-237.

42. Stack, J.H., et al., *Vesicle-mediated protein transport: regulatory interactions between the Vps15 protein kinase and the Vps34 PtdIns 3-kinase essential for protein sorting to the vacuole in yeast.* J Cell Biol, 1995. **129**(2): p. 321-34.
43. Okkenhaug, K., *Signalling by the phosphoinositide 3-kinase family in immune cells.* Annual review of immunology, 2013. **31**: p. 675-704.
44. Stephens, L.R., K.T. Hughes, and R.F. Irvine, *Pathway of phosphatidylinositol(3,4,5)-trisphosphate synthesis in activated neutrophils.* Nature, 1991. **351**(6321): p. 33-9.
45. Yu, J., et al., *Regulation of the p85/p110 phosphatidylinositol 3'-kinase: stabilization and inhibition of the p110alpha catalytic subunit by the p85 regulatory subunit.* Mol Cell Biol, 1998. **18**(3): p. 1379-87.
46. Zhang, X., et al., *Structure of lipid kinase p110beta/p85beta elucidates an unusual SH2-domain-mediated inhibitory mechanism.* Mol Cell, 2011. **41**(5): p. 567-78.
47. Burke, J.E., et al., *Dynamics of the phosphoinositide 3-kinase p110delta interaction with p85alpha and membranes reveals aspects of regulation distinct from p110alpha.* Structure, 2011. **19**(8): p. 1127-37.
48. Jimenez, C., et al., *The p85 regulatory subunit controls sequential activation of phosphoinositide 3-kinase by Tyr kinases and Ras.* J Biol Chem, 2002. **277**(44): p. 41556-62.
49. James, S.R., et al., *Specific binding of the Akt-1 protein kinase to phosphatidylinositol 3,4,5-trisphosphate without subsequent activation.* Biochemical Journal, 1996. **315**(Pt 3): p. 709-713.
50. Burgering, B.M. and P.J. Coffer, *Protein kinase B (c-Akt) in phosphatidylinositol-3-OH kinase signal transduction.* Nature, 1995. **376**(6541): p. 599-602.
51. Vanhaesebroeck, B., L. Stephens, and P. Hawkins, *PI3K signalling: the path to discovery and understanding.* Nat Rev Mol Cell Biol, 2012. **13**(3): p. 195-203.
52. Sundaresan, N.R., et al., *The deacetylase SIRT1 promotes membrane localization and activation of Akt and PDK1 during tumorigenesis and cardiac hypertrophy.* Sci Signal, 2011. **4**(182): p. ra46.
53. Alessi, D.R., et al., *Characterization of a 3-phosphoinositide-dependent protein kinase which phosphorylates and activates protein kinase Balpha.* Curr Biol, 1997. **7**(4): p. 261-9.
54. Sarbassov, D.D., et al., *Phosphorylation and regulation of Akt/PKB by the rictor-mTOR complex.* Science, 2005. **307**(5712): p. 1098-101.
55. Maehama, T. and J.E. Dixon, *The tumor suppressor, PTEN/MMAC1, dephosphorylates the lipid second messenger, phosphatidylinositol 3,4,5-trisphosphate.* J Biol Chem, 1998. **273**(22): p. 13375-8.
56. Damen, J.E., et al., *The 145-kDa protein induced to associate with Shc by multiple cytokines is an inositol tetraphosphate and phosphatidylinositol 3,4,5-triphosphate 5-phosphatase.* Proc Natl Acad Sci U S A, 1996. **93**(4): p. 1689-93.
57. Pesesse, X., et al., *Identification of a second SH2-domain-containing protein closely related to the phosphatidylinositol polyphosphate 5-phosphatase SHIP.* Biochem Biophys Res Commun, 1997. **239**(3): p. 697-700.
58. Jean, S. and A.A. Kiger, *Classes of phosphoinositide 3-kinases at a glance.* Journal of Cell Science, 2014. **127**(5): p. 923.
59. Vanhaesebroeck, B., et al., *P110delta, a novel phosphoinositide 3-kinase in leukocytes.* Proc Natl Acad Sci U S A, 1997. **94**(9): p. 4330-5.
60. Pacold, M.E., et al., *Crystal structure and functional analysis of Ras binding to its effector phosphoinositide 3-kinase gamma.* Cell, 2000. **103**(6): p. 931-43.

61. Gupta, S., et al., *Binding of ras to phosphoinositide 3-kinase p110alpha is required for ras-driven tumorigenesis in mice.* Cell, 2007. **129**(5): p. 957-68.
62. Guillermet-Guibert, J., et al., *The p110beta isoform of phosphoinositide 3-kinase signals downstream of G protein-coupled receptors and is functionally redundant with p110gamma.* Proc Natl Acad Sci U S A, 2008. **105**(24): p. 8292-7.
63. Bi, L., et al., *Early embryonic lethality in mice deficient in the p110beta catalytic subunit of PI 3-kinase.* Mamm Genome, 2002. **13**(3): p. 169-72.
64. Bi, L., et al., *Proliferative defect and embryonic lethality in mice homozygous for a deletion in the p110alpha subunit of phosphoinositide 3-kinase.* J Biol Chem, 1999. **274**(16): p. 10963-8.
65. Foukas, L.C., et al., *Critical role for the p110alpha phosphoinositide-3-OH kinase in growth and metabolic regulation.* Nature, 2006. **441**(7091): p. 366-70.
66. Ciraolo, E., et al., *Phosphoinositide 3-kinase p110beta activity: key role in metabolism and mammary gland cancer but not development.* Sci Signal, 2008. **1**(36): p. ra3.
67. Sopasakis, V.R., et al., *Specific roles of the p110alpha isoform of phosphatidylinsositol 3-kinase in hepatic insulin signaling and metabolic regulation.* Cell Metab, 2010. **11**(3): p. 220-30.
68. Jia, S., et al., *Kinase-dependent and -independent functions of the p110β phosphoinositide-3-kinase in cell growth, metabolic regulation and oncogenic transformation.* Nature, 2008. **454**(7205): p. 776-779.
69. Graupera, M., et al., *Angiogenesis selectively requires the p110alpha isoform of PI3K to control endothelial cell migration.* Nature, 2008. **453**(7195): p. 662-6.
70. Kumar, A., et al., *Nuclear but Not Cytosolic Phosphoinositide 3-Kinase Beta Has an Essential Function in Cell Survival.* Molecular and Cellular Biology, 2011. **31**(10): p. 2122-2133.
71. Davies, M.A., *Regulation, role, and targeting of Akt in cancer.* J Clin Oncol, 2011. **29**(35): p. 4715-7.
72. Rommel, C., M. Camps, and H. Ji, *PI3K delta and PI3K gamma: partners in crime in inflammation in rheumatoid arthritis and beyond?* Nat Rev Immunol, 2007. **7**(3): p. 191-201.
73. Hamann, B.L. and R.D. Blind, *Nuclear phosphoinositide regulation of chromatin.* J Cell Physiol, 2018. **233**(1): p. 107-123.
74. Shah, Z.H., et al., *Nuclear phosphoinositides and their impact on nuclear functions.* FEBS J, 2013. **280**(24): p. 6295-310.
75. Smith, C.D. and W.W. Wells, *Phosphorylation of rat liver nuclear envelopes. II. Characterization of in vitro lipid phosphorylation.* J Biol Chem, 1983. **258**(15): p. 9368-73.
76. Cocco, L., et al., *Synthesis of polyphosphoinositides in nuclei of Friend cells. Evidence for polyphosphoinositide metabolism inside the nucleus which changes with cell differentiation.* Biochem J, 1987. **248**(3): p. 765-70.
77. Divecha, N., H. Banfic, and R.F. Irvine, *The polyphosphoinositide cycle exists in the nuclei of Swiss 3T3 cells under the control of a receptor (for IGF-I) in the plasma membrane, and stimulation of the cycle increases nuclear diacylglycerol and apparently induces translocation of protein kinase C to the nucleus.* Embo J, 1991. **10**(11): p. 3207-14.
78. Cocco, L., et al., *Synthesis of polyphosphoinositides in nuclei of Friend cells. Evidence for polyphosphoinositide metabolism inside the nucleus which changes with cell differentiation.* The Biochemical journal, 1987. **248**(3): p. 765-70.

79. Cocco, L., et al., *Rapid changes in phospholipid metabolism in the nuclei of Swiss 3T3 cells induced by treatment of the cells with insulin-like growth factor I.* Biochem Biophys Res Commun, 1988. **154**(3): p. 1266-72.
80. Martelli, A.M., et al., *Mitogen-stimulated events in nuclei of Swiss 3T3 cells. Evidence for a direct link between changes of inositol lipids, protein kinase C requirement and the onset of DNA synthesis.* FEBS Lett, 1991. **283**(2): p. 243-6.
81. Blind, R.D., *Disentangling biological signaling networks by dynamic coupling of signaling lipids to modifying enzymes.* Adv Biol Regul, 2014. **54**: p. 25-38.
82. Blind, R.D., M. Suzawa, and H.A. Ingraham, *Direct modification and regulation of a nuclear receptor-PIP(2) complex by the nuclear inositol-lipid kinase IPMK.* Science Signaling, 2012. **5**(229): p. ra44-ra44.
83. Lete, Marta G., et al., *Histones and DNA Compete for Binding Polyphosphoinositides in Bilayers.* Biophysical Journal, 2014. **106**(5): p. 1092-1100.
84. Yu, H., et al., *Phosphatidylinositol 4,5-bisphosphate reverses the inhibition of RNA transcription caused by histone H1.* Eur J Biochem, 1998. **251**(1-2): p. 281-7.
85. Barlow, C.A., R.S. Laishram, and R.A. Anderson, *Nuclear Phosphoinositides: A Signaling Enigma Wrapped in a Compartmental Conundrum.* Trends in cell biology, 2010. **20**(1): p. 25.
86. Lindsay, Y., et al., *Localization of agonist-sensitive PtdIns(3,4,5)P3 reveals a nuclear pool that is insensitive to PTEN expression.* J Cell Sci, 2006. **119**(Pt 24): p. 5160-8.
87. Kwon, I.S., et al., *PI(3,4,5)P3 regulates the interaction between Akt and B23 in the nucleus.* BMB Rep, 2010. **43**(2): p. 127-32.
88. Ahn, J.Y., et al., *Nucleophosmin/B23, a nuclear PI(3,4,5)P(3) receptor, mediates the antiapoptotic actions of NGF by inhibiting CAD.* Mol Cell, 2005. **18**(4): p. 435-45.
89. Wickramasinghe, V.O., et al., *Human inositol polyphosphate multikinase regulates transcript-selective nuclear mRNA export to preserve genome integrity.* Mol Cell, 2013. **51**(6): p. 737-50.
90. Sablin, E.P., et al., *Structure of Liver Receptor Homolog-1 (NR5A2) with PIP3 hormone bound in the ligand binding pocket.* J Struct Biol, 2015. **192**(3): p. 342-8.
91. Tanaka, K., et al., *A target of phosphatidylinositol 3,4,5-trisphosphate with a zinc finger motif similar to that of the ADP-ribosylation-factor GTPase-activating protein and two pleckstrin homology domains.* Eur J Biochem, 1997. **245**(2): p. 512-9.
92. Hu, Y., Z. Liu, and K. Ye, *Phosphoinositol lipids bind to phosphatidylinositol 3 (PI3)-kinase enhancer GTPase and mediate its stimulatory effect on PI3-kinase and Akt signalings.* Proceedings of the National Academy of Sciences of the United States of America, 2005. **102**(46): p. 16853-16858.
93. Tanaka, K., et al., *Evidence that a phosphatidylinositol 3,4,5-trisphosphate-binding protein can function in nucleus.* J Biol Chem, 1999. **274**(7): p. 3919-22.
94. Krylova, I.N., et al., *Structural analyses reveal phosphatidyl inositols as ligands for the NR5 orphan receptors SF-1 and LRH-1.* Cell, 2005. **120**(3): p. 343-55.
95. Zhao, K., et al., *Rapid and phosphoinositol-dependent binding of the SWI/SNF-like BAF complex to chromatin after T lymphocyte receptor signaling.* Cell, 1998. **95**(5): p. 625-36.
96. Osborne, S.L., et al., *Nuclear PtdIns(4,5)P2 assembles in a mitotically regulated particle involved in pre-mRNA splicing.* J Cell Sci, 2001. **114**(Pt 13): p. 2501-11.
97. Mellman, D.L., et al., *A PtdIns4,5P2-regulated nuclear poly(A) polymerase controls expression of select mRNAs.* Nature, 2008. **451**(7181): p. 1013-7.

98. Rando, O.J., et al., *Phosphatidylinositol-dependent actin filament binding by the SWI/SNF-like BAF chromatin remodeling complex.* Proc Natl Acad Sci U S A, 2002. **99**(5): p. 2824-9.
99. Toska, E., et al., *Repression of transcription by WT1-BASP1 requires the myristoylation of BASP1 and the PIP2-dependent recruitment of histone deacetylase.* Cell Rep, 2012. **2**(3): p. 462-9.
100. Mortier, E., et al., *Nuclear speckles and nucleoli targeting by PIP(2)–PDZ domain interactions.* The EMBO Journal, 2005. **24**(14): p. 2556-2565.
101. Kaadige, M.R. and D.E. Ayer, *The polybasic region that follows the plant homeodomain zinc finger 1 of Pf1 is necessary and sufficient for specific phosphoinositide binding.* J Biol Chem, 2006. **281**(39): p. 28831-6.
102. Viiri, K.M., et al., *DNA-binding and -bending activities of SAP30L and SAP30 are mediated by a zinc-dependent module and monophosphoinositides.* Mol Cell Biol, 2009. **29**(2): p. 342-56.
103. Gozani, O., et al., *The PHD finger of the chromatin-associated protein ING2 functions as a nuclear phosphoinositide receptor.* Cell, 2003. **114**(1): p. 99-111.
104. Gelato, K.A., et al., *Accessibility of different histone H3-binding domains of UHRF1 is allosterically regulated by phosphatidylinositol 5-phosphate.* Mol Cell, 2014. **54**(6): p. 905-19.
105. Stijf-Bultsma, Y., et al., *The basal transcription complex component TAF3 transduces changes in nuclear phosphoinositides into transcriptional output.* Mol Cell, 2015. **58**(3): p. 453-67.
106. Bua, D.J., et al., *Nuclear phosphatidylinositol-5-phosphate regulates ING2 stability at discrete chromatin targets in response to DNA damage.* Scientific Reports, 2013. **3**: p. 2137.
107. Davis, W.J., P.Z. Lehmann, and W. Li, *Nuclear PI3K signaling in cell growth and tumorigenesis.* Frontiers in Cell and Developmental Biology, 2015. **3**: p. 24.
108. Martelli, A.M., et al., *The emerging multiple roles of nuclear Akt.* Biochim Biophys Acta, 2012. **1823**(12): p. 2168-78.
109. Planchon, S.M., K.A. Waite, and C. Eng, *The nuclear affairs of PTEN.* J Cell Sci, 2008. **121**(Pt 3): p. 249-53.
110. Resnick, A.C., et al., *Inositol polyphosphate multikinase is a nuclear PI3-kinase with transcriptional regulatory activity.* Proc Natl Acad Sci U S A, 2005. **102**(36): p. 12783-8.
111. Kumar, A., O. Fernandez-Capetillo, and A.C. Carrera, *Nuclear phosphoinositide 3-kinase beta controls double-strand break DNA repair.* Proc Natl Acad Sci U S A, 2010. **107**(16): p. 7491-6.
112. Marques, M., et al., *Phosphoinositide 3-kinases p110alpha and p110beta regulate cell cycle entry, exhibiting distinct activation kinetics in G1 phase.* Mol Cell Biol, 2008. **28**(8): p. 2803-14.
113. Marques, M., et al., *Specific function of phosphoinositide 3-kinase beta in the control of DNA replication.* Proc Natl Acad Sci U S A, 2009. **106**(18): p. 7525-30.
114. Didichenko, S.A. and M. Thelen, *Phosphatidylinositol 3-kinase c2alpha contains a nuclear localization sequence and associates with nuclear speckles.* J Biol Chem, 2001. **276**(51): p. 48135-42.
115. Spector, D.L. and A.I. Lamond, *Nuclear Speckles.* Cold Spring Harbor Perspectives in Biology, 2011. **3**(2): p. a000646.
116. Meier, R., et al., *Mitogenic activation, phosphorylation, and nuclear translocation of protein kinase Bbeta.* J Biol Chem, 1997. **272**(48): p. 30491-7.

117. Wang, R. and M.G. Brattain, *AKT can be activated in the nucleus.* Cell Signal, 2006. **18**(10): p. 1722-31.
118. Deleris, P., et al., *SHIP-2 and PTEN are expressed and active in vascular smooth muscle cell nuclei, but only SHIP-2 is associated with nuclear speckles.* J Biol Chem, 2003. **278**(40): p. 38884-91.
119. Shen, W.H., et al., *Essential role for nuclear PTEN in maintaining chromosomal integrity.* Cell, 2007. **128**(1): p. 157-70.
120. Song, M.S., et al., *Nuclear PTEN regulates the APC-CDH1 tumor-suppressive complex in a phosphatase-independent manner.* Cell, 2011. **144**(2): p. 187-99.
121. Liu, J.-L., et al., *Nuclear PTEN-Mediated Growth Suppression Is Independent of Akt Down-Regulation.* Molecular and Cellular Biology, 2005. **25**(14): p. 6211-6224.
122. Nemeth, A. and G. Langst, *Genome organization in and around the nucleolus.* Trends Genet, 2011. **27**(4): p. 149-56.
123. Zhao, R., M.S. Bodnar, and D.L. Spector, *Nuclear neighborhoods and gene expression.* Curr Opin Genet Dev, 2009. **19**(2): p. 172-9.
124. Nerurkar, P., et al., *Eukaryotic Ribosome Assembly and Nuclear Export.* Int Rev Cell Mol Biol, 2015. **319**: p. 107-40.
125. Caburet, S., et al., *Human ribosomal RNA gene arrays display a broad range of palindromic structures.* Genome Res, 2005. **15**(8): p. 1079-85.
126. Sylvester, J.E., et al., *The human ribosomal RNA genes: structure and organization of the complete repeating unit.* Hum Genet, 1986. **73**(3): p. 193-8.
127. Ritossa, F.M. and S. Spiegelman, *Localization of DNA Complementary to Ribosomal RNA in the Nucleolus Organizer Region of Drosophila melanogaster.* Proceedings of the National Academy of Sciences of the United States of America, 1965. **53**(4): p. 737-745.
128. McStay, B., *Nucleolar organizer regions: genomic 'dark matter' requiring illumination.* Genes Dev, 2016. **30**(14): p. 1598-610.
129. Grummt, I., *Wisely chosen paths--regulation of rRNA synthesis: delivered on 30 June 2010 at the 35th FEBS Congress in Gothenburg, Sweden.* Febs j, 2010. **277**(22): p. 4626-39.
130. Lempiainen, H. and D. Shore, *Growth control and ribosome biogenesis.* Curr Opin Cell Biol, 2009. **21**(6): p. 855-63.
131. Henras, A.K., et al., *An overview of pre-ribosomal RNA processing in eukaryotes.* Wiley Interdiscip Rev RNA, 2015. **6**(2): p. 225-42.
132. McStay, B. and I. Grummt, *The epigenetics of rRNA genes: from molecular to chromosome biology.* Annu Rev Cell Dev Biol, 2008. **24**: p. 131-57.
133. Scheer, U. and R. Hock, *Structure and function of the nucleolus.* Curr Opin Cell Biol, 1999. **11**(3): p. 385-90.
134. Leung, A. and A. I Lamond, *The Dynamics of the Nucleolus*. Vol. 13. 2003. 39-54.
135. Shaw, P.J. and E.G. Jordan, *The nucleolus.* Annu Rev Cell Dev Biol, 1995. **11**: p. 93-121.
136. Guetg, C. and R. Santoro, *Formation of nuclear heterochromatin: The nucleolar point of view.* Epigenetics, 2012. **7**(8): p. 811-814.
137. Németh, A., et al., *Initial Genomics of the Human Nucleolus.* PLoS Genetics, 2010. **6**(3): p. e1000889.
138. Ghetti, A., et al., *hnRNP I, the polypyrimidine tract-binding protein: distinct nuclear localization and association with hnRNAs.* Nucleic Acids Res, 1992. **20**(14): p. 3671-8.
139. Pollock, C. and S. Huang, *The Perinucleolar Compartment.* Journal of cellular biochemistry, 2009. **107**(2): p. 189-193.

140. Nguyen le, X.T. and B.S. Mitchell, *Akt activation enhances ribosomal RNA synthesis through casein kinase II and TIF-IA.* Proc Natl Acad Sci U S A, 2013. **110**(51): p. 20681-6.
141. Sobol, M., et al., *UBF complexes with phosphatidylinositol 4,5-bisphosphate in nucleolar organizer regions regardless of ongoing RNA polymerase I activity.* Nucleus, 2013. **4**(6): p. 478-86.
142. Drakas, R., X. Tu, and R. Baserga, *Control of cell size through phosphorylation of upstream binding factor 1 by nuclear phosphatidylinositol 3-kinase.* Proc Natl Acad Sci U S A, 2004. **101**(25): p. 9272-6.
143. Vinayagam, A., et al., *An Integrative Analysis of the InR/PI3K/Akt Network Identifies the Dynamic Response to Insulin Signaling.* Cell Rep, 2016. **16**(11): p. 3062-74.
144. Li, P., et al., *Identification of nucleolus-localized PTEN and its function in regulating ribosome biogenesis.* Mol Biol Rep, 2014. **41**(10): p. 6383-90.
145. Ehm, P., et al., *The tumor suppressor SHIP1 colocalizes in nucleolar cavities with p53 and components of PML nuclear bodies.* Nucleus, 2015. **6**(2): p. 154-64.
146. Kakuk, A., et al., *Nucleolar localization of phosphatidylinositol 4-kinase PI4K230 in various mammalian cells.* Cytometry A, 2006. **69**(12): p. 1174-83.
147. Kakuk, A., et al., *Nuclear and nucleolar localization signals and their targeting function in phosphatidylinositol 4-kinase PI4K230.* Exp Cell Res, 2008. **314**(13): p. 2376-88.
148. Chakrabarti, R., et al., *Phosphatidylinositol-4-phosphate 5-Kinase 1alpha Modulates Ribosomal RNA Gene Silencing through Its Interaction with Histone H3 Lysine 9 Trimethylation and Heterochromatin Protein HP1-alpha.* J Biol Chem, 2015. **290**(34): p. 20893-903.
149. Lucas, C.L., et al., *PI3Kdelta and primary immunodeficiencies.* Nat Rev Immunol, 2016. **16**(11): p. 702-714.
150. Okkenhaug, K., M. Graupera, and B. Vanhaesebroeck, *Targeting PI3K in Cancer: Impact on Tumor Cells, Their Protective Stroma, Angiogenesis, and Immunotherapy.* Cancer Discov, 2016. **6**(10): p. 1090-1105.
151. Cully, M., et al., *Beyond PTEN mutations: the PI3K pathway as an integrator of multiple inputs during tumorigenesis.* Nat Rev Cancer, 2006. **6**(3): p. 184-92.
152. Rozengurt, E., H.P. Soares, and J. Sinnet-Smith, *Suppression of feedback loops mediated by PI3K/mTOR induces multiple overactivation of compensatory pathways: an unintended consequence leading to drug resistance.* Mol Cancer Ther, 2014. **13**(11): p. 2477-88.
153. Li, J., et al., *PTEN, a putative protein tyrosine phosphatase gene mutated in human brain, breast, and prostate cancer.* Science, 1997. **275**(5308): p. 1943-7.
154. Angulo, I., et al., *Phosphoinositide 3-kinase delta gene mutation predisposes to respiratory infection and airway damage.* Science, 2013. **342**(6160): p. 866-71.
155. Samuels, Y., et al., *High frequency of mutations of the PIK3CA gene in human cancers.* Science, 2004. **304**(5670): p. 554.
156. Jia, S., et al., *Essential roles of PI(3)K-p110beta in cell growth, metabolism and tumorigenesis.* Nature, 2008. **454**(7205): p. 776-9.
157. Wee, S., et al., *PTEN-deficient cancers depend on PIK3CB.* Proceedings of the National Academy of Sciences of the United States of America, 2008. **105**(35): p. 13057-13062.
158. Ni, J., et al., *Functional characterization of an isoform-selective inhibitor of PI3K-p110β as a potential anti-cancer agent.* Cancer discovery, 2012. **2**(5): p. 425-433.

159. Kang, S., et al., *Oncogenic transformation induced by the p110β, -γ, and -δ isoforms of class I phosphoinositide 3-kinase.* Proceedings of the National Academy of Sciences of the United States of America, 2006. **103**(5): p. 1289-1294.
160. Zoncu, R., A. Efeyan, and D.M. Sabatini, *mTOR: from growth signal integration to cancer, diabetes and ageing.* Nat Rev Mol Cell Biol, 2011. **12**(1): p. 21-35.
161. Carpten, J.D., et al., *A transforming mutation in the pleckstrin homology domain of AKT1 in cancer.* Nature, 2007. **448**(7152): p. 439-44.
162. Grabiner, B.C., et al., *A diverse array of cancer-associated MTOR mutations are hyperactivating and can predict rapamycin sensitivity.* Cancer Discov, 2014. **4**(5): p. 554-63.
163. Lim, M.A., et al., *Nuclear translocation of 3'-phosphoinositide-dependent protein kinase 1 (PDK-1): a potential regulatory mechanism for PDK-1 function.* Proc Natl Acad Sci U S A, 2003. **100**(24): p. 14006-11.
164. Kikani, C.K., et al., *Proliferative and antiapoptotic signaling stimulated by nuclear-localized PDK1 results in oncogenesis.* Sci Signal, 2012. **5**(249): p. ra80.
165. Ferlay, J., et al., *Cancer incidence and mortality worldwide: sources, methods and major patterns in GLOBOCAN 2012.* Int J Cancer, 2015. **136**(5): p. E359-86.
166. Siegel, R.L., K.D. Miller, and A. Jemal, *Cancer statistics, 2016.* CA Cancer J Clin, 2016. **66**(1): p. 7-30.
167. Wartko, P., et al., *Recent changes in endometrial cancer trends among menopausal-age U.S. women.* Cancer Epidemiol, 2013. **37**(4): p. 374-7.
168. Evans-Metcalf, E.R., et al., *Profile of women 45 years of age and younger with endometrial cancer.* Obstet Gynecol, 1998. **91**(3): p. 349-54.
169. Garg, K. and R.A. Soslow, *Endometrial carcinoma in women aged 40 years and younger.* Arch Pathol Lab Med, 2014. **138**(3): p. 335-42.
170. Morice, P., et al., *Endometrial cancer.* Lancet, 2016. **387**(10023): p. 1094-1108.
171. Bokhman, J.V., *Two pathogenetic types of endometrial carcinoma.* Gynecol Oncol, 1983. **15**(1): p. 10-7.
172. Murali, R., R.A. Soslow, and B. Weigelt, *Classification of endometrial carcinoma: more than two types.* Lancet Oncol, 2014. **15**(7): p. e268-78.
173. Levine, R.L., et al., *PTEN mutations and microsatellite instability in complex atypical hyperplasia, a precursor lesion to uterine endometrioid carcinoma.* Cancer Res, 1998. **58**(15): p. 3254-8.
174. Kandoth, C., et al., *Integrated genomic characterization of endometrial carcinoma.* Nature, 2013. **497**(7447): p. 67-73.
175. Cheung, L.W., et al., *High frequency of PIK3R1 and PIK3R2 mutations in endometrial cancer elucidates a novel mechanism for regulation of PTEN protein stability.* Cancer Discov, 2011. **1**(2): p. 170-85.
176. Miyake, T., et al., *PIK3CA gene mutations and amplifications in uterine cancers, identified by methods that avoid confounding by PIK3CA pseudogene sequences.* Cancer Lett, 2008. **261**(1): p. 120-6.
177. Stelloo, E., et al., *Improved Risk Assessment by Integrating Molecular and Clinicopathological Factors in Early-stage Endometrial Cancer-Combined Analysis of the PORTEC Cohorts.* Clin Cancer Res, 2016. **22**(16): p. 4215-24.
178. Mutter, G.L., et al., *Altered PTEN expression as a diagnostic marker for the earliest endometrial precancers.* J Natl Cancer Inst, 2000. **92**(11): p. 924-30.
179. Hayes, M.P., et al., *PIK3CA and PTEN mutations in uterine endometrioid carcinoma and complex atypical hyperplasia.* Clin Cancer Res, 2006. **12**(20 Pt 1): p. 5932-5.

180. Salvesen, H.B., et al., *Integrated genomic profiling of endometrial carcinoma associates aggressive tumors with indicators of PI3 kinase activation.* Proc Natl Acad Sci U S A, 2009. **106**(12): p. 4834-9.
181. Pazarentzos, E., et al., *Oncogenic activation of the PI3-kinase p110beta isoform via the tumor-derived PIK3Cbeta(D1067V) kinase domain mutation.* Oncogene, 2016. **35**(9): p. 1198-205.
182. An, H.J., et al., *Targeted RNA interference of phosphatidylinositol 3-kinase p110-beta induces apoptosis and proliferation arrest in endometrial carcinoma cells.* J Pathol, 2007. **212**(2): p. 161-9.
183. Karlsson, T., et al., *Endometrial cancer cells exhibit high expression of p110β and its selective inhibition induces variable responses on PI3K signaling, cell survival and proliferation.* Oncotarget, 2017. **8**(3): p. 3881-3894.
184. Makker, V., et al., *Phase II trial of GDC-0980 (dual PI3K/mTOR inhibitor) in patients with advanced endometrial carcinoma: Final study results.* Journal of Clinical Oncology, 2014. **32**(15_suppl): p. 5513-5513.
185. Konstantinopoulos, P., et al., *Phase II, single stage, cohort expansion study of MK-2206 in recurrent endometrial serous cancer.* Journal of Clinical Oncology, 2014. **32**(15_suppl): p. 5515-5515.
186. Matulonis, U., et al., *Phase II study of the PI3K inhibitor pilaralisib (SAR245408; XL147) in patients with advanced or recurrent endometrial carcinoma.* Gynecol Oncol, 2015. **136**(2): p. 246-53.
187. Girouard, J., et al., *Involvement of Akt isoforms in chemoresistance of endometrial carcinoma cells.* Gynecol Oncol, 2013. **128**(2): p. 335-43.
188. Bradford, L.S., et al., *Assessing the efficacy of targeting the phosphatidylinositol 3-kinase/AKT/mTOR signaling pathway in endometrial cancer.* Gynecol Oncol, 2014. **133**(2): p. 346-52.
189. Mateo, J., et al., *A first-time-in-human study of GSK2636771, a phosphoinositide 3 kinase beta-selective inhibitor, in patients with advanced solid tumors.* Clinical Cancer Research, 2017.
190. Ali, A.T., et al., *Adipocyte and adipogenesis.* Eur J Cell Biol, 2013. **92**(6-7): p. 229-36.
191. Rutkowski, J.M., J.H. Stern, and P.E. Scherer, *The cell biology of fat expansion.* The Journal of Cell Biology, 2015. **208**(5): p. 501-512.
192. Wu, J., et al., *Beige adipocytes are a distinct type of thermogenic fat cell in mouse and human.* Cell, 2012. **150**(2): p. 366-76.
193. Lefterova, M.I. and M.A. Lazar, *New developments in adipogenesis.* Trends Endocrinol Metab, 2009. **20**(3): p. 107-14.
194. Tang, Q.Q. and M.D. Lane, *Adipogenesis: from stem cell to adipocyte.* Annu Rev Biochem, 2012. **81**: p. 715-36.
195. Green, H. and O. Kehinde, *Sublines of mouse 3T3 cells that accumulate lipid.* Cell, 1974. **1**(3): p. 113-116.
196. Poulos, S.P., M.V. Dodson, and G.J. Hausman, *Cell line models for differentiation: preadipocytes and adipocytes.* Exp Biol Med (Maywood), 2010. **235**(10): p. 1185-93.
197. Zebisch, K., et al., *Protocol for effective differentiation of 3T3-L1 cells to adipocytes.* Anal Biochem, 2012. **425**(1): p. 88-90.
198. Czech, M.P., et al., *Insulin signalling mechanisms for triacylglycerol storage.* Diabetologia, 2013. **56**(5): p. 949-64.
199. Cuatrecasas, P., *Insulin--receptor interactions in adipose tissue cells: direct measurement and properties.* Proc Natl Acad Sci U S A, 1971. **68**(6): p. 1264-8.

200. Roth, R.A. and D.J. Cassell, *Insulin receptor: evidence that it is a protein kinase.* Science, 1983. **219**(4582): p. 299-301.
201. Kwok, Y.C., et al., *Kinetic properties of the insulin receptor tyrosine protein kinase: activation through an insulin-stimulated tyrosine-specific, intramolecular autophosphorylation.* Arch Biochem Biophys, 1986. **244**(1): p. 102-13.
202. Cushman, S.W. and L.J. Wardzala, *Potential mechanism of insulin action on glucose transport in the isolated rat adipose cell. Apparent translocation of intracellular transport systems to the plasma membrane.* J Biol Chem, 1980. **255**(10): p. 4758-62.
203. Ishiki, M., et al., *Insulin regulates the membrane arrival, fusion, and C-terminal unmasking of glucose transporter-4 via distinct phosphoinositides.* J Biol Chem, 2005. **280**(31): p. 28792-802.
204. Okada, T., et al., *Essential role of phosphatidylinositol 3-kinase in insulin-induced glucose transport and antilipolysis in rat adipocytes. Studies with a selective inhibitor wortmannin.* J Biol Chem, 1994. **269**(5): p. 3568-73.
205. Clarke, J.F., et al., *Inhibition of the translocation of GLUT1 and GLUT4 in 3T3-L1 cells by the phosphatidylinositol 3-kinase inhibitor, wortmannin.* Biochem J, 1994. **300 (Pt 3)**: p. 631-5.
206. Kohn, A.D., et al., *Expression of a constitutively active Akt Ser/Thr kinase in 3T3-L1 adipocytes stimulates glucose uptake and glucose transporter 4 translocation.* J Biol Chem, 1996. **271**(49): p. 31372-8.
207. Hill, M.M., et al., *A role for protein kinase Bbeta/Akt2 in insulin-stimulated GLUT4 translocation in adipocytes.* Mol Cell Biol, 1999. **19**(11): p. 7771-81.
208. Siersbaek, R., R. Nielsen, and S. Mandrup, *Transcriptional networks and chromatin remodeling controlling adipogenesis.* Trends Endocrinol Metab, 2012. **23**(2): p. 56-64.
209. Brun, R.P., et al., *Adipocyte differentiation: a transcriptional regulatory cascade.* Curr Opin Cell Biol, 1996. **8**(6): p. 826-32.
210. Myers, M.G., Jr., et al., *IRS-1 activates phosphatidylinositol 3'-kinase by associating with src homology 2 domains of p85.* Proc Natl Acad Sci U S A, 1992. **89**(21): p. 10350-4.
211. Kimura, K., et al., *Neurite outgrowth of PC12 cells is suppressed by wortmannin, a specific inhibitor of phosphatidylinositol 3-kinase.* J Biol Chem, 1994. **269**(29): p. 18961-7.
212. Tomiyama, K., et al., *Wortmannin, a specific phosphatidylinositol 3-kinase inhibitor, inhibits adipocytic differentiation of 3T3-L1 cells.* Biochem Biophys Res Commun, 1995. **212**(1): p. 263-9.
213. Asano, T., et al., *p110 beta is up-regulated during differentiation of 3T3-L1 cells and contributes to the highly insulin-responsive glucose transport activity.* Journal of Biological Chemistry, 2000. **275**(23): p. 17671-17676.
214. Kim, J.E., P.R. Shepherd, and C. Chaussade, *Investigating the role of class-IA PI 3-kinase isoforms in adipocyte differentiation.* Biochem Biophys Res Commun, 2009. **379**(4): p. 830-4.
215. Jacobsen, R.G., et al., *DNA Topoisomerase IIalpha contributes to the early steps of adipogenesis in 3T3-L1 cells.* Cell Signal, 2016. **28**(10): p. 1593-603.
216. Knight, Z.A., et al., *A pharmacological map of the PI3-K family defines a role for p110alpha in insulin signaling.* Cell, 2006. **125**(4): p. 733-47.
217. Chaussade, C., et al., *Evidence for functional redundancy of class IA PI3K isoforms in insulin signalling.* The Biochemical Journal, 2007. **404**(Pt 3): p. 449-458.
218. Brown, R.A., et al., *Insulin activates the alpha isoform of class II phosphoinositide 3-kinase.* J Biol Chem, 1999. **274**(21): p. 14529-32.

219. Engelman, J.A., J. Luo, and L.C. Cantley, *The evolution of phosphatidylinositol 3-kinases as regulators of growth and metabolism.* Nat Rev Genet, 2006. **7**(8): p. 606-19.
220. Meder, V.S., et al., *PARP-1 and PARP-2 interact with nucleophosmin/B23 and accumulate in transcriptionally active nucleoli.* J Cell Sci, 2005. **118**(Pt 1): p. 211-22.
221. Boamah, E.K., et al., *Poly(ADP-Ribose) polymerase 1 (PARP-1) regulates ribosomal biogenesis in Drosophila nucleoli.* PLoS Genet, 2012. **8**(1): p. e1002442.
222. Katso, R., et al., *Cellular function of phosphoinositide 3-kinases: implications for development, homeostasis, and cancer.* Annu Rev Cell Dev Biol, 2001. **17**: p. 615-75.
223. Beloribi-Djefaflia, S., S. Vasseur, and F. Guillaumond, *Lipid metabolic reprogramming in cancer cells.* Oncogenesis, 2016. **5**(1): p. e189.
224. Menendez, J.A., *Fine-tuning the lipogenic/lipolytic balance to optimize the metabolic requirements of cancer cell growth: molecular mechanisms and therapeutic perspectives.* Biochim Biophys Acta, 2010. **1801**(3): p. 381-91.
225. Baenke, F., et al., *Hooked on fat: the role of lipid synthesis in cancer metabolism and tumour development.* Disease Models & Mechanisms, 2013. **6**(6): p. 1353.
226. Kandel, E.S., et al., *Activation of Akt/Protein Kinase B Overcomes a G(2)/M Cell Cycle Checkpoint Induced by DNA Damage.* Molecular and Cellular Biology, 2002. **22**(22): p. 7831-7841.
227. Stambolic, V., et al., *Negative regulation of PKB/Akt-dependent cell survival by the tumor suppressor PTEN.* Cell, 1998. **95**(1): p. 29-39.
228. Sun, H., et al., *PTEN modulates cell cycle progression and cell survival by regulating phosphatidylinositol 3,4,5,-trisphosphate and Akt/protein kinase B signaling pathway.* Proc Natl Acad Sci U S A, 1999. **96**(11): p. 6199-204.
229. Liu, F., et al., *PTEN enters the nucleus by diffusion.* J Cell Biochem, 2005. **96**(2): p. 221-34.
230. Chung, J.H., M.E. Ginn-Pease, and C. Eng, *Phosphatase and tensin homologue deleted on chromosome 10 (PTEN) has nuclear localization signal-like sequences for nuclear import mediated by major vault protein.* Cancer Res, 2005. **65**(10): p. 4108-16.
231. Walker, S.M., C.P. Downes, and N.R. Leslie, *TPIP: a novel phosphoinositide 3-phosphatase.* Biochem J, 2001. **360**(Pt 2): p. 277-83.
232. Elong Edimo, W., et al., *Evidence of SHIP2 Ser132 phosphorylation, its nuclear localization and stability.* Biochem J, 2011. **439**(3): p. 391-401.
233. Belin, S., et al., *Dysregulation of ribosome biogenesis and translational capacity is associated with tumor progression of human breast cancer cells.* PLoS One, 2009. **4**(9): p. e7147.
234. Boisvert, F.M., et al., *The multifunctional nucleolus.* Nat Rev Mol Cell Biol, 2007. **8**(7): p. 574-85.
235. Hein, N., et al., *The nucleolus: an emerging target for cancer therapy.* Trends Mol Med, 2013. **19**(11): p. 643-54.
236. Koller, P.C., *THE NUCLEUS OF THE CANCER CELL. A HISTORICAL REVIEW.* Exp Cell Res, 1963. **24**: p. Suppl9:3-14.
237. Montanaro, L., D. Trere, and M. Derenzini, *Changes in ribosome biogenesis may induce cancer by down-regulating the cell tumor suppressor potential.* Biochim Biophys Acta, 2012. **1825**(1): p. 101-10.

238. Rose, H.G. and J.H. Frenster, *Composition and metabolism of lipids within repressed and active chromatin of interphase lymphocytes.* Biochim Biophys Acta, 1965. **106**(3): p. 577-91.
239. Brighenti, E., et al., *Interleukin 6 downregulates p53 expression and activity by stimulating ribosome biogenesis: a new pathway connecting inflammation to cancer.* Oncogene, 2014. **33**(35): p. 4396-406.
240. Donati, G., et al., *5S ribosomal RNA is an essential component of a nascent ribosomal precursor complex that regulates the Hdm2-p53 checkpoint.* Cell Rep, 2013. **4**(1): p. 87-98.
241. Donati, G., et al., *The balance between rRNA and ribosomal protein synthesis up- and downregulates the tumour suppressor p53 in mammalian cells.* Oncogene, 2011. **30**(29): p. 3274-88.
242. Korgaonkar, C., et al., *Nucleophosmin (B23) targets ARF to nucleoli and inhibits its function.* Mol Cell Biol, 2005. **25**(4): p. 1258-71.
243. Hamilton, G., et al., *AKT regulates NPM dependent ARF localization and p53(mut) stability in tumors.* Oncotarget, 2014. **5**(15): p. 6142-6167.
244. Derenzini, M., et al., *Key role of the achievement of an appropriate ribosomal RNA complement for G1-S phase transition in H4-II-E-C3 rat hepatoma cells.* J Cell Physiol, 2005. **202**(2): p. 483-91.
245. Ogawa, L.M. and S.J. Baserga, *Crosstalk between the nucleolus and the DNA damage response.* Mol Biosyst, 2017. **13**(3): p. 443-455.
246. Box, J.K., et al., *Nucleophosmin: from structure and function to disease development.* BMC Molecular Biology, 2016. **17**(1): p. 19.
247. Kurfurstova, D., et al., *DNA damage signalling barrier, oxidative stress and treatment-relevant DNA repair factor alterations during progression of human prostate cancer.* Mol Oncol, 2016. **10**(6): p. 879-94.
248. Oei, A.L., et al., *Enhancing synthetic lethality of PARP-inhibitor and cisplatin in BRCA-proficient tumour cells with hyperthermia.* Oncotarget, 2017. **8**(17): p. 28116-28124.
249. De Vos, M., V. Schreiber, and F. Dantzer, *The diverse roles and clinical relevance of PARPs in DNA damage repair: current state of the art.* Biochem Pharmacol, 2012. **84**(2): p. 137-46.
250. Fakan, S., et al., *Immunoelectron microscopical distribution of poly(ADP-ribose)polymerase in the mammalian cell nucleus.* Experimental Cell Research, 1988. **179**(2): p. 517-526.
251. Calkins, A.S., J.D. Iglehart, and J.B. Lazaro, *DNA damage-induced inhibition of rRNA synthesis by DNA-PK and PARP-1.* Nucleic Acids Res, 2013. **41**(15): p. 7378-86.
252. van Sluis, M. and B. McStay, *Nucleolar reorganization in response to rDNA damage.* Curr Opin Cell Biol, 2017. **46**: p. 81-86.
253. Jordan, P., et al., *In vivo evidence that TATA-binding protein/SL1 colocalizes with UBF and RNA polymerase I when rRNA synthesis is either active or inactive.* J Cell Biol, 1996. **133**(2): p. 225-34.
254. Kotova, E., M. Jarnik, and A.V. Tulin, *Poly (ADP-ribose) polymerase 1 is required for protein localization to Cajal body.* PLoS Genet, 2009. **5**(2): p. e1000387.
255. Shin, Y. and C.P. Brangwynne, *Liquid phase condensation in cell physiology and disease.* Science, 2017. **357**(6357).
256. Mao, Y.S., B. Zhang, and D.L. Spector, *Biogenesis and function of nuclear bodies.* Trends in Genetics, 2011. **27**(8): p. 295-306.

257. Shin, Y., et al., *Spatiotemporal Control of Intracellular Phase Transitions Using Light-Activated optoDroplets.* Cell. **168**(1): p. 159-171.e14.
258. Feric, M., et al., *Coexisting Liquid Phases Underlie Nucleolar Subcompartments.* Cell, 2016. **165**(7): p. 1686-1697.
259. Fajas, L., *Adipogenesis: a cross-talk between cell proliferation and cell differentiation.* Ann Med, 2003. **35**(2): p. 79-85.
260. Ali, S.A., et al., *Phenotypic transcription factors epigenetically mediate cell growth control.* Proc Natl Acad Sci U S A, 2008. **105**(18): p. 6632-7.
261. Donati, G., L. Montanaro, and M. Derenzini, *Ribosome biogenesis and control of cell proliferation: p53 is not alone.* Cancer Res, 2012. **72**(7): p. 1602-7.
262. Tajrishi, M.M., R. Tuteja, and N. Tuteja, *Nucleolin: The most abundant multifunctional phosphoprotein of nucleolus.* Communicative & Integrative Biology, 2011. **4**(3): p. 267-275.
263. Ugrinova, I., et al., *Inactivation of nucleolin leads to nucleolar disruption, cell cycle arrest and defects in centrosome duplication.* BMC Mol Biol, 2007. **8**: p. 66.

I

Nuclear upregulation of PI3K p110β correlates with increased rRNA transcription in endometrial cancer cells

Fatemeh Mazloumi Gavgani[1*], Thomas Karlsson[1*], Victoria Smith Arnesen[1], Ole Horvli[1], Pamela Pollock[4], Ingvild L Tangen[2,3], Camilla Krakstad[2,3] and Aurélia E Lewis[1§]

[1] Department of Molecular Biology, University of Bergen

[2] Centre for Cancer Biomarkers, Department of Clinical Science, University of Bergen [3] Department of Gynecology and Obstetrics, Haukeland University Hospital, Bergen, Norway.

[4] Queensland University of Technology (QUT), Brisbane, Australia.

* equal authorship

§ Corresponding author: Aurélia E. Lewis, Department of Molecular Biology, University of Bergen, PO Box 7803, N-5020 Bergen, Norway. Email: aurelia.lewis@uib.no.

Abstract

Endometrial cancer (EC) is often cured by surgery but tumours recur unpredictably in about 20% of cases and have poor response to current treatments and targeted therapeutics are not available for routine clinical use. Genes encoding for components of the phosphoinositide 3-kinase (PI3K) signalling pathway are frequently mutated in EC, including inactivating mutations of *PTEN* and activating mutations of *PIK3CA*. These genetic alterations do not however account for all tumours and other alterations in other genes of the pathway could contribute. Analysing cell lines and annotated clinical samples, we have previously found that p110β (encoded by *PIK3CB*) is highly expressed in cancer cells and that *PIK3CB* mRNA levels increase early in tumourigenesis. Selective inhibition of PI3K p110α and p110β led to different effects on cell signalling and cell function, p110α activity being correlated to cell survival in *PIK3CA* mutant cells and p110β with cell proliferation in PTEN-deficient cells. To understand the mechanisms governing the differential roles of these isoforms, we assessed their sub-cellular localisation. p110α was cytoplasmic whereas p110β was both cytoplasmic and nuclear with increased levels in both compartments in cancer cells. Immunohistochemistry of p110β in clinically annotated patient tumour sections revealed cytoplasmic staining in intact endometrial glands in low grade tumours and nuclear staining in higher grades. Consistent with this, the presence of high levels of p110β in the nuclei of EC cells, correlated with high levels of its product phosphatidylinositol 3,4,5-trisphosphate (PtdIns(3,4,5)P_3) in the nucleus. In addition, we observed that p110β and its lipid product PtdIns(3,4,5)P_3 were localised in the nucleoli of EC cell lines. PTEN-deficient EC cells with the highest amount of nuclear PtdIns(3,4,5)P_3 and p110β showed elevated nucleolar activity as assessed by the increase in the pre-rRNA transcriptional levels. Altogether these results present a nucleolar role for the PI3K pathway that may contribute to tumour progression in endometrial cancers.

Introduction

The phosphatidylinositol 3-kinase (PI3K) signalling pathway is frequently hyperactivated in cancer, often due to genetic or epigenetic alterations in several gene members of the pathway (1-3). Class I PI3Ks consist of heterodimers of catalytic subunits (p110α, β, δ or γ) and adaptor proteins (p85α and its variants, p85β or p55γ) (4) and phosphorylate the 3'-hydroxyl group of the phospholipid phosphatidylinositol 4,5-bisphosphate (PtdIns(4,5)P_2) to generate phosphatidylinositol 3,4,5-trisphosphate (PtdIns(3,4,5)P_3). PtdIns(3,4,5)P_3 binds to effector proteins including the serine/threonine kinases AKT/Protein Kinase B (PKB), 3-phosphoinositide-dependent protein kinase 1 (PDK1) and SIN1 via their phosphoinositide-binding plextrin homology (PH) domain (5-7). AKT is further activated by phosphorylation on Thr308 and Ser473 by PDK1 and mammalian target of rapamycin complex 2 (mTORC2) respectively (8). Activated AKT can act at different intracellular sites, where it phosphorylates a myriad of substrates that regulate cell survival, cell proliferation and growth as well as metabolism (9). The production of PtdIns(3,4,5)P_3 is regulated by phosphatase and tensin homolog deleted on chromosome 10 (PTEN), a lipid phosphatase which dephosphorylates PtdIns(3,4,5)P_3 back to PtdIns(4,5)P_2, thereby opposing PI3K-mediated signalling and hence limiting the potential cancer-promoting effects of class I PI3K activity (10).

p110α and p110β are ubiquitously expressed, share the same enzymatic properties and generate the same lipid product, and initiate the same signalling cascade. Despite these shared features, the two isoforms are both essential for development as individual knockout mice are embryonically lethal, hence suggesting non-redundant functions (11, 12). Moreover, their mode of activation is distinct, with p110α carrying out most of receptor tyrosine kinase (RTK)-mediated PI3K signalling and p110β being regulated by G-protein coupled receptors (GPCR) (3, 13-15) through different adaptor proteins (16). In cancer, the oncogenic properties of p110α are due to activating mutations of its gene *PIK3CA* (17). In contrast, *PIK3CB*, the gene encoding p110β, is rarely mutated in cancer, with only two reports so far describing activating mutations (18, 19). *PIK3CB* was however shown to be the key isoform mediating tumorigenesis in PTEN-deficient tumours in particular in breast, prostate and ovarian cancer cells (20-24), possibly due to its ability to promote oncogenic transformation in its wild type state (25). Furthermore, the importance of p110β in tumorigenesis was recently highlighted in a study by Juric *et al* (26). This study showed that *PIK3CA* mutant breast cancer cells which were initially sensitive to p110α specific inhibition eventually developed resistance with

acquired loss of PTEN in metastatic lesions. These cells could however revers the resistance when p110β inhibition was combined. Regarding their functions, a few studies have reported that the two isoforms can contribute differently to cell survival and proliferation, with p110α playing more of a role in cell survival and p110β in cell cycle progression and DNA replication (27-29). Another distinguishing feature about these two isoforms is their sub-cellular localisation. Although p110α and β are both found in the cytoplasm and share/compete for similar upstream receptor activation and downstream signalling cascades, p110β is also found in the nucleoplasm and in the chromatin fraction (29, 30). Moreover, we have recently reported the presence of p110β and PtdIns(3,4,5)P_3 in the nucleolus (31).

The PI3K pathway is the signalling pathway most frequently altered in endometrial cancer (EC) with more than 80% of tumours harbouring somatic alteration in at least one gene component of the pathway, including high frequency mutations in *PTEN*, *PIK3CA* and *PIK3R1* (encoding p85α) and low frequency in *Akt* and *PIK3R2* (encoding p85β) (32, 33). Loss of function of the tumour suppressor gene *PTEN*, due to loss of heterozygosity or somatic mutations is the most common event in Endometriod EC (EEC) and occurs early in 18-48% of lesions with atypical hyperplasia (34, 35). *PIK3CA*, the gene encoding the catalytic p110α subunit of class I PI3K, is frequently mutated in 10-39% of EEC but in contrast to *PTEN* has a low frequency in early lesions and a high frequency in aggressive, invasive less differentiated tumours (35, 36). In addition, mutations in *PTEN* were found to co-exist with those of *PIK3CA* or *PIK3R1*, thereby leading to enhanced activation of the PI3K pathway (36-39). *PIK3CA* gene amplification can also account for other mechanisms for PI3K pathway activation and was found to correlate with a PI3K activation profile, segregated more frequently to aggressive and invasive tumours whereas point mutations segregated to non-aggressive (40) or to lower grade tumours (36). In contrast to *PIK3CA*, mutation events are rare in *PIK3CB* with 2.2% in EC according to data from COSMIC release v80 –Feb 2017 ((41) http://cancer.sanger.ac.uk/cosmic), including a recently characterized oncogenic mutation in its catalytic domain (19). *PIK3CB* mRNA levels were found to be elevated in endometrial tumours compared to normal tissue in a few patient samples (42). In a recent study, we have shown that the p110β protein levels are elevated in EC cell lines and that mRNA levels are increased in grade 1 endometrioid endometrial lesions compared to complex hyperplasias (43). We have recently reported the presence of p110β and of its product PtdIns(3,4,5)P_3 in the nucleolus of the breast cancer cell line AU565 (31). In this study, we showed an increase in the nuclear levels of both p110β and PtdIns(3,4,5)P_3 in EC cells. We further showed that high p110β levels correlated with high rRNA transcription which suggests

the involvement of this kinase and its lipid product PtdIns(3,4,5)P_3 in increased nucleolar activity in cancer.

Results

p110β is cytoplasmic and nuclear in endometrial cancer cell lines and patient tumours

Previous studies have shown that p110α and p110β are differently localized and that this may contribute to the variable function of both catalytic subunits (29-31). We determined the subcellular localization of catalytic isoforms, as well as the two regulatory subunits p85α and p85β, in EM and endometrial cancer cells by Western immunoblotting. As shown in Figure 1A, p110α concentrated to the cytoplasmic fraction in all cell lines. p110β expression was low in EM cells detected mostly in the cytoplasmic fraction and with very low levels in nuclear fractions. All cancer cell lines had higher levels of p110β in the cytoplasmic fraction than EM cells. In the nuclear fractions, all cancer cell lines demonstrated high p110β levels except for EFE-184 cells. In the majority of cell lines p85α was restricted to the cytoplasmic fraction. In contrast, p85β was mostly undetectable in the cytoplasmic fraction in all cells except for MFE-280 cells, but was concentrated to the nuclear fraction, with high levels in EM, KLE, EFE-184 and MFE-280 cells and lower levels in the remaining cells (Figure 1A). When detected by immunostaining, p110β was localized in the cytoplasm as well as in nucleoli together with the nucleolar protein nucleophosmin (Figure 1B). The localisation of p110β in the nucleoplasm varied amongst cell lines. To determine if the localization pattern of p110β could also be observed in human tissues, we examined a patient cohort including 727 primary endometrial tumours by immunohistochemistry. While most patients showed p110β cytoplasmic detection with various degrees of intensity, 23% of all cases showed nuclear staining (Fig. 2A). In addition, a significant correlation was observed between high nuclear to cytoplasmic localisation-intensity ratio for p110β and high grade or histological type II endometrial tumour (Figure 2B).

The levels of PtdIns(3,4,5)P_3 are increased in nuclei of EC cells in a p110β-dependent manner

We next determined if the presence of p110β in the nucleus correlates with nuclear PI3K pathway activity by first assessing the presence of active p-S473-AKT. As shown in Figure 3A, the cytoplasmic and nuclear levels of p-S473-Akt were low in EM, KLE, EFE-184 and MFE-280 cells, while high levels were observed in MFE-296, MFE-319, RL95-2 and

Ishikawa cells, consistent with our previous study using total cell extracts in the same cells (43). Interestingly, high nuclear p-S473-Akt levels were inversely correlated with low levels of p85β (Figure 1A). Furthermore, we determined the nuclear level of PtdIns(3,4,5)P_3 of all cells examined following nuclear isolation, lipid extraction, and detection with GST-GRP1-PH, a PtdIns(3,4,5)P_3 specific probe (Figure 3B). The purity of the fractionation was verified by Western immunoblotting using markers for the cytoplasm, nucleus and endoplasmic reticulum (Supplementary Figure S1). PtdIns(3,4,5)P_3 levels were high in most cancer cells and highest in RL95-2 cells compared to EM cells (Figure 3C). To test if p110β is responsible for the synthesis of nuclear PtdIns(3,4,5)P_3 when PTEN is lost, we treated the PTEN-deficient cell line RL95-2 with TGX-221, a p110β selective inhibitor. Treatment for 3 days reduced the levels of nuclear PtdIns(3,4,5)P_3 (Figure 3D) and nuclear p-S473-Akt (Figure 3E). However, the levels of total Akt were increased in the cytosol while it was decreased in the nucleus following p110β inhibition. The decrease in nuclear p-Akt may hence be due to loss of translocation of active pAkt from the cytoplasm.

High nucleolar p110β levels correlates with high rRNA transcription

Using immunofluorescence microscopy, we show that p110β is found together with PtdIns(3,4,5)P_3 both in the nucleoplasmic and nucleolar compartments of RL95-2 (Figure 4A) and MFE-319 cells (Supplementary Figure S2). Furthermore, AKT was found to associate with the nucleolar pool of p110β and its active p-S473 form with the nucleolar protein nucleophosmin as discrete foci (Supplementary Figure S3). Nucleolar fractionation of RL95-2 cells confirmed the presence of p110β in the same compartments (Figure 4B). Tubulin, fibrillarin and lamin A/C were used as cytoplasmic, nuclear and nucleolar markers, respectively to validate the fractionation procedure. Lamin A/C was found in both the nucleoplasmic and nucleolar compartments as previously reported (44). In order to characterize the molecular composition of the PtdIns(3,4,5)P_3 species present in the nucleus, we performed targeted LC-MS/MS on the lipid extracted from different subcellular fractions of RL95-2 cells, which harbour the high nuclear PtdIns(3,4,5)P_3 levels. In particular, the species PtdIns(3,4,5)P_3 (38:4) was detected in the nucleolar fraction (Supplementary Table S1). Interestingly, the same PtdIns(4,5)P_2 (38:4) molecular species was also detected in the same fraction and can be hence thought as a possible substrate for p110β in the nucleolus.

The main function of the nucleolus is to synthesise ribosomes which involves rRNA transcription and processing (45). Elevated levels of nucleolar activity have been correlated to an increased risk of cancer development (46). We next examined whether EC cells with high

levels of p110β and PtdIns(3,4,5)P_3 in the nucleus had high level of rRNA transcription. Consistently, RL95-2 cells, showed the highest level of pre-rRNA synthesis when compared to EM cells (Figure 4C). Surprisingly, MFE 319 cells showed very little difference in transcription.

Discussion

Cellular compartmentalisation provides an additional important mode of regulation for signalling cascades in order to achieve specificity and to precisely coordinate cellular outputs. The PI3K pathway has been extensively studied from a cytoplasmic perspective. However, a few studies have detailed the distinct intracellular localisation of PI3K enzymes. For example, p110α is found to be restricted to the cytoplasm while p110β is present both in the cytoplasm and the nucleus, in particular in the nucleoplasm, the chromatin fraction and the nucleolus (29-31). The compartmentalisation of these enzymes is likely to impact on signalling networks and to mediate different cell functions, hence accounting for the pleiotropic effects attributed to PI3K signalling. Although the PI3K signalling pathway is pivotal in cancer, the impact of the subcellular localisation of PI3K in processes attributed to tumourigenesis is still poorly understood. Our findings demonstrate that p110α and p110β are differently compartmentalised in EC cells. Consistent with previous studies (29, 30), p110α is cytoplasmic and p110β nuclear. p110α and p110β isoforms may hence share some of the functions attributed to PI3K signalling operating in the cytoplasm, perhaps due to their recently reported cross-activation (47). In addition, the presence of genetic mutations affecting *PIK3CA* or *PTEN* would influence PtdIns(3,4,5)P_3-mediated downstream functions induced by p110α and p110β respectively in this compartment. Furthermore, we found that the levels of p110β is high in the nucleus of EC cell lines compared to EM cells. In clinically annotated tumour samples, we show a correlation between the nuclear p110β levels and an increase in endometrial cancer progression as tumours with higher grade histology presented high p110β nuclear to cytoplasmic ratio. These results would indicate the importance of the regulation of the levels of this isoform. Indeed, the overexpression of p110β has previously been shown to lead to cell transformation in its wild type state (48). Furthermore, our studies demonstrate that EC cells, not only have high nuclear levels of p110β, but also elevated levels of PtdIns(3,4,5)P_3, its lipid product as well as the active form of the oncoprotein AKT, p-S473-Akt, the critical signalling effector of PtdIns(3,4,5)P_3. Here, we demonstrate that upon p110β inhibition, the levels of the active form of Akt, p-S473-Akt, were decreased in EC

nuclei. The nuclear PtdIns(3,4,5)P_3 levels were also reduced in these cells following p110β inhibition, which suggests that the nuclear pool of PtdIns(3,4,5)P_3 is, at least partly, the product of the kinase activity of p110β. The existence of a molecular link within the nucleus between PtdIns(3,4,5)P_3 and Akt is however not clear from this study. Additional mechanisms of regulation required for the activation of Akt were not explored in this study. These would include the PtdIns(3,4,5)P_3-dependent activation of PDK1 and mTORC2, known to be critical for the phosphorylation and full activation of Akt (6, 7).

A clear relationship between elevated nucleolar activity and increased risk of cancer has been shown (46). Thus, nucleolar processes need to be tightly regulated with high fidelity to ensure appropriate cell growth and proliferation in response to external signals. One potential molecular link regulating these processes is the PI3K pathway. A few studies have shown that the transcription and processing of the pre rRNA is stimulated in a PI3K and mTOR-dependent manner (49-51). In addition, the PtdIns(3,4,5)P_3 effector protein nucleophosmin (52) as well mTORC1 are known to also localize to the nucleolus, where they can regulate nucleolar function (51, 53-55). Nuclear Akt has also been shown to regulate rRNA transcription by activating the TIF-I transcription factor (56). How PI3K, Akt and mTOR are activated in a nucleolar context is however not known. Moreover, the responsible PI3K isoform was not identified in those studies. In this study, we showed that both PtdIns(3,4,5)P_3 and p110β were localised in the nucleolar compartment, raising the possibility of p110β acting as a regulator of nucleolar functions in a kinase-dependent manner. The detection of PtdIns(3,4,5)P_3 in the nucleolus was further confirmed by LC-MS/MS analyses in the form of 38:4 (carbons:double bonds) for its acyl chains, which is consistent with the reported most common chemical form of fatty acyl chains for polyphosphoinositides (PPIn) (57). We could not identify PtdIns(3,4,5)P_3 in the cytoplasmic and nucleoplasmic fractions by LC-MS/MS, which may be due to the high amount of protein present in these fractions. PPIn and in particular PtdIns(3,4,5)P_3 are minor components, which could potentially get lost in the protein interphase during extractions. Immunofluorescent staining indicated also of the presence of both total Akt and phosphorylated Akt in nucleoli, which can suggest a local activation of this protein by PtdIns(3,4,5)P_3 present in nucleoli. Again, this would need to be explored further.

Our findings demonstrate that the RL95-2 endometrial cancer cells, high in nuclear PtdIns(3,4,5)P_3 and p110β levels, have significantly increased pre-rRNA transcription. The proliferation of these cells was shown to be at least partly dependent upon the activity of p110β (43). It would therefore be sensible to speculate that an increase in ribosome

production will help increase cell proliferation and subsequently cancer progression. Nucleolar p110β would hence provide a mode of regulation of ribosome synthesis necessary for protein synthesis and ultimately cell division. p110β can therefore potentially increase tumour progression in EC cells by producing the nucleolar pool of PtdIns(3,4,5)P_3 and thereby increasing the biogenesis of ribosomes required for tumour growth. However, the exact molecular mechanisms by which PtdIns(3,4,5)P_3 or p110β can influence nucleolar function remains to be further explored.

Materials and methods

Reagents

Antibodies used in Western immunoblotting and immunostaining are listed in Supplementary table S2.

Patient series

Tissue was collected from patients diagnosed with endometrial cancer at Haukeland University hospital during the period from 2001-2013 and included a total of 234 clinical samples with 18 endometrial cancer precursor lesions (complex atypical hyperplasias, CAH), 174 primary tumours and 42 metastases. Clinical data were collected as described earlier (58, 59). The patient cohort used for p110β immunohistochemistry is described in detail in Tangen *et al* (59). This study was conducted in line with Norwegian legislation and international demands for ethical review, approved by the Norwegian Data Inspectorate, Norwegian Social Sciences Data Services and the Western Regional Committee for Medical and Health Research Ethics (NSD15501; REK 052.01). Patients signed an informed consent.

Cell lines and cell culture conditions

Cancer cell lines were obtained from ATCC (KLE, RL95-2), DSMZ Germany (MFE-296, MFE-319, EFE-184 and MFE-280) and Sigma-Aldrich (Ishikawa). EM-E6/E7-hTERT (EM), a non-transformed endometrial cell line isolated from glandular endometrial tissue and immortalized with E6/E7 and human TERT (60, 61), was a gift from Professor PM Pollock (University of Queensland, Australia). All cells were authenticated by short tandem repeat DNA profiling (IdentiCell Service, Dept. Molecular Medicine, Aarhus University Hospital, Denmark for all cancer cell lines and MD Anderson Cancer Center, USA for EM cells), as previously described (43). All cancer cells were cultured in Dulbecco's modified Eagle's

medium (DMEM) supplemented with 10% fetal bovine serum (FBS) and antibiotics (100 IU/ml penicillin and 100 µg/ml streptomycin). EM cells were cultured in DMEM/Ham's F12 supplemented with Insulin-Transferrin-Selenium, 10% FBS and antibiotics and changed to DMEM containing 10% FBS and antibiotics 24 h before harvest. Cells were harvested when they reached a maximum of 80% confluence.

Whole cell extracts, subcellular fractionation and Western immunoblotting

Whole cell extracts were prepared in radioimmunoprecipitation assay (RIPA) lysis buffer (50 mM Tris pH 8.0, 0.5% deoxycholic acid, 150 mM NaCl, 1% NP-40, 0.1% SDS) supplemented with 5 mM NaF, 2 mM Na3VO4 and 1x Sigma Protease Inhibitor Cocktail. Nuclear fractionation was carried out according to O'Caroll et al. (62) and nuclear pellets were lysed in RIPA buffer. RL95-2 cells required an additional syringing step of the nuclear pellet resuspended in wash buffer (10 mM Tris-HCl pH 7.5 and 2 mM MgCl2) to avoid cytoplasmic contamination. The nucleoli were isolated according to the protocole described in Lam *et al* 2006 (63). In brief cells were grown in 10 large 15cm dishes up to 70% confluency. Fresh medium was added to the cells 1 hour prior to the fractionation. Cells were trypsinized and washed 3 x with cold PBS. The cell pellet was collected by centrifugation and re-suspend in 5ml of buffer A containing 10 mM HEPES pH 7.9, 1.5 mM MgCl2, 10 mM KCl, 0,5mM DDT, 1 % Igepal and protease inhibitor cocktail. After 5 min of incubation on ice the cells were syringed by passed through a 23-gauge needle 16 times. After centrifugation at 218x g for 5 min at 4°C the supernatant was collected as the cytosolic fraction and the nuclear pellet was re-suspended in 3 ml of buffer S1 (0.25 M sucrose, 10 mM $MgCl_2$ and protease inhibitor cocktail). The suspension was layered over 3ml of buffer S2 (0.35 M sucrose, 0.5 mM $MgCl_2$ and protease inhibitor cocktail) and centrifugation was performed at 1430 x g for 5 min at 4°C. The pellet was then re-suspended in 3 ml of S2 before sonicating (7 times: 10 sec on/10sec off) on ice. The lysate was then layered over 3 ml of S3 (0.88 M Sucrose, 0.5 mM $MgCl_2$ and protease inhibitor cocktail) and centrifugation was performed at 3000 x g for 10 min at 4°C. The top layer was collected as the nucleoplasmic fraction and the pellet which contained the nucleoli was washed once with 500µl of S2. Equal amount of proteins (40-50 µg) were resolved by SDS-PAGE, immunoblotted as described previously (64) and detected by enhanced chemiluminescence using the SuperSignal West Pico Chemiluminescent Substrate (Pierce) and visualized with a BioRad ChemiDocTM Xrs+. See table S3 for antibodies and dilutions.

RNA extraction

After pelleting the cells were washed two times with PBS and resuspended in 1ml TriReagent (Sigma) and incubated at room temperature for 5 min. 200µl of chloroform was added and mixed vigorously before incubating at room temperature for 1 min and centrifuging (at 12000 x g and 4°C) for 15 min. Phenol -chloroform-isoamyl alcohol mixture (Sigma) was added (500µl) to the upper phase and after mixing was incubated at room temperature for 2 min before centrifuging (at 12000 x g and 4°C) for 10 min. To the upper phase chloroform (500µl) was added and after mixing and incubating at room temperature for 1 min it was centrifuged (at 12000 x g and 4°C) for 10 min. 20 µg of RNA grade glycogen (Thermo Fisher Scientific) and 500 µl isopropanol was added to the upper phase and after mixing well it was incubated at room temperature for 20 min before centrifuging (at 13000 x g and 4°C) for 20 min. The pellet was resuspended in 1 ml of ice cold ethanol (70%) and centrifuged (at 8000 x g and 4°C) for 5 min. The extracted RNA was dissolved in water for RT-qPCR analysis.

RT-qPCR

From total RNA extracts of RL952, MFE319 and EM cells 1µgr was used to make cDNA with random primers according to the protocol from the High-Capacity cDNA Reverse Transcription Kit (Thermo Fisher scientific). Real-time PCR was performed on Roche Light Cycler 480 using PowerUp SYBR Green Master Mix (Thermo Fisher scientific). Primers used for the target pre-rRNA gene (5' external transcribed spacer region) were: 5'-GAACGGTGGTGTGTCGTTC-3' and 5'-GCGTCTCGTCTCGTCTCACT-3' (65) and for the RPS12 gene (as reference gene) were: 5′-ATTCAGCTTCACCCGTAACC-3′ and 5′-CAACCACTTTACGGGGATTC-3′ (66).

Lipid Extraction from nuclear fractions

Following cell fractionation, the nuclear pellets were resuspended in nuclear resuspension buffer (10 mM Tris pH 7,4, 1 mM EGTA, 1,5 mM KCL, 5mM $MgCL_2$, 320 mM sucrose) and counted. Lipids were extracted from each nuclear fraction using a method adapted from Grey *et al* (67). Nuclei were incubated in 1 mL MeOH/$CHCl_3$ 2:1 to extract neutral lipids for 10 min at room temperature with shaking at 1200 rpm and vortexed 3-4 times. The samples were centrifuged at 3000 g for 5 min at 4 °C and supernatants were discarded and the same procedure was repeated. The acidic lipids were then extracted with 750 µL MeOH/$CHCl_3$/0.1 M HCl 80:40:1 2:1:0.8 and incubated for 15 min at room temperature and vortexed 4 times during the incubation followed by centrifugation at 3000 g for 5 min at 4 °C. The pellets were

resuspended with 250 µL $CHCl_3$ and 450 µL 0.1 M HCl and centrifuged at 3000 g for 5 min at 4 °C and a phase split between the organic and aqueous phases was apparent. The organic phase (bottom phase) was collected in conical glass tubes and dried at 60°C under N_2 gas. Lipids were resuspended with 4-6 µl of MeOH/CHCl3/H_2O 2:1:0.8, vortexed for 30 seconds before being sonicated in an ice bath for 5 min and vortexed again for 30 seconds. Proteins were recovered from lipid extraction and the protein concentration was estimated for validation of the fractionation by western blotting.

Lipid Overlay Assay

Lipids obtained from lipid extraction were spotted on Hybond™-CExtra membranes, 2 µl at a time. The membranes were left to dry for 1 hour at room temperature protected from light. The membranes were next blocked for 1 h at room temperature with the appropriate blocking buffer (1% fat-free milk in PBS pH 7.4) and further incubated with 0.5 µg/mL GST-GRP1-PH in the same buffer overnight at 4°C and protected from light. GST-GRP1-PH was expressed and purified as described previously (68). The membranes were washed 6 x 5 min in PBS-T (0.05% Tween 20) and then incubated with anti-GST conjugated to HRP (1:30 000) in blocking buffer for 1 h at room temperature. The blots were washed 6 x 5 min with PBS-T. The signal was detected by ECL using the SuperSignal West Pico Chemiluminescent Substrate or with SuperSignal West Femto Maximum Sensitivity Substrate (Thermo Fisher scientific) and detected with a BioRad ChemiDoc™ Xrs+. Lipid spot densitometry was quantified using ImageJ.

Immunostaining, immunohistochemistry and microscopy

Cells grown on coverslips were fixed with 3.7% paraformaldehyde/PBS for 10 min, washed thrice with PBS, permeabilised with 0.25% Triton X-100/PBS for 10 min, blocked for 1 h with blocking buffer (3% BSA in 0.05% Triton X-100/PBS) and incubated with primary antibodies diluted in blocking buffer overnight at 4°C and subsequently with fluorescently-labelled secondaary antibodies diluted in blocking buffer for 1 h at room temperature. Washes were performed with 0.05% Tween-20/PBS after antibody incubation. The coverslips were mounted in ProLong Gold Antifade Reagent containing 4',6-diamidino-2-phenylindole (DAPI). Images were acquired with a Leica DMI6000B fluorescence microscope using x40 or x100 objectives or Leica TCS SP5 confocal laser scanning microscope using a 63x/1.4 oil immersion lens. Images were processed with a Leica application suite V 4.0. TMA sections from a cohort including 727 patients were stained and scored for p110β expression following

a protocol previously described (59). Briefly, three cylinders of 0.6 mm were retrieved from high tumour purity areas using a custom-made precision instrument (Beecher Instruments, Silver Spring, MD, USA) and mounted in a paraffin block. TMA sections (5 μm) were stained for p110β expression and scored visually by light microscopy by 2 independent observers (CK and ILT). Scoring was performed blinded for information regarding clinical characteristics and outcome. A semi quantitative and subjective scoring method was used, and a staining index was calculated as a product of staining intensity (0-3) and area of positive tumour cells (1≤10%, 2=10-50% and 3≥50%).

Acknowledgments

We would like to thank Professor Bernard Payrastre, Dr. Gaëtan Chicanne, Justine Bertrand-Michel and Fanny Viars (The MetaToul lipidomic facility at the Université Toulouse III Paul Sabatier, France) for their help in the lipid extraction and LC-MS/MS analyses. This work was funded by the University of Bergen, the Norwegian cancer society and the Meltzer foundation.

References

1. Engelman JA. Targeting PI3K signalling in cancer: opportunities, challenges and limitations. Nat Rev Cancer. 2009;9(8):550-62.

2. Fruman DA, Rommel C. PI3K and cancer: lessons, challenges and opportunities. Nat Rev Drug Discov. 2014;13(2):140-56.

3. Thorpe LM, Yuzugullu H, Zhao JJ. PI3K in cancer: divergent roles of isoforms, modes of activation and therapeutic targeting. Nat Rev Cancer. 2015;15(1):7-24.

4. Vanhaesebroeck B, Stephens L, Hawkins P. PI3K signalling: the path to discovery and understanding. Nat Rev Mol Cell Biol. 2012;13(3):195-203.

5. Davies MA. Regulation, role, and targeting of Akt in cancer. J Clin Oncol. 2011;29(35):4715-7.

6. Currie RA, Walker KS, Gray A, Deak M, Casamayor A, Downes CP, et al. Role of phosphatidylinositol 3,4,5-trisphosphate in regulating the activity and localization of 3-phosphoinositide-dependent protein kinase-1. Biochem J. 1999;337 (Pt 3):575-83.

7. Liu P, Gan W, Chin YR, Ogura K, Guo J, Zhang J, et al. PtdIns(3,4,5)P3-Dependent Activation of the mTORC2 Kinase Complex. Cancer Discov. 2015;5(11):1194-209.

8. Salamon RS, Backer JM. Phosphatidylinositol-3,4,5-trisphosphate: tool of choice for class I PI 3-kinases. Bioessays. 2013;35(7):602-11.

9. Hers I, Vincent EE, Tavare JM. Akt signalling in health and disease. Cell Signal. 2011;23(10):1515-27.

10. Chalhoub N, Baker SJ. PTEN and the PI3-kinase pathway in cancer. Annu Rev Pathol. 2009;4:127-50.

11. Bi L, Okabe I, Bernard DJ, Nussbaum RL. Early embryonic lethality in mice deficient in the p110beta catalytic subunit of PI 3-kinase. Mamm Genome. 2002;13(3):169-72.

12. Bi L, Okabe I, Bernard DJ, Wynshaw-Boris A, Nussbaum RL. Proliferative defect and embryonic lethality in mice homozygous for a deletion in the p110alpha subunit of phosphoinositide 3-kinase. J Biol Chem. 1999;274(16):10963-8.

13. Ciraolo E, Iezzi M, Marone R, Marengo S, Curcio C, Costa C, et al. Phosphoinositide 3-kinase p110beta activity: key role in metabolism and mammary gland cancer but not development. Science signaling. 2008;1(36).

14. Guillermet-Guibert J, Bjorklof K, Salpekar A, Gonella C, Ramadani F, Bilancio A, et al. The p110beta isoform of phosphoinositide 3-kinase signals downstream of G protein-coupled receptors and is functionally redundant with p110gamma. Proc Natl Acad Sci U S A. 2008;105(24):8292-7.

15. Jia S, Liu Z, Zhang S, Liu P, Zhang L, Lee SH, et al. Essential roles of PI(3)K-p110beta in cell growth, metabolism and tumorigenesis. Nature. 2008;454(7205):776-9.

16. Fritsch R, de Krijger I, Fritsch K, George R, Reason B, Kumar MS, et al. RAS and RHO families of GTPases directly regulate distinct phosphoinositide 3-kinase isoforms. Cell. 2013;153(5):1050-63.

17. Samuels Y, Wang Z, Bardelli A, Silliman N, Ptak J, Szabo S, et al. High frequency of mutations of the PIK3CA gene in human cancers. Science. 2004;304(5670):554.

18. Dbouk HA, Khalil BD, Wu H, Shymanets A, Nurnberg B, Backer JM. Characterization of a tumor-associated activating mutation of the p110beta PI 3-kinase. PLoS One. 2013;8(5):e63833.

19. Pazarentzos E, Giannikopoulos P, Hrustanovic G, St John J, Olivas VR, Gubens MA, et al. Oncogenic activation of the PI3-kinase p110beta isoform via the tumor-derived PIK3Cbeta(D1067V) kinase domain mutation. Oncogene. 2016;35(9):1198-205.

20. Torbett NE, Luna-Moran A, Knight ZA, Houk A, Moasser M, Weiss W, et al. A chemical screen in diverse breast cancer cell lines reveals genetic enhancers and suppressors of sensitivity to PI3K isoform-selective inhibition. Biochem J. 2008;415(1):97-110.

21. Jia S, Liu Z, Zhang S, Liu P, Zhang L, Lee SH, et al. Kinase-dependent and -independent functions of the p110β phosphoinositide-3-kinase in cell growth, metabolic regulation and oncogenic transformation. Nature. 2008;454(7205):776-9.

22. Wee S, Wiederschain D, Maira SM, Loo A, Miller C, deBeaumont R, et al. PTEN-deficient cancers depend on PIK3CB. Proc Natl Acad Sci U S A. 2008;105(35):13057-62.

23. Ni J, Liu Q, Xie S, Carlson C, Von T, Vogel K, et al. Functional characterization of an isoform-selective inhibitor of PI3K-p110beta as a potential anticancer agent. Cancer Discov. 2012;2(5):425-33.

24. Schmit F, Utermark T, Zhang S, Wang Q, Von T, Roberts TM, et al. PI3K isoform dependence of PTEN-deficient tumors can be altered by the genetic context. Proc Natl Acad Sci U S A. 2014;111(17):6395-400.

25. Kang S, Denley A, Vanhaesebroeck B, Vogt PK. Oncogenic transformation induced by the p110β, -γ, and -δ isoforms of class I phosphoinositide 3-kinase. P Natl Acad Sci USA. 2006;103(5):1289-94.

26. Juric D, Castel P, Griffith M, Griffith OL, Won HH, Ellis H, et al. Convergent loss of PTEN leads to clinical resistance to a PI(3)Kalpha inhibitor. Nature. 2014.

27. Benistant C, Chapuis H, Roche S. A specific function for phosphatidylinositol 3-kinase alpha (p85alpha-p110alpha) in cell survival and for phosphatidylinositol 3-kinase beta (p85alpha-p110beta) in de novo DNA synthesis of human colon carcinoma cells. Oncogene. 2000;19(44):5083-90.

28. Marques M, Kumar A, Cortes I, Gonzalez-Garcia A, Hernandez C, Moreno-Ortiz MC, et al. Phosphoinositide 3-kinases p110alpha and p110beta regulate cell cycle entry, exhibiting distinct activation kinetics in G1 phase. Mol Cell Biol. 2008;28(8):2803-14.

29. Marques M, Kumar A, Poveda AM, Zuluaga S, Hernandez C, Jackson S, et al. Specific function of phosphoinositide 3-kinase beta in the control of DNA replication. Proc Natl Acad Sci U S A. 2009;106(18):7525-30.

30. Kumar A, Redondo-Munoz J, Perez-Garcia V, Cortes I, Chagoyen M, Carrera AC. Nuclear but not cytosolic phosphoinositide 3-kinase beta has an essential function in cell survival. Mol Cell Biol. 2011;31(10):2122-33.

31. Karlsson T, Altankhuyag A, Dobrovolska O, Turcu DC, Lewis AE. A polybasic motif in ErbB3-binding protein 1 (EBP1) has key functions in nucleolar localization and polyphosphoinositide interaction. Biochem J. 2016;473(14):2033-47.

32. O'Hara AJ, Bell DW. The genomics and genetics of endometrial cancer. Adv Genomics Genet. 2012;2012(2):33-47.

33. Cheung LW, Hennessy BT, Li J, Yu S, Myers AP, Djordjevic B, et al. High frequency of PIK3R1 and PIK3R2 mutations in endometrial cancer elucidates a novel mechanism for regulation of PTEN protein stability. Cancer Discov. 2011;1(2):170-85.

34. Mutter GL, Lin MC, Fitzgerald JT, Kum JB, Baak JP, Lees JA, et al. Altered PTEN expression as a diagnostic marker for the earliest endometrial precancers. Journal of the National Cancer Institute. 2000;92(11):924-30.

35. Hayes MP, Wang H, Espinal-Witter R, Douglas W, Solomon GJ, Baker SJ, et al. PIK3CA and PTEN mutations in uterine endometrioid carcinoma and complex atypical hyperplasia. Clinical cancer research : an official journal of the American Association for Cancer Research. 2006;12(20 Pt 1):5932-5.

36. Konopka B, Janiec-Jankowska A, Kwiatkowska E, Najmola U, Bidzinski M, Olszewski W, et al. PIK3CA mutations and amplification in endometrioid endometrial carcinomas: relation to other genetic defects and clinicopathologic status of the tumors. Hum Pathol. 2011;42(11):1710-9.

37. Oda K, Stokoe D, Taketani Y, McCormick F. High frequency of coexistent mutations of PIK3CA and PTEN genes in endometrial carcinoma. Cancer research. 2005;65(23):10669-73.

38. Oda K, Okada J, Timmerman L, Rodriguez-Viciana P, Stokoe D, Shoji K, et al. PIK3CA cooperates with other phosphatidylinositol 3'-kinase pathway mutations to effect oncogenic transformation. Cancer research. 2008;68(19):8127-36.

39. Urick ME, Rudd ML, Godwin AK, Sgroi D, Merino M, Bell DW. PIK3R1 (p85alpha) is somatically mutated at high frequency in primary endometrial cancer. Cancer research. 2011;71(12):4061-7.

40. Salvesen HB, Carter SL, Mannelqvist M, Dutt A, Getz G, Stefansson IM, et al. Integrated genomic profiling of endometrial carcinoma associates aggressive tumors with indicators of PI3 kinase activation. Proc Natl Acad Sci U S A. 2009;106(12):4834-9.

41. Forbes SA, Bindal N, Bamford S, Cole C, Kok CY, Beare D, et al. COSMIC: mining complete cancer genomes in the Catalogue of Somatic Mutations in Cancer. Nucleic Acids Res. 2011;39(Database issue):D945-50.

42. An HJ, Cho NH, Yang HS, Kwak KB, Kim NK, Oh DY, et al. Targeted RNA interference of phosphatidylinositol 3-kinase p110-beta induces apoptosis and proliferation arrest in endometrial carcinoma cells. J Pathol. 2007;212(2):161-9.

43. Karlsson T, Krakstad C, Tangen IL, Hoivik EA, Pollock PM, Salvesen HB, et al. Endometrial cancer cells exhibit high expression of p110beta and its selective inhibition induces variable responses on PI3K signaling, cell survival and proliferation. Oncotarget. 2017;8(3):3881-94.

44. Martin C, Chen S, Maya-Mendoza A, Lovric J, Sims PF, Jackson DA. Lamin B1 maintains the functional plasticity of nucleoli. Journal of cell science. 2009;122(Pt 10):1551-62.

45. Boisvert FM, van Koningsbruggen S, Navascues J, Lamond AI. The multifunctional nucleolus. Nat Rev Mol Cell Biol. 2007;8(7):574-85.

46. Montanaro L, Trere D, Derenzini M. Changes in ribosome biogenesis may induce cancer by down-regulating the cell tumor suppressor potential. Biochim Biophys Acta. 2012;1825(1):101-10.

47. Perez-Garcia V, Redondo-Munoz J, Kumar A, Carrera AC. Cell activation-induced phosphoinositide 3-kinase alpha/beta dimerization regulates PTEN activity. Mol Cell Biol. 2014.

48. Kang S, Denley A, Vanhaesebroeck B, Vogt PK. Oncogenic transformation induced by the p110beta, -gamma, and -delta isoforms of class I phosphoinositide 3-kinase. Proc Natl Acad Sci U S A. 2006;103(5):1289-94.

49. Hannan KM, Brandenburger Y, Jenkins A, Sharkey K, Cavanaugh A, Rothblum L, et al. mTOR-dependent regulation of ribosomal gene transcription requires S6K1 and is mediated by phosphorylation of the carboxy-terminal activation domain of the nucleolar transcription factor UBF. Mol Cell Biol. 2003;23(23):8862-77.

50. James MJ, Zomerdijk JC. Phosphatidylinositol 3-kinase and mTOR signaling pathways regulate RNA polymerase I transcription in response to IGF-1 and nutrients. J Biol Chem. 2004;279(10):8911-8.

51. Iadevaia V, Zhang Z, Jan E, Proud CG. mTOR signaling regulates the processing of pre-rRNA in human cells. Nucleic Acids Res. 2012;40(6):2527-39.

52. Ahn JY, Liu X, Cheng D, Peng J, Chan PK, Wade PA, et al. Nucleophosmin/B23, a nuclear PI(3,4,5)P(3) receptor, mediates the antiapoptotic actions of NGF by inhibiting CAD. Molecular cell. 2005;18(4):435-45.

53. Hamilton G, Abraham AG, Morton J, Sampson O, Pefani DE, Khoronenkova S, et al. AKT regulates NPM dependent ARF localization and p53(mut) stability in tumors. Oncotarget. 2014;5(15):6142-67.

54. Lee SB, Xuan Nguyen TL, Choi JW, Lee KH, Cho SW, Liu Z, et al. Nuclear Akt interacts with B23/NPM and protects it from proteolytic cleavage, enhancing cell survival. Proc Natl Acad Sci U S A. 2008;105(43):16584-9.

55. Lindstrom MS. NPM1/B23: A Multifunctional Chaperone in Ribosome Biogenesis and Chromatin Remodeling. Biochemistry research international. 2011;2011:195209.

56. Nguyen le XT, Mitchell BS. Akt activation enhances ribosomal RNA synthesis through casein kinase II and TIF-IA. Proc Natl Acad Sci U S A. 2013;110(51):20681-6.

57. Traynor-Kaplan A, Kruse M, Dickson EJ, Dai G, Vivas O, Yu H, et al. Fatty-acyl chain profiles of cellular phosphoinositides. Biochimica et biophysica acta. 2017;1862(5):513-22.

58. Berg A, Hoivik EA, Mjos S, Holst F, Werner HM, Tangen IL, et al. Molecular profiling of endometrial carcinoma precursor, primary and metastatic lesions suggests different targets for treatment in obese compared to non-obese patients. Oncotarget. 2014.

59. Tangen IL, Werner HM, Berg A, Halle MK, Kusonmano K, Trovik J, et al. Loss of progesterone receptor links to high proliferation and increases from primary to metastatic endometrial cancer lesions. European journal of cancer. 2014;50(17):3003-10.

60. Kyo S, Nakamura M, Kiyono T, Maida Y, Kanaya T, Tanaka M, et al. Successful immortalization of endometrial glandular cells with normal structural and functional characteristics. The American journal of pathology. 2003;163(6):2259-69.

61. Mizumoto Y, Kyo S, Ohno S, Hashimoto M, Nakamura M, Maida Y, et al. Creation of tumorigenic human endometrial epithelial cells with intact chromosomes by introducing defined genetic elements. Oncogene. 2006;25(41):5673-82.

62. O'Carroll SJ, Mitchell MD, Faenza I, Cocco L, Gilmour RS. Nuclear PLCbeta1 is required for 3T3-L1 adipocyte differentiation and regulates expression of the cyclin D3-cdk4 complex. Cell Signal. 2009;21(6):926-35.

63. Lam Y, I. Lamond A. Isolation of Nucleoli2006. 103-7 p.

64. Aumo L, Rusten M, Mellgren G, Bakke M, Lewis AE. Functional roles of protein kinase A (PKA) and exchange protein directly activated by 3',5'-cyclic adenosine 5'-monophosphate (cAMP) 2 (EPAC2) in cAMP-mediated actions in adrenocortical cells. Endocrinology. 2010;151(5):2151-61.

65. Murayama A, Ohmori K, Fujimura A, Minami H, Yasuzawa-Tanaka K, Kuroda T, et al. Epigenetic control of rDNA loci in response to intracellular energy status. Cell. 2008;133(4):627-39.

66. Gabriel JM, Higgins MJ, Gebuhr TC, Shows TB, Saitoh S, Nicholls RD. A model system to study genomic imprinting of human genes. P Natl Acad Sci USA. 1998;95(25):14857-62.

67. Gray A, Olsson H, Batty IH, Priganica L, Peter Downes C. Nonradioactive methods for the assay of phosphoinositide 3-kinases and phosphoinositide phosphatases and selective detection of signaling lipids in cell and tissue extracts. Anal Biochem. 2003;313(2):234-45.

68. Lewis AE, Sommer L, Arntzen MO, Strahm Y, Morrice NA, Divecha N, et al. Identification of nuclear phosphatidylinositol 4,5-bisphosphate-interacting proteins by neomycin extraction. Mol Cell Proteomics. 2011;10(2):M110 003376.

Figure legends

Figure 1: p110α and p110β demonstrate different subcellular compartmentalisation

(A) Actively growing cells were fractionated into cytoplasmic and nuclear fractions. Equal protein concentrations were resolved by SDS-PAGE and analysed by Western immunoblotting using the antibodies as indicated. **(B)** Co-immunostaining of p110β and nucleophosmin in actively growing KLE, MFE-319 and RL95-2 cells and imaged by epifluorescence microscopy. Scale bar 10 μm (x100).

Figure 2: High nuclear levels of p110β are more prevalent in high grade and type II endometrial tumours

(A) Representative histochemistry images of cytoplasmic and nuclear p110β staining in primary endometrial tumours detected with anti-p110β. **(B)** Quantitative graphs of nuclear (N) to cytoplasmic (C) ratio measured following p110β histochemistry of 728 patient histology samples. G represents the grade of the tumour.

Figure 3: Nuclear PtdIns(3,4,5)P_3 levels are elevated in endometrial cancer cells

(A) Actively growing cells were fractionated into cytoplasmic and nuclear fractions. Equal protein concentrations were resolved by SDS-PAGE and analysed by Western immunoblotting using the antibodies as indicated. **(B)** PIP array spotted with 1.56 to 100 picoM of each of the seven PPIn species incubated with GST-GRP1-PH and an anti-GST-HRP conjugated antibody. **(C)** PtdIns(3,4,5)P_3 (PIP3) detection from nuclear acidic lipids extracted from actively growing cells, by overlay assay with GST-GRP1-PH domain and anti-GST-HRP conjugated antibody (upper panel). PIP3 signal/mg nuclear protein were calculated and expressed as folds compared to EM values (lower panel–graph. n=3, * $p< 0.05$ t-test). **(D)** PtdIns(3,4,5)P_3 (PIP3) detection by overlay assay with GST-GRP1-PH domain and anti-GST-HRP conjugated antibody from nuclear acidic lipids extracted from RL95-2 cells treated with or without 10 μM TGX-221 for three days. **(E)** Western immunoblotting of cytoplasmic (cyt) and nuclear (nuc) fractions from RL95-2 cells treated with or without 10 μM TGX-221 for three days.

Figure 4: Pre-rRNA expression is increased in RL95-2 cells with high nuclear levels of p110β.

(A) Confocal microscopy of actively growing RL95-2 cells co-stained with the indicated antibodies (Scale bar 5 μm). **(B)** Sub-cellular fractionation of RL95-2 cells showing the nucleolar presence of p110β **(C)** Relative pre-rRNA expresstion to RPS12 gene in RL95-2, MFE 319 and EM cells is shown in the graph. The expressions of all samples were normalized to EM cells.

Figure 1

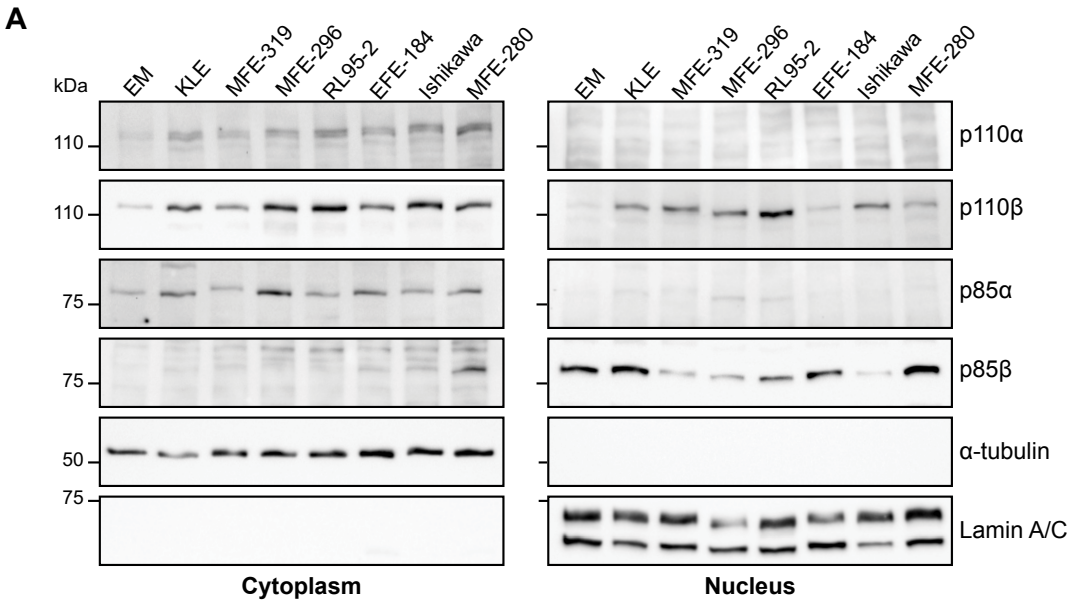
A
kDa
EM
KLE
MFE-319
MFE-296
RL95-2
EFE-184
Ishikawa
MFE-280
110
110
75
75
50
75
p110α
p110β
p85α
p85β
α-tubulin
Lamin A/C
Cytoplasm
Nucleus

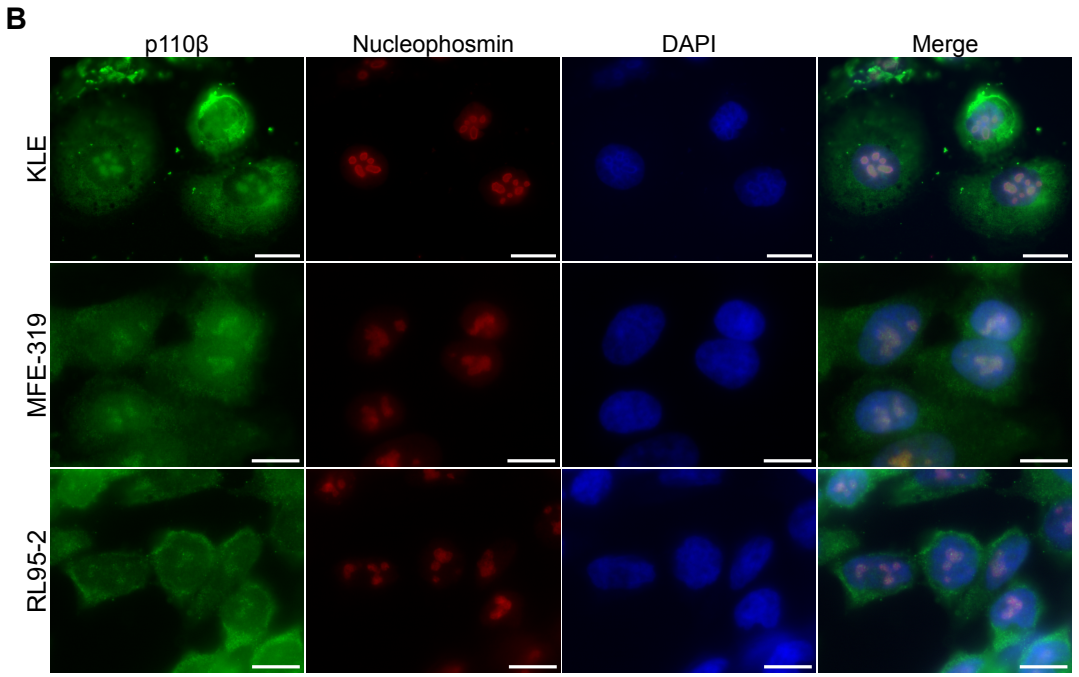
B
p110β
Nucleophosmin
DAPI
Merge
KLE
MFE-319
RL95-2

Figure 2

A

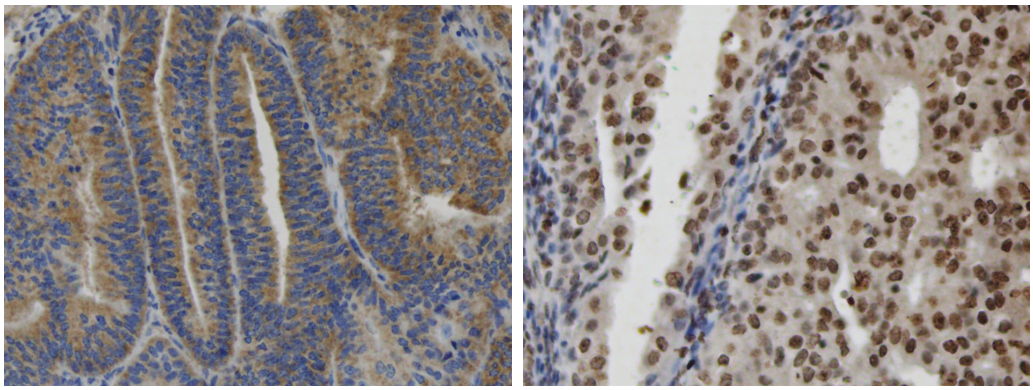

B

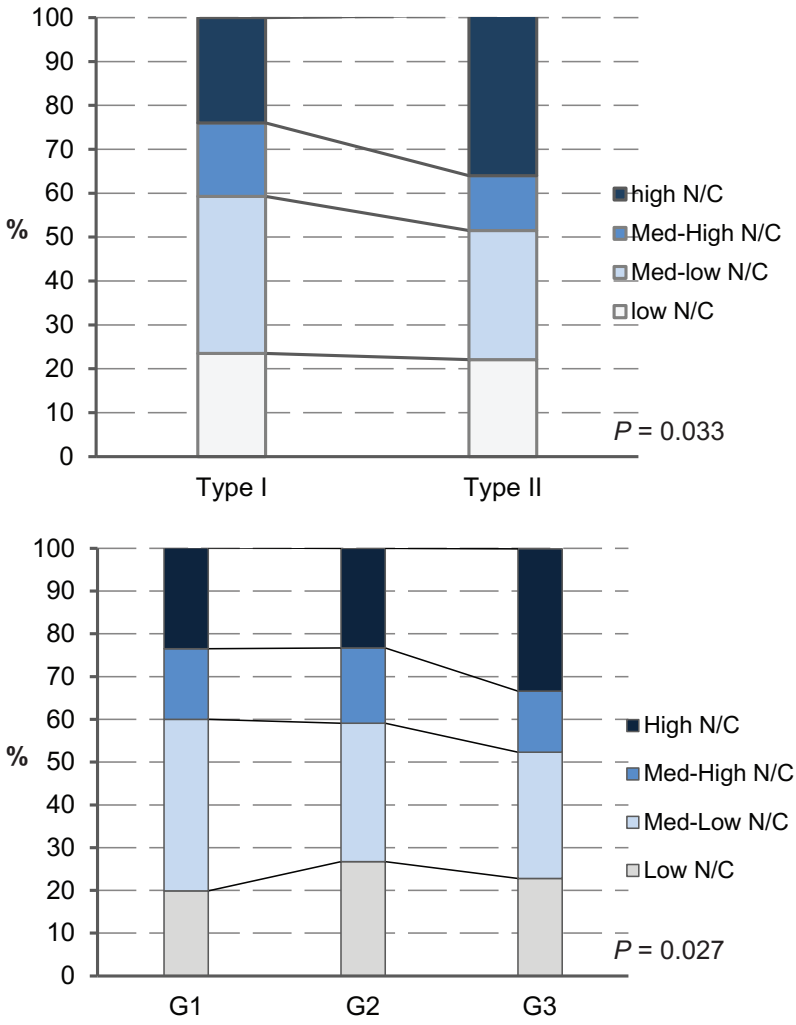
100
90
80
70
60
50
40
30
20
10
0
%
high N/C
Med-High N/C
Med-low N/C
low N/C
P = 0.033
Type I
Type II
High N/C
Med-High N/C
Med-Low N/C
Low N/C
P = 0.027
G1
G2
G3

Figure 3

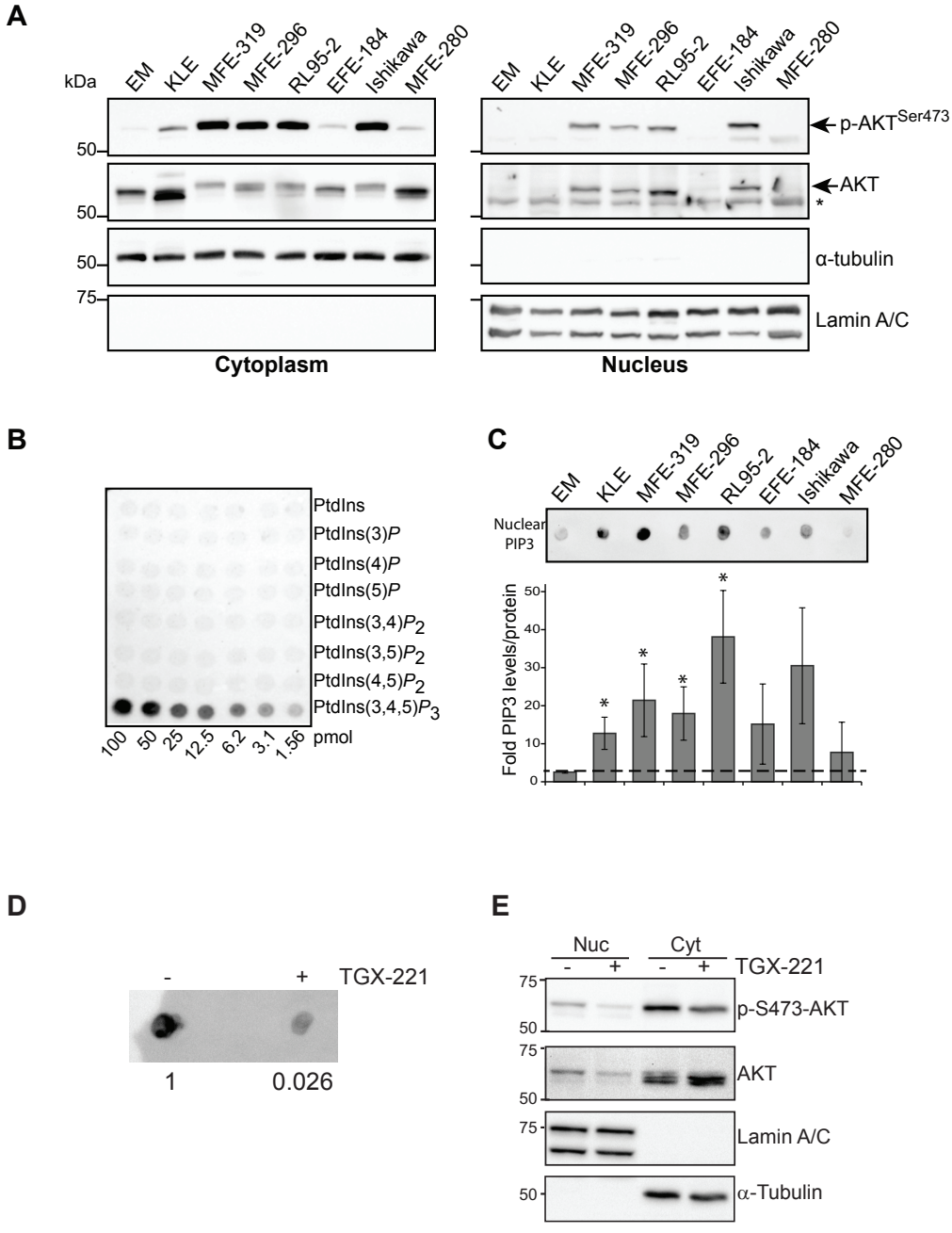
A
kDa
EM
KLE
MFE-319
MFE-296
RL95-2
EFE-184
Ishikawa
MFE-280
50
50
50
75
Cytoplasm
Nucleus
p-AKTSer473
AKT
*
α-tubulin
Lamin A/C
B
PtdIns
PtdIns(3)P
PtdIns(4)P
PtdIns(5)P
PtdIns(3,4)P2
PtdIns(3,5)P2
PtdIns(4,5)P2
PtdIns(3,4,5)P3
100
50
25
12.5
6.2
3.1
1.56
pmol
C
Nuclear PIP3
Fold PIP3 levels/protein
0
10
20
30
40
50
D
-
+
TGX-221
1
0.026
E
Nuc
Cyt
TGX-221
p-S473-AKT
AKT
Lamin A/C
α-Tubulin
75
50

Figure 4

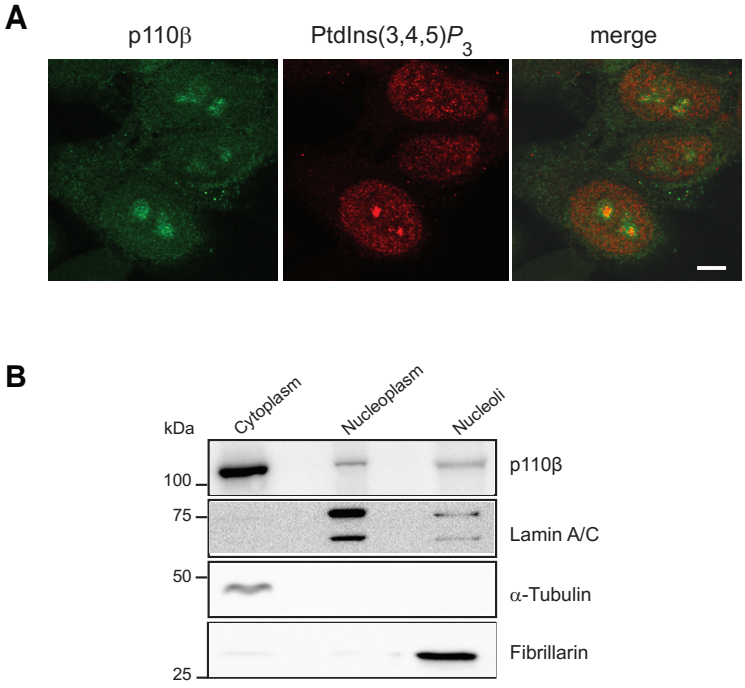
A
p110β
PtdIns(3,4,5)P3
merge
B
kDa
Cytoplasm
Nucleoplasm
Nucleoli
100
75
50
25
p110β
Lamin A/C
α-Tubulin
Fibrillarin
C
pre- rRNA transcription
Relative level of expression Normalized to EM
0
1
2
3
4
5
6
EM
MFE 319
RL952

Supplementary material

Nuclear upregulation of PI3K p110β correlates with increased rRNA transcription in endometrial cancer cells

Fatemeh Mazloumi Gavgani[1*], Thomas Karlsson[1*], Victoria Smith Arnesen[1], Ole Horvli[1], Ingvild L Tangen[2,3], Camilla Krakstad[2,3], Pamela Pollock[4] and Aurélia E Lewis[1§]

[1] Department of Molecular Biology, University of Bergen [2] Centre for Cancer Biomarkers, Department of Clinical Science, University of Bergen [3] Department of Gynecology and Obstetrics, Haukeland University Hospital, Bergen, Norway. [4] Queensland University of Technology (QUT), Brisbane, Australia.

Supplementary methods

LC-MS and lipid extraction from cytoplasmic, nuclear and nucleolar fractions

Cytoplasmic, nuclear and nucleolar fractions were isolated from RL95-2 cells. Prior to lipid extraction, the cytoplasmic and nuclear fractions were pelleted at 48 000 g for 1 hour in a TLi 100.2 rotor. The lipid extraction procedure described in Clark & al. (2011) was followed. Extraction: Fractionated pellets were resuspended in 170 µL H2O, sonicated with rod for 5 sec and transferred to 2 mL Eppendorf-tubes. The original tubes were rinsed with 750 µL of quench mix (MeOH:$CHCl_3$:HCl 484:242:23.55 by volume) and then added to the 2 mL-tubes. The tubes were shaken by hand 3 times for 10 sec and sonicated in ultrabath for 30 sec. Subsequently 20 ng of each internal standard (PIP/PIP2 and PIP3) was added to each tube, and a blank tube with only internal standard was also prepared. The tubes were again shaken by hand for 3 times for 10 sec, and let to stand for 5 min. To each tube was added 725 µL $CHCl_3$ and 170 µL 2 M HCl. The tubes were shaken by hand 3 times for 10 sec, and centrifuged at 1500 g for 5 min. The lower phases were transferred to new 2 mL tubes, and 708 µL pre derivatization mix (MeOH:$CHCl_3$:HCl 12:24:9 by volume) was added. The tubes were shaken by hand 2 times for 10 sec, and centrifuged at 1500 g for 3 min. The upper phases (most of it) were removed and discarded, and the lower phases were carefully transferred to new 2 mL tubes. To each tube 50 µL TMS-diazomethane was added. The tubes were let to stand for 10 min, and then 6 µL concentrated acetic acid was added. 700 µL post derivatization mix (MeOH:CHCl3:H2O 12:24:9 by volume) was added, and the tubes were shaken by hand 2 times for 10 sec, and centrifuged at 1500 g for 3 min. The lower phases were transferred to new 2 mL tubes, and 700 µL post derivatization mix was added. The tubes were shaken by hand 2 times for 10 sec, and centrifuged at 1500 g for 3 min. Now the lower phases were transferred to glass tubes, and 100 µL methanol: H_2O (9:1) was added, and the tubes were vortexed and gently concentrated under nitrogen-flow to about 10 µL left. Then 80 µL MeOH was added to each tube, and they were sonicated in ultrabath for 30 sec and transferred to MS-sample vials and after evaporation with nitrogen gas they were stored in the glass tubes at -20 °C. LC-MS: An Agilent triple quad MS (model 6460) was used directly connected to an Agilent HPLC system. PIP/PIP2 and PIP3 samples (in 80:20 MeOH:H_2O) were injected (2 µL) and separated on a C4 column, and introduced to the MS at full scan acquisition. Data were analyzed by the provided software (Agilent MassHunter).

Supplementary Table S1. LC-MS/MS analysis of PtdIns(4,5)P_2 and PtdIns(3,4,5)P_3 in different subcellular fractions of RL95-2 cells.

NQ: non-quantifiable.

PPIn species	Cytoplasm	Nucleus	Nucleolus
PIP3 32:0	0,00	NQ	0,00
PIP3 32:1	0,00	NQ	0,00
PIP3 32:2	0,00	NQ	0,00
PIP3 34:0	0,00	NQ	0,00
PIP3 34:1	0,00	NQ	0,00
PIP2 34:1	**457,73**	NQ	0,00
PIP3 34:2	0,00	NQ	0,00
PIP2 36:1	**511,29**	NQ	0,00
PIP3 36:2	0,00	NQ	0,00
PIP2 36:2	**452,03**	NQ	0,00
PIP3 36:3	0,00	NQ	0,00
PIP3 36:4	0,00	NQ	0,00
PIP3 38:0	0,00	NQ	0,00
PIP2 38:0	0,00	NQ	**30,86**
PIP3 38:1	0,00	NQ	0,00
PIP3 38:2	0,00	NQ	0,00
PIP3 38:3	0,00	NQ	0,00
PIP2 38:3	**749,90**	NQ	**2324,82**
PIP3 38:4	0,00	NQ	**113,15**
PIP2 38:4	512,51	NQ	**1463,64**
PIP3 38:5	0,00	NQ	0,00
PIP3-16:17	0,00	NQ	0,00
PIP3-36:0	0,00	NQ	0,00
PIP3-36:1	0,00	NQ	0,00

Supplementary Table S2. Antibodies used for immunofluorescence (IMF), Immunohistochemistry (IHC) or Western immunoblotting (WB)

Antibody	Catalog number	Company	Dilution
PtdIns(3,4,5)P_3	Z-P345b	Echelon	**IMF:** 1:400
Nucleolin	12247	Cell signaling Technology	**IMF:** 1:100
Nucleophosmin	32-5200	Zymed/Life Tech	**IMF:** 1:1000
PI3K p85α	05-212	Millipore	**WB:** 1:2000
PI3K p85β	S3089	Epitomics	**WB:** 1:5000
PI3K p110α	1683-1 4249	Epitomics Cell signaling Technology	**WB:** 1:5000
PI3K p110β	ab151549 3011	Abcam Cell signaling Technology	**IHC/IMF:** 1:50 **WB:**1:1000
α-Tubulin	T5168	Sigma	**WB:** 1:20000
p-S473-AKT	9271	Cell signaling Technology	**WB:** 1:1000
Total AKT	2920	Cell signaling Technology	**WB:** 1:2000
Lamin A/C	sc-376248	Santa Cruz Biotechnology	**WB**: 1:10000
GST-HRP	ab3416	Abcam	**WB**: 1:30000
Goat anti-Mouse IgG Alexa Fluor 594	A-11005	Thermo Fisher Scientific	**IMF**: 1:200
Goat anti-Rabbit Alexa Fluor 488	A-11008	Thermo Fisher Scientific	**IMF**: 1:200
Calnexin	ab22595	Abcam	**WB:** 1:2000

Supplementary Figure S1

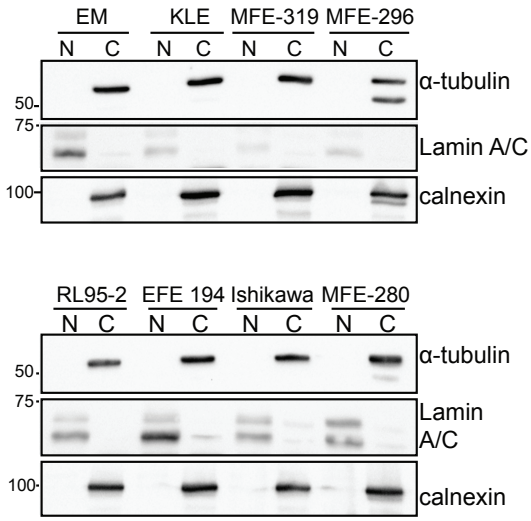

Supplementary Figure S1: Purity of fractionation
Actively growing cells were fractionated into cytoplasmic and nuclear fractions. Equal protein concentrations were resolved by SDS-PAGE and analysed by Western immunoblotting using the antibodies as indicated.

Supplementary Figure S2

MEF-319

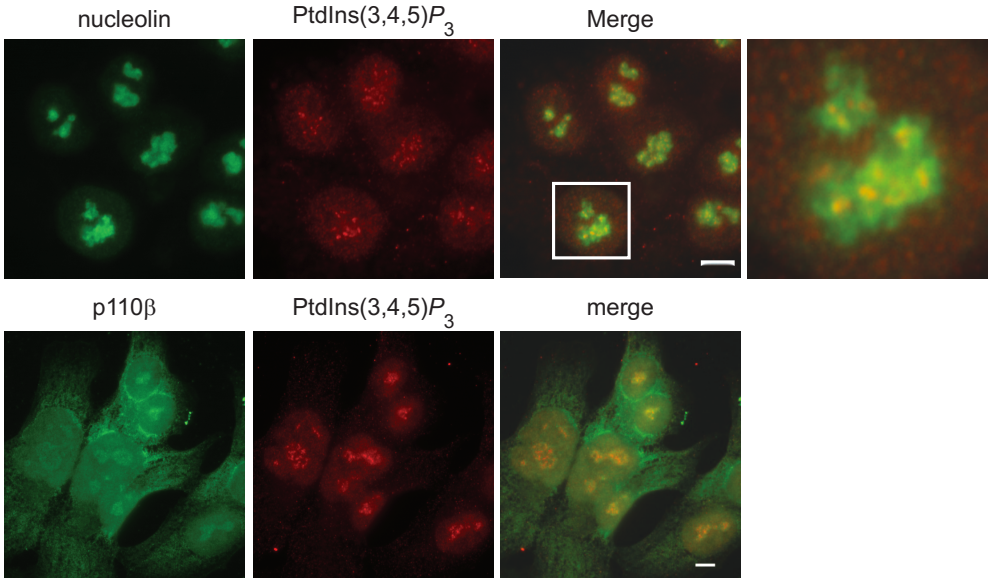

Supplementary Figure S2: p110β and PtdIns(3,4,5)P_3 are nucleolar in MFE-319 cells
Actively growing MFE-319 cells were immunostained using the antibodies as indicated and imaged using epifluorescent microscopy. Scale bars are of 5 μM.

Supplementary Figure S3

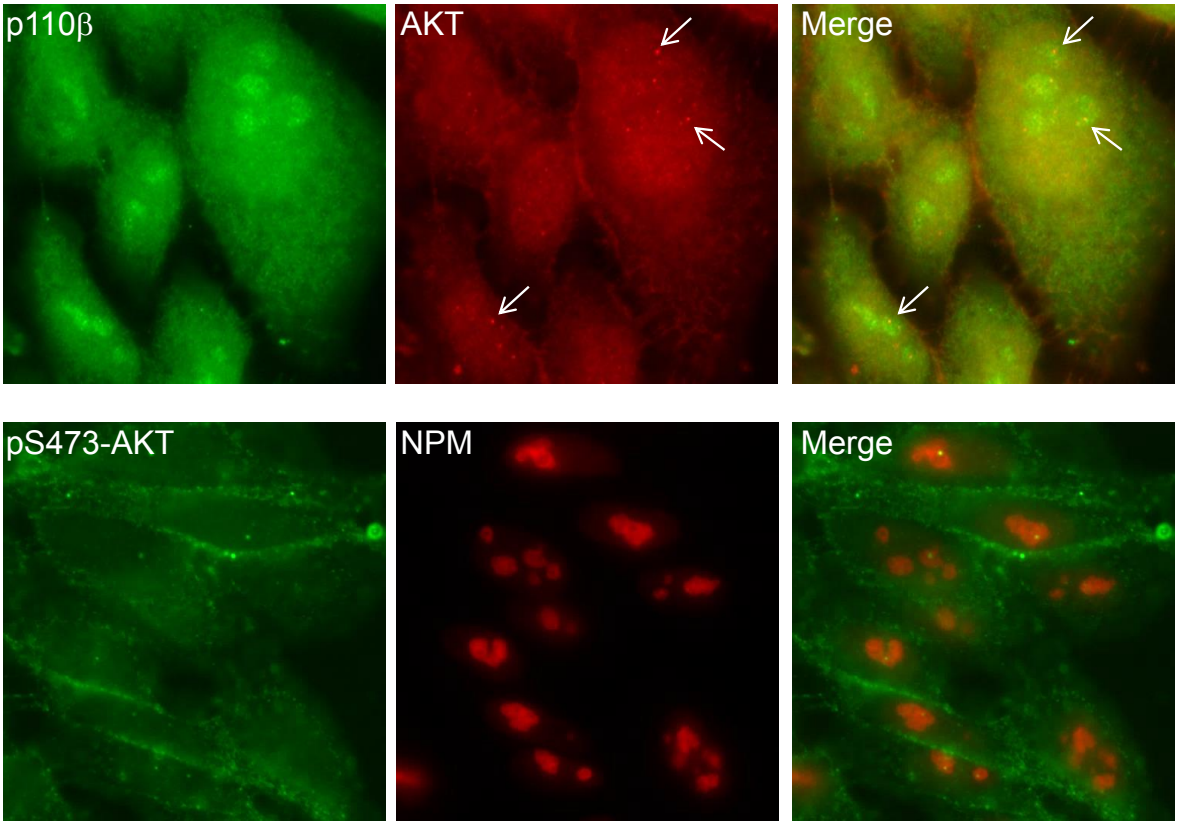

Supplementary Figure S3. AKT and its active form pS473-AKT are nucleolar.
Actively growing RL95-2 cells were co-stained with the indicated antibodies and imaged by epifluorescence microscopy. NPM indicates nucleophosmin.

II

Nuclear phosphatidylinositol 3,4,5-triphosphate interactome

Fatemeh Mazloumi Gavgani[1], Diana C. Turcu[1], Julie Guillermet-Guibert [2], Rein Aasland[3], Clive D'Santos [4] and Aurélia E. Lewis[1*]

[1] Department of Molecular Biology, University of Bergen, Bergen, Norway

[2] Centre de Recherches en Cancérologie de Toulouse (CRCT), Institut National de la Santé et de la Recherche Médicale (INSERM), Université Toulouse III Paul Sabatier, Toulouse, France.

[3] Department of Bioscience, University of Oslo, Oslo, Norway

[4] CRUK Cambridge Institute, Cambridge University, Cambridge, UK.

* To whom correspondence should be addressed:
Aurélia E. Lewis
Department of Molecular Biology
University of Bergen
PO Box 7803, N-5020 Bergen
Norway.
Phone: +47-55584521
E.mail: aurelia.lewis@uib.no.

Abstract

Phosphoinositides (PIs) play essential functions as signalling molecules, either directly or by acting as precursors to other signalling molecules. Although their functions have been mostly elucidated in the cytoplasm, PIs are also intranuclear where they contribute to chromatin remodelling, transcription and mRNA processing. In particular, the PPIn phosphatidylinositol 3,4,5-triphosphate (PtdIns(3,4,5)P_3) and its producing kinase, class I phosphoinositide -3 kinase p110β, have been previously mapped to the nucleus and nucleoli. To gain further insights into the nuclear functions of this PPIn, we applied a previously developed quantitative mass spectrometry-based approach to identify the nuclear targets of PtdIns(3,4,5)P_3. We found 219 potential PtdIns(3,4,5)P_3 interacting proteins that were enriched in RNA processing, cytokinesis and DNA repair functions. Interestingly, many of these interactors were identified as nucleolar proteins, some of which had dual functions in both rRNA transcription and DNA repair. Poly(ADP-Ribose) Polymerase 1 was one of the identified proteins which was then found to interact directly with PtdIns(3,4,5)P_3 and its localization together with this lipid in nucleoli was dependent on active polymerase I transcription. In conclusion, we report a potential role for p110β and its lipid product PtdIns(3,4,5)P_3 in regulating nucleolar function.

Introduction

Polyphosphoinositides (PPIn) are low abundant glycerophospholipids consisting of phosphorylated derivatives of phosphatidylinositol (PtdIns) (PPIn nomenclature from (1)). PtdIns consists of two fatty acyl chains coupled to a glycerol backbone, which is itself bound to a *myo*-inositol group via a phosphodiester linkage (2). The inositol ring can be reversely phosphorylated at the 3', 4' and 5' hydroxyl groups, producing seven different PPIn, *i.e.* the monophosphorylated PtdIns3*P*, PtdIns4*P* and PtdIns5*P*, the diphosphorylated PtdIns(3,4)P_2, PtdIns(3,5)P_2 and PtdIns(4,5)P_2, and finally the triphosphorylated PtdIns(3,4,5)P_3 (2). These lipids are precursors of second messengers or can act directly as signalling molecules. They are synthesised in different subcellular compartments due to the presence of specific PPIn metabolizing kinases and phosphatases (3, 4). Their presence in the nucleus was discovered over three decades ago (5) and the notion of PPIn metabolism and signalling occurring in the nucleus independently of the cytoplasm became evident shortly after in several studies (6-9). With the exception of PtdIns(3,4)P_2 and PtdIns(3,5)P_2, the remaining five PPIn have been

detected or quantified in the nucleus (6, 8, 10-20). Since then, several studies have identified multiple nuclear processes attributed to nuclear PPIn including mRNA processing, splicing and export, chromatin remodelling transcription as well as cell cycle progression (21-27). Nuclear PPIn regulate these processes mostly by interacting with proteins containing polybasic regions (PBR)/K/R motifs (20, 28, 29) rather than structured PPIn-binding domains harboured by cytoplasmic proteins (30).

So far several nuclear PPIn-interacting proteins have been individually identified and characterized (27, 31, 32). In addition, global PPIn interactomics studies have been performed mostly from whole cell extracts to gain further insight into PPIn nuclear roles (33-40). To focus on nuclear PPIn-interacting proteins, nuclear fractionation was then combined to PPIn interactomics (41). Using this approach led to the identification of PtdIns(4,5)P_2 nuclear interacting partners involved in mRNA transcription regulation, mRNA splicing and protein folding (41). Two of these nuclear proteins were further validated to interact directly with PPIn (20, 41). Considering that PtdIns(3,4,5)P_3, a key signalling PPIn, is also present in the nucleus (15, 19) and in particular in the nucleolus together with the class I phosphoinositide - 3 kinase (PI3K) p110β (20), we performed quantitative mass spectrometry-based PtdIns(3,4,5)P_3 interactomics from isolated HeLa nuclei according to the method that we have previously developed (41). We identified 219 potential PtdIns(3,4,5)P_3 interactors with functions highly enriched in RNA processing, mRNA splicing, cytokinesis and DNA repair. Interestingly, 29% of these proteins belonged to the nucleolar database (42), many of which were annotated to the DNA repair category, including the Poly(ADP-Ribose) Polymerase 1 (PARP1) protein.

Results

Both p110β and PtdIns(3,4,5)P_3 localize to the nucleoli in HeLa cells

To extend our previous findings on the nucleolar localisation of p110β and PtdIns(3,4,5)P_3 in the breast cancer cell line AU565 (20), we first determined their exact subcellular localization in HeLa cells by immunofluorescence staining and confocal microscopy using specific antibodies for p110β and PtdIns(3,4,5)P_3 (Figure 1). We found that p110β localized to the cytoplasm and nucleoplasm with strong staining in the nucleoli where it co-localized with the RNA polymerase I subunit RPA194 (Figure 1A). The presence of p110β in these compartments was further validated by Western immunoblotting following the

nucleolar fractionation of HeLa cells. Equal amounts of protein from each cytoplasmic, nucleoplasmic and nucleolar fractions were analysed by western blotting and p110β was detected in all three fractions (Figure 1B). PtdIns(3,4,5)P_3 was also detected in all three cellular compartments by immunofluorescence staining (Figure 1C). The nucleolar staining of PtdIns(3,4,5)P_3 showed intense foci that colocalised with the key nucleolar proteins nucleolin and the transcription factor upstream binding factor (UBF) (Figure 1C). In addition, PtdIns(3,4,5)P_3 and p110β were found to colocalise in the nucleolus in some cells, as indicated with an asterisk, but not in others (Figure 1D). This may suggest that the activation of p110β and the synthesis of PtdIns(3,4,5)P_3 may be cell cycle dependent.

p110β produces the nucleolar pool of PtdIns(3,4,5)P_3 and colocalizes with RNA polymerase I as the cells exit mitosis

p110β is activated during G1 in the nucleus and contributes to G1 to S phase transition (43, 44). In parallel, rRNA transcription oscillates during the cell cycle, as it is lowest during mitosis and is re-activated in G1 phase with highest activity thereafter in S and G2 phases (45). We therefore next examined the appearance of p110β and PtdIns(3,4,5)P_3 during the reformation of nucleoli after mitosis (Figure 2). We performed a combination of nocodazol treatment and mitotic shake-off to synchronize and enrich for mitotic HeLa cells. After re-plating the collected mitotic cells on coverslips, the cells were fixed at different time points and immunostained. After 1 h, the cells were still in mitosis and both p110β and PtdIns(3,4,5)P_3 were present mostly in non-DNA regions. We found that p110β colocalises with RPA194 3 h after replating, as the cells exit mitosis and the nucleoli start to reform. With a lag of up to 2 to 5 h, PtdIns(3,4,5) P_3 started to reappear in the nucleoli. To determine if the pool of PtdIns(3,4,5)P_3 present in the nucleoli is produced due to the kinase activity of p110β, we compared the nucleolar appearance of PtdIns(3,4,5)P_3 in p110β kinase inactive and WT mouse embryonic fibroblast (MEF) cells using the same synchronisation method. Four hours post-replating, cells were labelled with a GFP-GRP1-PH probe and an anti-nucleophosmin antibody as a nucleolar marker (Supplementary Figure S1). In line with our results in HeLa cells, PtdIns(3,4,5)P_3 was detected together with nucleophosmin in the p110β WT MEFs. In contrast, the p110β kinase inactive MEF demonstrated a substantial decrease in PtdIns(3,4,5)P_3 nucleolar staining .

Nuclear PtdIns(3,4,5)P_3-binding proteins are enriched in RNA processing and splicing factors

In order to identify the interacting partners of PtdIns(3,4,5)P_3 in the nucleus we employed a quantitative proteomics method that we have previously developed for the identification of nuclear PtdIns(4,5)P_2 effector proteins (41). Following SILAC labelling of HeLa S3 cells, nuclei were isolated and incubated with neomycin to enrich for and displace potential PPIn-binding proteins from nuclei (Figure 3A). Equal protein amounts obtained from heavy labelled and light labelled cell populations were incubated with PtdIns(3,4,5)P_3-conjugated beads or control beads respectively. The specificity of the PtdIns(3,4,5)P_3 affinity beads was validated by incubating them with GST-tagged PH domain of the GRP1 protein (well known for its affinity to PtdIns(3,4,5)P_3) (46) (Figure 3B). The control beads showed no affinity whereas the PtdIns(3,4,5)P_3 beads were able to pull down the GST-GRP1-PH domain. Importantly, this interaction was competed out by the pre-incubation of free PtdIns(3,4,5)P_3 with the probe. The pull down eluates were combined and separated by polyacrylamide gel electrophoresis (PAGE). Following trypsin digestion, the peptides were analysed by LC-MS/MS and identified and quantified using Proteome explorer. Statistical analyses demonstrated 219 proteins to be specifically pulled down by PtdIns(3,4,5)P_3 including proteins with previous history as PtdIns(3,4,5)P_3 interacting proteins, i.e. nucleophosmin (47) and ALY (48) (Supplementary Table S1). We further examined the presence lysine/arginine rich motif (K/R-($X_{n=3-7}$)-K-X-K/R-K/R), which has previously been reported to be a motif enriched in PtdIns(4,5)P_2-binding proteins (41) and found that 38% of these proteins harbour at least one of them (Supplementary Table S2 and Figure 3C). For a better understanding of the biological processes of these proteins, they were annotated to the Gene Ontology (GO) database for biological processes and enrichment was performed using the PANTHER web tool (49).The biological functions that were over represented by 2 fold are shown in Figure 3D. In particular, RNA splicing, cytokinesis, mRNA processing, induction of apoptosis and DNA repair were functions particularly enriched in the PtdIns(3,4,5)P_3 pull down protein list by over 5 fold. Furthermore, 29% of all potential PtdIns(3,4,5)P_3 interactors are annotated to the nucleolar database and 47% to the T cell nucleome (50) including 28 common to both nucleome lists (Supplementary Table S1).

PtdIns(3,4,5)P_3 co-localizes with PARP1 in the nucleoli

Considering the presence of PtdIns(3,4,5)P_3 in nucleoli, a large number of potential PtdIns(3,4,5)P_3 interacting proteins were also linked or annotated to the nucleolus. Searching

through the literature for clear evidence of nucleolar localization of the PtdIns(3,4,5)P_3-binding protein list, we focused on PARP1, a chromatin-associated protein that is highly abundant in nucleoli (51, 52). PARP1 is one of the thirteen protein annotated to the DNA repair enriched biological process and has a PtdIns(3,4,5)P_3 /control ratio of 1.5 and harbours one K/R motif (Table 1). We first validated the direct interaction of PARP1 with PPIn by lipid overlay assay using phospholipid-immobilized strips and the GST-PARP1 protein (Figure 4A-B). PARP1 was found to interact with all PPIns except PtdIns(3,4)P_2 as well as phosphatidic acid and phosphatidylserine. Furthermore, immunofluorescent staining showed that PtdIns(3,4,5)P_3 co-localizes with PARP1 in the nucleolus of HeLa cells (Figure 4C).

The nucleolar localisation pattern of PtdIns(3,4,5)P_3 is affected by RNA Polymerase I inhibition

To understand the conditions that determine PtdIns(3,4,5) P_3 and PARP1 association in the nucleolus, we inhibited RNA polymerase I transcription by treating HeLa cells with actinomycin D. Three hours of treatment led to the loss of co-localization between PtdIns(3,4,5)P_3 and PARP1. Indeed, PtdIns(3,4,5)P_3 formed a compact structure towards the interior of the nucleoli whereas PARP1 translocated to the periphery of the nucleolus (Figure 5A). It is already known that nucleolar proteins from the fibrillar center and the dense fibrillar component translocate to the perinucleolar caps (clusters found around the nucleolus), or the nucleoplasm upon inhibition of rRNA transcription (52, 53). We also examined the localisation of p110β upon actinomycin D treatment and found that this kinase changed its pattern as well from a relatively homogenous staining within nucleoli (Figure 1A) to a more focused pattern (Figure 5B). Since the nucleolar presence of PARP1 is dependent on active polymerase I transcription (52), these results would suggest that p110β as well as the PtdIns(3,4,5)P_3-PARP1 association in nucleoli rely on active rRNA transcription. To assess that PtdIns(3,4,5)P_3 is indeed involved in rRNA transcription we used a specific p110β inhibitor to reduce the pool of nucleolar PtdIns(3,4,5)P_3. Preliminary results showed a gradual decrease in rRNA transcription level from 18 to 42 hours of treatment (Supplementary Figure S2). These results indicate therefore a potential role for p110β and/or PtdIns(3,4,5) P_3 in ribosomal RNA transcription.

Discussion

Evidence of the presence of PPIn in the nucleus together with their producing kinases is now well established (23, 27, 32, 54, 55). Interestingly, they are found in RNA rich compartments, such as the nuclear speckles and nucleolus in particular for PtdIns(4,5)P_2 (16-18, 56) and PtdIns(3,4,5)P_3 (20). In this study, we have extended our previous findings (20) by showing a common localization of p110β as well as its product PtdIns(3,4,5)P_3 in the nucleolus in an additional cell line, namely HeLa cells. Importantly, we showed that the presence of PtdIns(3,4,5)P_3 in the nucleolus was dependent upon the activity of p110β. To support these findings, a minor pool of PtdIns(4,5)P_2 has been reported in the nucleolus and could hence substantiate the nucleolar synthesis of PtdIns(3,4,5)P_3 (17, 57). In addition, both the PPIn kinase isoforms, PI4K IIα and PIP5K Iα, which synthesise PtdIns 4*P* and PtdIns(4,5)P_2, respectively, were also reported present in the nucleolus (58, 59). Recent studies also identified the PtdIns(3,4,5)P_3 phosphatases PTEN and SHIP1 in the nucleolus (60, 61). All the components allowing a PI3K metabolic cycle to be operational are therefore in place in the nucleolus for the regulation of PtdIns(3,4,5)*P3* synthesis and a potential role in this sub-nuclear compartment. Indeed, a potential role for p110β regulating rRNA transcription is shown in this study using a selective inhibitor. The remaining question about the biophysical existence of PtdIns(3,4,5)*P3* in a non-membranous environment such as the nucleolus is still unanswered. Studies pointing to the existence of different phase environments due to specific arrangements of RNA binding proteins such as nucleophosmin and RNA in the nucleolus may be worth exploring to tackle this issue.

To further decipher the role of nuclear PtdIns(3,4,5)P_3, we applied a PPIn interactomics method that we previously developed but to identify PtdIns(4,5)P_2 effectors (28). To this end, we have identified 219 proteins specific for the PtdIns(3,4,5)P_3 pull down that were highly enriched in RNA processing and splicing factors. The nucleolus, which contains a large amount of rRNA species, is mostly known to be a compartment where rRNA transcription and processing occur (62). However, it is also associated with other functions such as DNA repair (63). Indeed, a growing body of evidence indicates that some of the identified nucleolar DNA repair proteins also possess roles in ribosome biogenesis, such as the nucleophosmin, nucleolin, APEX1 (apurinic/apyrimidinic endodeoxyribonuclease 1), and PARP1 proteins (63-66). Interestingly, among the PtdIns(3,4,5)P_3 interacting proteins identified, there was a 6 fold enrichment of DNA repair proteins listing 13 proteins, ten of which were found in at least one of the nucleolome datasets previously published, including

PARP1 and APEX1. Some of the identified PtdIns(3,4,5)P_3 effector proteins may not be direct binders as some of them do not harbour any PPIn interaction site. They could hence be pulled down as multiprotein complexes. In contrast, PARP1 harbours one K/R motif, binds to PPIn directly and associate with PtdIns(3,4,5)P_3 in the nucleolus. In this case, it may be possible that this PPIn regulates the complex formation of PARP1 with several of these factors.

Nucleophosmin has been shown to bind the DNA binding domains of both PARP-1 and PARP-2 (52) and it is a well-known PtdIns(3,4,5)P_3 interacting protein (47). When cells are not under stress condition, an enrichment of both PARP1 and poly ADP-ribose can be observed in the nucleolus (67). The dense fibrillar component of the nucleolus is where PARP has been shown to localize (68) and our immunofluorescent staining indicate a co-localization with PtdIns(3,4,5)P_3 in this area. Upon RNA polymerase I inhibition, PARP1 delocalizes from the nucleolus, indicating that the presence of PARP1 in the nucleolus is dynamic and dependent on RNA polymerase I transcriptional activity. This delocalization from the nucleolus is accompanied by other nucleolar proteins such as NPM and UBF (52, 69, 70). In this study, inhibition of RNA pol I led to the expected change of pattern for PARP1 but also prevented the colocalisation with PtdIns(3,4,5)P_3, which relocalised to UBF-labelled nucleolar caps. Interestingly, the pattern of localisation of p110β changed dramatically from a diffuse pattern to concentrated foci. Alltogether, these studies suggest that the organisation of proteins and lipids within the nucleolus is affected by the active transcription of rRNAs. Alternatively, PtdIns(3,4,5)P_3, itself may potentially regulate rRNA transcription through its binding to histone H1. Histone H1 is emerging to play important roles in the nucleolar structure and integrity (71). Both PARP1 and NPM are also histone H1 interacting proteins. Histone 1, as a linker histone, plays an important role in forming compact chromatin (72) and its PARylation by PARP1 has been shown to remove H1 from the chromatin, hence causing it to relax (73). NPM binds to histone H1.5 and has a silencing effect on this linker histone (74). At the same time histone H1 has been shown to bind to PtdIns(4,5)P_2 via its C-terminal region can (75). Although we did not study the possible interaction of histone with PtdIns(3,4,5)P_3, this PPIn may form a complex with PARP1, nucleophosmin and H1 to regulate the architecture of the nucleolus to allow transcription to occur.

Materials and methods

Cell culture and SILAC labeling:

HeLa cells were grown in DMEM medium containing 10% fetal bovine serum (FBS) in 5% CO_2 at 37°C. p110β$^{D931A/D931A}$ kinase inactive and p110β$^{WT/WT}$ MEFs were from Dr Julie Guillermet-Guibert (Université Toulouse III-Paul Sabatier, Toulouse, France) and grown in the same medium as HeLa cells. For SILAC (Stable isotope labelling with amino acids in cell culture) labelling, HeLa S3 cells were grown in heavy ($^{13}C_6$,$^{15}N_2$-labelled lysine and $^{13}C_6$, $^{15}N_4$-labelled arginine) or light (unlabelled amino acids) DMEM medium (Silantes, cat# 280001300) supplemented with 10% dialyzed FBS (Silantes, cat# 281000900). To examine the efficiency of SILAC labelling the incorporation of heavy amino acids was validated by LC-MS by Dr Bernd Thiede (University of Oslo, Norway).

Cellular fractionation

The nucleolar isolation was adapted from Lam *et al* 2006 (76). In brief, cells were grown in 10 x 15 cm dishes up to 70% confluency. 1 hour after adding fresh medium, the cells were washed, trypsinized and washed again 3 times (this time with ice cold PBS). The cell pellet was re-suspended in 5 ml of buffer A (10 mM HEPES pH 7.9, 1.5 mM $MgCl_2$, 10 mM KCl, 0,5mM DDT, 1 % Igepal and protease inhibitor cocktail) and incubated on ice for 5 min. The cells were then passed 12 times through a 23-gauge needle to disrupt the cell membrane. The lysates were then centrifuged at 218x g for 5 min at 4 °C. The supernatant was collected as the cytosolic fraction and the pellet containing the nuclei was re-suspended in 3 ml of buffer S1 (0.25 M sucrose, 10 mM $MgCl_2$ and protease inhibitor cocktail) and layered over 3ml of buffer S2 (0.35 M sucrose, 0.5 mM $MgCl_2$ and protease inhibitor cocktail) and centrifuged at 1430xg for 5 min (4 °C). The supernatant was removed and the pellet was re-suspended in 3 ml of buffer S2 and sonicated 7 times 10 sec on/10 sec off on ice. The nuclear lysate was layered over 3 ml of S3 (0.88 M Sucrose, 0.5 mM $MgCl_2$ and protease inhibitor cocktail) and Centrifuged at 3000xg for 10 min (4°C). The nucleoplasmic fraction (3 ml of the top layer) was collected and the nucleoli pellet was washed once with 500 µl of the S2 buffer.

Neomycin extraction and PtdIns(3,4,5)P_3 pull down

Nuclei were isolated and washed with retention buffer containing 20 mM Tris pH 7.5, 70 mM NaCl, 20 mM KCl, 5 mM $MgCl_2$, 3 mM $CaCl_2$ and protease inhibitor cocktail. The nuclei were then incubated with freshly prepared 5 mM neomycin (Neomycin trisulfate salt, Sigma-Aldrich) in retention buffer, rotating for 30 min at RT. After centrifugation at 13000 rpm for 5 min, the supernatant containing the neomycin-displaced protein extract was collected. Neomycin supernatants were dialysed three times in 900 ml of cold lipid pulldown buffer containing 20 mM HEPES pH 7.5, 150 mM NaCl, 5 mM EDTA, 0.1 % Igepal using Slide-A-Lyser Mini dialysis units (Thermo Fisher) for 1 h at 4°C each time. The protein concentration was measured using BCA (bicinchoninic acid) protein assay (ThermoFisher Scientific) and equal amount of extracts were used for each lipid pulldown. The GST-GRP1-PH protein was expressed as previously described (28). The heavy extracts were incubated with PtdIns(3,4,5)P_3 beads (Echelon Biosciences p-B345a) and the light extracts were incubated with control beads (Echelon Biosciences P-B000) for 1 hour rotating at 4°C. The beads were then washed 3x with the lipid pulldown buffer containing phosphatase (5mM β-glycerophosphate, 5 mM NaF and 2 mM Na_3VO_4) and protease inhibitor cocktail. For testing the efficiency of the lipid pull downs GST-GRP1-PH (purified as described in (41)) was used combined with a competition with free 20μM PtdIns(3,4,5)P_3 diC8 (Echelon p-3908).

Proteomics

In-gel digestion

In-gel trypsin digestion was performed as described (77) with some modifications. Briefly, the Coomassie brilliant blue-stained protein bands were excised, and following several washes, the gel pieces were subjected to a reduction step using 10 mM DTT in 100 mM ammonium bicarbonate (NH_4HCO_3) buffer for 45 min at 56°C. Alkylation was performed with 55 mM iodoacetamide in 100 mM NH_4HCO_3 for 30 min at room temperature in the dark. Digestion was performed with 10 μl of trypsin (10 mg/l in 50 mM NH_4HCO_3) overnight at 37^0C. Eluted peptides were recovered, and the gel pieces were subsequently washed in 2.5% formic acid/80% acetonitrile for 30 min at 37^0C. The acid wash was combined with the original peptide eluate and dried. Samples were resuspended in 0.1% formic acid and analysed directly by nano-LC-MS/MS.

Nano LC-MSMS

Digested peptide mixtures were analysed by nano-LC-MS/MS. Mass spectrometry (MS) was performed using a QExactive HF (Thermo Scientific) coupled to an Ultimate

RSLCnano-LC system (Dionex). Optimal separation conditions resulting in maximal peptide coverage were achieved using an Acclaim PepMap 100 column (C18, 3 μm, 100 Å) (Dionex) with an internal diameter of 75 μm and capillary length of 25 cm. A flow rate of 300 nl/min was used with a solvent gradient of 5% B to 45% B in 85 min followed by increasing the gradient to 95% B over 5 min. Solvent A was 0.1% (v/v) formic acid, 5%DMSO in water, whereas the composition of solvent B was 80% (v/v) acetonitrile, 0.1% (v/v) formic acid, 5% DMSO in water.

The mass spectrometer was operated in positive ion mode using an N^{th} order double-play method to automatically switch between Full scan acquisition of peptide precursor ions and HCD generated fragments both using the Orbitrap mass analyser. Survey full-scan MS spectra (from 400 to 1,600 m/z) were acquired in the Orbitrap with resolution (R) 60,000 at 400 m/z (after accumulation to a target of 3,000,000 charges). The method used allowed sequential isolation of the 10 most intense ions for fragmentation, depending on signal intensity, using HCD at a target value of 20,000 charges and resolution of 30,000. Target ions already selected for MS/MS were dynamically excluded for 30 s. Unassigned and 1+ charges were excluded from fragmentation selection. General MS conditions were electrospray voltage, 2.5 kV with no sheath or auxiliary gas flow, an ion selection threshold of 2,000 counts for MS/MS, an activation Q value of 0.25, activation time of 12 ms, capillary temperature of 200^0C, and an S-Lens RF level of 60% were also applied. Charge state screening was enabled, and precursors with unknown charge state or a charge state of 1 were excluded. Raw MS data files were processed using Proteome Discoverer v.2.1 (Thermo Scientific). Processed files were searched against the SwissProt human database using the Mascot search engine version 2.3.0. Searches were done with tryptic specificity allowing up to one missed cleavage and a tolerance on mass measurement of 10 ppm in MS mode and 20 ppm for MS/MS ions. Structure modifications allowed were oxidized methionine, and deamidation of asparagine and glutamine residues, which were searched as variable modifications. Using a reversed decoy database, false discovery rate (FDR) was less than 1%.

Cell synchronization

HeLa cells grown up to 70% confluency were treated with 50 ng/mL of nocodazole for 16 h. After treatment most of the growth medium was removed from the cells and transferred to a 50 ml tube leaving only 3 ml on the dish. The mitotic cells were collected by mechanical shake-off and transferred to a centrifuge tube. The shake-off procedure was repeated by adding 10 ml PBS and was added to the same centrifugation tube. The cells were pelleted by

centrifugation at 70 g for 5 min. After washing the pellet twice with 10 ml of growth medium the cell pellet was re-suspended in growth medium again and plated on cell culture dishes with coverslips covered with poly-L-Lysine. The cells were collected at different time points after re-plating.

Immunofluorescence staining

HeLa cells grown on 12 mm coverslips were fixed with 3.7 % paraformaldehyde for 10 min and washed twice with PBS and then permeabilised with 0.25 % Triton X-100 in PBS for 10 min at room temperature. Cells were blocked for 1 h with 5% goat serum in PBS- 0.1% Triton. Primary antibody (diluted in blocking buffer) incubation was performed overnight at 4°C followed by secondary antibody conjugated to Alexa-488 or Alexa-594 incubation for 1 h at room temperature. Washes were performed with PBS-T (0.05% Tween20), between each antibody incubation. Nucleic acid staining was performed by 15 min incubation with Hoechst 33342 diluted in PBS. For antibody dilutions, see the supplementary Table S3.

SDS-PAGE and Western Immunoblotting

Proteins were resolved by SDS-PAGE and then transferred to nitrocellulose membranes. The membrane was then blocked with 7% milk in PBS-T (PBS pH 7.4, 0.05 % Tween-20) for 1 hour at room temperature before incubation with primary antibodies overnight at 4°C (for antibody dilutions see the supplementary Table S3). After washing with PBS-T, the membrane was incubated with HRP conjugated secondary antibodies for 1 hour at room temperature. The enhanced chemiluminescence (ThermoFisher Scientific) was added and the Chemidoc XRS+ imaging system from Bio-Rad was used for visualization.

Lipid overlay assay

Lipid overlay assay were performed according to Karlson *et al* (20) using 0.5 µg/mL of recombinant GST (purified as described in (20)) or GST-PARP1 obtained from BPS Bioscience.

Table 1. List of potential PtdIns(3,4,5)P_3 binding protein annotated to DNA repair.
Proteins pulled down by PtdIns(3,4,5)P_3 and annotated to the DNA repair enriched process, identified with at least 2 peptides, with heavy/light log2 ratios >0.5, are indicated in this table. Their presence (+) or absence (-) in the nucleolar database (NoDB) (42), the T cell nucleome (50) and/or the HeLa nucleome (78) is indicated.

Uniprot ID	Name description	Gene symbol	Ratio	K/R motif	No DB	T cell	HeLa
P46063	ATP-dependent DNA helicase Q1	RECQL	2.271	KNTGAKKRK	-	+	-
Q09028	Histone-binding protein RBBP4	RBBP4	2.3	-	-	+	-
Q16531	DNA damage-binding protein 1	DDB1	2.101	-	-	+	-
P29372	DNA-3-methyladenine glycosylase	MPG	18.81	-	+	-	-
P78527	DNA-dependent protein kinase catalytic subunit	PRKDC	2.112	KHVSLNKAKKRR	-	+	-
P49916	DNA ligase 3	LIG3	2.119	KRHWLKVKK	-	+	-
O60934	Nibrin	NBN	1.575	KNFKKFKK RYNPYLKRRR KEEEEEEKPKR KKEEIKDEKIKK	-	-	-
P09874	**Poly [ADP-ribose] polymerase 1**	**PARP1**	1.5	RWDDQQKVKK	+	+	-
Q9BQ67	Glutamate-rich WD repeat-containing protein 1	GRWD1	3.158	-	-	-	+
Q14683	Structural maintenance of chromosomes protein 1A	SMC1A	1.772	KVEDELKEKK KHYKKRK KAVDKLKEKK RNIREFEEEKVKR KKDENEIEKLKK	-	+	-
Q92466	DNA damage-binding protein 2	DDB2	2.474	-	-	-	-
P27695	DNA-(apurinic or apyrimidinic site) lyase	APEX1	3.9	-	+	-	-
Q16576	Histone-binding protein RBBP7	RBBP7	2.003	-	-	-	-

Acknowledgments

We would like to thank Dr Bernd Thiede (University of Oslo, Norway) for validating the efficiency of the incorporation of heavy amino acids for SILAC labelling. This project was funded by the University of Bergen and the Meltzer foundation.

References

1. Michell RH, Heath VL, Lemmon MA, Dove SK. Phosphatidylinositol 3,5-bisphosphate: metabolism and cellular functions. Trends Biochem Sci. 2006;31(1):52-63.
2. Maffucci T. An introduction to phosphoinositides. Current topics in microbiology and immunology. 2012;362:1-42.
3. Viaud J, Mansour R, Antkowiak A, Mujalli A, Valet C, Chicanne G, et al. Phosphoinositides: Important lipids in the coordination of cell dynamics. Biochimie. 2016;125:250-8.
4. Schink KO, Tan KW, Stenmark H. Phosphoinositides in Control of Membrane Dynamics. Annu Rev Cell Dev Biol. 2016;32:143-71.
5. Smith CD, Wells WW. Phosphorylation of rat liver nuclear envelopes. II. Characterization of in vitro lipid phosphorylation. The Journal of biological chemistry. 1983;258(15):9368-73.
6. Cocco L, Gilmour RS, Ognibene A, Letcher AJ, Manzoli FA, Irvine RF. Synthesis of polyphosphoinositides in nuclei of Friend cells. Evidence for polyphosphoinositide metabolism inside the nucleus which changes with cell differentiation. The Biochemical journal. 1987;248(3):765-70.
7. Cocco L, Martelli AM, Gilmour RS, Ognibene A, Manzoli FA, Irvine RF. Rapid changes in phospholipid metabolism in the nuclei of Swiss 3T3 cells induced by treatment of the cells with insulin-like growth factor I. Biochem Biophys Res Commun. 1988;154(3):1266-72.
8. Divecha N, Banfic H, Irvine RF. The polyphosphoinositide cycle exists in the nuclei of Swiss 3T3 cells under the control of a receptor (for IGF-I) in the plasma membrane, and stimulation of the cycle increases nuclear diacylglycerol and apparently induces translocation of protein kinase C to the nucleus. Embo J. 1991;10(11):3207-14.
9. Martelli AM, Gilmour RS, Neri LM, Manzoli L, Corps AN, Cocco L. Mitogen-stimulated events in nuclei of Swiss 3T3 cells. Evidence for a direct link between changes of inositol lipids, protein kinase C requirement and the onset of DNA synthesis. FEBS Lett. 1991;283(2):243-6.
10. Vann LR, Wooding FB, Irvine RF, Divecha N. Metabolism and possible compartmentalization of inositol lipids in isolated rat-liver nuclei. Biochem J. 1997;327 (Pt 2):569-76.
11. Clarke JH, Letcher AJ, D'Santos C S, Halstead JR, Irvine RF, Divecha N. Inositol lipids are regulated during cell cycle progression in the nuclei of murine erythroleukaemia cells. Biochem J. 2001;357(Pt 3):905-10.
12. Jones DR, Bultsma Y, Keune WJ, Halstead JR, Elouarrat D, Mohammed S, et al. Nuclear PtdIns5P as a transducer of stress signaling: an in vivo role for PIP4Kbeta. Molecular cell. 2006;23(5):685-95.
13. Sarkes D, Rameh LE. A novel HPLC-based approach makes possible the spatial characterization of cellular PtdIns5P and other phosphoinositides. Biochem J. 2010;428:375-84.
14. Gillooly DJ, Morrow IC, Lindsay M, Gould R, Bryant NJ, Gaullier JM, et al. Localization of phosphatidylinositol 3-phosphate in yeast and mammalian cells. The EMBO journal. 2000;19(17):4577-88.

15. Lindsay Y, McCoull D, Davidson L, Leslie N, Fairservice A, Gray A, et al. Localization of agonist-sensitive PtdIns(3,4,5)P3 reveals a nuclear pool that is insensitive to PTEN expression. Journal of cell science. 2006;119(Pt 24):5160-8.
16. Boronenkov IV, Loijens JC, Umeda M, Anderson RA. Phosphoinositide signaling pathways in nuclei are associated with nuclear speckles containing pre-mRNA processing factors. Molecular biology of the cell. 1998;9(12):3547-60.
17. Osborne SL, Thomas CL, Gschmeissner S, Schiavo G. Nuclear PtdIns(4,5)P2 assembles in a mitotically regulated particle involved in pre-mRNA splicing. J Cell Sci. 2001;114(Pt 13):2501-11.
18. Watt SA, Kular G, Fleming IN, Downes CP, Lucocq JM. Subcellular localization of phosphatidylinositol 4,5-bisphosphate using the pleckstrin homology domain of phospholipase C delta1. Biochem J. 2002;363(Pt 3):657-66.
19. Kwon IS, Lee KH, Choi JW, Ahn JY. PI(3,4,5)P3 regulates the interaction between Akt and B23 in the nucleus. BMB reports. 2010;43(2):127-32.
20. Karlsson T, Altankhuyag A, Dobrovolska O, Turcu DC, Lewis AE. A polybasic motif in ErbB3-binding protein 1 (EBP1) has key functions in nucleolar localization and polyphosphoinositide interaction. Biochem J. 2016;473(14):2033-47.
21. Irvine RF. Nuclear lipid signalling. Nat Rev Mol Cell Biol. 2003;4(5):349-60.
22. Okada M, Ye K. Nuclear phosphoinositide signaling regulates messenger RNA export. RNA Biol. 2009;6(1):12-6.
23. Martelli AM, Ognibene A, Buontempo F, Fini M, Bressanin D, Goto K, et al. Nuclear phosphoinositides and their roles in cell biology and disease. Critical reviews in biochemistry and molecular biology. 2011;46(5):436-57.
24. Viiri K, Maki M, Lohi O. Phosphoinositides as regulators of protein-chromatin interactions. Sci Signal. 2012;5(222):pe19.
25. Musille PM, Kohn JA, Ortlund EA. Phospholipid--driven gene regulation. FEBS Lett. 2013;587(8):1238-46.
26. Davis WJ, Lehmann PZ, Li W. Nuclear PI3K signaling in cell growth and tumorigenesis. Front Cell Dev Biol. 2015;3:24.
27. Hamann BL, Blind RD. Nuclear phosphoinositide regulation of chromatin. Journal of cellular physiology. 2018;233(1):107-23.
28. Lewis AE, Sommer L, Arntzen MO, Strahm Y, Morrice NA, Divecha N, et al. Identification of nuclear phosphatidylinositol 4,5-bisphosphate-interacting proteins by neomycin extraction. Mol Cell Proteomics. 2011;10(2):M110 003376.
29. Bidlingmaier S, Wang Y, Liu Y, Zhang N, Liu B. Comprehensive analysis of yeast surface displayed cDNA library selection outputs by exon microarray to identify novel protein-ligand interactions. Mol Cell Proteomics. 2011;10(3):M110 005116.
30. Hammond GR, Balla T. Polyphosphoinositide binding domains: Key to inositol lipid biology. Biochim Biophys Acta. 2015;1851(6):746-58.
31. Schramp M, Hedman A, Li W, Tan X, Anderson R. PIP Kinases from the Cell Membrane to the Nucleus. Sub-cellular biochemistry. 2012;58:25-59.
32. Shah ZH, Jones DR, Sommer L, Foulger R, Bultsma Y, D'Santos C, et al. Nuclear phosphoinositides and their impact on nuclear functions. The FEBS journal. 2013;280(24):6295-310.
33. Catimel B, Schieber C, Condron M, Patsiouras H, Connolly L, Catimel J, et al. The PI(3,5)P2 and PI(4,5)P2 interactomes. J Proteome Res. 2008;7(12):5295-313.
34. Catimel B, Yin MX, Schieber C, Condron M, Patsiouras H, Catimel J, et al. PI(3,4,5)P3 Interactome. Journal of proteome research. 2009;8(7):3712-26.
35. Catimel B, Kapp E, Yin MX, Gregory M, Wong LS, Condron M, et al. The PI(3)P interactome from a colon cancer cell. J Proteomics. 2013;82:35-51.
36. Osborne SL, Wallis TP, Jimenez JL, Gorman JJ, Meunier FA. Identification of secretory granule phosphatidylinositol 4,5-bisphosphate-interacting proteins using an affinity pulldown strategy. Mol Cell Proteomics. 2007;6(7):1158-69.

37. Pasquali C, Bertschy-Meier D, Chabert C, Curchod ML, Arod C, Booth R, et al. A chemical proteomics approach to phosphatidylinositol 3-kinase signaling in macrophages. Mol Cell Proteomics. 2007;6(11):1829-41.
38. Dixon MJ, Gray A, Boisvert FM, Agacan M, Morrice NA, Gourlay R, et al. A screen for novel phosphoinositide 3-kinase effector proteins. Mol Cell Proteomics. 2011;10(4):M110 003178.
39. Rowland MM, Bostic HE, Gong D, Speers AE, Lucas N, Cho W, et al. Phosphatidylinositol 3,4,5-trisphosphate activity probes for the labeling and proteomic characterization of protein binding partners. Biochemistry. 2011;50(51):11143-61.
40. Jungmichel S, Sylvestersen KB, Choudhary C, Nguyen S, Mann M, Nielsen ML. Specificity and commonality of the phosphoinositide-binding proteome analyzed by quantitative mass spectrometry. Cell reports. 2014;6(3):578-91.
41. Lewis AE, Sommer L, Arntzen MO, Strahm Y, Morrice NA, Divecha N, et al. Identification of nuclear phosphatidylinositol 4,5-bisphosphate-interacting proteins by neomycin extraction. Molecular & cellular proteomics : MCP. 2011;10(2):M110.003376.
42. Scott MS, Troshin PV, Barton GJ. NoD: a Nucleolar localization sequence detector for eukaryotic and viral proteins. BMC bioinformatics. 2011;12:317.
43. Marques M, Kumar A, Cortes I, Gonzalez-Garcia A, Hernandez C, Moreno-Ortiz MC, et al. Phosphoinositide 3-kinases p110alpha and p110beta regulate cell cycle entry, exhibiting distinct activation kinetics in G1 phase. Molecular and cellular biology. 2008;28(8):2803-14.
44. Marques M, Kumar A, Poveda AM, Zuluaga S, Hernandez C, Jackson S, et al. Specific function of phosphoinositide 3-kinase beta in the control of DNA replication. Proc Natl Acad Sci U S A. 2009;106(18):7525-30.
45. Grummt I. Life on a planet of its own: regulation of RNA polymerase I transcription in the nucleolus. Genes Dev. 2003;17(14):1691-702.
46. Guillou H, Lecureuil C, Anderson KE, Suire S, Ferguson GJ, Ellson CD, et al. Use of the GRP1 PH domain as a tool to measure the relative levels of PtdIns(3,4,5)P3 through a protein-lipid overlay approach. J Lipid Res. 2007;48(3):726-32.
47. Ahn JY, Liu X, Cheng D, Peng J, Chan PK, Wade PA, et al. Nucleophosmin/B23, a nuclear PI(3,4,5)P(3) receptor, mediates the antiapoptotic actions of NGF by inhibiting CAD. Molecular cell. 2005;18(4):435-45.
48. Okada M, Jang SW, Ye K. Akt phosphorylation and nuclear phosphoinositide association mediate mRNA export and cell proliferation activities by ALY. Proc Natl Acad Sci U S A. 2008;105(25):8649-54.
49. Mi H, Muruganujan A, Casagrande JT, Thomas PD. Large-scale gene function analysis with the PANTHER classification system. Nat Protoc. 2013;8(8):1551-66.
50. Jarboui MA, Wynne K, Elia G, Hall WW, Gautier VW. Proteomic profiling of the human T-cell nucleolus. Mol Immunol. 2011;49(3):441-52.
51. Calkins AS, Iglehart JD, Lazaro JB. DNA damage-induced inhibition of rRNA synthesis by DNA-PK and PARP-1. Nucleic acids research. 2013;41(15):7378-86.
52. Meder VS, Boeglin M, de Murcia G, Schreiber V. PARP-1 and PARP-2 interact with nucleophosmin/B23 and accumulate in transcriptionally active nucleoli. Journal of cell science. 2005;118(Pt 1):211-22.
53. van Sluis M, McStay B. Nucleolar reorganization in response to rDNA damage. Current opinion in cell biology. 2017;46:81-6.
54. Barlow CA, Laishram RS, Anderson RA. Nuclear phosphoinositides: a signaling enigma wrapped in a compartmental conundrum. Trends in cell biology. 2010;20(1):25-35.
55. Fiume R, Keune WJ, Faenza I, Bultsma Y, Ramazzotti G, Jones DR, et al. Nuclear phosphoinositides: location, regulation and function. Sub-cellular biochemistry. 2012;59:335-61.
56. Tabellini G, Bortul R, Santi S, Riccio M, Baldini G, Cappellini A, et al. Diacylglycerol kinase-theta is localized in the speckle domains of the nucleus. Exp Cell Res. 2003;287(1):143-54.

57. Yildirim S, Castano E, Sobol M, Philimonenko VV, Dzijak R, Venit T, et al. Involvement of phosphatidylinositol 4,5-bisphosphate in RNA polymerase I transcription. Journal of cell science. 2013;126(Pt 12):2730-9.
58. Chakrabarti R, Sanyal S, Ghosh A, Bhar K, Das C, Siddhanta A. Phosphatidylinositol-4-phosphate 5-Kinase 1alpha Modulates Ribosomal RNA Gene Silencing through Its Interaction with Histone H3 Lysine 9 Trimethylation and Heterochromatin Protein HP1-alpha. The Journal of biological chemistry. 2015;290(34):20893-903.
59. Kakuk A, Friedlander E, Vereb G, Jr., Kasa A, Balla A, Balla T, et al. Nucleolar localization of phosphatidylinositol 4-kinase PI4K230 in various mammalian cells. Cytometry Part A : the journal of the International Society for Analytical Cytology. 2006;69(12):1174-83.
60. Ehm P, Nalaskowski MM, Wundenberg T, Jucker M. The tumor suppressor SHIP1 colocalizes in nucleolar cavities with p53 and components of PML nuclear bodies. Nucleus (Austin, Tex). 2015;6(2):154-64.
61. Li P, Wang D, Li H, Yu Z, Chen X, Fang J. Identification of nucleolus-localized PTEN and its function in regulating ribosome biogenesis. Molecular biology reports. 2014;41(10):6383-90.
62. Boisvert FM, van Koningsbruggen S, Navascues J, Lamond AI. The multifunctional nucleolus. Nature reviews Molecular cell biology. 2007;8(7):574-85.
63. Ogawa LM, Baserga SJ. Crosstalk between the nucleolus and the DNA damage response. Molecular bioSystems. 2017;13(3):443-55.
64. Scott DD, Oeffinger M. Nucleolin and nucleophosmin: nucleolar proteins with multiple functions in DNA repair. Biochemistry and cell biology = Biochimie et biologie cellulaire. 2016;94(5):419-32.
65. Boamah EK, Kotova E, Garabedian M, Jarnik M, Tulin AV. Poly(ADP-Ribose) polymerase 1 (PARP-1) regulates ribosomal biogenesis in Drosophila nucleoli. PLoS genetics. 2012;8(1):e1002442.
66. Box JK, Paquet N, Adams MN, Boucher D, Bolderson E, O'Byrne KJ, et al. Nucleophosmin: from structure and function to disease development. BMC Mol Biol. 2016;17(1):19.
67. Rancourt A, Satoh MS. Delocalization of nucleolar poly(ADP-ribose) polymerase-1 to the nucleoplasm and its novel link to cellular sensitivity to DNA damage. DNA repair. 2009;8(3):286-97.
68. Fakan S, Leduc Y, Lamarre D, Brunet G, Poirier GG. Immunoelectron microscopical distribution of poly(ADP-ribose)polymerase in the mammalian cell nucleus. Experimental Cell Research. 1988;179(2):517-26.
69. Brodska B, Holoubek A, Otevrelova P, Kuzelova K. Low-Dose Actinomycin-D Induces Redistribution of Wild-Type and Mutated Nucleophosmin Followed by Cell Death in Leukemic Cells. J Cell Biochem. 2016;117(6):1319-29.
70. Jordan P, Mannervik M, Tora L, Carmo-Fonseca M. In vivo evidence that TATA-binding protein/SL1 colocalizes with UBF and RNA polymerase I when rRNA synthesis is either active or inactive. The Journal of cell biology. 1996;133(2):225-34.
71. Szerlong HJ, Herman JA, Krause CM, DeLuca JG, Skoultchi A, Winger QA, et al. Proteomic characterization of the nucleolar linker histone H1 interaction network. Journal of molecular biology. 2015;427(11):2056-71.
72. Thoma F, Koller T, Klug A. Involvement of histone H1 in the organization of the nucleosome and of the salt-dependent superstructures of chromatin. The Journal of cell biology. 1979;83(2 Pt 1):403-27.
73. Sellou H, Lebeaupin T, Chapuis C, Smith R, Hegele A, Singh HR, et al. The poly(ADP-ribose)-dependent chromatin remodeler Alc1 induces local chromatin relaxation upon DNA damage. Molecular biology of the cell. 2016;27(24):3791-9.
74. Holmberg Olausson K, Elsir T, Moazemi Goudarzi K, Nister M, Lindstrom MS. NPM1 histone chaperone is upregulated in glioblastoma to promote cell survival and maintain nucleolar shape. Scientific reports. 2015;5:16495.
75. Yu H, Fukami K, Watanabe Y, Ozaki C, Takenawa T. Phosphatidylinositol 4,5-bisphosphate reverses the inhibition of RNA transcription caused by histone H1. European journal of biochemistry. 1998;251(1-2):281-7.

76. Lam Y, I. Lamond A. Isolation of Nucleoli2006. 103-7 p.
77. Mohammed H, D'Santos C, Serandour AA, Ali HR, Brown GD, Atkins A, et al. Endogenous purification reveals GREB1 as a key estrogen receptor regulatory factor. Cell reports. 2013;3(2):342-9.
78. Boisvert FM, Ahmad Y, Gierlinski M, Charriere F, Lamont D, Scott M, et al. A quantitative spatial proteomics analysis of proteome turnover in human cells. Mol Cell Proteomics. 2012;11(3):M111 011429.

Figure legends

Figure 1. p110β and PtdIns(3,4,5)P_3 are nucleolar.

(A, C, D) Co-immunostaining of HeLa cells was performed with the indicated antibodies and imaged by confocal microscopy. RPA194 indicates RNA polymerase I subunit, PIP3; PtdIns(3,4,5)P_3; UBF, upstream binding factor. Scale bar represents 5μm. (B) HeLa cells were fractionated into cytosolic, nucleoplasmic and nucleolar fractions. Equal amounts of proteins (60 μg) were separated by SDS-PAGE and western immunoblotting was performed using antibodies for the specified proteins.

Figure 2. Co-localization of p110β with RNA polymerase I at the exit of mitosis.

HeLa cells were treated with nocodazole (50 ng/ mL) for 16 hours before mitotic cells were collected by shake-off. The collected mitotic cells were re-plated on cover slips covered with poly-L-Lysine and fixed at the different time points as indicated. Immunofluorescent staining was then performed with the indicated antibodies and imaged by confocal microscopy. Scale bar represents 10μm.

Figure 3. Nuclear PtdIns(3,4,5)P_3 interactome.

(A) The experimental setup is shown where the SILAC labelled and unlabelled HeLa S3 nuclei are incubated with 5 mM neomycin and the displaced proteins are pull down using control beads or PtdIns(3,4,5)P_3 conjugated beads and subsequently analysed by LC-MS/MS. (B) GST-GRP1-PH (2 μg) pull down with control or PtdIns(3,4,5)P_3 conjugated beads with or without 20 μM free PtdIns(3,4,5)P_3. Eluates were western immunoblotted using an anti-GST antibody conjugated to horse radish peroxidase. (C) Biological processes Gene ontology enrichment of the proteins pulled down specifically by the PtdIns(3,4,5)P_3 conjugated beads.

Figure 4. PtdIns(3,4,5)P3 colocalises with PARP1 in the nucleolus.

(A) PIP strip schematic showing the positions of the spotted lipids (www.echelon-inc.com). LPA, lysophosphatidic acid; LPC, lysophosphatidylcholine; PI, phosphatidylinositol; PE, phosphatidylethanolamine; PC, phosphatidylcholine; S1P, sphingosine-1-phosphate; PA, phosphatidic acid; PS, phosphatidylserine. (B) PIP strips incubated with recombinant GST or GST-PARP1 and detection of protein-lipid interactions using an anti-GST-HRP conjugated antibody. (C) HeLa cells co-stained with anti-PARP1 and PtdIns(3,4,5)P_3 antibodies and imaged by confocal microscopy. Scale bar represents 20μm in the top image and 10μm in the bottom image.

Figure 5. Inhibition of RNA polymerase I leads to altered nucleolar patterns of PARP1, PtdIns(3,4,5)P_3 and p110β. Co-immunostaining of HeLa cells treated with 200 ng/mL actinomycin D for 3 h with indicated antibodies and confocal microscopy imaging. Scale bar indicates 5μm.

Figure 1

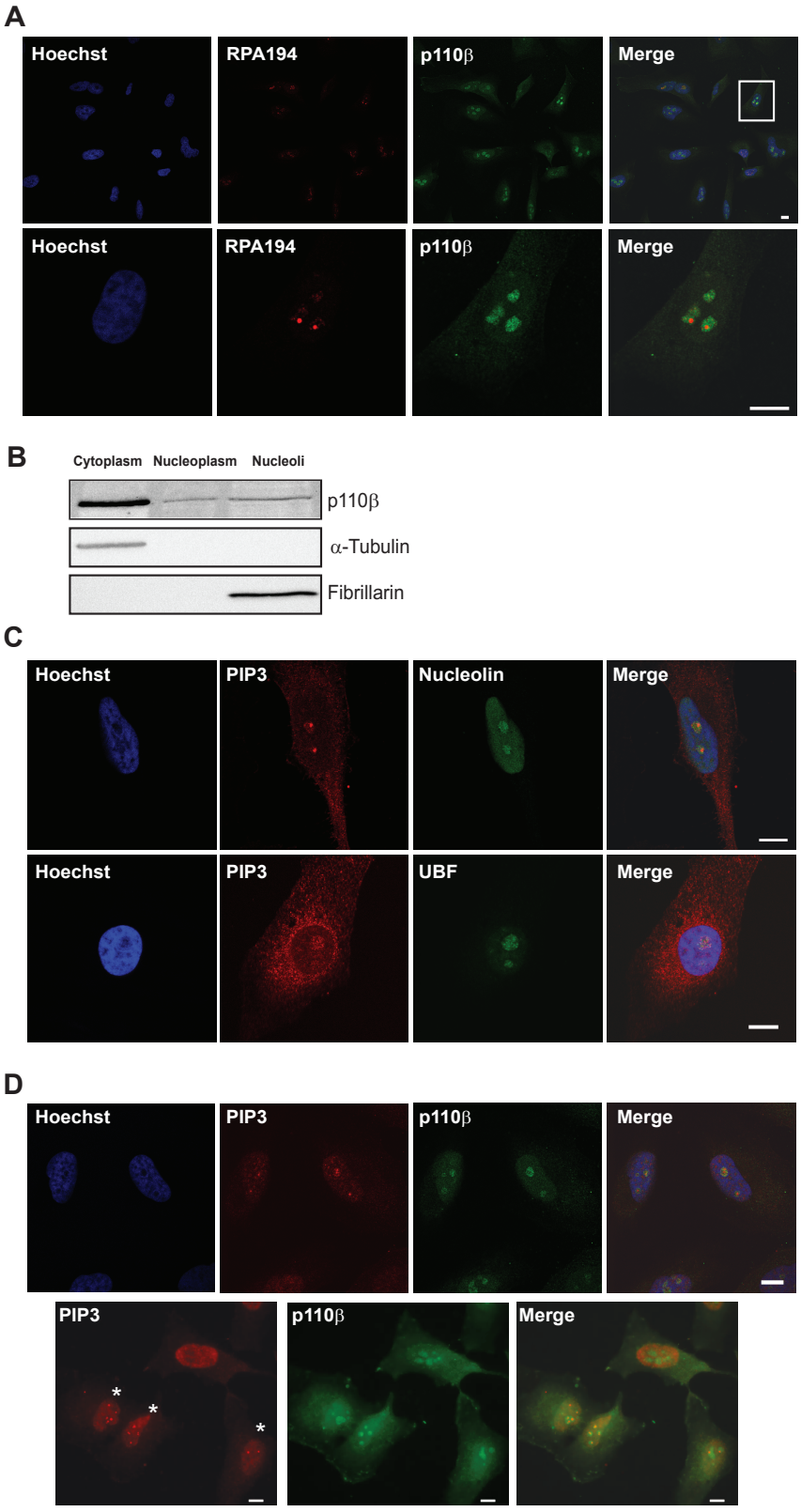
A
Hoechst
RPA194
p110β
Merge
Hoechst
RPA194
p110β
Merge
B
Cytoplasm
Nucleoplasm
Nucleoli
p110β
α-Tubulin
Fibrillarin
C
Hoechst
PIP3
Nucleolin
Merge
Hoechst
PIP3
UBF
Merge
D
Hoechst
PIP3
p110β
Merge
PIP3
p110β
Merge

Figure 2

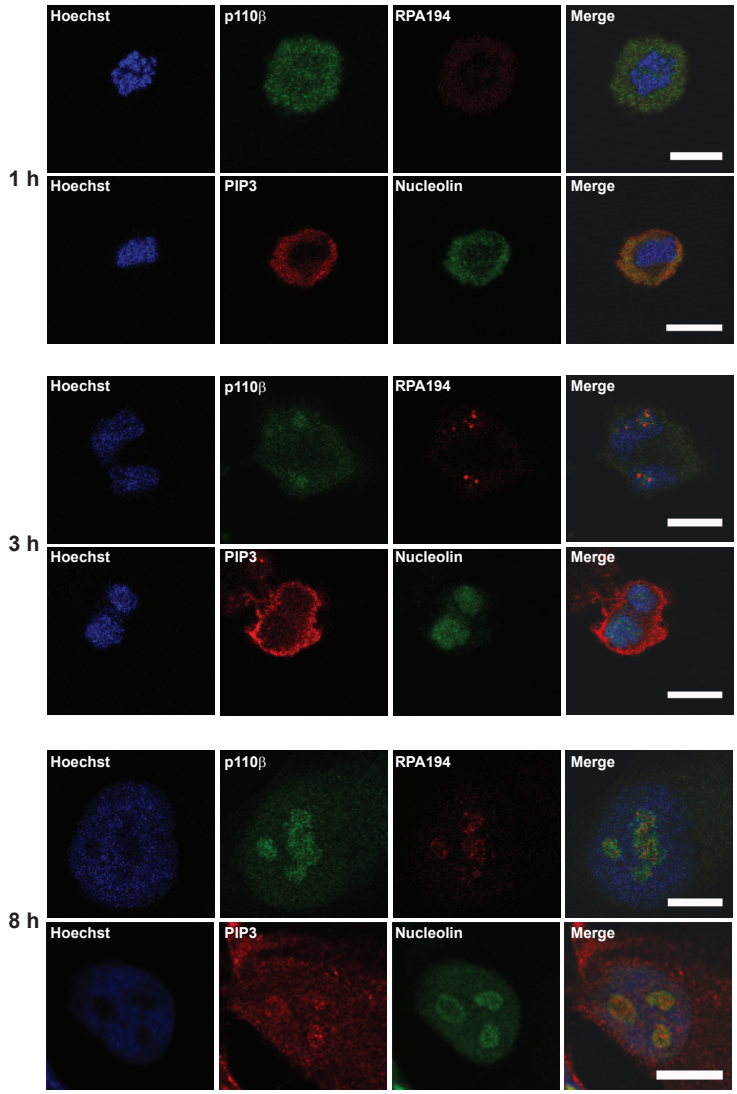
1 h
Hoechst
p110β
RPA194
Merge
Hoechst
PIP3
Nucleolin
Merge
3 h
Hoechst
p110β
RPA194
Merge
Hoechst
PIP3
Nucleolin
Merge
8 h
Hoechst
p110β
RPA194
Merge
Hoechst
PIP3
Nucleolin
Merge

Figure 3

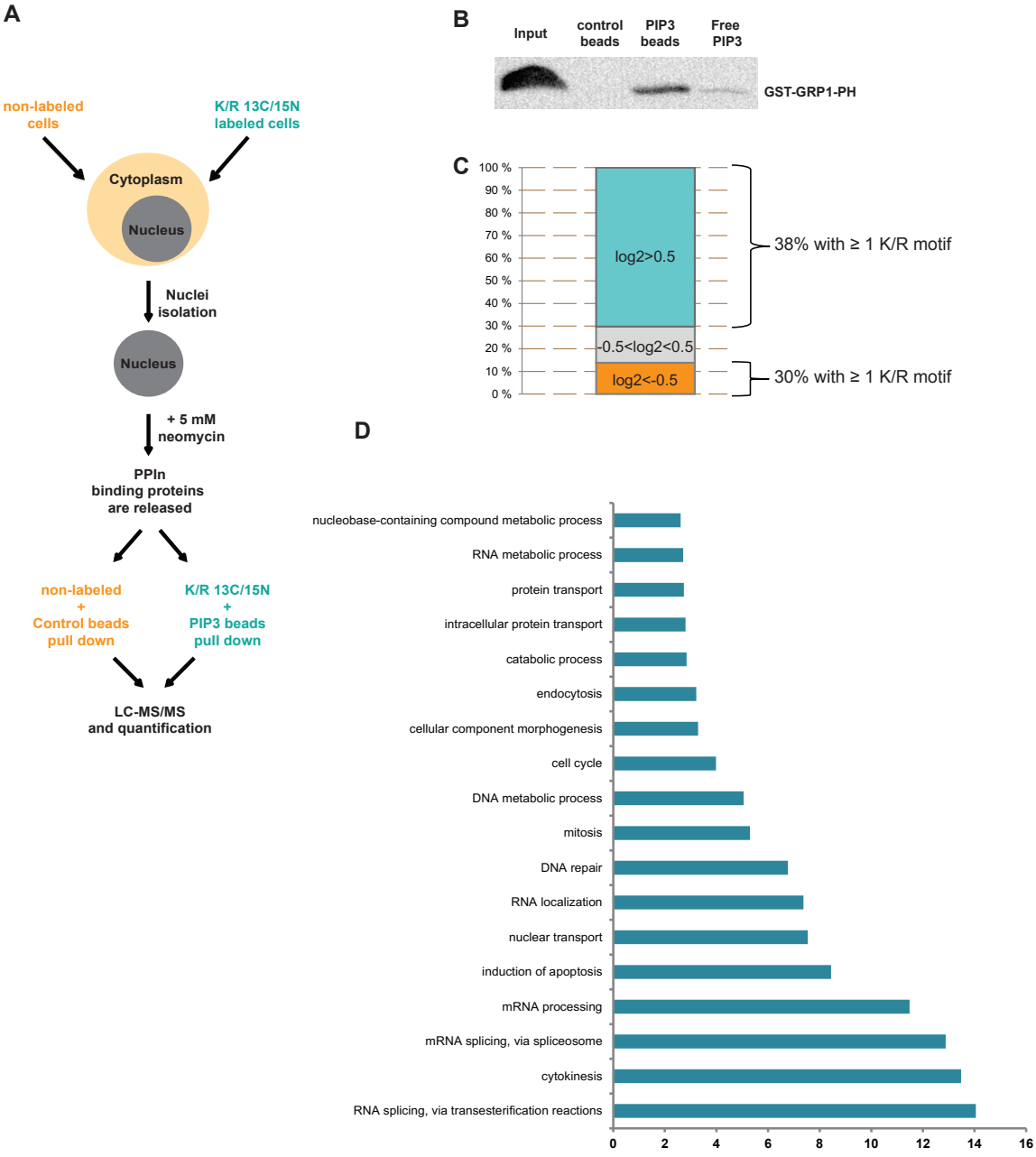
A
non-labeled cells
K/R 13C/15N labeled cells
Cytoplasm
Nucleus
Nuclei isolation
Nucleus
+ 5 mM neomycin
PPIn binding proteins are released
non-labeled + Control beads pull down
K/R 13C/15N + PIP3 beads pull down
LC-MS/MS and quantification
B
Input
control beads
PIP3 beads
Free PIP3
GST-GRP1-PH
C
100 %
90 %
80 %
70 %
60 %
50 %
40 %
30 %
20 %
10 %
0 %
log2>0.5
-0.5<log2<0.5
log2<-0.5
38% with ≥ 1 K/R motif
30% with ≥ 1 K/R motif
D
nucleobase-containing compound metabolic process
RNA metabolic process
protein transport
intracellular protein transport
catabolic process
endocytosis
cellular component morphogenesis
cell cycle
DNA metabolic process
mitosis
DNA repair
RNA localization
nuclear transport
induction of apoptosis
mRNA processing
mRNA splicing, via spliceosome
cytokinesis
RNA splicing, via transesterification reactions
0
2
4
6
8
10
12
14
16

Figure 4

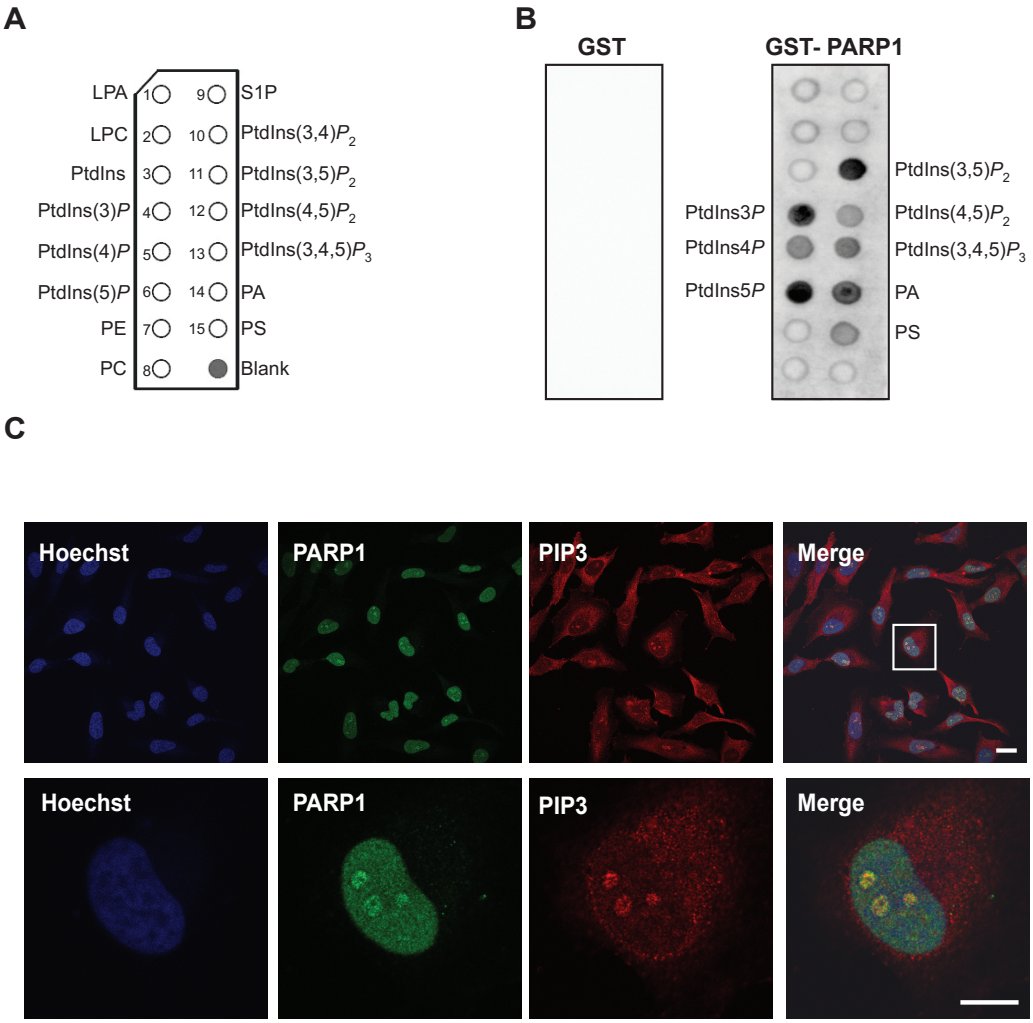
A
LPA
LPC
PtdIns
PtdIns(3)P
PtdIns(4)P
PtdIns(5)P
PE
PC
1
2
3
4
5
6
7
8
9
10
11
12
13
14
15
S1P
PtdIns(3,4)P2
PtdIns(3,5)P2
PtdIns(4,5)P2
PtdIns(3,4,5)P3
PA
PS
Blank
B
GST
GST- PARP1
PtdIns3P
PtdIns4P
PtdIns5P
PtdIns(3,5)P2
PtdIns(4,5)P2
PtdIns(3,4,5)P3
PA
PS
C
Hoechst
PARP1
PIP3
Merge
Hoechst
PARP1
PIP3
Merge

Figure 5

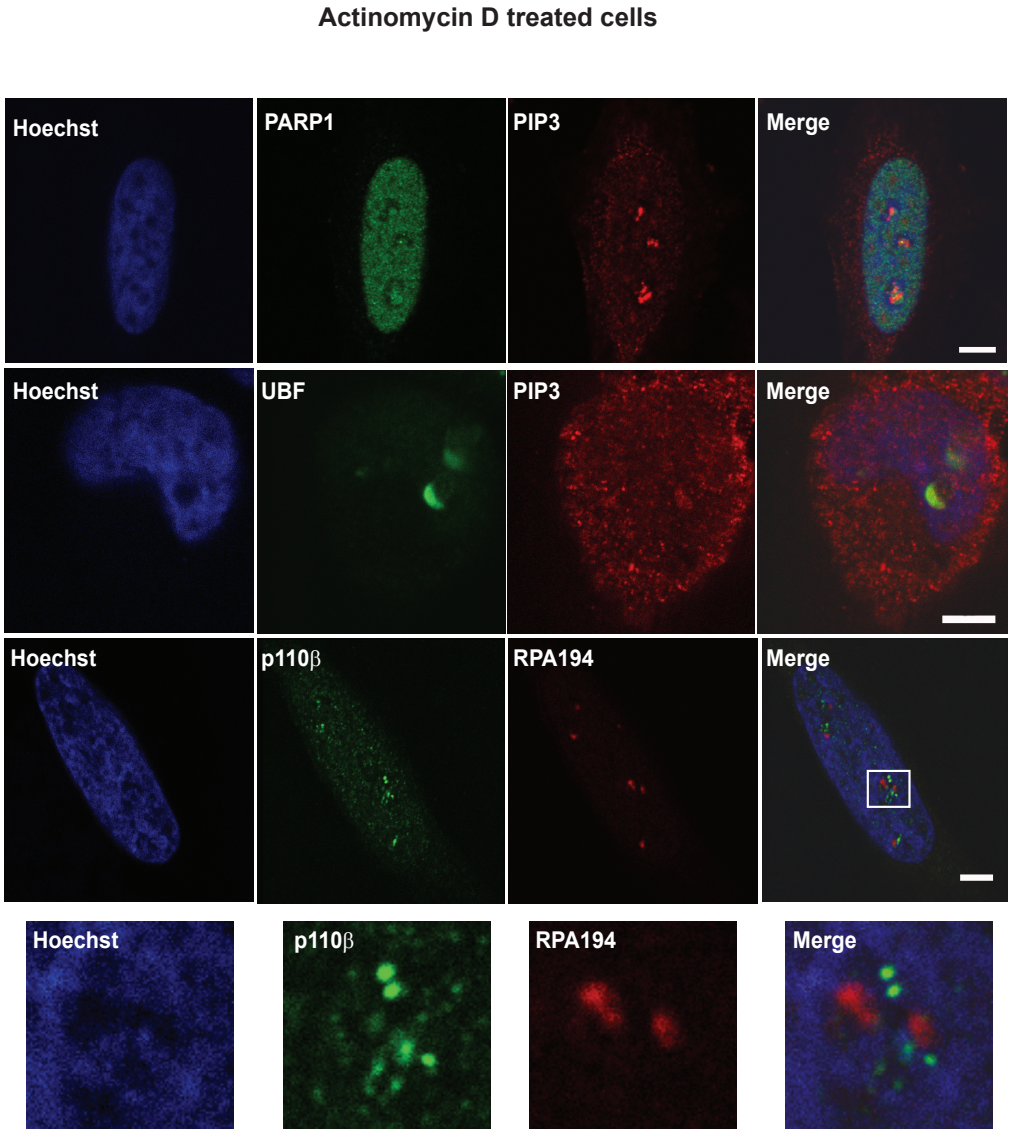
Actinomycin D treated cells
Hoechst
PARP1
PIP3
Merge
Hoechst
UBF
PIP3
Merge
Hoechst
p110β
RPA194
Merge
Hoechst
p110β
RPA194
Merge

SUPPLEMENTARY METHODS and DATA

Nuclear phosphatidylinositol 3,4,5-triphosphate interactome

Fatemeh Mazloumi Gavgani[1], Diana C. Turcu[1], Julie Guillermet-Guibert [2], Rein Aasland[3], Clive D'Santos [4] and Aurélia E. Lewis[1*]

1 Department of Molecular Biology, University of Bergen, Bergen, Norway
2 Centre de Recherches en Cancérologie de Toulouse (CRCT), Institut National de la Santé et de la Recherche Médicale (INSERM), Université Toulouse III Paul Sabatier, Toulouse, France.
3 Department of Bioscience, University of Oslo, Oslo, Norway
4 CRUK Cambridge Institute, Cambridge University, Cambridge, UK.

Supplementary methods

RNA extraction: HeLa cells were collected by centrifugation and after two washes with PBS**,** the cell pellet was suspended in 1ml TriReagent (Sigma) and incubated at room temperature (RT) for 5 minutes. Chloroform (200µl) was added and after vigorous shaking was incubated at RT for 1 minute before centrifugation (4°C at 12000 x g) for 15 minutes. To the upper phase 500µl of Phenol -chloroform - isoamyl alcohol mixture (Sigma) was added and after vigorous shaking was incubated at RT for 2 minute before centrifugation (4°C at 12000 x g) for 10 min. Chloroform (500µl) was added to the upper phase after mixing was incubated at RT for 1 min before centrifugation (4°C at 12000 x g) for 10 minutes. To the upper phase 20 µg of RNA grade glycogen (Thermo Fisher Scientific) and 500 µl isopropanol was added after mixing was incubated at RT for 20 minutes before centrifugation (4°C at 13000 x g) for 20 min. To the pellet 1 ml of ice cold 70% ethanol was added and after mixing was centrifuged (4°C at 8000 x g) for 5 min. The RNA pellet was dissolved in water for RT-qPCR analysis.

RT-qPCR: cDNA was made from total RNA extracts of HeLa cells using the High-Capacity cDNA Reverse Transcription Kit (Thermo Fisher scientific). PowerUp™ SYBR™ Green Master Mix (Thermo Fisher scientific) was used for the real-time PCRs, performed using Roche Light Cycler 480. To amplify the target pre-rRNA, we used the following primers for the 5' external transcribed spacer region: 5'-GAACGGTGGTGTGTCGTTC-3' and 5'-GCGTCTCGTCTCGTCTCACT-3' (1). As a reference gene we used RPS12: 5′-ATTCAGCTTCACCCGTAACC-3′ and 5′-CAACCACTTTACGGGGATTC-3′ (2).

References

1. Murayama A, Ohmori K, Fujimura A, Minami H, Yasuzawa-Tanaka K, Kuroda T, et al. Epigenetic control of rDNA loci in response to intracellular energy status. Cell. 2008;133(4):627-39.
2. Gabriel JM, Higgins MJ, Gebuhr TC, Shows TB, Saitoh S, Nicholls RD. A model system to study genomic imprinting of human genes. P Natl Acad Sci USA. 1998;95(25):14857-62.

Supplementary figures

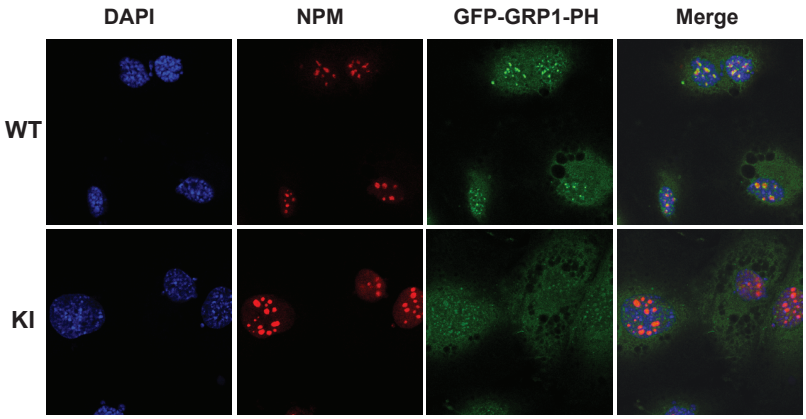

Supplementary figure S1- Co localization of PtdIns(3,4,5)P3 with Nucleophosmin at the exit of mitosis. MEF p110β WT and Kinase inactive (KI) cells were treated for 16 hours with 50ng/ml nocodazole as described in the methods and collected after mitotic shake-off. Cells were fixed after 4 hours of replating. Immunoflourescent staining was performed using GFP-GRP1-PH and the Nucleophosmin antibody.

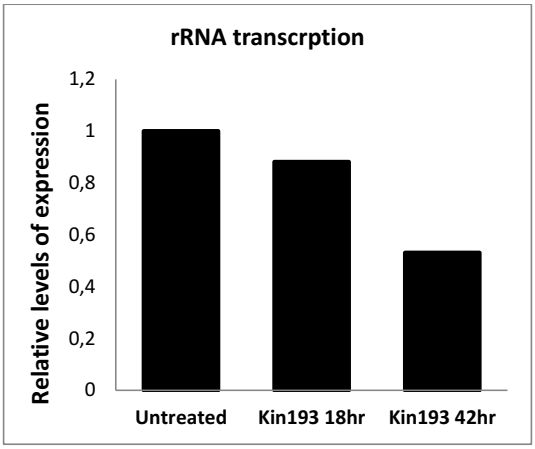

Supplementary Figure S2. pre-rRNA transcription levels are reduced upon p110β inhibition. HeLa cells were treated with the selective p110β inhibitor (10 μM) for the times indicated and pre- rRNA qPCR was performed. Relative pre-rRNA expression to RPS12 gene are shown where the levels decreased in a time dependent manner.

Supplementary Table S1. PIP3 specific with log2 >0.5

proteins commun to T cell nucleolar list

proteins common with NoDB

proteins commun to Lamont 2012 nucleolar list

Protein FDR Confidence	Master	Accession	Description	Sum PEP Score	Coverage	# Peptides	# PSMs	# Unique Peptides	# AAs	MW [kDa]	Abundance Ratio: (F1, Heavy) / (F1, Light)	log 2 ratio	Abundance: F1: Light, Control	Abundance: F1: Heavy, Sample	Abundances Count: F1: Light, Control	Abundances Count: F1: Heavy, Sample	emPAI	# Razor Peptides	Score Sequest HT
High	Master Protein	Q05639	Elongation factor 1-alpha 2 OS=Homo sapiens GN=EEF1A2 PE=1 SV=1	29,32876857	16,1987	7	18	1	463	50,438	100	6,644		1214000		1	1,754	0	16,6119
High	Master Protein	Q06787	Fragile X mental retardation protein 1 OS=Homo sapiens GN=FMR1 PE=1 SV=1	5,451668942	3,322785	2	2	1	632	71,131	100	6,644		965000		1	0,122	0	2,23895
High	Master Protein	Q99873	Protein arginine N-methyltransferase 1 OS=Homo sapiens GN=PRMT1 PE=1 SV=2	5,429119212	6,648199	2	2	2	361	41,489	23,861	4,577	186600	4452000	1	2	0,245	0	0
High	Master Protein	P60900	Proteasome subunit alpha type-6 OS=Homo sapiens GN=PSMA6 PE=1 SV=1	2,360984418	8,943089	2	2	2	246	27,382	23,644	4,563	146500	3465000	1	2	0,359	0	0
High	Master Protein	Q9BRX2	Protein pelota homolog OS=Homo sapiens GN=PELO PE=1 SV=2	6,509226556	11,68831	4	4	4	385	43,332	19,83	4,31	502600	9966000	3	3	0,407	0	0
High	Master Protein	P29372	DNA-3-methyladenine glycosylase OS=Homo sapiens GN=MPG PE=1 SV=3	10,34565189	19,12752	4	4	4	298	32,848	18,812	4,234	856800	16120000	2	2	0,719	0	2,35561
High	Master Protein	P62258	14-3-3 protein epsilon OS=Homo sapiens GN=YWHAE PE=1 SV=1	4,186015707	8,235294	2	3	1	255	29,155	14,189	3,827	292700	4153000	1	1	0,468	0	0
High	None	P07900	Heat shock protein HSP 90-alpha OS=Homo sapiens GN=HSP90AA1 PE=1 SV=5	7,723860059	5,327869	3	4	3	732	84,607	13,62	3,768	698400	9511000	3	4	0,245	0	3,85125
High	Master Protein	Q8NFW8	N-acylneuraminate cytidylyltransferase OS=Homo sapiens GN=CMAS PE=1 SV=2	5,189136666	6,221198	3	3	3	434	48,349	10,727	3,423	519700	5575000	2	3	0,259	0	0
High	Master Protein	P08238	Heat shock protein HSP 90-beta OS=Homo sapiens GN=HSP90AB1 PE=1 SV=4	15,09708343	11,04972	6	7	6	724	83,212	10,343	3,371	1484000	15350000	4	6	0,455	0	8,02137
High	Master Protein	Q9UPQ0	LIM and calponin homology domains-containing protein 1 OS=Homo sapiens GN=LIMCH1 PE=1 SV=4	5,156917712	3,693444	3	3	3	1083	121,792	9,439	3,239	463800	4378000	2	3	0,105	0	0
High	None	Q58FF8	Putative heat shock protein HSP 90-beta 2 OS=Homo sapiens GN=HSP90AB2P PE=1 SV=2	3,811228059	5,774278	2	2	2	381	44,321	8,559	3,097	1018000	8712000	2	2	0,202	0	3,52215

High	Master Protein	Q00059	Transcription factor A, mitochondrial OS=Homo sapiens GN=TFAM PE=1 SV=1	4,852543815	9,349593	2	2	2	246	29,078	7,543	2,915	469700	3543000	2	2	0,259	0	1,87049
High	Master Protein	Q8N8S7	Protein enabled homolog OS=Homo sapiens GN=ENAH PE=1 SV=2	5,958037664	3,722504	2	3	2	591	66,47	6,076	2,603	2007000	12200000	2	2	0,318	0	0
High	Master Protein	P35241	Radixin OS=Homo sapiens GN=RDX PE=1 SV=1	12,63010832	6,689537	4	11	1	583	68,521	5,822	2,542	143600	836100	1	1	0,413	0	5,19114
High	None	P35580	Myosin-10 OS=Homo sapiens GN=MYH10 PE=1 SV=3	13,3843106	2,530364	4	10	4	1976	228,858	5,623	2,491	7546000	42430000	4	4	0,115	0	1,91406
High	Master Protein	Q16527	Cysteine and glycine-rich protein 2 OS=Homo sapiens GN=CSRP2 PE=1 SV=3	3,16855078	12,95337	2	2	2	193	20,94	5,519	2,464	855800	4723000	2	2	0,425	0	0
High	Master Protein	P35579	Myosin-9 OS=Homo sapiens GN=MYH9 PE=1 SV=4	83,91708313	22,2449	31	52	31	1960	226,392	5,071	2,342	54210000	274900000	26	30	1,006	0	23,0832
High	Master Protein	O94979	Protein transport protein Sec31A OS=Homo sapiens GN=SEC31A PE=1 SV=3	4,126438029	2,459016	3	3	3	1220	132,931	5,049	2,336	766100	3868000	2	3	0,139	0	0
High	Master Protein	P30419	Glycylpeptide N-tetradecanoyltransferase 1 OS=Homo sapiens GN=NMT1 PE=1 SV=2	6,485077644	8,669355	3	3	3	496	56,77	4,954	2,309	2426000	12020000	2	3	0,194	0	0
High	None	P35749	Myosin-11 OS=Homo sapiens GN=MYH11 PE=1 SV=3	6,419145944	2,789047	4	4	4	1972	227,199	4,617	2,207	2011000	9285000	2	3	0,056	0	0
High	Master Protein	Q92785	Zinc finger protein ubi-d4 OS=Homo sapiens GN=DPF2 PE=1 SV=2	2,815731318	5,882353	2	2	2	391	44,127	4,304	2,106	717300	3087000	1	2	0,212	0	0
High	Master Protein	P51116	Fragile X mental retardation syndrome-related protein 2 OS=Homo sapiens GN=FXR2 PE=1 SV=2	9,472176546	9,212481	5	5	4	673	74,178	4,28	2,098	2999000	12840000	4	4	0,299	0	0
High	Master Protein	Q92879	CUGBP Elav-like family member 1 OS=Homo sapiens GN=CELF1 PE=1 SV=2	5,764974088	6,790123	3	3	3	486	52,03	4,226	2,079	1045000	4414000	1	3	0,413	0	1,6752
High	Master Protein	O00148	ATP-dependent RNA helicase DDX39A OS=Homo sapiens GN=DDX39A PE=1 SV=2	21,70500665	21,31148	8	12	3	427	49,098	4,105	2,037	1804000	7407000	1	2	1,471	0	8,96566
High	Master Protein	P15311	Ezrin OS=Homo sapiens GN=EZR PE=1 SV=4	19,31504553	11,94539	7	15	4	586	69,37	4,007	2,003	5127000	20540000	4	4	0,805	0	8,39886
High	Master Protein	P67809	Nuclease-sensitive element-binding protein 1 OS=Homo sapiens GN=YBX1 PE=1 SV=3	15,69439557	20,37037	4	6	1	324	35,903	3,974	1,991	4611000	18320000	1	1	1,683	0	8,01324
High	None	Q7Z406	Myosin-14 OS=Homo sapiens GN=MYH14 PE=1 SV=2	8,98286617	2,406015	4	5	4	1995	227,732	3,962	1,986	12580000	49830000	3	4	0,094	0	1,89528
High	Master Protein Candidate	P31946	14-3-3 protein beta/alpha OS=Homo sapiens GN=YWHAB PE=1 SV=3	4,388550092	7,723577	2	3	1	246	28,065	3,95	1,982	1239000	4894000	2	2	0,501	0	0
High	Master Protein	P61981	14-3-3 protein gamma OS=Homo sapiens GN=YWHAG PE=1 SV=2	4,388550092	7,692308	2	3	1	247	28,285	3,95	1,982	1239000	4894000	2	2	0,468	1	0
High	Master Protein	P27695	DNA-(apurinic or apyrimidinic site) lyase OS=Homo sapiens GN=APEX1 PE=1 SV=2	5,292621467	8,176101	2	2	2	318	35,532	3,9	1,963	2536000	9891000	2	2	0,292	0	0
High	Master Protein	O43242	26S proteasome non-ATPase regulatory subunit 3 OS=Homo sapiens GN=PSMD3 PE=1 SV=2	6,235280136	8,426966	4	4	4	534	60,939	3,851	1,945	1803000	6943000	4	4	0,266	0	0

High	Master Protein	Q92945	Far upstream element-binding protein 2 OS=Homo sapiens GN=KHSRP PE=1 SV=4	7,492468256	7,876231	4	4	4	711	73,07	3,831	1,938	1659000	6357000	4	4	0,245	0	1,76768
High	Master Protein	P26196	Probable ATP-dependent RNA helicase DDX6 OS=Homo sapiens GN=DDX6 PE=1 SV=2	8,157557655	10,97308	4	4	4	483	54,382	3,708	1,891	1174000	4353000	3	3	0,374	0	1,79457
High	Master Protein	Q13200	26S proteasome non-ATPase regulatory subunit 2 OS=Homo sapiens GN=PSMD2 PE=1 SV=3	5,654164408	5,726872	4	4	4	908	100,136	3,706	1,89	3571000	13240000	3	4	0,169	0	0
High	Master Protein	P16989	Y-box-binding protein 3 OS=Homo sapiens GN=YBX3 PE=1 SV=4	19,79727882	13,70968	4	7	1	372	40,066	3,613	1,853	21670000	78310000	5	5	1,239	4	10,1186
High	Master Protein	Q99460	26S proteasome non-ATPase regulatory subunit 1 OS=Homo sapiens GN=PSMD1 PE=1 SV=2	4,523069434	3,043022	3	3	3	953	105,769	3,599	1,848	1469000	5287000	3	3	0,134	0	0
High	Master Protein	P54886	Delta-1-pyrroline-5-carboxylate synthase OS=Homo sapiens GN=ALDH18A1 PE=1 SV=2	15,14798412	9,18239	6	6	6	795	87,248	3,509	1,811	2923000	10260000	5	5	0,318	0	6,94965
High	None	Q9Y2T7	Y-box-binding protein 2 OS=Homo sapiens GN=YBX2 PE=1 SV=2	14,52241064	9,89011	3	5	0	364	38,495	3,497	1,806	19350000	67650000	4	4	0,896	0	8,01324
High	Master Protein	Q13838	Spliceosome RNA helicase DDX39B OS=Homo sapiens GN=DDX39B PE=1 SV=1	22,26326494	21,26168	8	13	3	428	48,96	3,301	1,723	18640000	61510000	6	6	1,471	4	10,826
High	None	Q32P51	Heterogeneous nuclear ribonucleoprotein A1-like 2 OS=Homo sapiens GN=HNRNPA1L2 PE=2 SV=2	37,88698968	26,25	9	22	7	320	34,204	3,272	1,71	12650000	41400000	5	6	4,995	0	26,8986
High	Master Protein	P51114	Fragile X mental retardation syndrome-related protein 1 OS=Homo sapiens GN=FXR1 PE=1 SV=3	20,81741297	14,65378	7	8	6	621	69,678	3,229	1,691	19350000	62460000	6	7	0,604	1	5,1025
High	Master Protein	Q9BQ67	Glutamate-rich WD repeat-containing protein 1 OS=Homo sapiens GN=GRWD1 PE=1 SV=1	3,833110168	5,156951	2	2	2	446	49,388	3,158	1,659	839700	2652000	2	2	0,259	0	0
High	Master Protein	P42166	Lamina-associated polypeptide 2, isoform alpha OS=Homo sapiens GN=TMPO PE=1 SV=2	8,886581796	3,458213	2	3	2	694	75,446	3,096	1,63	3500000	10830000	2	2	0,189	0	5,73058
High	Master Protein	Q13112	Chromatin assembly factor 1 subunit B OS=Homo sapiens GN=CHAF1B PE=1 SV=1	4,228310791	4,11449	2	2	2	559	61,454	3,057	1,612	3055000	9339000	2	2	0,155	0	3,6286
High	Master Protein	O75150	E3 ubiquitin-protein ligase BRE1B OS=Homo sapiens GN=RNF40 PE=1 SV=4	10,04304865	4,595405	4	4	4	1001	113,581	3,037	1,603	4658000	14150000	4	4	0,16	0	3,51063
High	Master Protein	P78344	Eukaryotic translation initiation factor 4 gamma 2 OS=Homo sapiens GN=EIF4G2 PE=1 SV=1	7,163198281	4,63065	4	5	4	907	102,297	3,021	1,595	3284000	9921000	4	4	0,22	0	1,65249
High	Master Protein	P26599	Polypyrimidine tract-binding protein 1 OS=Homo sapiens GN=PTBP1 PE=1 SV=1	53,12333827	31,63842	9	36	9	531	57,186	2,991	1,581	26600000	79570000	8	7	2,981	0	40,7997
High	Master Protein	P53396	ATP-citrate synthase OS=Homo sapiens GN=ACLY PE=1 SV=3	93,6328283	25,79473	22	42	22	1101	120,762	2,985	1,578	89230000	266400000	23	23	2,003	0	44,5275
High	Master Protein	Q13765	Nascent polypeptide-associated complex subunit alpha OS=Homo sapiens	4,518535242	12,55814	2	2	2	215	23,37	2,953	1,562	1817000	5367000	2	1	0,931	0	3,58437

	Candidate		GN=NACA PE=1 SV=1																
High	Master Protein	E9PAV3	Nascent polypeptide-associated complex subunit alpha, muscle-specific form OS=Homo sapiens GN=NACA PE=1 SV=1	4,518535242	1,299326	2	2	2	2078	205,295	2,953	1,562	1817000	5367000	2	1	0,04	0	3,58437
High	Master Protein	P46060	Ran GTPase-activating protein 1 OS=Homo sapiens GN=RANGAP1 PE=1 SV=1	12,13542232	8,517888	4	4	4	587	63,502	2,952	1,562	6117000	18060000	4	4	0,311	0	5,72772
High	Master Protein	Q15366	Poly(rC)-binding protein 2 OS=Homo sapiens GN=PCBP2 PE=1 SV=1	12,02775737	13,42466	4	5	4	365	38,556	2,944	1,558	13520000	39790000	4	4	0,778	0	5,58496
High	Master Protein	Q08J23	tRNA (cytosine(34)-C(5))-methyltransferase OS=Homo sapiens GN=NSUN2 PE=1 SV=2	2,515951982	2,216428	2	2	2	767	86,416	2,905	1,539	1935000	5620000	2	2	0,101	0	0
High	Master Protein	Q96AE4	Far upstream element-binding protein 1 OS=Homo sapiens GN=FUBP1 PE=1 SV=3	5,774433501	3,26087	2	4	1	644	67,518	2,866	1,519	108900	312000	1	1	0,283	0	0
High	Master Protein	Q96I24	Far upstream element-binding protein 3 OS=Homo sapiens GN=FUBP3 PE=1 SV=2	18,81035607	13,11189	7	9	6	572	61,602	2,846	1,509	11960000	34030000	6	6	0,725	2	6,04151
High	Master Protein	Q8WX93	Palladin OS=Homo sapiens GN=PALLD PE=1 SV=3	10,72460816	3,832249	5	6	5	1383	150,47	2,844	1,508	8322000	23670000	5	5	0,199	0	3,71834
High	Master Protein	Q6UXN9	WD repeat-containing protein 82 OS=Homo sapiens GN=WDR82 PE=1 SV=1	3,710511205	8,306709	2	2	2	313	35,056	2,841	1,506	2001000	5685000	2	2	0,259	0	0
High	Master Protein	P11586	C-1-tetrahydrofolate synthase, cytoplasmic OS=Homo sapiens GN=MTHFD1 PE=1 SV=3	41,63432933	15,40107	13	17	13	935	101,495	2,84	1,506	23270000	66080000	13	13	0,848	0	18,2531
High	Master Protein	P46940	Ras GTPase-activating-like protein IQGAP1 OS=Homo sapiens GN=IQGAP1 PE=1 SV=1	80,98847867	17,01871	27	41	27	1657	189,134	2,825	1,498	127600000	360500000	26	27	1,393	0	21,1853
High	Master Protein	P63104	14-3-3 protein zeta/delta OS=Homo sapiens GN=YWHAZ PE=1 SV=1	4,552406895	9,795918	2	3	1	245	27,728	2,824	1,498	1151000	3251000	1	1	0,438	0	0
High	Master Protein	P13010	X-ray repair cross-complementing protein 5 OS=Homo sapiens GN=XRCC5 PE=1 SV=3	72,05753782	28,14208	15	30	15	732	82,652	2,817	1,494	74380000	209500000	12	13	2,594	0	26,4698
High	Master Protein	Q9Y295	Developmentally-regulated GTP-binding protein 1 OS=Homo sapiens GN=DRG1 PE=1 SV=1	5,049762288	5,722071	2	2	2	367	40,517	2,728	1,448	1803000	4918000	2	2	0,194	0	1,83874
High	None	P36873	Serine/threonine-protein phosphatase PP1-gamma catalytic subunit OS=Homo sapiens GN=PPP1CC PE=1 SV=1	5,013071455	11,14551	3	3	3	323	36,96	2,72	1,444	2495000	6787000	3	3	0,413	0	1,9523
High	Master Protein Candidate	Q05193	Dynamin-1 OS=Homo sapiens GN=DNM1 PE=1 SV=2	7,609984771	2,430556	2	4	2	864	97,347	2,719	1,443	2576000	7005000	2	2	0,172	0	2,18965
High	Master Protein	P50570	Dynamin-2 OS=Homo sapiens GN=DNM2 PE=1 SV=2	7,609984771	2,413793	2	4	2	870	98,003	2,719	1,443	2576000	7005000	2	2	0,175	0	2,18965
High	Master Protein Candidate	Q9UQ16	Dynamin-3 OS=Homo sapiens GN=DNM3 PE=1 SV=4	7,609984771	2,416571	2	4	2	869	97,685	2,719	1,443	2576000	7005000	2	2	0,169	0	2,18965
High	Master	P08651	Nuclear factor 1 C-type OS=Homo sapiens	5,658181828	4,92126	2	3	2	508	55,64	2,695	1,43	2789000	7517000	2	2	0,318	0	0

	Protein		GN=NFIC PE=1 SV=2																
High	Master Protein	O00571	ATP-dependent RNA helicase DDX3X OS=Homo sapiens GN=DDX3X PE=1 SV=3	12,0280286	5,135952	3	6	2	662	73,198	2,688	1,427	2549000	6851000	2	2	0,315	0	8,03162
High	Master Protein Candidate	O15523	ATP-dependent RNA helicase DDX3Y OS=Homo sapiens GN=DDX3Y PE=1 SV=2	12,0280286	5,151515	3	6	2	660	73,108	2,688	1,427	2549000	6851000	2	2	0,299	0	8,03162
High	None	P57721	Poly(rC)-binding protein 3 OS=Homo sapiens GN=PCBP3 PE=2 SV=2	4,077652963	6,738544	2	2	2	371	39,44	2,658	1,41	8485000	22560000	2	2	0,259	0	1,6574
High	Master Protein	Q15019	Septin-2 OS=Homo sapiens GN=SEPT2 PE=1 SV=1	23,01003054	29,63989	7	11	7	361	41,461	2,647	1,404	18070000	47810000	6	6	1,404	0	6,92691
High	Master Protein	P60842	Eukaryotic initiation factor 4A-I OS=Homo sapiens GN=EIF4A1 PE=1 SV=1	34,28815487	28,81773	11	18	11	406	46,125	2,626	1,393	40250000	105700000	11	13	3,642	0	16,331
High	Master Protein	Q99729	Heterogeneous nuclear ribonucleoprotein A/B OS=Homo sapiens GN=HNRNPAB PE=1 SV=2	8,701373456	9,337349	3	4	2	332	36,202	2,604	1,381	5733000	14930000	2	2	0,848	0	3,53746
High	None	P0CG38	POTE ankyrin domain family member I OS=Homo sapiens GN=POTEI PE=3 SV=1	6,129954764	2,232558	2	4	2	1075	121,205	2,592	1,374	28230000	73180000	2	2	0,11	0	0
High	Master Protein	Q13283	Ras GTPase-activating protein-binding protein 1 OS=Homo sapiens GN=G3BP1 PE=1 SV=1	34,20340477	24,46352	8	16	8	466	52,132	2,589	1,372	37420000	96860000	4	5	2,831	0	9,73081
High	Master Protein	O43719	HIV Tat-specific factor 1 OS=Homo sapiens GN=HTATSF1 PE=1 SV=1	5,943343149	2,781457	2	3	2	755	85,801	2,572	1,363	2259000	5811000	2	2	0,126	0	1,63746
High	Master Protein	Q9Y2L1	Exosome complex exonuclease RRP44 OS=Homo sapiens GN=DIS3 PE=1 SV=2	3,696122146	3,340292	3	3	3	958	108,934	2,565	1,359	1532000	3931000	3	3	0,129	0	0
High	Master Protein	P12814	Alpha-actinin-1 OS=Homo sapiens GN=ACTN1 PE=1 SV=2	111,8803186	27,01794	21	86	9	892	102,993	2,56	1,356	10960000	28050000	5	6	3,042	0	98,4668
High	Master Protein	Q7KZF4	Staphylococcal nuclease domain-containing protein 1 OS=Homo sapiens GN=SND1 PE=1 SV=1	49,23601559	25,93407	19	26	19	910	101,934	2,552	1,352	60480000	154300000	17	18	1,239	0	15,1439
High	Master Protein	Q00341	Vigilin OS=Homo sapiens GN=HDLBP PE=1 SV=2	29,90150612	13,17035	14	16	14	1268	141,368	2,548	1,349	24510000	62430000	14	14	0,532	0	12,6067
High	None	P62140	Serine/threonine-protein phosphatase PP1-beta catalytic subunit OS=Homo sapiens GN=PPP1CB PE=1 SV=3	3,496230665	6,727829	2	2	2	327	37,163	2,537	1,343	1730000	4389000	2	2	0,259	0	1,9523
High	Master Protein	P26038	Moesin OS=Homo sapiens GN=MSN PE=1 SV=3	22,931281	18,89081	10	19	7	577	67,778	2,535	1,342	36080000	91440000	11	11	0,962	4	8,73277
High	Master Protein	Q15424	Scaffold attachment factor B1 OS=Homo sapiens GN=SAFB PE=1 SV=4	2,438492848	2,295082	2	2	2	915	102,58	2,535	1,342	1766000	4477000	2	2	0,094	0	0
High	Master Protein	P17844	Probable ATP-dependent RNA helicase DDX5 OS=Homo sapiens GN=DDX5 PE=1 SV=1	29,08900711	16,28664	10	15	4	614	69,105	2,525	1,336	3115000	7865000	2	3	1,448	0	9,98749
High	Master Protein	P20042	Eukaryotic translation initiation factor 2 subunit 2 OS=Homo sapiens GN=EIF2S2 PE=1 SV=2	9,468810301	12,61261	3	4	3	333	38,364	2,505	1,325	6828000	17100000	3	3	0,52	0	2,35044

High	Master Protein	P09874	Poly [ADP-ribose] polymerase 1 OS=Homo sapiens GN=PARP1 PE=1 SV=4	80,00810362	26,82446	22	37	22	1014	113,012	2,5	1,322	165600000	414000000	19	20	1,994	0	39,3181
High	None	Q2VIR3	Putative eukaryotic translation initiation factor 2 subunit 3-like protein OS=Homo sapiens GN=EIF2S3L PE=5 SV=2	13,36729042	12,07627	5	7	5	472	51,196	2,497	1,32	15310000	38240000	4	6	1,015	0	3,44028
High	Master Protein	P26368	Splicing factor U2AF 65 kDa subunit OS=Homo sapiens GN=U2AF2 PE=1 SV=4	7,090099677	7,578947	3	5	3	475	53,467	2,497	1,32	5352000	13360000	4	4	0,551	0	2,04845
High	Master Protein	Q69YN4	Protein virilizer homolog OS=Homo sapiens GN=KIAA1429 PE=1 SV=2	16,61135797	5,573951	8	9	8	1812	201,898	2,474	1,307	9706000	24010000	7	7	0,209	0	1,68385
High	Master Protein	Q92466	DNA damage-binding protein 2 OS=Homo sapiens GN=DDB2 PE=1 SV=1	3,04793441	4,683841	2	2	2	427	47,833	2,474	1,307	2256000	5580000	2	2	0,179	0	1,74063
High	None	Q14240	Eukaryotic initiation factor 4A-II OS=Homo sapiens GN=EIF4A2 PE=1 SV=2	21,52213569	16,46192	6	11	6	407	46,373	2,459	1,298	24390000	59970000	5	7	1,371	0	9,80257
High	Master Protein	P09661	U2 small nuclear ribonucleoprotein A' OS=Homo sapiens GN=SNRPA1 PE=1 SV=2	7,848166526	14,5098	3	4	3	255	28,398	2,443	1,289	4607000	11260000	3	3	0,848	0	0
High	Master Protein	Q8NE71	ATP-binding cassette sub-family F member 1 OS=Homo sapiens GN=ABCF1 PE=1 SV=2	8,519357924	5,798817	4	5	4	845	95,866	2,426	1,279	12020000	29170000	4	4	0,278	0	2,11527
High	Master Protein	Q9NSD9	Phenylalanine--tRNA ligase beta subunit OS=Homo sapiens GN=FARSB PE=1 SV=3	19,75074837	15,95925	9	13	9	589	66,074	2,415	1,272	27440000	66260000	9	9	0,8	0	13,3394
High	Master Protein	Q52LJ0	Protein FAM98B OS=Homo sapiens GN=FAM98B PE=1 SV=1	8,065347452	8,181818	2	2	2	330	37,167	2,408	1,268	2206000	5312000	2	2	0,259	0	4,33705
High	Master Protein	O75475	PC4 and SFRS1-interacting protein OS=Homo sapiens GN=PSIP1 PE=1 SV=1	3,418456681	3,207547	2	2	2	530	60,067	2,407	1,267	3170000	7629000	2	2	0,133	0	1,75941
High	Master Protein	Q13263	Transcription intermediary factor 1-beta OS=Homo sapiens GN=TRIM28 PE=1 SV=5	21,0256917	12,09581	8	9	8	835	88,493	2,383	1,253	20450000	48730000	7	8	0,658	0	7,58258
High	Master Protein	Q8N684	Cleavage and polyadenylation specificity factor subunit 7 OS=Homo sapiens GN=CPSF7 PE=1 SV=1	24,17134713	16,13588	5	6	5	471	52,018	2,377	1,249	2472000	5875000	4	4	0,738	0	12,8828
High	Master Protein	P52272	Heterogeneous nuclear ribonucleoprotein M OS=Homo sapiens GN=HNRNPM PE=1 SV=3	39,26020347	25,89041	14	21	14	730	77,464	2,37	1,245	35210000	83440000	16	16	1,31	0	13,1737
High	Master Protein	P41091	Eukaryotic translation initiation factor 2 subunit 3 OS=Homo sapiens GN=EIF2S3 PE=1 SV=3	15,38724158	15,04237	6	8	6	472	51,077	2,367	1,243	25200000	59660000	5	7	1,154	0	3,44028
High	Master Protein	O43707	Alpha-actinin-4 OS=Homo sapiens GN=ACTN4 PE=1 SV=2	265,9574554	65,75192	46	175	34	911	104,788	2,366	1,242	671300000	1588000000	57	54	27,861	18	185,602
High	Master Protein	P0DMV9	Heat shock 70 kDa protein 1B OS=Homo sapiens GN=HSPA1B PE=1 SV=1	41,21365779	17,62871	9	19	7	641	70,009	2,355	1,236	23890000	56250000	8	8	1,801	0	19,9078
High	Master Protein	Q14103	Heterogeneous nuclear ribonucleoprotein D0 OS=Homo sapiens GN=HNRNPD PE=1 SV=1	17,25077632	12,67606	5	8	4	355	38,41	2,345	1,23	40780000	95620000	5	5	1,929	1	9,17725
High	Master Protein	P23284	Peptidyl-prolyl cis-trans isomerase B OS=Homo sapiens GN=PPIB PE=1 SV=2	18,68389239	31,48148	7	10	7	216	23,728	2,342	1,228	23750000	55620000	7	7	2,162	0	4,34278

High	Master Protein	Q9P258	Protein RCC2 OS=Homo sapiens GN=RCC2 PE=1 SV=2	34,21722849	30,65134	14	18	14	522	56,049	2,305	1,205	36230000	83510000	15	15	2,162	0	1,78161
High	Master Protein	Q09028	Histone-binding protein RBBP4 OS=Homo sapiens GN=RBBP4 PE=1 SV=3	13,92593586	15,52941	6	7	6	425	47,626	2,305	1,205	14670000	33800000	6	6	1,239	0	1,68677
High	Master Protein	P09651	Heterogeneous nuclear ribonucleoprotein A1 OS=Homo sapiens GN=HNRNPA1 PE=1 SV=5	42,33369091	26,88172	10	24	8	372	38,723	2,286	1,193	38830000	88760000	6	8	5,31	0	26,8986
High	Master Protein	P46063	ATP-dependent DNA helicase Q1 OS=Homo sapiens GN=RECQL PE=1 SV=3	13,37008251	10,01541	5	7	5	649	73,41	2,271	1,183	12310000	27950000	4	5	0,512	0	4,06008
High	None	P48741	Putative heat shock 70 kDa protein 7 OS=Homo sapiens GN=HSPA7 PE=5 SV=2	22,98557725	13,62398	4	10	2	367	40,22	2,269	1,182	10910000	24750000	3	3	1,994	0	11,7797
High	Master Protein	P26640	Valine--tRNA ligase OS=Homo sapiens GN=VARS PE=1 SV=4	4,920518592	3,243671	3	3	3	1264	140,387	2,265	1,18	1817000	4116000	3	3	0,104	0	0
High	Master Protein	P33991	DNA replication licensing factor MCM4 OS=Homo sapiens GN=MCM4 PE=1 SV=5	9,273803654	6,025492	5	6	5	863	96,498	2,264	1,179	10920000	24730000	4	4	0,311	0	1,6578
High	Master Protein	P05198	Eukaryotic translation initiation factor 2 subunit 1 OS=Homo sapiens GN=EIF2S1 PE=1 SV=3	28,00838771	23,49206	7	10	7	315	36,089	2,249	1,169	29400000	66130000	7	7	1,848	0	11,1706
High	None	Q6S8J3	POTE ankyrin domain family member E OS=Homo sapiens GN=POTEE PE=1 SV=3	16,15979127	3,72093	3	7	3	1075	121,286	2,243	1,165	40380000	90570000	3	3	0,187	0	5,32513
High	None	A5A3E0	POTE ankyrin domain family member F OS=Homo sapiens GN=POTEF PE=1 SV=2	16,15979127	3,72093	3	7	3	1075	121,367	2,243	1,165	40380000	90570000	3	3	0,184	0	5,32513
High	Master Protein	P60709	Actin, cytoplasmic 1 OS=Homo sapiens GN=ACTB PE=1 SV=1	31,91791225	34,93333	9	18	9	375	41,71	2,241	1,164	106700000	239100000	7	7	2,675	0	5,32513
High	Master Protein Candidate	P63261	Actin, cytoplasmic 2 OS=Homo sapiens GN=ACTG1 PE=1 SV=1	31,91791225	34,93333	9	18	9	375	41,766	2,241	1,164	106700000	239100000	7	7	2,675	0	5,32513
High	Master Protein	P78347	General transcription factor II-I OS=Homo sapiens GN=GTF2I PE=1 SV=2	22,73861014	9,018036	8	12	8	998	112,346	2,236	1,161	21320000	47670000	9	9	0,505	0	5,62424
High	Master Protein	Q14157	Ubiquitin-associated protein 2-like OS=Homo sapiens GN=UBAP2L PE=1 SV=2	4,612892557	2,115915	2	2	2	1087	114,465	2,216	1,148	3609000	7997000	2	2	0,141	0	2,29976
High	Master Protein	P12956	X-ray repair cross-complementing protein 6 OS=Homo sapiens GN=XRCC6 PE=1 SV=2	69,72371585	38,09524	18	40	18	609	69,799	2,215	1,147	116300000	257500000	15	15	3,732	0	34,4228
High	Master Protein	P78527	DNA-dependent protein kinase catalytic subunit OS=Homo sapiens GN=PRKDC PE=1 SV=3	150,3803369	14,00194	50	74	50	4128	468,788	2,212	1,145	215600000	476800000	49	52	0,911	0	51,9631
High	Master Protein	P62826	GTP-binding nuclear protein Ran OS=Homo sapiens GN=RAN PE=1 SV=3	6,963519043	14,81481	3	3	3	216	24,408	2,205	1,141	8081000	17820000	3	3	0,874	0	1,93105
High	Master Protein	O43684	Mitotic checkpoint protein BUB3 OS=Homo sapiens GN=BUB3 PE=1 SV=1	19,48760944	19,5122	5	13	5	328	37,131	2,164	1,114	22580000	48850000	6	6	2,594	0	7,69858
High	Master Protein	Q05048	Cleavage stimulation factor subunit 1 OS=Homo sapiens GN=CSTF1 PE=1 SV=1	7,52419712	14,84919	5	6	5	431	48,327	2,146	1,102	6649000	14270000	4	5	0,874	0	0
High	Master Protein	Q15393	Splicing factor 3B subunit 3 OS=Homo sapiens GN=SF3B3 PE=1 SV=4	9,791593135	5,094495	5	5	5	1217	135,492	2,139	1,097	5610000	12000000	5	5	0,194	0	3,82531

High	None	P54652	Heat shock-related 70 kDa protein 2 OS=Homo sapiens GN=HSPA2 PE=1 SV=1	33,06005342	11,89358	7	15	4	639	69,978	2,136	1,095	89960000	192200000	10	10	1,322	0	15,3062
High	Master Protein	P49916	DNA ligase 3 OS=Homo sapiens GN=LIG3 PE=1 SV=2	12,74158503	6,342914	6	6	6	1009	112,835	2,119	1,083	7043000	14920000	5	6	0,225	0	4,38436
High	Master Protein	Q16531	DNA damage-binding protein 1 OS=Homo sapiens GN=DDB1 PE=1 SV=1	11,06157647	4,473684	5	6	5	1140	126,887	2,101	1,071	5212000	10950000	5	5	0,254	0	3,45183
High	Master Protein	Q15428	Splicing factor 3A subunit 2 OS=Homo sapiens GN=SF3A2 PE=1 SV=2	4,366147398	5,603448	2	3	2	464	49,224	2,094	1,066	9760000	20440000	2	2	0,54	0	0
High	None	Q9BYX7	Putative beta-actin-like protein 3 OS=Homo sapiens GN=POTEKP PE=5 SV=1	14,09514736	7,733333	2	6	2	375	41,989	2,092	1,065	31130000	65130000	2	2	0,492	0	5,32513
High	Master Protein	P26358	DNA (cytosine-5)-methyltransferase 1 OS=Homo sapiens GN=DNMT1 PE=1 SV=2	10,24678291	2,908416	5	5	5	1616	183,05	2,079	1,056	4825000	10030000	4	5	0,132	0	3,61956
High	Master Protein	Q8NCA5	Protein FAM98A OS=Homo sapiens GN=FAM98A PE=1 SV=1	7,85664939	9,441233	3	4	3	519	55,366	2,079	1,056	4074000	8470000	3	3	0,425	0	1,69269
High	Master Protein	P29692	Elongation factor 1-delta OS=Homo sapiens GN=EEF1D PE=1 SV=5	19,93659583	26,69039	5	7	5	281	31,103	2,078	1,055	15430000	32060000	4	4	1,239	0	7,38508
High	Master Protein	Q8N163	Cell cycle and apoptosis regulator protein 2 OS=Homo sapiens GN=CCAR2 PE=1 SV=2	7,800968892	3,466956	3	4	3	923	102,838	2,078	1,055	3742000	7775000	3	3	0,182	0	3,80208
High	Master Protein	Q8NBJ5	Procollagen galactosyltransferase 1 OS=Homo sapiens GN=COLGALT1 PE=1 SV=1	17,87815106	8,842444	5	8	5	622	71,59	2,069	1,049	6801000	14070000	4	4	0,567	0	8,0284
High	Master Protein	Q1KMD3	Heterogeneous nuclear ribonucleoprotein U-like protein 2 OS=Homo sapiens GN=HNRNPUL2 PE=1 SV=1	32,27212646	19,81258	11	20	11	747	85,052	2,036	1,026	57750000	117600000	12	11	1,276	0	11,3131
High	None	Q96F07	Cytoplasmic FMR1-interacting protein 2 OS=Homo sapiens GN=CYFIP2 PE=1 SV=2	4,712411462	1,72144	2	2	2	1278	148,302	2,032	1,023	2323000	4720000	2	2	0,059	0	1,64902
High	Master Protein	Q7L576	Cytoplasmic FMR1-interacting protein 1 OS=Homo sapiens GN=CYFIP1 PE=1 SV=1	6,883172034	2,873105	3	3	3	1253	145,089	2,029	1,021	2632000	5339000	3	3	0,095	0	1,64902
High	None	Q14141	Septin-6 OS=Homo sapiens GN=SEPT6 PE=1 SV=4	3,459170748	4,608295	2	2	2	434	49,685	2,029	1,021	3157000	6404000	2	2	0,194	0	0
High	Master Protein	O43670	BUB3-interacting and GLEBS motif-containing protein ZNF207 OS=Homo sapiens GN=ZNF207 PE=1 SV=1	4,526907577	5,020921	2	3	2	478	50,717	2,025	1,018	6310000	12770000	2	2	1,154	0	0
High	Master Protein	O75718	Cartilage-associated protein OS=Homo sapiens GN=CRTAP PE=1 SV=1	2,515278601	5,236908	2	2	2	401	46,532	2,024	1,017	2282000	4618000	1	1	0,186	0	0
High	Master Protein	Q01780	Exosome component 10 OS=Homo sapiens GN=EXOSC10 PE=1 SV=2	2,590100067	3,389831	2	2	2	885	100,768	2,009	1,006	1494000	3003000	2	2	0,076	0	0
High	Master Protein	P68104	Elongation factor 1-alpha 1 OS=Homo sapiens GN=EEF1A1 PE=1 SV=1	48,40257977	27,48918	9	40	3	462	50,109	2,007	1,005	275700000	553300000	8	8	4,248	6	38,9906
High	Master Protein Candidate	Q5VTE0	Putative elongation factor 1-alpha-like 3 OS=Homo sapiens GN=EEF1A1P5 PE=5 SV=1	48,40257977	27,48918	9	40	3	462	50,153	2,007	1,005	275700000	553300000	8	8	4,248	0	38,9906
High	None	P68032	Actin, alpha cardiac muscle 1 OS=Homo sapiens GN=ACTC1 PE=1 SV=1	13,6015804	10,07958	3	5	3	377	41,992	2,003	1,002	21380000	42820000	2	2	0,492	0	5,32513

High	None	P68133	Actin, alpha skeletal muscle OS=Homo sapiens GN=ACTA1 PE=1 SV=1	13,6015804	10,07958	3	5	3	377	42,024	2,003	1,002	21380000	42820000	2	2	0,492	0	5,32513
High	None	P62736	Actin, aortic smooth muscle OS=Homo sapiens GN=ACTA2 PE=1 SV=1	13,6015804	10,07958	3	5	3	377	41,982	2,003	1,002	21380000	42820000	2	2	0,492	0	5,32513
High	None	P63267	Actin, gamma-enteric smooth muscle OS=Homo sapiens GN=ACTG2 PE=1 SV=1	13,6015804	10,10638	3	5	3	376	41,85	2,003	1,002	21380000	42820000	2	2	0,52	0	5,32513
High	None	Q16576	Histone-binding protein RBBP7 OS=Homo sapiens GN=RBBP7 PE=1 SV=1	3,453947181	3,529412	2	2	2	425	47,79	2,003	1,002	6077000	12170000	2	2	0,259	0	0
High	Master Protein	Q2TAY7	WD40 repeat-containing protein SMU1 OS=Homo sapiens GN=SMU1 PE=1 SV=2	4,287597374	7,407407	3	3	3	513	57,507	2,001	1,001	2342000	4686000	3	3	0,233	0	0
High	Master Protein	P11142	Heat shock cognate 71 kDa protein OS=Homo sapiens GN=HSPA8 PE=1 SV=1	65,98225441	30,65015	17	33	14	646	70,854	1,999	0,999	153100000	306100000	20	20	5,236	5	32,6489
High	Master Protein	Q9UN86	Ras GTPase-activating protein-binding protein 2 OS=Homo sapiens GN=G3BP2 PE=1 SV=2	10,85774742	8,091286	3	6	3	482	54,088	1,999	0,999	20410000	40800000	3	3	0,359	0	1,77134
High	Master Protein	Q9BR76	Coronin-1B OS=Homo sapiens GN=CORO1B PE=1 SV=1	12,81741915	12,26994	6	7	6	489	54,2	1,988	0,991	15190000	30190000	6	6	0,905	0	6,96191
High	Master Protein Candidate	Q14839	Chromodomain-helicase-DNA-binding protein 4 OS=Homo sapiens GN=CHD4 PE=1 SV=2	4,188315898	1,307531	2	2	2	1912	217,867	1,988	0,991	1465000	2912000	2	2	0,045	0	0
High	Master Protein	Q8TDI0	Chromodomain-helicase-DNA-binding protein 5 OS=Homo sapiens GN=CHD5 PE=1 SV=1	4,188315898	1,279427	2	2	2	1954	222,909	1,988	0,991	1465000	2912000	2	2	0,042	0	0
High	Master Protein	Q9Y3I0	tRNA-splicing ligase RtcB homolog OS=Homo sapiens GN=RTCB PE=1 SV=1	31,50556514	23,16832	10	15	10	505	55,175	1,971	0,979	42850000	84460000	10	10	2,162	0	7,62417
High	Master Protein	P62136	Serine/threonine-protein phosphatase PP1-alpha catalytic subunit OS=Homo sapiens GN=PPP1CA PE=1 SV=1	6,642003593	13,93939	4	4	4	330	37,488	1,939	0,955	5118000	9925000	4	4	0,585	0	1,9523
High	Master Protein	P50552	Vasodilator-stimulated phosphoprotein OS=Homo sapiens GN=VASP PE=1 SV=3	15,47407295	12,36842	4	7	4	380	39,805	1,927	0,946	12430000	23960000	4	4	1,448	0	2,21387
High	Master Protein	Q16181	Septin-7 OS=Homo sapiens GN=SEPT7 PE=1 SV=2	14,91601014	12,12815	4	8	4	437	50,648	1,915	0,937	27390000	52440000	5	5	0,817	0	2,22222
High	Master Protein	Q14444	Caprin-1 OS=Homo sapiens GN=CAPRIN1 PE=1 SV=2	23,80806383	9,308886	6	9	6	709	78,318	1,911	0,934	57640000	110100000	6	6	1,031	0	7,41021
High	Master Protein	Q9NVA2	Septin-11 OS=Homo sapiens GN=SEPT11 PE=1 SV=3	10,322004	10,25641	4	5	4	429	49,367	1,911	0,934	16890000	32270000	4	4	0,585	0	1,95787
High	Master Protein	Q15007	Pre-mRNA-splicing regulator WTAP OS=Homo sapiens GN=WTAP PE=1 SV=2	6,63706055	6,060606	2	2	2	396	44,217	1,907	0,931	3147000	6002000	2	2	0,194	0	0
High	Master Protein	P14866	Heterogeneous nuclear ribonucleoprotein L OS=Homo sapiens GN=HNRNPL PE=1 SV=2	15,30277069	20,03396	7	10	7	589	64,092	1,895	0,922	40990000	77690000	6	6	0,848	0	3,92411
High	None	O94973	AP-2 complex subunit alpha-2 OS=Homo sapiens GN=AP2A2 PE=1 SV=2	3,549977338	2,342918	2	2	2	939	103,895	1,895	0,922	2695000	5108000	2	2	0,086	0	0
High	Master Protein	Q12874	Splicing factor 3A subunit 3 OS=Homo sapiens GN=SF3A3 PE=1 SV=1	22,2158795	16,56687	6	10	6	501	58,812	1,873	0,905	29650000	55550000	5	6	1,276	0	1,8833

High	Master Protein	Q12996	Cleavage stimulation factor subunit 3 OS=Homo sapiens GN=CSTF3 PE=1 SV=1	19,01167317	6,415621	4	7	4	717	82,869	1,855	0,891	12860000	23850000	4	4	0,482	0	7,91133
High	Master Protein	Q15459	Splicing factor 3A subunit 1 OS=Homo sapiens GN=SF3A1 PE=1 SV=1	37,44318882	20,80706	14	20	14	793	88,831	1,854	0,891	80060000	148400000	13	13	1,683	0	10,904
High	Master Protein	P42285	Superkiller viralicidic activity 2-like 2 OS=Homo sapiens GN=SKIV2L2 PE=1 SV=3	9,545270471	4,606526	4	5	4	1042	117,729	1,85	0,888	5241000	9695000	4	4	0,204	0	1,87461
High	Master Protein	Q92499	ATP-dependent RNA helicase DDX1 OS=Homo sapiens GN=DDX1 PE=1 SV=2	40,26918239	25,54054	16	24	16	740	82,38	1,846	0,884	77670000	143400000	17	16	1,798	0	12,488
High	Master Protein	Q14676	Mediator of DNA damage checkpoint protein 1 OS=Homo sapiens GN=MDC1 PE=1 SV=3	3,221468185	0,957396	2	2	2	2089	226,529	1,832	0,873	2318000	4247000	2	2	0,048	0	0
High	Master Protein	Q14315	Filamin-C OS=Homo sapiens GN=FLNC PE=1 SV=3	37,42546034	4,807339	11	26	6	2725	290,841	1,829	0,871	4696000	8588000	5	5	0,228	0	27,3135
High	Master Protein	Q01844	RNA-binding protein EWS OS=Homo sapiens GN=EWSR1 PE=1 SV=1	19,58684643	7,317073	3	5	3	656	68,436	1,806	0,853	10490000	18940000	4	4	0,65	0	6,76824
High	Master Protein	Q00610	Clathrin heavy chain 1 OS=Homo sapiens GN=CLTC PE=1 SV=5	51,64730069	9,313433	12	21	12	1675	191,493	1,794	0,843	41960000	75260000	11	12	0,664	0	15,8353
High	Master Protein	P11021	78 kDa glucose-regulated protein OS=Homo sapiens GN=HSPA5 PE=1 SV=2	44,6400291	20,94801	10	19	8	654	72,288	1,787	0,838	20960000	37450000	7	7	1,598	0	20,6935
High	Master Protein	O00303	Eukaryotic translation initiation factor 3 subunit F OS=Homo sapiens GN=EIF3F PE=1 SV=1	28,4342601	15,68627	4	6	4	357	37,54	1,785	0,836	9694000	17310000	4	4	1,254	0	15,2488
High	Master Protein	P38646	Stress-70 protein, mitochondrial OS=Homo sapiens GN=HSPA9 PE=1 SV=2	10,00420043	5,44919	3	4	3	679	73,635	1,777	0,829	3791000	6737000	3	3	0,233	0	3,84852
High	Master Protein	O14979	Heterogeneous nuclear ribonucleoprotein D-like OS=Homo sapiens GN=HNRNPDL PE=1 SV=3	9,514777855	7,857143	3	4	2	420	46,409	1,775	0,828	3524000	6256000	1	1	0,468	0	3,53746
High	Master Protein	Q14683	Structural maintenance of chromosomes protein 1A OS=Homo sapiens GN=SMC1A PE=1 SV=2	18,79835695	6,082725	7	10	7	1233	143,144	1,772	0,825	12520000	22180000	7	7	0,299	0	3,5649
High	Master Protein	O60341	Lysine-specific histone demethylase 1A OS=Homo sapiens GN=KDM1A PE=1 SV=2	4,144466308	2,934272	2	2	2	852	92,845	1,772	0,825	1715000	3039000	2	2	0,099	0	1,65597
High	Master Protein	Q9UMS4	Pre-mRNA-processing factor 19 OS=Homo sapiens GN=PRPF19 PE=1 SV=1	19,04741968	18,65079	6	11	6	504	55,146	1,766	0,82	26650000	47060000	5	6	1,462	0	1,75836
High	Master Protein	Q15717	ELAV-like protein 1 OS=Homo sapiens GN=ELAVL1 PE=1 SV=2	16,99536891	15,95092	5	6	5	326	36,069	1,762	0,817	15710000	27690000	5	5	1,254	0	11,1315
High	Master Protein	P25205	DNA replication licensing factor MCM3 OS=Homo sapiens GN=MCM3 PE=1 SV=3	5,634374881	2,10396	2	3	2	808	90,924	1,757	0,813	1674000	2942000	2	2	0,129	0	1,7803
High	Master Protein	O43809	Cleavage and polyadenylation specificity factor subunit 5 OS=Homo sapiens GN=NUDT21 PE=1 SV=1	16,94191713	28,63436	5	7	5	227	26,211	1,752	0,809	39640000	69460000	6	6	1,738	0	6,14376
High	Master Protein	P43243	Matrin-3 OS=Homo sapiens GN=MATR3 PE=1 SV=2	15,3508069	6,847698	4	8	4	847	94,565	1,743	0,802	11720000	20420000	4	4	0,265	0	6,11155
High	Master Protein	Q00839	Heterogeneous nuclear ribonucleoprotein U OS=Homo sapiens GN=HNRNPU PE=1	72,28348714	19,87879	14	44	14	825	90,528	1,742	0,801	291400000	507700000	16	17	3,642	0	28,0231

			SV=6																
High	Master Protein	Q9Y285	Phenylalanine--tRNA ligase alpha subunit OS=Homo sapiens GN=FARSA PE=1 SV=3	23,42304123	16,73228	7	10	7	508	57,528	1,74	0,799	30210000	52550000	7	7	1,043	0	11,7282
High	Master Protein	Q09666	Neuroblast differentiation-associated protein AHNAK OS=Homo sapiens GN=AHNAK PE=1 SV=2	6,792358263	1,290323	4	4	4	5890	628,699	1,737	0,797	3216000	5587000	3	3	0,017	0	0
High	Master Protein	O15294	UDP-N-acetylglucosamine--peptide N-acetylglucosaminyltransferase 110 kDa subunit OS=Homo sapiens GN=OGT PE=1 SV=3	11,0246926	6,214149	6	6	6	1046	116,85	1,725	0,787	11720000	20220000	6	6	0,292	0	5,45924
High	Master Protein	P22626	Heterogeneous nuclear ribonucleoproteins A2/B1 OS=Homo sapiens GN=HNRNPA2B1 PE=1 SV=2	37,96066483	35,41076	11	25	9	353	37,407	1,723	0,785	152900000	263400000	10	10	5,158	2	25,0172
High	None	Q10567	AP-1 complex subunit beta-1 OS=Homo sapiens GN=AP1B1 PE=1 SV=2	10,98111953	3,898841	3	4	3	949	104,57	1,719	0,782	4086000	7024000	3	3	0,202	0	3,76177
High	Master Protein	Q86YP4	Transcriptional repressor p66-alpha OS=Homo sapiens GN=GATAD2A PE=1 SV=1	8,610535637	7,424961	3	4	2	633	68,021	1,716	0,779	6186000	10620000	3	3	0,239	1	1,75693
High	Master Protein	Q96ST3	Paired amphipathic helix protein Sin3a OS=Homo sapiens GN=SIN3A PE=1 SV=2	4,097231115	2,513747	3	3	3	1273	145,085	1,709	0,773	5779000	9875000	3	3	0,105	0	1,70041
High	Master Protein	O75534	Cold shock domain-containing protein E1 OS=Homo sapiens GN=CSDE1 PE=1 SV=2	4,238858811	3,759398	2	2	2	798	88,829	1,708	0,772	4556000	7781000	2	2	0,086	0	1,71216
High	Master Protein	Q05682	Caldesmon OS=Homo sapiens GN=CALD1 PE=1 SV=3	16,11166047	10,34048	6	6	6	793	93,175	1,705	0,77	46600000	79450000	6	6	0,369	0	4,2196
High	Master Protein	P46821	Microtubule-associated protein 1B OS=Homo sapiens GN=MAP1B PE=1 SV=2	13,6224974	4,497569	9	9	9	2468	270,468	1,698	0,764	20580000	34930000	9	9	0,185	0	1,77594
High	Master Protein	P49736	DNA replication licensing factor MCM2 OS=Homo sapiens GN=MCM2 PE=1 SV=4	20,35026023	8,185841	6	9	6	904	101,832	1,68	0,748	13710000	23050000	6	6	0,49	0	6,57963
High	None	P53675	Clathrin heavy chain 2 OS=Homo sapiens GN=CLTCL1 PE=1 SV=2	11,45200628	2,378049	3	5	3	1640	186,91	1,675	0,744	13200000	22120000	3	3	0,123	0	2,24835
High	Master Protein	P55072	Transitional endoplasmic reticulum ATPase OS=Homo sapiens GN=VCP PE=1 SV=4	10,81360657	8,312655	6	6	6	806	89,266	1,672	0,742	14040000	23480000	6	6	0,334	0	7,27259
High	Master Protein	Q02809	Procollagen-lysine,2-oxoglutarate 5-dioxygenase 1 OS=Homo sapiens GN=PLOD1 PE=1 SV=2	11,352989	8,66575	5	7	5	727	83,497	1,651	0,723	15960000	26340000	5	5	0,334	0	3,58637
High	Master Protein	Q7L014	Probable ATP-dependent RNA helicase DDX46 OS=Homo sapiens GN=DDX46 PE=1 SV=2	3,269940805	2,036857	2	2	2	1031	117,29	1,648	0,721	2336000	3848000	2	2	0,078	0	0
High	Master Protein	P06748	Nucleophosmin OS=Homo sapiens GN=NPM1 PE=1 SV=2	40,8122091	18,02721	3	15	3	294	32,555	1,639	0,713	56730000	92990000	4	3	2,594	0	21,1334
High	Master Protein	O14776	Transcription elongation regulator 1 OS=Homo sapiens GN=TCERG1 PE=1 SV=2	2,168806127	1,821494	2	2	2	1098	123,823	1,634	0,708	3157000	5160000	2	2	0,094	0	0
High	Master	Q16630	Cleavage and polyadenylation specificity	33,62983754	17,05989	6	9	6	551	59,173	1,632	0,707	37650000	61450000	5	5	1,462	0	18,6049

	Protein		factor subunit 6 OS=Homo sapiens GN=CPSF6 PE=1 SV=2																
High	Master Protein	P13639	Elongation factor 2 OS=Homo sapiens GN=EEF2 PE=1 SV=4	19,92567589	9,90676	9	11	9	858	95,277	1,631	0,706	36220000	59060000	9	9	0,598	0	5,40519
High	Master Protein	P51610	Host cell factor 1 OS=Homo sapiens GN=HCFC1 PE=1 SV=2	25,35235221	4,324324	7	10	7	2035	208,602	1,626	0,701	18130000	29470000	7	7	0,371	0	8,78622
High	Master Protein	Q9UHD8	Septin-9 OS=Homo sapiens GN=SEPT9 PE=1 SV=2	47,01497851	23,54949	11	18	11	586	65,361	1,616	0,692	67780000	109600000	10	10	1,661	0	17,0032
High	Master Protein	P60228	Eukaryotic translation initiation factor 3 subunit E OS=Homo sapiens GN=EIF3E PE=1 SV=1	8,420753258	9,213483	4	5	4	445	52,187	1,599	0,677	12330000	19710000	4	4	0,433	0	0
High	Master Protein	Q13347	Eukaryotic translation initiation factor 3 subunit I OS=Homo sapiens GN=EIF3I PE=1 SV=1	14,76101049	19,07692	6	7	6	325	36,479	1,592	0,671	20610000	32810000	6	6	1,015	0	5,57335
High	Master Protein	P02545	Prelamin-A/C OS=Homo sapiens GN=LMNA PE=1 SV=1	116,5897686	44,72892	28	54	28	664	74,095	1,585	0,664	390800000	619300000	32	33	11,915	0	47,7351
High	Master Protein	P23258	Tubulin gamma-1 chain OS=Homo sapiens GN=TUBG1 PE=1 SV=2	3,057080439	3,769401	2	2	2	451	51,138	1,579	0,659	3759000	5934000	2	2	0,233	0	0
High	Master Protein	O60934	Nibrin OS=Homo sapiens GN=NBN PE=1 SV=1	2,776773805	3,183024	2	2	2	754	84,906	1,575	0,655	269500	424400	1	1	0,105	0	0
High	Master Protein	O14497	AT-rich interactive domain-containing protein 1A OS=Homo sapiens GN=ARID1A PE=1 SV=3	2,683692421	1,181619	2	2	2	2285	241,892	1,571	0,652	1261000	1982000	2	2	0,027	0	0
High	Master Protein	Q92841	Probable ATP-dependent RNA helicase DDX17 OS=Homo sapiens GN=DDX17 PE=1 SV=2	49,54077618	23,59396	15	24	9	729	80,222	1,569	0,65	56880000	89260000	15	15	2,548	7	18,9405
High	Master Protein	Q9Y262	Eukaryotic translation initiation factor 3 subunit L OS=Homo sapiens GN=EIF3L PE=1 SV=1	17,63808076	14,53901	8	9	8	564	66,684	1,568	0,649	20070000	31460000	8	8	0,874	0	3,65644
High	Master Protein	P26641	Elongation factor 1-gamma OS=Homo sapiens GN=EEF1G PE=1 SV=3	48,39879974	24,48513	10	28	10	437	50,087	1,565	0,646	137800000	215600000	13	13	4,179	0	33,9619
High	Master Protein	Q86V81	THO complex subunit 4 OS=Homo sapiens GN=ALYREF PE=1 SV=3	12,45520649	24,51362	3	6	3	257	26,872	1,56	0,642	18810000	29340000	4	4	1,512	0	3,85696
High	Master Protein	Q12905	Interleukin enhancer-binding factor 2 OS=Homo sapiens GN=ILF2 PE=1 SV=2	19,97417517	11,53846	4	12	4	390	43,035	1,552	0,634	19020000	29510000	5	4	1,404	0	5,74894
High	Master Protein	P33992	DNA replication licensing factor MCM5 OS=Homo sapiens GN=MCM5 PE=1 SV=5	18,02517311	9,400545	5	8	5	734	82,233	1,538	0,621	6122000	9417000	4	5	0,468	0	7,59551
High	Master Protein	Q14152	Eukaryotic translation initiation factor 3 subunit A OS=Homo sapiens GN=EIF3A PE=1 SV=1	15,54398407	5,716353	7	9	7	1382	166,468	1,537	0,62	14820000	22770000	6	6	0,247	0	2,12863
High	Master Protein	P61978	Heterogeneous nuclear ribonucleoprotein K OS=Homo sapiens GN=HNRNPK PE=1 SV=1	53,48635139	35,42117	13	36	13	463	50,944	1,532	0,615	168100000	257600000	15	15	6,279	0	37,2453
High	Master Protein	Q99613	Eukaryotic translation initiation factor 3 subunit C OS=Homo sapiens GN=EIF3C	25,8143019	9,309967	8	12	8	913	105,278	1,528	0,612	28550000	43620000	6	7	0,778	0	15,7155

	Candidate		PE=1 SV=1																
High	Master Protein	B5ME19	Eukaryotic translation initiation factor 3 subunit C-like protein OS=Homo sapiens GN=EIF3CL PE=3 SV=1	25,8143019	9,299781	8	12	8	914	105,407	1,528	0,612	28550000	43620000	6	7	0,778	0	15,7155
High	Master Protein	Q96KR1	Zinc finger RNA-binding protein OS=Homo sapiens GN=ZFR PE=1 SV=2	6,991222182	4,003724	3	3	3	1074	116,939	1,52	0,604	4007000	6090000	3	3	0,151	0	2,06474
High	Master Protein	P33993	DNA replication licensing factor MCM7 OS=Homo sapiens GN=MCM7 PE=1 SV=4	21,61747157	15,85535	9	10	9	719	81,257	1,516	0,6	12500000	18940000	8	7	0,6	0	5,66968
High	Master Protein	P35637	RNA-binding protein FUS OS=Homo sapiens GN=FUS PE=1 SV=1	31,5596365	18,06084	6	20	6	526	53,394	1,513	0,597	100700000	152400000	7	7	4,275	0	11,22
High	Master Protein Candidate	Q92922	SWI/SNF complex subunit SMARCC1 OS=Homo sapiens GN=SMARCC1 PE=1 SV=3	7,935490803	2,533937	4	5	4	1105	122,79	1,513	0,597	12390000	18740000	3	4	0,204	0	1,64998
High	Master Protein	Q8TAQ2	SWI/SNF complex subunit SMARCC2 OS=Homo sapiens GN=SMARCC2 PE=1 SV=1	7,935490803	2,306425	4	5	4	1214	132,797	1,513	0,597	12390000	18740000	3	4	0,224	0	1,64998
High	Master Protein	O60506	Heterogeneous nuclear ribonucleoprotein Q OS=Homo sapiens GN=SYNCRIP PE=1 SV=2	83,24147388	39,80738	19	45	14	623	69,56	1,504	0,589	260400000	391700000	17	20	6,079	6	41,7264
High	Master Protein	P51659	Peroxisomal multifunctional enzyme type 2 OS=Homo sapiens GN=HSD17B4 PE=1 SV=3	16,41670559	11,68478	7	8	7	736	79,636	1,504	0,589	14530000	21840000	7	7	0,52	0	7,61166
High	Master Protein	O15372	Eukaryotic translation initiation factor 3 subunit H OS=Homo sapiens GN=EIF3H PE=1 SV=1	4,493890951	5,113636	2	2	2	352	39,905	1,504	0,589	5029000	7563000	2	2	0,212	0	2,04845
High	None	Q92804	TATA-binding protein-associated factor 2N OS=Homo sapiens GN=TAF15 PE=1 SV=1	5,634210262	3,885135	2	4	2	592	61,793	1,487	0,572	42800000	63650000	2	2	0,189	0	3,58116
High	Master Protein	O96019	Actin-like protein 6A OS=Homo sapiens GN=ACTL6A PE=1 SV=1	14,8714966	21,21212	7	7	7	429	47,43	1,467	0,553	17280000	25360000	7	7	1,154	0	7,49098
High	Master Protein	Q13435	Splicing factor 3B subunit 2 OS=Homo sapiens GN=SF3B2 PE=1 SV=2	15,99268158	6,368715	5	6	5	895	100,165	1,465	0,551	16960000	24850000	5	5	0,304	0	6,36927
High	Master Protein	Q86XP3	ATP-dependent RNA helicase DDX42 OS=Homo sapiens GN=DDX42 PE=1 SV=1	18,64514936	8,315565	6	8	6	938	102,912	1,463	0,549	17070000	24980000	6	6	0,389	0	6,2212
High	Master Protein	O95782	AP-2 complex subunit alpha-1 OS=Homo sapiens GN=AP2A1 PE=1 SV=3	6,95275645	4,503582	4	4	4	977	107,478	1,43	0,516	4653000	6654000	4	4	0,163	0	0

Supplementary table S2. KR motifs of the PIP3 specific pull down proteins

Entry	Entry name	Protein name	Gene name	Line number containing the KR motif
Q58FF8	H90B2_HUMAN	Putative heat shock protein HSP 90-...	HSP90AB2P HSP90BB	5:DDSGKDKKKKTKKIKEKYIDQEELNKTKPIWTRNTEDITQEEYGEFYKSLTNDWKDHLAV
P42167	LAP2B_HUMAN	Lamina-associated polypeptide 2, is...	TMPO LAP2	5:DRYSDNEEDSKIELKLEKREPLKGRAKTPVTLKQRRVEHNQSYSQAGITETEWTSGSSKG
P07900	HS90A_HUMAN	Heat shock protein HSP 90-alpha	HSP90AA1 HSP90A, HSPC1, HSPCA	6:KEEEKEKEEKESEDKPEIEDVGSDEEEEKKDGDKKKKKKIKEKYIDQEELNKTKPIWTRN
P35580	MYH10_HUMAN	Myosin-10	MYH10	18:EEEGARQKLQLEKVTAEAKIKKMEEEILLLEDQNSKFIKEKKLMEDRIAECSSQLAEEEE 19:KAKNLAKIRNKQEVMISDLEERLKKEEKTRQELEKAKRKLDGETTDLQDQIAELQAQIDE 22:HATALEELSEQLEQAKRFKANLEKNKQGLETDNKELACEVKVLQQVKAESEHKRKKLDAQ 27:EFERQNKQLRADMEDLMSSKDDVGKNVHELEKSKRALEQQVEEMRTQLEELEDELQATED
P35241	RADI_HUMAN	Radixin	RDX	7:EVQQMKAQAREEKHQKQLERAQLENEKKKREIAEKEKERIEREKEELMERLKQIEEQTIK 8:AQKELEEQTRKALELDQERKRAKEEAERLEKERRAAEEAKSAIAKQAADQMKNQEQLAAE 9:LAEFTAKIALLEEAKKKKEEEATEWQHKAFAAQEDLEKTKEELKTVMSAPPPPPPPPVIP
P08238	HS90B_HUMAN	Heat shock protein HSP 90-beta	HSP90AB1 HSP90B, HSPC2, HSPCB	6:DKDDEEKPKIEDVGSDEEDDSGKDKKKKTKKIKEKYIDQEELNKTKPIWTRNPDDITQEE
P35579	MYH9_HUMAN	Myosin-9	MYH9	9:TYERMFRWLVLRINKALDKTKRQGASFIGILDIAGFEIFDLNSFEQLCINYTNEKLQQLF 18:KLQLEKVTTEAKLKKLEEEQIILEDQNCKLAKEKKLLEDRIAEFTTNLTEEEEKSKSLAK 19:LKNKHEAMITDLEERLRREEKQRQELEKTRRKLEGDSTDLSDQIAELQAQIAELKMQLAK

				20:KEEELQAALARVEEEAAQKNMALKKIRELESQISELQEDLESERASRNKAEKQKRDLGEE 22:LAEQLEQTKRVKANLEKAKQTLENERGELANEVKVLLQGKGDSEHKRKKVEAQLQELQVK 27:QFRTEMEDLMSSKDDVGKSVHELEKSKRALEQQVEEMKTQLEELEDELQATEDAKLRLEV
P35749	MYH11_HUMAN	Myosin-11	MYH11 KIAA0866	4:FCVVVNPYKHLPIYSEKIVDMYKGKKRHEMPPHIYAIADTAYRSMLQDREDQSILCTGES 18:EEEAARQKLQLEKVTAEAKIKKLEDEILVMDDQNNKLSKERKLLEERISDLTTNLAEEEE 19:KAKNLTKLKNKHESMISELEVRLKKEEKSRQELEKLKRKLEGDASDFHEQIADLQAQIAE 22:HAQAVEELTEQLEQFKRAKANLDKNKQTLEKENADLAGELRVLGQAKQEVEHKKKKLEAQ 27:ELERTNKMLKAEMEDLVSSKDDVGKNVHELEKSKRALETQMEEMKTQLEELEDELQATED 32:LHEMEGAVKSKFKSTIAALEAKIAQLEEQVEQEAREKQAATKSLKQKDKKLKEILLQVED
Q9UPQ0	LIMC1_HUMAN	LIM and calponin homology domains-c...	LIMCH1 KIAA1102	12:SPLELKQDNGSIEINIKKPNSVPQELAATTEKTEPNSQEDKNDGGKSRKGNIELASSEPQ
Q7Z406	MYH14_HUMAN	Myosin-14	MYH14 KIAA2034, FP17425	18:EKKRLQQHIQELEAHLEAEEGARQKLQLEKVTTEAKMKKFEEDLLLLEDQNSKLSKERKL 19:LEDRLAEFSSQAAEEEEKVKSLNKLRLKYEATIADMEDRLRKEEKGRQELEKLKRRLDGE 21:QEDLESERVARTKAEKQRRDLGEELEALRGELEDTLDSTNAQQELRSKREQEVTELKKTL
Q13838	DX39B_HUMAN	Spliceosome RNA helicase DDX39B	DDX39B BAT1, UAP56	6:KFMQDPMEIFVDDETKLTLHGLQQYYVKLKDNEKNRKLFDLLDVLEFNQVVIFVKSVQRC
Q9UQ16	DYN3_HUMAN	Dynamin-3	DNM3 KIAA0820	11:KGGSKGYWFVLTAESLSWYKDDEEKEKKYMLPLDNLKVRDVEKSFMSSKHIFALFNTEQR
O00148	DX39A_HUMAN	ATP-dependent RNA helicase DDX39A	DDX39A DDX39	6:FMQDPMEVFVDDETKLTLHGLQQYYVKLKDSEKNRKLFDLLDVLEFNQVIIFVKSVQRCM

O00139	KIF2A_HUMAN	Kinesin-like protein KIF2A	KIF2A KIF2, KNS2	3:SLNPDLVPDEEIEPSPETPPPPASSAKVNKIVKNRRTVASIKNDPPSRDNRVVGSARARP
Q05193	DYN1_HUMAN	Dynamin-1	DNM1 DNM	11:YWFVLTAENLSWYKDDEEKEKKYMLSVDNLKLRDVEKGFMSSKHIFALFNTEQRNVYKDY
P50570	DYN2_HUMAN	Dynamin-2	DNM2 DYN2	11:YWFVLTAESLSWYKDEEEKEKKYMLPLDNLKIRDVEKGFMSNKHVFAIFNTEQRNVYKDL
Q7KZF4	SND1_HUMAN	Staphylococcal nuclease domain-cont...	SND1 TDRD11	7:IAVYTRGAEKLRAAERFAKERRLRIWRDYVAPTANLDQKDKQFVAKVMQVLNADAIVVKL
O43719	HTSF1_HUMAN	HIV Tat-specific factor 1	HTATSF1	5:KGDGLCCYLKRESVELALKLLDEDEIRGYKLHVEVAKFQLKGEYDASKKKKKCKDYKKKL
Q13200	PSMD2_HUMAN	26S proteasome non-ATPase regulator...	PSMD2 TRAP2	2:MEEGGRDKAPVQPQQSPAAAPGGTDEKPSGKERRDAGDKDKEQELSEEDKQLQDELEMLV 12:AGSGNVLKVQQLLHICSEHFDSKEKEEDKDKKEKKDKDKKEAPADMGAHQGVAVLGIALI
P26358	DNMT1_HUMAN	DNA (cytosine-5)-methyltransferase ...	DNMT1 AIM, CXXC9, DNMT	5:QEESERAKSDESIKEEDKDQDEKRRRVTSRERVARPLPAEEPERAKSGTRTEKEEERDEK 7:EKEPEKVNPQISDEKDEDEKEEKRRKTTPKEPTEKKMARAKTVMNSKTHPPKCIQCGQYL 12:RQTIRHSTREKDRGPTKATTTKLVYQIFDTFFAEQIEKDDREDKENAFKRRRCGVCEVCQ
P46940	IQGA1_HUMAN	Ras GTPase-activating-like protein ...	IQGAP1 KIAA0051	25:ARTILLNTKRLIVDVIRFQPGETLTEILETPATSEQEAEHQRAMQRRAIRDAKTPDKMKK 27:AELVKLQQTYAALNSKATFYGEQVDYYKSYIKTCLDNLASKGKVSKKPREMKGKKSKKIS
Q00341	VIGLN_HUMAN	Vigilin	HDLBP HBP, VGL	4:KDQGLSIMVSGKLDAVMKARKDIVARLQTQASATVAIPKEHHRFVIGKNGEKLQDLELKT 6:YNRLVGEIMQETGTRINIPPPSVNRTEIVFTGEKEQLAQAVARIKKIYEEKKKKTTTIAV 13:PAKLHNSLIGTKGRLIRSIMEECGGVHIHFPVEGSGSDTVVIRGPSSDVEKAKKQLLHLA 14:EEKQTKSFTVDIRAKPEYHKFLIGKGGGKIRKVRDSTGARVIFPAAEDKDQDLITIIGKE
Q9H2U1	DHX36_HUMAN	ATP-dependent RNA	DHX36 DDX36, KIAA1488,	11:PPGVRKIVIATNIAETSITIDDVVYVIDGGKIKETHFDTQNNISTMSAEWVSKANAKQRK

		helicase DHX36	MLEL1, RHAU	16:PKVAKIRLNLGKKRKMVKVYTKTDGLVAVHPKSVNVEQTDFHYNWLIYHLKMRTSSIYLY
P15311	EZRI_HUMAN	Ezrin	EZR VIL2	7:EVQQMKAQAREEKHQKQLERQQLETEKKRRETVEREKEQMMREKEELMLRLQDYEEKTKK
P51114	FXR1_HUMAN	Fragile X mental retardation syndro...	FXR1	11:ISRAESQSRQRNLPRETLAKNKKEMAKDVIEEHGPSEKAINGPTSASGDDISKLQRTPGE
Q8NE71	ABCF1_HUMAN	ATP-binding cassette sub-family F m...	ABCF1 ABC50	2:MPKAPKQQPPEPEWIGDGESTSPSDKVVKKGKKDKKIKKTFFEELAVEDKQAGEEEKVLK 3:EKEQQQQQQQQQQKKKRDTRKGRRKKDVDDDGEEKELMERLKKLSVPTSDEEDEVPAPKP 5:EKSKGKAKPQNKFAALDNEEEDKEEEIIKEKEPPKQGKEKAKKAEQGSEEEGEGEEEEEE 6:GGESKADDPYAHLSKKEKKKLKKQMEYERQVASLKAANAAENDFSVSQAEMSSRQAMLEN 11:QQKQKELLKQYEKQEKKLKELKAGGKSTKQAEKQTKEALTRKQQKCRRKNQDEESQEAPE
Q9NRZ9	HELLS_HUMAN	Lymphoid-specific helicase	HELLS PASG, SMARCA6, Nbla10143	3:TEIRYRRLQHLLEKSNIYSKFLLTKMEQQQLEEQKKKEKLERKKESLKVKKGKNSIDASE
Q8N163	CCAR2_HUMAN	Cell cycle and apoptosis regulator ...	CCAR2 DBC1, KIAA1967	5:FPARGPHGRLDQGRSDDYDSKKRKQRAGGEPWGAKKPRHDLPPYRVHLTPYTVDSPICDF
Q14694	UBP10_HUMAN	Ubiquitin carboxyl-terminal hydrola...	USP10 KIAA0190	4:ALALDGSSNVEAEVLENDGVSGGLGQRERKKKKKRPPGYYSYLKDGGDDSISTEALVNGH
O14776	TCRG1_HUMAN	Transcription elongation regulator ...	TCERG1 CA150, TAF2S	13:ARMKQFKDMLLERGVSAFSTWEKELHKIVFDPRYLLLNPKERKQVFDQYVKTRAEEERRE
Q9UKF6	CPSF3_HUMAN	Cleavage and polyadenylation specif...	CPSF3 CPSF73	2:MSAIPAEESDQLLIRPLGAGQEVGRSCIILEFKGRKIMLDCGIHPGLEGMDALPYIDLID
P26599	PTBP1_HUMAN	Polypyrimidine tract-	PTBP1 PTB	10:VKGFKFFQKDRKMALIQMGSVEEAVQALIDLHNHDLGENHHLRVSFSKSTI

		binding protei...		
P26038	MOES_HUMAN	Moesin	MSN	7:EVQQMKAQAREEKHQKQMERAMLENEKKKREMAEKEKEKIEREKEELMERLKQIEEQTKK
O43707	ACTN4_HUMAN	Alpha-actinin-4	ACTN4	5:KNVNVQNFHISWKDGLAFNALIHRHRPELIEYDKLRKDDPVTNLNNAFEVAEKYLDIPKM
P49916	DNLI3_HUMAN	DNA ligase 3	LIG3	13:DVKGTYEPGKRHWLKVKKDYLNEGAMADTADLVVLGAFYGQGSKGGMMSIFLMGCYDPGS
Q08043	ACTN3_HUMAN	Alpha-actinin-3	ACTN3	5:QNFHTSWKDGLALCALIHRHRPDLIDYAKLRKDDPIGNLNTAFEVAEKYLDIPKMLDAED
P20042	IF2B_HUMAN	Eukaryotic translation initiation f...	EIF2S2 EIF2B	2:MSGDEMIFDPTMSKKKKKKKKPFMLDEEGDTQTEETQPSETKEVEPEPTEDKDLEADEED 3:TRKKDASDDLDDLNFFNQKKKKKKTKKIFDIDEAEEGVKDLKIESDVQEPTEPEDDLDIM
P09874	PARP1_HUMAN	Poly [ADP-ribose] polymerase 1	PARP1 ADPRT, PPOL	3:GHSIRHPDVEVDGFSELRWDDQQKVKKTAEAGGVTGKGQDGIGSKAEKTLGDFAAEYAKS
P05198	IF2A_HUMAN	Eukaryotic translation initiation f...	EIF2S1 EIF2A	4:YTKDEQLESLFQRTAWVFDDKYKRPGYGAYDAFKHAVSDPSILDSLDLNEDEREVLINNI
Q14683	SMC1A_HUMAN	Structural maintenance of chromosom...	SMC1A DXS423E, KIAA0178, SB1.8, SMC1, SMC1L1	6:ELASKNKEIEKDKKRMDKVEDELKEKKKELGKMMREQQQIEKEIKEKDSELNQKRPQYIK 7:AKENTSHKIKKLEAAKKSLQNAQKHYKKRKGDMDELEKEMLSVEKARQEFEERMEEESQS 13:AKARRWDEKAVDKLKEKKERLTEELKEQMKAKRKEAELRQVQSQAHGLQMRLKYSQSDLE 15:CREIGVRNIREFEEEKVKRQNEIAKKRLEFENQKTRLGIQLDFEKNQLKEDQDKVHMWEQ 16:TVKKDENEIEKLKKEEQRHMKIIDETMAQLQDLKNQHLAKKSEVNDKNHEMEEIRKKLGG
P62826	RAN_HUMAN	GTP-binding nuclear protein Ran	RAN ARA24, OK/SW-cl.81	4:GNKVDIKDRKVKAKSIVFHRKKNLQYYDISAKSNYNFEKPFLWLARKLIGDPNLEFVAMP
Q5VTR2	BRE1A_HUMAN	E3 ubiquitin-protein ligase BRE1A	RNF20 BRE1A	2:MSGIGNKRAAGEPGTSMPPEKKAAVEDSGTTVETIKLGGVSSTEELDIRTLQTKNRKLAE

				13:VQLMAAEKKSKAELEDLRQRLKDLEDKEKKENKKMADEDALRKIRAVEEQIEYLQKKLAM
O75150	BRE1B_HUMAN	E3 ubiquitin-protein ligase BRE1B	RNF40 BRE1B, KIAA0661	2:MSGPGNKRAAGDGGSGPPEKKLSREEKTTTTLIEPIRLGGISSTEEMDLKVLQFKNKKLA 17:ESFNLKRAQEDISRLRRKLEKQRKVEVYADADEILQEEIKEYKARLTCPCCNTRKKDAVL
Q9Y3I0	RTCB_HUMAN	tRNA-splicing ligase RtcB homolog	RTCB C22orf28, HSPC117	9:ETFGTTCHGAGRALSRAKSRRNLDFQDVLDKLADMGIAIRVASPKLVMEEAPESYKNVTD
P42285	SK2L2_HUMAN	Superkiller viralicidic activity 2-...	SKIV2L2 DOB1, KIAA0052, Mtr4	19:NKFAEGITKIKRDIVFAASLYL
P12814	ACTN1_HUMAN	Alpha-actinin-1	ACTN1	5:ALIHRHRPELIDYGKLRKDDPLTNLNTAFDVAEKYLDIPKMLDAEDIVGTARPDEKAIMT
P78527	PRKDC_HUMAN	DNA-dependent protein kinase cataly...	PRKDC HYRC, HYRC1	21:KHVSLNKAKKRRLPRGFPPSASLCLLDLVKWLLAHCGRPQTECRHKSIELFYKFVPLLPG
Q01780	EXOSX_HUMAN	Exosome component 10	EXOSC10 PMSCL, PMSCL2, RRP6	5:IRPQLKFREKIDNSNTPFLPKIFIKPNAQKPLPQALSKERRERPQDRPEDLDVPPALADF
Q16181	SEPT7_HUMAN	Septin-7	SEPT7 CDC10	7:TNNVHYENYRSRKLAAVTYNGVDNNKNKGQLTKSPLAQMEEERREHVAKMKKMEMEMEQV 9:QNSSRTLEKNKKKGKIF
P14866	HNRPL_HUMAN	Heterogeneous nuclear ribonucleopro...	HNRNPL HNRPL, P/OKcl.14	2:MSRRLLPRAEKRRRRLEQRQQPDEQRRRSGAMVKMAAAGGGGGGGRYYGGGSEGGRAPKR
Q14676	MDC1_HUMAN	Mediator of DNA damage checkpoint p...	MDC1 KIAA0170, NFBD1	6:ATVEAKQSEAEVVTEIQLEKDQPLVKERDNDTKVKRGAGNGVVPAGVILERSQPPGEDSD
Q15459	SF3A1_HUMAN	Splicing factor 3A subunit 1	SF3A1 SAP114	5:FLTQLMQKEQRNYQFDFLRPQHSLFNYFTKLVEQYTKILIPPKGLFSKLKKEAENPREVL
P11021	GRP78_HUMAN	78 kDa glucose-	HSPA5 GRP78	6:VFEVVATNGDTHLGGEDFDQRVMEHFIKLYKKKTGKDVRKDNRAVQKLRREVEKAKRALS

		regulated protein		
Q7L014	DDX46_HUMAN	Probable ATP-dependent RNA helicase...	DDX46 KIAA0801	3:RSRDRKRLRRSRSRERDRSRERRRSRSRDRRRSRSRSRGRRSRSSSPGNKSKKTENRSRS 4:KEKTDGGESSKEKKKDKDDKEDEKEKDAGNFDQNKLEEEMRKRKERVEKWREEQRKKAME
O00571	DDX3X_HUMAN	ATP-dependent RNA helicase DDX3X	DDX3X DBX, DDX3	5:SFSDVEMGEIIMGNIELTRYTRPTPVQKHAIPIIKEKRDLMACAQTGSGKTAAFLLPILS
O15523	DDX3Y_HUMAN	ATP-dependent RNA helicase DDX3Y	DDX3Y DBY	5:SDIDMGEIIMGNIELTRYTRPTPVQKHAIPIIKGKRDLMACAQTGSGKTAAFLLPILSQI
P46063	RECQ1_HUMAN	ATP-dependent DNA helicase Q1	RECQL RECQ1, RECQL1	12:ESSQTCHSEQGDKKMEEKNSGNFQKKAANMLQQSGSKNTGAKKRKIDDA
Q86XP3	DDX42_HUMAN	ATP-dependent RNA helicase DDX42	DDX42	4:AEVEDQAARDMKRLEEKDKERKNVKGIRDDIEEEDDQEAYFRYMAENPTAGVVQEEEEDN 12:LLTPKDSNFAGDLVRNLEGANQHVSKELLDLAMQNAWFRKSRFKGGKGKKLNIGGGGLGY
Q14566	MCM6_HUMAN	DNA replication licensing factor MC...	MCM6	3:LVVSFVDLEQFNQQLSTTIQEEFYRVYPYLCRALKTFVKDRKEIPLAKDFYVAFQDLPTR
Q00839	HNRPU_HUMAN	Heterogeneous nuclear ribonucleopro...	HNRNPU HNRPU, SAFA, U21.1	2:MSSSPVNVKKLKVSELKEELKKRRLSDKGLKAELMERLQAALDDEEAGGRPAMEPGNGSL
Q9UQE7	SMC3_HUMAN	Structural maintenance of chromosom...	SMC3 BAM, BMH, CSPG6, SMC3L1	9:EDTEANKEKNLEQYNKLDQDLNEVKARVEELDRKYYEVKNKKDELQSERNYLWREENAEQ
P62136	PP1A_HUMAN	Serine/threonine-protein phosphatas...	PPP1CA PPP1A	7:KNKGKYGQFSGLNPGGRPITPPRNSAKAKK
P46821	MAP1B_HUMAN	Microtubule-associated protein 1B	MAP1B	8:VPENLKNPEPNIKMKRSIEEACFTLQYLNKLSMKPEPLFRSVGNTIDPVILFQKMGVGKL 12:SVTEKEVPSKEEPSPVKAEVAEKQATDVKPKAAKEKTVKKETKVKPEDKKEEKEKPKKEV

				13:AKKEDKTPIKKEEKPKKEEVKKEVKKEIKKEEKKEPKKEVKKETPPKEVKKEVKKEEKKE 39:DPEALAIEQNLGKALKKDLKEKTKTKKPGTKTKSSSPVKKSDGKSKPLAASPKPAGLKES
O60934	NBN_HUMAN	Nibrin	NBN NBS, NBS1, P95	13:SLVIKNSTSRNPSGINDDYGQLKNFKKFKKVTYPGAGKLPHIIGGSDLIAHHARKNTELE 14:EWLRQEMEVQNQHAKEESLADDLFRYNPYLKRRR
Q05682	CALD1_HUMAN	Caldesmon	CALD1 CAD, CDM	5:EENKKEDKEKEEEEEEKPKRGSIGENQVEVMVEEKTTESQEETVVMSLKNGQISSEEPKQ 9:KKAQEDKLQTAVLKKQGEEKGTKVQAKREKLQEDKPTFKKEEIKDEKIKKDKEPKEEVKS
P49959	MRE11_HUMAN	Double-strand break repair protein ...	MRE11 HNGS1, MRE11A	6:VIWGHEHECKIAPTKNEQQLFYISQPGSSVVTSLSPGEAVKKHVGLLRIKGRKMNMHKIP
Q13330	MTA1_HUMAN	Metastasis-associated protein MTA1	MTA1	12:MPSRGLANHGQARHMGPSRNLLLNGKSYPTKVRLIRGGSLPPVKRRRMNWIDAPDDVFYM
Q96KR1	ZFR_HUMAN	Zinc finger RNA-binding protein	ZFR	7:AAWTGTTFTKKAPFQNKQLKPKQPPKPPQIHYCDVCKISCAGPQTYKEHLEGQKHKKKEA 12:LKGRRHRLQYKKKVNPDLQVEVKPSIRARKIQEEKMRKQMQKEEYWRRREEEERWRMEMR 19:LAFRQIHKVLGMDPLPQMSQRFNIHNNRKRRRDSDGVDGFEAEGKKDKKDYDNF
Q14152	EIF3A_HUMAN	Eukaryotic translation initiation f...	EIF3A EIF3S10, KIAA0139	13:LEELDPDFIMAKQVEQLEKEKKELQERLKNQEKKIDYFERAKRLEEIPLIKSAYEEQRIK
P43243	MATR3_HUMAN	Matrin-3	MATR3 KIAA0723	9:PFGVISNHLILNKINEAFIEMATTEDAQAAVDYYTTTPALVFGKPVRVHLSQKYKRIKKP 11:TREDAMAMVDHCLKKALWFQGRCVKVDLSEKYKKLVLRIPNRGIDLLKKDKSRKRSYSPD
O60216	RAD21_HUMAN	Double-strand-break repair protein ...	RAD21 HR21, KIAA0078, NXP1	7:EEAFALEPIDITVKETKAKRKRKLIVDSVKELDSKTIRAQLSDYSDIVTTLDLAPPTKKL
Q99459	CDC5L_HUMAN	Cell division cycle 5-like	CDC5L KIAA0432,	4:RKLKPGEIDPNPETKPARPDPIDMDEDELEMLSEARARLANTQGKKAKRKAREKQLEEAR

		protein	PCDC5RP	5:RLAALQKRRELRAAGIEIQKKRKRKRGVDYNAEIPFEKKPALGFYDTSEENYQALDADFR 6:KLRQQDLDGELRSEKEGRDRKKDKQHLKRKKESDLPSAILQTSGVSEFTKKRSKLVLPAP
O60506	HNRPQ_HUMAN	Heterogeneous nuclear ribonucleopro...	SYNCRIP HNRPQ, NSAP1	8:FGKLERVKKLKDYAFIHFDERDGAVKAMEEMNGKDLEGENIEIVFAKPPDQKRKERKAQR
Q10567	AP1B1_HUMAN	AP-1 complex subunit beta-1	AP1B1 ADTB1, BAM22, CLAPB2	2:MTDSKYFTTTKKGEIFELKAELNSDKKEKKKEAVKKVIASMTVGKDVSALFPDVVNCMQT
P33993	MCM7_HUMAN	DNA replication licensing factor MC...	MCM7 CDC47, MCM2	2:MALKDYALEKEKVKKFLQEFYQDDELGKKQFKYGNQLVRLAHREQVALYVDLDDVAEDDP
Q13435	SF3B2_HUMAN	Splicing factor 3B subunit 2	SF3B2 SAP145	7:RSSLGQSASETEEDTVSVSKKEKNRKRRNRKKKKKPQRVRGVSSESSGDREKDSTRSRGS 9:KKGFEEEHKDSDDDSSDDEQEKKPEAPKLSKKKLRRMNRFTVAELKQLVARPDVVEMHDV 16:TQKYEEHVREQQAQVEKEDFSDMVAEHAAKQKQKKRKAQPQDSRGGSKKYKEFKF
P25205	MCM3_HUMAN	DNA replication licensing factor MC...	MCM3	13:EKKRKKRSEDESETEDEEEKSQEDQEQKRKRRKTRQPDAKDGDSYDPYDFSDTEEEMPQV
P55884	EIF3B_HUMAN	Eukaryotic translation initiation f...	EIF3B EIF3S9	14:KKDLKKYSKIFEQKDRLSQSKASKELVERRRTMMEDFRKYRKMAQELYMEQKNERLELRG
Q86YP4	P66A_HUMAN	Transcriptional repressor p66-alpha	GATAD2A	10:TAPAQAKAEPTAAPHPVLKQVIKPRRKLAFRSGEARDWSNGAVLQASSQLSRGSATTPRG
Q16630	CPSF6_HUMAN	Cleavage and polyadenylation specif...	CPSF6 CFIM68	10:ESKSYGSGSRRERSRERDHSRSREKSRRHKSRSRDRHDDYYRERSRERERHRDRDRDRDR
B5ME19	EIFCL_HUMAN	Eukaryotic translation initiation f...	EIF3CL	2:MSRFFTTGSDSESESSLSGEELVTKPVGGNYGKQPLLLSEDEEDTKRVVRSAKDKRFEEL 4:WEDKEGKKKMNKNNAKALSTLRQKIRKYNRDFESHITSYKQNPEQSADEDAEKNEEDSEG

				6:DSEEEEGKQTALASRFLKKAPTTDEDKKAAEKKREDKAKKKHDRKSKRLDEEEEEDNEGG
Q99613	EIF3C_HUMAN	Eukaryotic translation initiation f...	EIF3C EIF3S8	2:MSRFFTTGSDSESESSLSGEELVTKPVGGNYGKQPLLLSEDEEDTKRVVRSAKDKRFEEL 4:WEDKEGKKKMNKNNAKALSTLRQKIRKYNRDFESHITSYKQNPEQSADEDAEKNEEDSEG 6:DSEEEEGKQTALASRFLKKAPTTDEDKKAAEKKREDKAKKKHDRKSKRLDEEEEDNEGGE
P28370	SMCA1_HUMAN	Probable global transcription activ...	SMARCA1 SNF2L, SNF2L1	19:SLIEKENMEIEERERAEKKKRATKTPMVKFSAFS

Supplementary Table S3- List of antibodies used and dilution for immunofluorescence (IMF) staining or western immunoblotting (WB)

Antibodies	Reference Number	Company name	Dilutions
PtdIns(3,4,5)P3	Z-P345b	Echelon	**IMF:** 1:400
Nucleolin	12247	Cell signaling Technology	**IMF:** 1:100
PI3K p110 beta	ab151549 3011	Abcam Cell signaling Technology	**IMF:** 1:50 **WB:**1:2000
Fibrillarin	2639S	Cell signaling Technology	**IMF:** 1:100 **WB:**1:5000
RPA194	sc-48385	Santa cruz	**IMF:** 1:100
UBF	sc-9131	Santacruz	**IMF:** 1:50
Nucleophosmin	32-5200	Zymed	**IMF:** 1:1000
Nucleolin	14574S	Cell signaling Technology	**IMF:** 1:100
αTubulin	T5168	Sigma	**WB:** 1:20000
Hochest 33342	C10330	Thermo Fisher Scientific	**IMF:** 1:1000
PARP1	9542S	Cell signaling Technology	**IMF:** 1:50
Goat anti-Mouse IgG Alexa Fluor 594	A-11005	Thermo Fisher Scientific	**IMF**: 1:200
Goat anti-Rabbit Alexa Fluor 594	A-11012	Thermo Fisher Scientific	**IMF**: 1:200
Goat anti-Rabbit Alexa Fluor 488	A-11008	Thermo Fisher Scientific	**IMF**: 1:200
Goat anti-Mouse IgG Alexa Fluor 488	A-11001	Thermo Fisher Scientific	**IMF**: 1:200

III

Synthesis of phosphatidylinositol 3,4-bisphosphate and phosphatidylinositol 3,4,5-trisphosphate in distinct nuclear sites upon adipocyte differentiation

Rhîan G. Jacobsen*, Marianne Goris*‡, Fatemeh Mazloumi Gavgani*, Thomas Karlsson, Vandana Ardawatia and Aurélia E. Lewis

1 Department of Molecular biology, University of Bergen, Norway

* Shared first authorship

‡ Current address Department of Biomedicine, University of Bergen, Norway

Running title: Nuclear PI3K and adipogenesis

Corresponding author:
Aurélia E Lewis
Department of Molecular Biology
University of Bergen
Høyteknologisenteret
Thormølensgate 55
5008 Bergen
Norway

Telephone: +47-55584521
E.mail: aurelia.lewis@uib.no

Abstract

Spatial organisation is critical in signalling events. In particular, phosphoinositide 3-kinase (PI3K) signalling events have been shown to occur in both the cytoplasm and the nucleus. However, little is known about the regulation of this pathway within the nucleus and its contribution to adipocyte differentiation. In this project, the nuclear PI3K pathway was studied in the context of adipogenesis using mouse 3T3-L1 pre-adipocyte cells. We have shown that the PI3K/Akt pathway is active upon the induction of differentiation in the cytoplasm as well as in the nuclear compartment but in a delayed manner. We have shown the presence of the class I PI3K catalytic subunits p110α and p110β and class II PI3KC2α in the cytoplasm. In addition, p110β was localized in nucleoli and PI3KC2α in foci in the nucleoplasm. The levels of the products of these enzymes, PtdIns(3,4)P_2 and PtdIns(3,4,5)P_3 respectively, were shown to increase in the nucleus upon short term stimulation and up to 24h. The distribution differed for these 3'-phosphorylated polyphosphoinositides (3P-PPIn) in the nucleus and coincided with the localisation of the PI3Ks. To characterise the nuclear role of these PPIn, we have identified several potential nuclear PPIn-interacting proteins that are differently regulated during adipogenesis in 3T3-L1 cells by mass spectrometry. Altogether, this study demonstrates the presence of an active PI3K-Akt pathway as well as 3P-PPIn in distinct nuclear sub-sites in the nuclei of differentiating adipocytes. We suggest that nuclear p110β and PI3KC2α and their 3P-PPIn products regulate distinct nuclear processes contributing to adipocyte differentiation.

Introduction

The adipose tissue is a major source of metabolic fuel and contributes to whole body energy homeostasis by regulating fatty acid storage and mobilisation depending upon hormonal and energetic cues [1]. In the fed state, adipocytes are under the influence of insulin, which induces glucose and fatty acid uptake, esterification into triglycerides (TAGs) and storage into droplets (major lipogenesis pathway in adipocytes) as well as inhibition of TAG lipolysis [2, 3]. Insulin activates signalling cascades through the insulin receptor (IR), by inducing the phosphorylation of IR substrates and the activation of the class IA phosphatidylinositol 3 kinase (PI3K) signalling pathway [4-7] as well as class IIα PI3K [8]. Ultimately, the transcription of specific insulin responsive gene products is activated enabling glucose and lipid homeostasis [2, 3, 7]. Activation of class I PI3K generates the polyphosphoinositide (PPIn) lipid product phosphatidylinositol(3,4,5) triphosphate (PtdIns(3,4,5)P_3) which can be dephosphorylated to PtdIns(3,4)P_2 by SHIP2 (Src-homology-2 (SH2) domain-containing inositol 5-phosphatase) [9, 10]. These PPIns bind to and recruit the protein kinases Akt and 3-phosphoinositide-dependent protein kinase-1 (PDK1) to the plasma membrane via their PPIn-binding module plecktrin homology (PH) domains and Akt becomes activated by sequential phosphorylation on Thr308 and Ser473 by PDK1 and mammalian target of rapamycin complex 2 (mTORC2) respectively [11, 12]. Activated Akt can translocate to different intracellular sites where it phosphorylates a myriad of substrates. When in the nucleus, Akt phosphorylates and inactivates the transcription factor FoxO1 by nuclear exclusion, thus permitting adipogenic gene transcription [13]. Although a central role for Akt downstream of PI3K activation has clearly been demonstrated genetically and biochemically in insulin actions in glucose uptake and lipid metabolism [14], other effectors such as atypical PKCs have been implicated [15]. Additional effector proteins of PtdIns(3,4,)P_2 and PtdIns(3,4,5)P_3 have also been identified in interactomics studies in different cell types [16-18] but the functional significance of these interactions is largely unknown. Furthermore, Akt-independent responses to insulin signalling have also emerged in recent years both in hepatocytes and adipocytes [19-22]. For example, insulin stimulates the stepwise translocation of vesicles containing the GLUT4 glucose transporter to the plasma membrane in both Akt-dependent and independent processes, but still in a PI3K-dependent manner in adipocytes [20]. Consistently, decrease in class I PI3K activity in insulin resistance did not always correlate with a decrease in Akt activity, despite the observed lower glucose uptake [23, 24] and elevated free fatty acids due to inappropriate lipolysis [25]. These studies

suggest therefore the existence of Akt-independent events and the potential contribution of other PPIn effector proteins in insulin actions but downstream from PI3K activity.

Class I PI3Ks are heterodimeric proteins of a catalytic subunit and a regulatory subunit and organised in 2 sub-classes. Class IA consists of p110α, β or δ and a regulatory protein (p85α, p85β, p50α, p55α or p55γ) and class 1B consists of p110γ which interacts with p87/p101. p110α and β are ubiquitously expressed whereas p110δ and γ are expressed in hematopoietic cells [10]. Adipocytes express both p110α and p110β and low levels of p110δ [4, 26-28]. Both p110α and β are activated by insulin and generate PtdIns(3,4,5)P_3, but pharmacological studies using isoform specific inhibitors have shown that p110α, is the dominant isoform necessary for acute Akt activation as well as their adipocyte differentiation, as shown in 3T3-L1 cells [6, 26, 28, 29] or p110α knockout MEFs [30]. Contrasting results have been shown for p110β where, on one hand its activity was stimulated by insulin and its expression increased upon differentiation of 3T3-L1 cells [4], and on the other hand its selective inhibition had little impact on adipocyte differentiation [28, 29]. p110β may however contribute to sustained and long-term insulin signalling as mice expressing a kinase dead *Pik3cb* develop mild insulin resistance with age [5]. Class II PI3KC2α can be activated by insulin [8] in adipocytes and generate PtdIns3*P* and/or PtdIns(3,4)P_2 depending on the cell type [31-33], the latter activating AKT [32, 34]. PI3KC2α kinase dead mice show increased adipogenesis [35]. The contribution of this enzyme in adipocyte function is however not clear at the molecular level [35, 36]. Most research on PI3K-mediated signal transduction has focused on events taking place at the plasma membrane. However, an elegant study using molecular tools to investigate the subcellular actions of Akt showed that Akt signalling, not only contributed to 3T3-L1 adipocyte differentiation at the plasma membrane, but also in the nucleus at different stages of the process [37]. In addition, previous studies have implied that PI3K translocates to the nucleus upon extracellular stimulation, which was accompanied by an increase of nuclear PtdIns(3,4,5)P_3 [38, 39]. In more recent studies, PI3K enzymes have been shown to be present in the nucleus with PI3KC2α in nuclear speckles [40] and p110β in the nucleoplasm, chromatin-enriched fraction [41] or the nucleolus [42]. This was substantiated by the detection of their products PtdIns(3,4,5)P_3, as well as PtdIns3*P* and PtdIns(3,4)P_2 in the nucleus [43-46] and nucleoli [42] of different cell types. We therefore propose that the sub-cellular compartmentalisation of PI3K isoforms provides a mode of regulation mediating the myriad functions of the PI3K pathway downstream from insulin. Considering that the class I and II PI3K enzymes, p110β and PI3KC2α, can be activated by

insulin, we assessed their presence and activation in the nucleus upon adipocyte differentiation in 3T3-L1 cells.

Here, we have shown an increase in the presence of PtdIns(3,4) P_2 and PtdIns(3,4,5)P_3 as well as active Akt in the nucleus following adipocyte differentiation. This was complemented by the presence of both p110β and PI3KC2α in distinct nuclear sites in these cells in addition to their cytoplasmic localisation. These results suggest that the spatial organisation of these enzymes and the local synthesis of their products contribute to the insulin actions in adipogenesis.

Results

Temporal and sub-cellular activation of the PI3K-Akt pathway upon adipocyte differentiation

Considering that both p110α and p110β contribute to insulin responses, but that p110β has been reported to be localized in the nucleus in some cells and both nuclear and plasma membrane Akt activity are required for adipocyte differentiation, we first determined if the PI3K-Akt pathway was active in the nucleus as well as in the cytoplasm in 3T3-L1 cells upon stimulation of differentiation (Figure 1). α-Tubulin and lamin A/C were used as markers for the cytoplasmic and nuclear fractions respectively, calnexin was used as a marker for the endoplasmic reticulum. Both acute (Figure 1A) and long term stimulation (Figure 1B) were examined to assess the subcellular localization of active phosphorylated Akt on S473 (p-S473-Akt) in cytoplasmic and nuclear fractions. We showed that the PI3K pathway was activated both in the cytoplasm and the nucleus in acute stimulation of up to 2 h. The appearance of active Akt was detected within 5 min in the cytoplasmic fraction but was delayed in the nucleus and appeared within 30 min. In the nucleus, p-S743-Akt was detected as a double band but only the upper band was sensitive to PI3K inhibition with LY294002 (Figure 1C). In long-term stimulation (Figure 1B), the levels of pS473-Akt tended however to increase in D1, to be lower at D2 but to increase again slightly at D3 and D5 in the cytoplasmic fractions. In the nucleus, Akt is found in its active form at D1, D2 and D3 compared to D0 and the levels decrease again at D5. Differentiation was monitored by demonstrating an increase in PPARγ1/2 levels in the nucleus overtime (Figure 1D) and oil red staining (not shown). Taken together, these results suggest that the PI3K-Akt pathway is found in its active form in the nucleus but at different time points compared to cytoplasmic events.

PtdIns(3,4)P_2 and PtdIns(3,4,5)P_3 levels increase in nuclear compartments

Contrasting reports (reviewed in [47]) have shown that the occurrence of active Akt in the nucleus may be due to prior activation in the cytoplasm followed by its translocation [48] or by its activation directly within the nucleus [49]. Detection of p-S473-Akt may not be a direct indicator of active PI3K and of the local production of PtdIns(3,4,5)P_3 in the nucleus. We have therefore adapted a method from Guillou *et al.* [50] to detect specifically the nuclear levels of both PtdIns(3,4)P_2 and PtdIns(3,4,5)P_3 following nuclear isolation, lipid extraction and lipid overlay assays. To this end, we have used the specific PtdIns(3,4)P_2 and PtdIns(3,4,5)P_3 probes, an anti-PtdIns(3,4)P_2 antibody and GST-GRP1-PH respectively [50, 51], as demonstrated in Figure S1A-C. Acidic lipids were extracted from cell fractions obtained at different time points of stimulation and analysed by lipid overlay assay to detect PtdIns(3,4)P_2 and PtdIns(3,4,5)P_3 (Figure 2A-B). The levels of both PPIns were increased in the nuclear fractions within 60-120 min of stimulation and this was maintained at D1 (Figure 2A-B). Consistently, an overall increase in PtdIns(3,4)P_2 nuclear intensity was apparent by immunofluorescence staining within 30 min (Supplementary Figure S2) and at D1 (Figure 2C). PtdIns(3,4)P_2 staining was particularly pronounced in numerous foci within nuclei, reminiscent of nuclear speckles (Supplementary Figure S2 and Figure 4D). Using a specific anti- PtdIns(3,4,5)P_3 antibody (Supplementary Figure S1D), PtdIns(3,4,5)P_3 could be detected in the nucleoplasm at all time points. Overall, changes in the nuclear intensity of PtdIns(3,4,5)P_3 were less apparent following stimulation (Supplementary Figure S3 and Figure 2D) but strong signals could be detected in nucleoli in some cells (Supplementary Figure S3 and Figure 4E-F), consistent with our previous study in the breast cancer cells AU565 [42]. In sum, we show an increase in the levels of PtdIns(3,4)P_2 and PtdIns(3,4,5)P_3 in distinct sub-nuclear sites upon adipocyte differentiation.

Class I p110β and class II PI3KC2α are localized in different sub-nuclear sites of 3T3-L1 Cells

We have recently showed that 3T3-L1 cells express class IA p110α, β and δ throughout their differentiation program [28]. In addition, using selective pharmacological inhibition of each enzyme, we showed that p110α plays a dominant role in adipogenesis compared to the two other isoforms. Both p110β and δ had a small contribution but it was not clear at which stage of the differentiation program [28]. Considering that p110β is known to reside not only in the cytoplasm but also in the nucleus [41] and in particular in the nucleolus [42], this isoform could be hence responsible, in part, for the production of nuclear

PtdIns(3,4,5)P_3. PtdIns(3,4)P_2 can be produced by the class II PI3Ks [32, 33] and PI3KC2α has been reported to localise to nuclear speckles [40]. We hence determined the sub-cellular localisation of these two enzymes in 3T3-L1 cells by Western immunoblotting following nuclear fractionation and immunofluorescence staining (Figure 3). As shown in Figure 3A, p110α was detected in the cytoplasm but not in the nuclear fractions at all time-points. In addition, p110β was mainly distributed in the cytoplasmic fractions throughout adipogenesis and was hardly detectable in the nuclear fraction using two different anti-p110β antibodies (Figure 3B and Supplementary Figure S4). In contrast, PI3KC2α was found in both compartments at D0 but with two different migrating bands (Figure 3A), as shown in HeLa cells [40]. The levels of the top band decreased thereafter in the cytoplasm and could not be detected from D3, while both bands were present in nuclear fractions at variable levels throughout the time course. Using immunofluorescence staining, we were able to strongly detect p110β in the cytoplasm but weakly in the nucleoplasm. However, discrete p110β foci were apparent in the nucleoli together with the RNA polymerase I subunit RPA 194 (Figure 3B). PI3KC2α was weakly detected in the cytoplasm but strongly in the nucleoplasm (Figure 3C). Taken together, these results show the presence of PI3K enzymes in the same sub-nuclear sites as their products.

Identification of Topo IIα and nucleolin as potential PPIn-binding proteins

Considering that we were able to map PtdIns(3,4)P_2 and PtdIns(3,4,5)P_3 as well as their metabolising enzymes to the nucleus, we attempted to identify binding proteins at time points when these PPIns are elevated. To this end, we applied a method we have previously developed to identify potential nuclear PPIn-binding protein in any cellular status [52]. We exploited the ability of PPIns to bind to the polybasic aminoglycoside neomycin [53] and predicted that neomycin would compete for binding to PPIns, therefore displacing PPIn-interacting proteins. Incubation of intact nuclei with neomycin resulted in the displacement of many proteins from nuclei to supernatants. By combining quantitative mass spectrometry using SILAC (stable isotope labelling with amino acids in cell culture) and nuclear fractionation, we identified 168 nuclear proteins displaced specifically by neomycin [52]. Importantly, a subset of these proteins were shown to interact with PtdIns(4,5)P_2. Similarly, by incubating 3T3-L1 nuclei with neomycin, we have identified several nuclear proteins displaced by neomycin only when nuclei were isolated from cells induced to differentiate for 24 h (Fig 4A – Day 1). These proteins include Topo IIα, DNMT1 (DNA methyltransferase 1), HSP90α (Heat shock protein 90α) and nucleolin (Supplementary table S2), which were also

displaced by neomycin in another cell line in our previous study [52]. These results were validated by Western immunoblotting for Topo IIα and nucleolin (Figure 4B). While Topo IIα was displaced specifically by neomycin and not by retention buffer alone, less clear differences were observed for nucleolin (Figure 4C). This may indicate that PPIn may contribute differently in the nuclear retention of these two proteins. Considering that Topo IIα can bind to both PtdIns(3,4)P_2 and PtdIns(3,4,5)P_3 *in vitro* (data not shown), we ascertained the localisation of Topo IIα at day 1 in relation to both PtdIns(3,4)P_2 and PtdIns(3,4,5)P_3 by immunofluorescence staining. Topo IIα localised in the nucleoplasm and strongly in foci, consistently with our previous study [28], known as centric/pericentric heterochromatin (PCH) [54] (Figure 4D-E). Overall, partial colocalisation could be observed between Topo IIα and either PPIn in some of the foci highlighted by PtdIns(3,4)P_2 (Figure 4D – white arrows) or in the nucleoplasm with PtdIns(3,4,5)P_3 but not in the nucleolus where strong intensity of the lipid can be detected (Figure 4E). The nucleolar protein, nucleolin, was in contrast detected with strong overlaps with PtdIns(3,4,5)P_3 (Figure 4F). We next determined the effect of p110β inhibition on neomycin-dependent displacement of these proteins (Figure 4G). The nuclear levels of these two proteins were affected differently by p110β inhibition with a decrease in Topo IIα but no change for nucleolin. In contrast both proteins were more displaced by neomycin following p110β inhibition. This may suggest that PtdIns(3,4,5)P_3 may affect the retention of nucleolin in the nucleolus and Topo IIα in the nucleoplasm.

Discussion

The PI3K pathway is essential in a myriad of cellular processes. The pathway is orchestrated by class I PI3K enzymes, which share the same enzymatic properties and generate the same lipid product, PtdIns(3,4,5)P_3, which recruits effector proteins. Despite these common properties, different signalling inputs as well as outputs, in particular towards Akt, are coupled to the different PI3K isoforms, which may explain some of the pleiotropic roles of PI3K signalling at cellular and organismal level [10, 55, 56]. In the case of ubiquitously expressed p110α and p110β, different cellular functions have been attributed to each isoform in different cell types [6, 57-60]. However, the molecular mode of regulation coupled to each of the p110α and p110β isoforms remain unclear. Nevertheless, one distinguishing feature between p110α and p110β is that p110β is nuclear as well as cytoplasmic in different cells [41, 60]. This could be compatible with the idea that the PI3K pathway could operate also in the nucleus, from where other processes could be regulated.

Consistent with this notion, we have shown, in this study, the presence of an active PI3K pathway in the nucleus upon short and long term stimulation of differentiation of 3T3-L1 cells by the detection of increased levels of active AKT and of the product of PI3K enzymes, *i.e.* PtdIns(3,4)P_2 and PtdIns(3,4,5)P_3. The presence of active nuclear AKT is documented in various cell lines and upon different external cues [41, 48, 49]. However, whether this is due to the prior activation of Akt in the cytoplasm followed by its translocation to the nucleus or its local activation within the nucleus itself is controversial [47]. In this study, total AKT was observed in the nuclear fractions of non-stimulated cells (D0) and treatment with the pan-PI3K inhibitor did not prevent the nuclear presence of AKT following stimulation. These observations may indicate the possibility of the local activation of AKT within the nuclear compartment upon insulin stimulation and reinforce the importance of a nuclear active pool of AKT in the differentiation program of 3T3-L1 cells [37]. Moreover, the increased detection of the AKT-binding PPIns, PtdIns(3,4)P_2 and PtdIns(3,4,5)P_3, in the nucleus prior to the increase in nuclear active AKT would support the idea that a similar mechanism to the cytoplasmic activation of AKT could operate in the nucleus. Interestingly, both PDK1 and mTORC2, which are known to be activated through interaction with PtdIns(3,4,5)P_3 and lead to the phosphorylation of AKT on T308 and S473 respectively, have previously been detected in the nucleus [61-64], hence implying the same mechanism of AKT activation at the nuclear level. So far, the interaction of AKT with PtdIns(3,4,5)P_3 in the nucleus has been implied in one study whereby PtdIns(3,4,5)P_3 regulates the AKT/NPM/B23 association in the nucleoplasm [65].

In this study, both PtdIns(3,4)P_2 and PtdIns(3,4,5)P_3 were increased in the nuclear compartment upon stimulation. The kinases known to produce these two PPIns and that could act in the nucleus are the PI3Ks, PI3KC2α and p110β, respectively. These two enzymes were indeed found localised in the nucleus of 3T3-L1 cells at overlapping sites of their lipid products, *i.e.* in the nucleolus for p110β and in foci resembling nuclear speckles for PI3KC2α. The nucleolar localisation of both p110β and PtdIns(3,4,5)P_3 in 3T3-L1 cells is consistent with our previous study in the breast cancer cell line AU565 using the same antibody [42], thus further indicating a general role for p110β in nucleolar processes. p110β could however only be detected in the nuclear fraction by immunofluorescence staining and not by Western immunoblotting. This may be due to low levels only found in the nucleolus and with very little signal in the rest of the nucleus in 3T3-L1 cells, as shown by immunostaining. In contrast, PtdIns(3,4,5)P_3 was detected diffusely in the nucleoplasm of these cells where p110β was hardly detectable. This would suggest that PtdIns(3,4,5)P_3 is generated by other

PtdIns(3,4,5)P_3-generating enzyme in the nucleoplasm. We have indeed observed that the nuclear increase in PtdIns(3,4,5)P_3 was not blocked by the PI3K inhibitor, LY294002 (data not shown), hence further supporting the notion that the synthesis of PtdIns(3,4,5)P_3 in the nucleoplasm may be due to PI3K activity that is insensitive to class I PI3K inhibitors. Inositol polyphosphate kinase (IPMK), initially discovered as an inositol (1,4,5) triphosphate (IP3) kinase, acts also as a nuclear PI3K by phosphorylating PtdIns(4,5)P_2 to PtdIns(3,4,5)P_3 and is insensitive to PI3K inhibitors [66, 67]. Immunofluorescence cellular imaging of the endogenous kinase, shows IPMK in the nucleoplasm in a punctate pattern [66] in different cell types (http://www.proteinatlas.org/ENSG00000151151-IPMK/cell, [68]) and excluded from nucleoli. Altogether, the nuclear synthesis of PtdIns(3,4,5)P_3 may arise from IPMK in the nucleoplasm and from p110β in nucleoli in 3T3-L1 cells. Nucleolar activity and especially that of ribosomal RNA transcription is decreased in cells undergoing differentiation, including during adipogenesis [69]. This could be consistent with the seemingly lower level of p110β in nucleoli of 3T3-L1 cells compared to the more active cancer cells AU565 cells. As for IPMK, it has recently been shown to contribute to myogenic differentiation in concert with the phospholipase Cβ1 [70]. A role for this kinase in the context of adipogenesis remains to be discovered.

The cytoplasmic fraction of PI3KC2α diminished greatly within 24 h of insulin stimulation while the nuclear fraction remained unchanged. The nuclear localisation in 3T3-L1 cells was reminiscent of that of HeLa cells as reported by Didichenko *et al.* in nuclear speckles [40]. One of the two possible PPIn product of this enzyme, PtdIns(3,4)P_2, localises seemingly at the same foci and this could hence suggest an enzymatic link. However, the exact product hydrolysed in the nucleus by PI3KC2α, PtdIns(4)*P* and/or PtdIns(3,4)P_2 remains to be demonstrated. Another possibility is the de-phosphorylation of PtdIns(3,4,5)P_3 to PtdIns(3,4)P_2 by SHIP2. Interestingly, a phosphorylated form of SHIP2 on S132 has previously been reported to be nuclear and in particular at nuclear speckles [71]. This nuclear pool of PtdIns(3,4,5)P_3, particularly in the nucleoplasm, could be used as a substrate by SHIP2. Consistently, Resnick *et al.* have demonstrated that PtdIns(3,4,5)P_3 synthesised by IPMK is indeed a substrate of SHIP2 [66]. Altogether, this would imply that the distinct nuclear localisation of IPMK and p110β could allow the synthesis of different pools of PtdIns(3,4,5)P_3, which can be remodelled due to the actions of different PtdIns(3,4,5)P_3 phosphatases. Hence, further studies characterising the regulation and activity of IPMK and SHIP2 in the nucleus upon differentiation is warranted.

To understand how the production of these two different PPIns could contribute to the response of pre-adipocytes to the induction of differentiation, we have attempted to identify nuclear effector proteins for these lipids. We have found Topo IIα and nucleolin as potential nuclear PPIn-effector proteins in 3T3-L1 cells. These two proteins show differential overlaps with PtdIns(3,4,5)P_3 at different sites of the nucleus in the nucleoplasm for Topo IIα and the nucleolus for nucleolin. Hence the production of PtdIns(3,4,5)P_3 at different sites in the nucleus permits the potential regulation of different effector proteins. The differential remodelling of this lipid in a spatial manner has also the potential to add an extra layer of regulation. Inhibition of p110β led to an increase in the displacement of both proteins by neomycin. Considering that both proteins can bind to nucleic acids, it may be conceivable that PPIn interaction may compete electrostatically or regulate allosterically the interaction of these proteins with nucleic acids. Consistently, a few studies have demonstrated these possible modes of regulations. For example, the HIV-1 viral protein Gag interacts both with PtdIns(4,5)P_2 and RNA via the same highly basic region, which offer distinct mode of regulation of the association of the protein with the plasma membrane [72]. In addition, ALY (alias THO complex subunit 4), a protein regulating mRNA export, binds PtdIns(3,4,5)P_3 via basic residues [73] and this interaction contributes to ALY-mediated recognition of specific mRNA transcripts for their nuclear export [74]. Similarly to the PPIn-effector protein EBP1 [42], Topo IIα and nucleolin harbour basic-rich motifs, seven and one respectively, that could be relevant for their interaction with PPIn and nucleic acids and the regulation of their functions.

In conclusion, this study suggests that nuclear PPIn provide an additional mode of regulation mediating the myriad functions of the PI3K pathway downstream from insulin. We have indeed shown the synthesis of the PPIns, PtdIns(3,4)P_2 and PtdIns(3,4,5)P_3, distinct sub-nuclear localisation, in the nucleoplasm, nuclear speckles as well as nucleoli, upon the induction of differentiation. This implies that these lipids contribute in different nuclear processes by affecting the function of distinct effector proteins at these sites. Further studies to clarify the nuclear roles of PPIn and their metabolising enzymes in adipogenesis are under way.

Materials and methods

Reagents and antibodies

Antibodies used in Western immunoblotting and immunostaining are listed in Supplementary Table S1.

Cell Culture and differentiation of 3T3-L1 cells

3T3-L1 fibroblasts were kindly provided by Ass. Professor Lise Madsen (University of Copenhagen, Denmark). 3T3-L1 cells were grown and differentiated as previously reported for up to a maximum of 7 days [28].

Cell fractionation

Cell fractionation was adapted from a method by O'Caroll *et al.* [75]. All steps were done on ice. Cells, grown in 10 cm dishes, were washed twice with PBS and quickly rinsed with a hypotonic buffer (10 mM Tris-HCl pH 7.8 with 1 % Igepal. Cells were scrapped into 500 µL of hypotonic buffer containing 1 mM DTT, 5 mM NaF, 2 mM Na_3VO_4 and 1x Protease Inhibitor Cocktail and incubated for 3 min on ice. 500 µL milliQ H_2O was added and the cells were incubated for 3 more min before they were subjected to 8 passages through a 23-gauge needle. The lysates were centrifuged at 400 g for 5-10 min at 4 °C. The supernatant, containing the cytoplasmic fraction, was spun again at 600 g for 5-8 min to avoid nuclear contamination. Isolated nuclei were washed in 1 mL wash buffer (10 mM Tris-HCl pH 7.5 and 2 mM $MgCl_2$) and spun at 600 g for 4-8 min, this wash step was then repeated. Nuclei were then used for neomycin extraction, for lipid extraction. Alternatively, nuclei were lysed in RIPA buffer (50 mM Tris pH 8.0, 0.5 % deoxycholic acid, 150 mM NaCl, 1 % Igepal, 0.1 % SDS) supplemented with 5 mM NaF, 2 mM Na_3VO_4 and 1x Protease Inhibitor Cocktail and sonicated in an ultrasonic bath for 1-2 min before being centrifuged at 13000 rpm. Protein concentration was then determined using BCA reagent (Pierce) on supernatants.

Neomycin extraction

Nuclei were isolated as described above but using an igepal-free hypotonic buffer was used. Nuclei were washed in retention buffer (20 mM Tris pH 7.5, 70 mM NaCl, 20 mM KCl, 5 mM $MgCl_2$, 3 mM $CaCl_2$) and centrifuged at 1300 g for 5 mins. Nuclei were then incubated in retention buffer containing 5 mM neomycin (Neomycin trisulfate salt, Sigma-Aldrich) for 30 min at room temperature in an eppendorf mixer at 700 rpm before being centrifuged at 13000

rpm for 5 mins and the supernatants collected (neomycin extracts). Neomycin extracts were dialysed using Slide-A-Lyser Mini dialysis units (Thermo Fisher) for 1 h at room temperature then overnight at 4^0C in 900 ml dialysis buffer (20 mM HEPES pH 7.5, 150 mM NaCl, 5 mM EDTA, 0.1 % IGEPAL). Protein concentration was then determined using BCA reagent (Thermo Fisher).

SDS-PAGE and Western Immunoblotting

Equal amount of proteins obtained from neomycin extraction samples or cytoplasmic and nuclear fractions were resolved by SDS-PAGE. Proteins were then transferred to nitrocellulose membranes which were then blocked in 7% fat-free milk in TBS-T (50 mM Tris pH 7.5, 150 mM NaCl, 0.1 % Tween-20) or PBS-T (PBS pH 7.4, 0.05 % Tween-20) for 1 h at room temperature or 4^0C overnight. Primary antibodies (*c.f.* Supplementary Table S1) were incubated overnight at 4^0C and secondary antibodies conjugated to HRP for 1 h at room temperature. To strip the membranes, membranes were first incubated for 20 min at RT in RestoreTM Western Blot Stripping Buffer (Thermo Fisher), before being blocked again and if required probed with the corresponding secondary antibody to detect any remaining signal prior to further immunoblotting. Equal protein loading and fraction purity were confirmed by immunodetection of α-tubulin and/or lamin A/C (incubated 1 h at room temperature). Bands were visualised using BioRad ChemiDoc^{TM} Xrs+ with enhanced chemiluminescence (ECL) with SuperSignal West Pico or Femto Chemiluminescent Substrate (Pierce). Band densities were assessed using ImageJ.

Lipid Extraction from nuclear fractions

Cells were seeded in 15 cm dishes and cell fractionation was performed as above (with 2.5 x the volume used for 10 cm dishes). The protein concentration was determined for each nuclear preparation and lipid extraction was performed from fractions with equal protein amount. Lipids were extracted from nuclear fractions using a method adapted from Gray *et al.* [76]. Nuclei were resuspended in 1 mL of MeOH/$CHCl_3$ (2:1, v:v) to extract neutral lipids and incubated for 10 min at room temperature with shaking at 1200 rpm with 3-4 vortexing. The samples were centrifuged at 3000 g for 5 min at 4 °C, the supernatant discarded and the same procedure was repeated. The acidic lipids were then extracted with 0.75 mL of MeOH/$CHCl_3$/concentrated HCl (80:40:1, v:v:v) and incubated for 15 min at room temperature with shaking at 1200 rpm and vortexed 4 times during the incubation 0.25 mL $CHCl_3$ and 0.45 mL 0.1 M HCl were added and the samples were vortexed and centrifuged at

3000 g for 5 min at 4 °C and a phase split between the organic and aqueous phases was apparent. The organic phase (lower phase) was collected in conical glass tubes and dried at 60^0C under N_2 gas and stored at -20°C until further use. Lipids were resuspended with 3 µl of MeOH/CHCl3/H_2O 2:1:0,8, vortexed for 30 seconds before being sonicated in an ice bath for 5 min and vortexed again for 30 sec.

Lipid Overlay Assay

Lipids were spotted on Hybond-CExtra membranes (Amersham Biosciences), 3 µl at a time. The membranes were left to dry for 1 h at room temperature protected from light. The membranes were next blocked for 1 h at room temperature with the appropriate blocking buffer (1% fat-free milk in PBS for PtdIns(3,4,5)P_3 and 3 % FAF BSA in PBS-T (0.1%) pH 7.4 for PtdINs(3,4)P_2) and further incubated with 0.5 µg/mL GST-GRP1-PH (for PtdIns(3,4,5)P_3 detection) or anti-PtdIns(3,4)P_2 antibody (1:2000) in the same buffer overnight at 4°C protected from light. GST-GRP1-PH was expressed and purified as described previously [52]. The membranes were washed 6 x 5 min in PBS or PBS-T and then incubated with anti-GST-HRP (1:80,000) or anti-mouse IgG conjugated to HRP (1:20,000) in blocking buffer for 1 h at room temperature. The blots were washed 6 x 5 min with PBS or PBS-T. Revelation was performed by ECL using the SuperSignal West Pico Chemiluminescent Substrate (Pierce) or with SuperSignal West Femto Maximum Sensitivity Substrate and detected with a BioRad ChemiDoc^{TM} Xrs+. Lipid spot densitometry was quantified using ImageJ.

Proteomics sample preparation for MALDI-TOF analyses

50 µg of dialysed neomycin extracts were run on long 5-15 % gradient gel and stained using imperial protein stain (Thermo Fisher). Gel bands were cut out and washed twice in 25 mM ammonium bicarbonate (Ambic) in 50% acetonitrile (ACN) and dried in a rotavapor. Cysteins were reduced by addition of 10 mM DTT in 100 mM Ambic for 45 mins at 56 ^{o}C and then alkylated using 55 mM iodoacetamide (IAA) in 100 mM Ambic incubated 30 mins in the dark at room temperature and then washed twice and dried. In gel protein digestion was done using 40 µl of 5 ng/µl porcine trypsin (Promega) in digestion buffer (50 mM Ambic) and rehydrated on ice for 30 mins before a further 16 h at 37 ^{o}C with additional digestion buffer. After cooling and spinning down supernatant was removed. Remaining gel pieces were incubated for 20 mins at room temperature with 50 µl 1 % trifluoroacetic acid (TFA) in an eppendorf mixer and supernatant pooled with the first. Gel pieces were then incubated with 50

µl 60 % ACN 0.1 % TFA for 20 mins room temperature in an eppendorf mixer and supernatant pooled with the previous two. Supernatant pool was then vacuum dried until 10-15 µl remained and frozen -20 ^{0}C until further use. A Stage Tip (STop And Go Extraction Tip) column with Empore nC_{18} 3M extraction disk (Varian) was prepared and washed 3 times with methanol and then wetted with 60 % ACN/0.1 % TFA and conditioned with 0.1 % TFA. Samples were then bound and washed in 0.1 % TFA before being dried. Peptides were eluted in alpha cyano-4-hydroxycinnamic acid (CHCA) matrix (6 mg/ml CHCA, 60 % ACN, 15% methanol, 0.1 % TFA) and analysed by MALDI-TOF/TOF (Ultraflex, Bruker Daltonics). Raw files were searched with MASCOT against a *mus musculus* database from Uniprot/Swissprot. The following search parameters were used; carbamidomethyl (Cys) as fixed modification and oxidation (Met) as a variable modification, peptide tolerance of 50 ppm were allowed for precursors.

Immunofluorescence staining

Immunofluorescence staining was performed according to our previous study [28] and images were acquired by confocal microscopy with a Leica TCS SP5 confocal laser scanning microscope equipped with a 63x/1.4 oil immersion lens and using 488nm and 633 nm laser lines. Images were processed with the Leica application suite version 4.4 and Photoshop.

Acknowledgments

We thank Ann Kristin Froyset (Department of Molecular Biology, University of Bergen) for her help with MALDI-TOF proteomics analyses.

This project was funded by Helse Bergen Vest (project number 911682), the Norwegian Diabetes and the Meltzer foundations.

References

1. Rutkowski, J.M., J.H. Stern, and P.E. Scherer, *The cell biology of fat expansion.* J Cell Biol, 2015. **208**(5): p. 501-12.
2. Foukas, L.C. and D.J. Withers, *Phosphoinositide signalling pathways in metabolic regulation.* Curr Top Microbiol Immunol, 2010. **346**: p. 115-41.
3. Czech, M.P., et al., *Insulin signalling mechanisms for triacylglycerol storage.* Diabetologia, 2013. **56**(5): p. 949-64.
4. Asano, T., et al., *p110beta is up-regulated during differentiation of 3T3-L1 cells and contributes to the highly insulin-responsive glucose transport activity.* J Biol Chem, 2000. **275**(23): p. 17671-6.
5. Ciraolo, E., et al., *Phosphoinositide 3-kinase p110beta activity: key role in metabolism and mammary gland cancer but not development.* Science signaling, 2008. **1**(36).
6. Knight, Z.A., et al., *A pharmacological map of the PI3-K family defines a role for p110alpha in insulin signaling.* Cell, 2006. **125**(4): p. 733-47.
7. Boucher, J., A. Kleinridders, and C.R. Kahn, *Insulin receptor signaling in normal and insulin-resistant states.* Cold Spring Harb Perspect Biol, 2014. **6**(1).
8. Brown, R., et al., *Insulin activates the alpha isoform of class II phosphoinositide 3-kinase.* The Journal of biological chemistry, 1999. **274**(21): p. 14529-14532.
9. Sasaki, T., et al., *Mammalian phosphoinositide kinases and phosphatases.* Prog Lipid Res, 2009. **48**(6): p. 307-43.
10. Vanhaesebroeck, B., L. Stephens, and P. Hawkins, *PI3K signalling: the path to discovery and understanding.* Nat Rev Mol Cell Biol, 2012. **13**(3): p. 195-203.
11. Bunney, T.D. and M. Katan, *Phosphoinositide signalling in cancer: beyond PI3K and PTEN.* Nat Rev Cancer, 2010. **10**(5): p. 342-52.
12. Salamon, R.S. and J.M. Backer, *Phosphatidylinositol-3,4,5-trisphosphate: tool of choice for class I PI 3-kinases.* Bioessays, 2013. **35**(7): p. 602-11.
13. Tzivion, G., M. Dobson, and G. Ramakrishnan, *FoxO transcription factors; Regulation by AKT and 14-3-3 proteins.* Biochim Biophys Acta, 2011. **1813**(11): p. 1938-45.
14. Fayard, E., et al., *Protein kinase B (PKB/Akt), a key mediator of the PI3K signaling pathway.* Curr Top Microbiol Immunol, 2010. **346**: p. 31-56.
15. Farese, R.V., M.P. Sajan, and M.L. Standaert, *Atypical protein kinase C in insulin action and insulin resistance.* Biochem Soc Trans, 2005. **33**(Pt 2): p. 350-3.
16. Pasquali, C., et al., *A chemical proteomics approach to phosphatidylinositol 3-kinase signaling in macrophages.* Mol Cell Proteomics, 2007. **6**(11): p. 1829-41.
17. Catimel, B., et al., *PI(3,4,5)P3 Interactome.* J Proteome Res, 2009. **8**(7): p. 3712-26.
18. Dixon, M.J., et al., *A screen for novel phosphoinositide 3-kinase effector proteins.* Mol Cell Proteomics, 2011. **10**(4): p. M110 003178.
19. Choi, S., et al., *Insulin regulates adipocyte lipolysis via an Akt-independent signaling pathway.* Molecular and cellular biology, 2010. **30**(21): p. 5009-5020.
20. Gonzalez, E. and T. McGraw, *Insulin signaling diverges into Akt-dependent and -independent signals to regulate the recruitment/docking and the fusion of GLUT4 vesicles to the plasma membrane.* Molecular biology of the cell, 2006. **17**(10): p. 4484-4493.
21. Lu, M., et al., *Insulin regulates liver metabolism in vivo in the absence of hepatic Akt and Foxo1.* Nature medicine, 2012. **18**(3): p. 388-395.
22. Yuan, M., et al., *Identification of Akt-independent regulation of hepatic lipogenesis by mammalian target of rapamycin (mTOR) complex 2.* The Journal of biological chemistry, 2012. **287**(35): p. 29579-29588.
23. Bjornholm, M., et al., *Insulin signal transduction and glucose transport in human adipocytes: effects of obesity and low calorie diet.* Diabetologia, 2002. **45**(8): p. 1128-35.
24. Smith, U., *Impaired ('diabetic') insulin signaling and action occur in fat cells long before glucose intolerance--is insulin resistance initiated in the adipose tissue?* Int J Obes Relat Metab Disord, 2002. **26**(7): p. 897-904.
25. Savage, D.B., K.F. Petersen, and G.I. Shulman, *Disordered lipid metabolism and the pathogenesis of insulin resistance.* Physiol Rev, 2007. **87**(2): p. 507-20.
26. Chaussade, C., et al., *Evidence for functional redundancy of class IA PI3K isoforms in insulin signalling.* Biochem J, 2007. **404**(3): p. 449-58.
27. Geering, B., et al., *Class IA phosphoinositide 3-kinases are obligate p85-p110 heterodimers.* Proc Natl Acad Sci U S A, 2007. **104**(19): p. 7809-14.

28. Jacobsen, R.G., et al., *DNA Topoisomerase IIα contributes to the early steps of adipogenesis in 3T3-L1 cells.* Cellular Signalling, 2016. **28**(10): p. 1593-1603.
29. Kim, J.E., P.R. Shepherd, and C. Chaussade, *Investigating the role of class-IA PI 3-kinase isoforms in adipocyte differentiation.* Biochem Biophys Res Commun, 2009. **379**(4): p. 830-4.
30. Zhao, J.J., et al., *The p110alpha isoform of PI3K is essential for proper growth factor signaling and oncogenic transformation.* Proc Natl Acad Sci U S A, 2006. **103**(44): p. 16296-300.
31. Gao, Z., et al., *Inhibition of insulin sensitivity by free fatty acids requires activation of multiple serine kinases in 3T3-L1 adipocytes.* Mol Endocrinol, 2004. **18**(8): p. 2024-34.
32. Leibiger, B., et al., *Insulin-feedback via PI3K-C2alpha activated PKBalpha/Akt1 is required for glucose-stimulated insulin secretion.* FASEB J, 2010. **24**(6): p. 1824-1837.
33. Falasca, M., et al., *The role of phosphoinositide 3-kinase C2alpha in insulin signaling.* J Biol Chem, 2007. **282**(38): p. 28226-36.
34. Campa, C.C., I. Franco, and E. Hirsch, *PI3K-C2alpha: One enzyme for two products coupling vesicle trafficking and signal transduction.* FEBS Lett, 2015. **589**(14): p. 1552-8.
35. Alliouachene, S., et al., *Inactivation of class II PI3K-C2alpha induces leptin resistance, age-dependent insulin resistance and obesity in male mice.* Diabetologia, 2016. **59**(7): p. 1503-12.
36. Mazza, S. and T. Maffucci, *Class II phosphoinositide 3-kinase C2alpha: what we learned so far.* International journal of biochemistry and molecular biology, 2011. **2**(2): p. 168-182.
37. Maiuri, T., J. Ho, and V. Stambolic, *Regulation of adipocyte differentiation by distinct subcellular pools of protein kinase B (PKB/Akt).* J Biol Chem, 2010. **285**(20): p. 15038-47.
38. Neri, L.M., et al., *Erythropoietin-induced erythroid differentiation of K562 cells is accompanied by the nuclear translocation of phosphatidylinositol 3-kinase and intranuclear generation of phosphatidylinositol (3,4,5) trisphosphate.* Cell Signal, 2002. **14**(1): p. 21-9.
39. Neri, L.M., et al., *Increase in nuclear phosphatidylinositol 3-kinase activity and phosphatidylinositol (3,4,5) trisphosphate synthesis precede PKC-zeta translocation to the nucleus of NGF-treated PC12 cells.* FASEB J, 1999. **13**(15): p. 2299-310.
40. Didichenko, S.A. and M. Thelen, *Phosphatidylinositol 3-kinase c2alpha contains a nuclear localization sequence and associates with nuclear speckles.* The Journal of biological chemistry, 2001. **276**(51): p. 48135-42.
41. Kumar, A., et al., *Nuclear but not cytosolic phosphoinositide 3-kinase beta has an essential function in cell survival.* Mol Cell Biol, 2011. **31**(10): p. 2122-33.
42. Karlsson, T., et al., *A polybasic motif in ErbB3-binding protein 1 (EBP1) has key functions in nucleolar localization and polyphosphoinositide interaction.* Biochem J, 2016. **473**(14): p. 2033-47.
43. Lindsay, Y., et al., *Localization of agonist-sensitive PtdIns(3,4,5)P3 reveals a nuclear pool that is insensitive to PTEN expression.* Journal of cell science, 2006. **119**(Pt 24): p. 5160-5168.
44. Kumar, A., O. Fernandez-Capetillo, and A.C. Carrera, *Nuclear phosphoinositide 3-kinase beta controls double-strand break DNA repair.* Proc Natl Acad Sci U S A, 2010. **107**(16): p. 7491-6.
45. Gillooly, D.J., et al., *Localization of phosphatidylinositol 3-phosphate in yeast and mammalian cells.* Embo j, 2000. **19**(17): p. 4577-88.
46. Sindic, A., et al., *Activation of phosphoinositide 3-kinase C2 beta in the nuclear matrix during compensatory liver growth.* Adv Enzyme Regul, 2006. **46**: p. 280-7.
47. Martelli, A., et al., *The emerging multiple roles of nuclear Akt.* Biochimica et biophysica acta, 2012. **1823**(12): p. 2168-2178.
48. Xuan Nguyen, T.L., et al., *Akt phosphorylation is essential for nuclear translocation and retention in NGF-stimulated PC12 cells.* Biochem Biophys Res Commun, 2006. **349**(2): p. 789-98.
49. Wang, R. and M.G. Brattain, *AKT can be activated in the nucleus.* Cell Signal, 2006. **18**(10): p. 1722-31.
50. Guillou, H., et al., *Use of the GRP1 PH domain as a tool to measure the relative levels of PtdIns(3,4,5)P3 through a protein-lipid overlay approach.* J Lipid Res, 2007. **48**(3): p. 726-32.
51. Venkateswarlu, K., et al., *Nerve growth factor- and epidermal growth factor-stimulated translocation of the ADP-ribosylation factor-exchange factor GRP1 to the plasma membrane of PC12 cells requires activation of phosphatidylinositol 3-kinase and the GRP1 pleckstrin homology domain.* Biochem J, 1998. **335 (Pt 1)**: p. 139-46.
52. Lewis, A.E., et al., *Identification of nuclear phosphatidylinositol 4,5-bisphosphate-interacting proteins by neomycin extraction.* Mol Cell Proteomics, 2011. **10**(2): p. M110 003376.
53. Schacht, J., *Purification of polyphosphoinositides by chromatography on immobilized neomycin.* J Lipid Res, 1978. **19**(8): p. 1063-7.

54. Guetg, C. and R. Santoro, *Formation of nuclear heterochromatin: the nucleolar point of view.* Epigenetics, 2012. **7**(8): p. 811-4.
55. Vanhaesebroeck, B., et al., *The emerging mechanisms of isoform-specific PI3K signalling.* Nat Rev Mol Cell Biol, 2010. **11**(5): p. 329-41.
56. Jean, S. and A.A. Kiger, *Classes of phosphoinositide 3-kinases at a glance.* J Cell Sci, 2014. **127**(Pt 5): p. 923-8.
57. Benistant, C., H. Chapuis, and S. Roche, *A specific function for phosphatidylinositol 3-kinase alpha (p85alpha-p110alpha) in cell survival and for phosphatidylinositol 3-kinase beta (p85alpha-p110beta) in de novo DNA synthesis of human colon carcinoma cells.* Oncogene, 2000. **19**(44): p. 5083-90.
58. Foukas, L.C., et al., *Critical role for the p110alpha phosphoinositide-3-OH kinase in growth and metabolic regulation.* Nature, 2006. **441**(7091): p. 366-70.
59. Kingham, E. and M. Welham, *Distinct roles for isoforms of the catalytic subunit of class-IA PI3K in the regulation of behaviour of murine embryonic stem cells.* J Cell Sci, 2009. **122**(Pt 13): p. 2311-21.
60. Marques, M., et al., *Specific function of phosphoinositide 3-kinase beta in the control of DNA replication.* Proc Natl Acad Sci U S A, 2009. **106**(18): p. 7525-30.
61. Lim, M.A., et al., *Nuclear translocation of 3'-phosphoinositide-dependent protein kinase 1 (PDK-1): a potential regulatory mechanism for PDK-1 function.* Proc Natl Acad Sci U S A, 2003. **100**(24): p. 14006-11.
62. Scheid, M.P., M. Parsons, and J.R. Woodgett, *Phosphoinositide-dependent phosphorylation of PDK1 regulates nuclear translocation.* Mol Cell Biol, 2005. **25**(6): p. 2347-63.
63. Sephton, C.F., et al., *The nuclear localization of 3'-phosphoinositide-dependent kinase-1 is dependent on its association with the protein tyrosine phosphatase SHP-1.* Cell Signal, 2009. **21**(11): p. 1634-44.
64. Rosner, M. and M. Hengstschlager, *Cytoplasmic and nuclear distribution of the protein complexes mTORC1 and mTORC2: rapamycin triggers dephosphorylation and delocalization of the mTORC2 components rictor and sin1.* Hum Mol Genet, 2008. **17**(19): p. 2934-48.
65. Kwon, I.S., et al., *PI(3,4,5)P3 regulates the interaction between Akt and B23 in the nucleus.* BMB Rep, 2010. **43**(2): p. 127-32.
66. Resnick, A.C., et al., *Inositol polyphosphate multikinase is a nuclear PI3-kinase with transcriptional regulatory activity.* Proc Natl Acad Sci U S A, 2005. **102**(36): p. 12783-8.
67. Maag, D., et al., *Inositol polyphosphate multikinase is a physiologic PI3-kinase that activates Akt/PKB.* Proc Natl Acad Sci U S A, 2011. **108**(4): p. 1391-6.
68. Uhlen, M., et al., *Proteomics. Tissue-based map of the human proteome.* Science, 2015. **347**(6220): p. 1260419.
69. Ali, S.A., et al., *Phenotypic transcription factors epigenetically mediate cell growth control.* Proc Natl Acad Sci U S A, 2008. **105**(18): p. 6632-7.
70. Ramazzotti, G., et al., *IPMK and beta-catenin mediate PLC-beta1-dependent signaling in myogenic differentiation.* Oncotarget, 2016. **7**(51): p. 84118-84127.
71. Elong Edimo, W., et al., *Evidence of SHIP2 Ser132 phosphorylation, its nuclear localization and stability.* Biochem J, 2011. **439**(3): p. 391-401.
72. Chukkapalli, V., S.J. Oh, and A. Ono, *Opposing mechanisms involving RNA and lipids regulate HIV-1 Gag membrane binding through the highly basic region of the matrix domain.* Proc Natl Acad Sci U S A, 2010. **107**(4): p. 1600-5.
73. Okada, M., S.W. Jang, and K. Ye, *Akt phosphorylation and nuclear phosphoinositide association mediate mRNA export and cell proliferation activities by ALY.* Proc Natl Acad Sci U S A, 2008. **105**(25): p. 8649-54.
74. Wickramasinghe, V.O., et al., *Human inositol polyphosphate multikinase regulates transcript-selective nuclear mRNA export to preserve genome integrity.* Mol Cell, 2013. **51**(6): p. 737-50.
75. O'Carroll, S.J., et al., *Nuclear PLCbeta1 is required for 3T3-L1 adipocyte differentiation and regulates expression of the cyclin D3-cdk4 complex.* Cell Signal, 2009. **21**(6): p. 926-35.
76. Gray, A., et al., *Nonradioactive methods for the assay of phosphoinositide 3-kinases and phosphoinositide phosphatases and selective detection of signaling lipids in cell and tissue extracts.* Anal Biochem, 2003. **313**(2): p. 234-45.

Figures legends

Figure 1. Active Akt levels increase in both cytoplasm and the nucleus upon adipocyte differentiation

Two days post-confluent (D0) 3T3-L1 preadipocytes were incubated with the differentiation cocktail for **(A)** 5 to 120 min, **(C)** 30 or 60 min in the absence (-) or presence (+) of 20 μM LY294002 or **(B-D)** induced to differentiate for up to 7 days (D7). Cells were fractionated into cytoplasmic and nuclear fractions and equal protein amounts were resolved by SDS-PAGE and analysed by Western immunobloting with the indicated antibodies. α-tubulin, calnexin (ER marker) and lamin A/C were used as loading and fractionation controls. Densitometric analyses of three different experiments + SDs are shown as fold increase of the pS473-Akt/Akt ratios compared to D0.

Figure 2. Increased levels of PtdIns(3,4)P_2 and PtdIns(3,4,5)P_3 in the nucleus

(A-B) Acidic lipids were extracted from 3T3-L1 nuclear cell fractions, spotted on nitrocellulose membrane and probed with anti-PtdIns(3,4)P_2 antibody (A) and GST-GRP1-PH (B) by lipid overlay assay. (**C**). Confocal images of immunostained 3T3-L1 cells fixed at day 0 (D0) and day 1 (D1) with anti-PtdIns(3,4)P_2 and PtdIns(3,4,5)P_3 antibodies and counterstained with TO-PRO-3. Scale bar indicates 10 μm (63x).

Figure 3. Sub-cellular compartmentalisation of PI3Ks

(A) Two days post-confluent (D0) 3T3-L1 preadipocytes were incubated with the differentiation cocktail for 1 day (D1) and up to 7 days (D7) and cells were fractionated into cytoplasmic and nuclear fractions. Equal protein amounts of cytoplasmic extracts (40 μg) and nuclear extracts (60-70 μg) were resolved by SDS-PAGE and analysed by Western immunobloting using the indicated antibodies. α-tubulin, calnexin and lamin A/C were used as loading and fractionation controls. **(B-C)** Confocal images of immunostained 3T3-L1 cells fixed at day 0 (D0) and day 1 (D1) with anti-p110β and the RNA polymerase I subunit A1 (RPA194) (B) or PI3KC2α (C) and counterstained with TO-PRO-3. Scale bar indicates 10 μm (63x).

Figure 4. Displacement of Topo IIα and nucleolin by neomycin from nuclei

A-B) Nuclei were fractionated in the absence of detergent from 3T3-L1 cells obtained at day 0 (D0) or 60 min, 120 min or 1 day (D1) after the addition of the differentiation cocktail and

were incubated with 5 mM neomycin in retention buffer. 50 µg (A) of collected supernatants were resolved on a long 5-15% gradient SDS-polyacrylamide gel and stained with imperial protein stain. Protein bands apparent in D1 were cut out and identified by MALDI-TOF as DNA methyl transferase 1 (DNMT1), DNA Topoisomerase IIα (Topo IIα) and nucleolin. 5 µg (B) were resolved by SDS-PAGE and Western immunoblotted to detect candidate proteins identified from the gel in A as well as lamin A/C. **(C)** Day 1 nuclei were incubated in retention buffer with (+) or without (-) 5 mM neomycin. 2 µg were resolved by SDS-PAGE and Western immunoblotted to detect Topo IIα, nucleolin and lamin A/C. **(D-E)** Confocal images of 3T3-L1 cells fixed at day 1 immunostained with anti-Topo IIα and anti-PtdIns(3,4)P_2 (D) or PtdIns(3,4,5)P_3 (E). scale bar indicate 10 µm (63x). (**F**) Confocal images of 3T3-L1 cells fixed at day 1 immunostained with anti-nucleolin and anti-PtdIns(3,4,5)P_3 antibodies. Scale bar indicates 5 µm (63x). **(G)** Nuclei were obtained from D0, or D1 pre-incubated with vehicle (DMSO) or 10 µM KIN-193 (p110β inhibitor) and split in two for either neomycin extraction or direct lysis (inputs) prior to SDS-PAGE (2 µg and 20 µg resolved respectively) and Western immunoblotting.

Figure 1

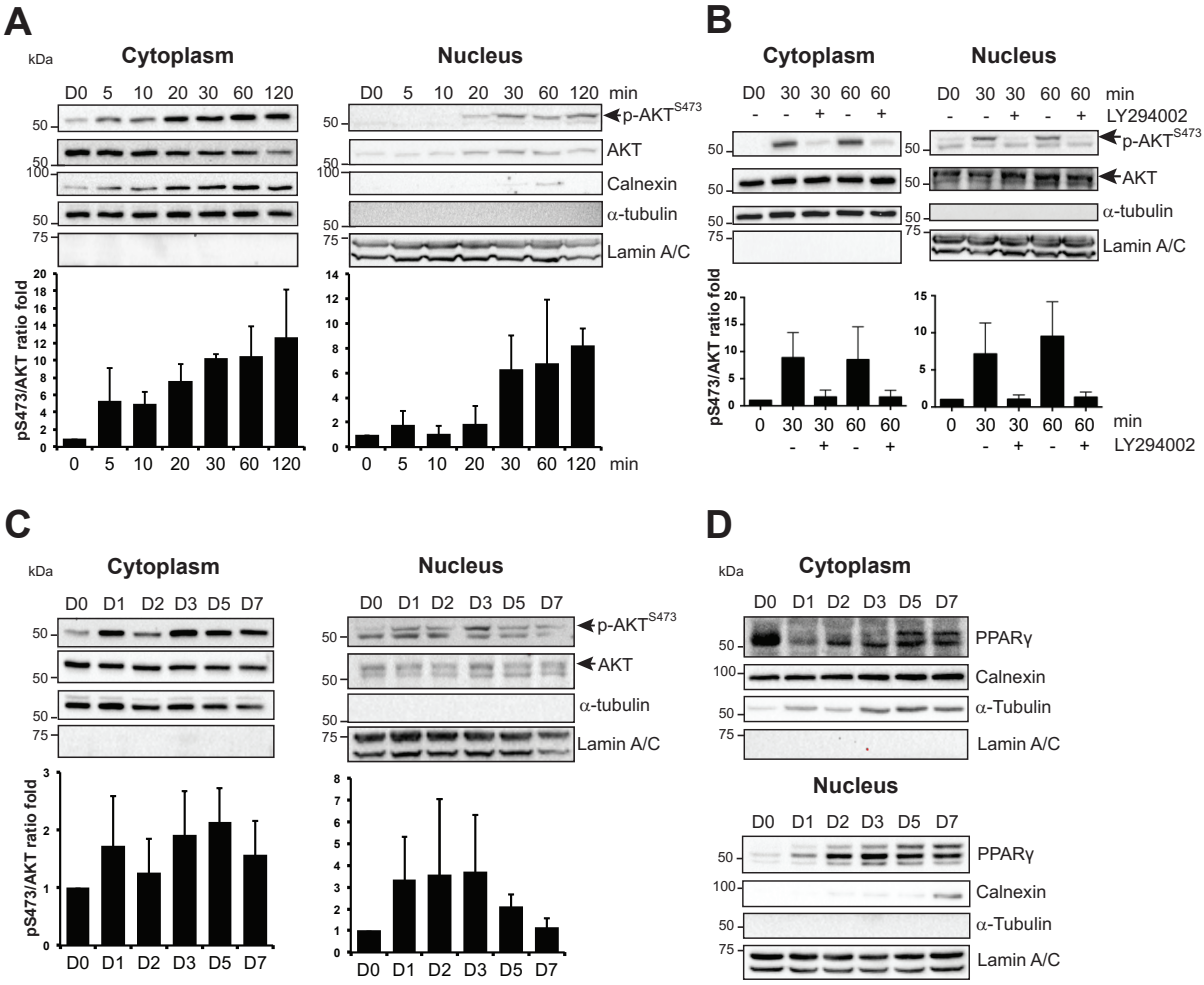
A
kDa
Cytoplasm
Nucleus
D0 5 10 20 30 60 120
min
p-AKT S473
AKT
Calnexin
α-tubulin
Lamin A/C
pS473/AKT ratio fold
B
Cytoplasm
Nucleus
D0 30 30 60 60
LY294002
p-AKT S473
AKT
α-tubulin
Lamin A/C
pS473/AKT ratio fold
C
Cytoplasm
Nucleus
D0 D1 D2 D3 D5 D7
p-AKT S473
AKT
α-tubulin
Lamin A/C
pS473/AKT ratio fold
D
Cytoplasm
Nucleus
PPARγ
Calnexin
α-Tubulin
Lamin A/C

Figure 2

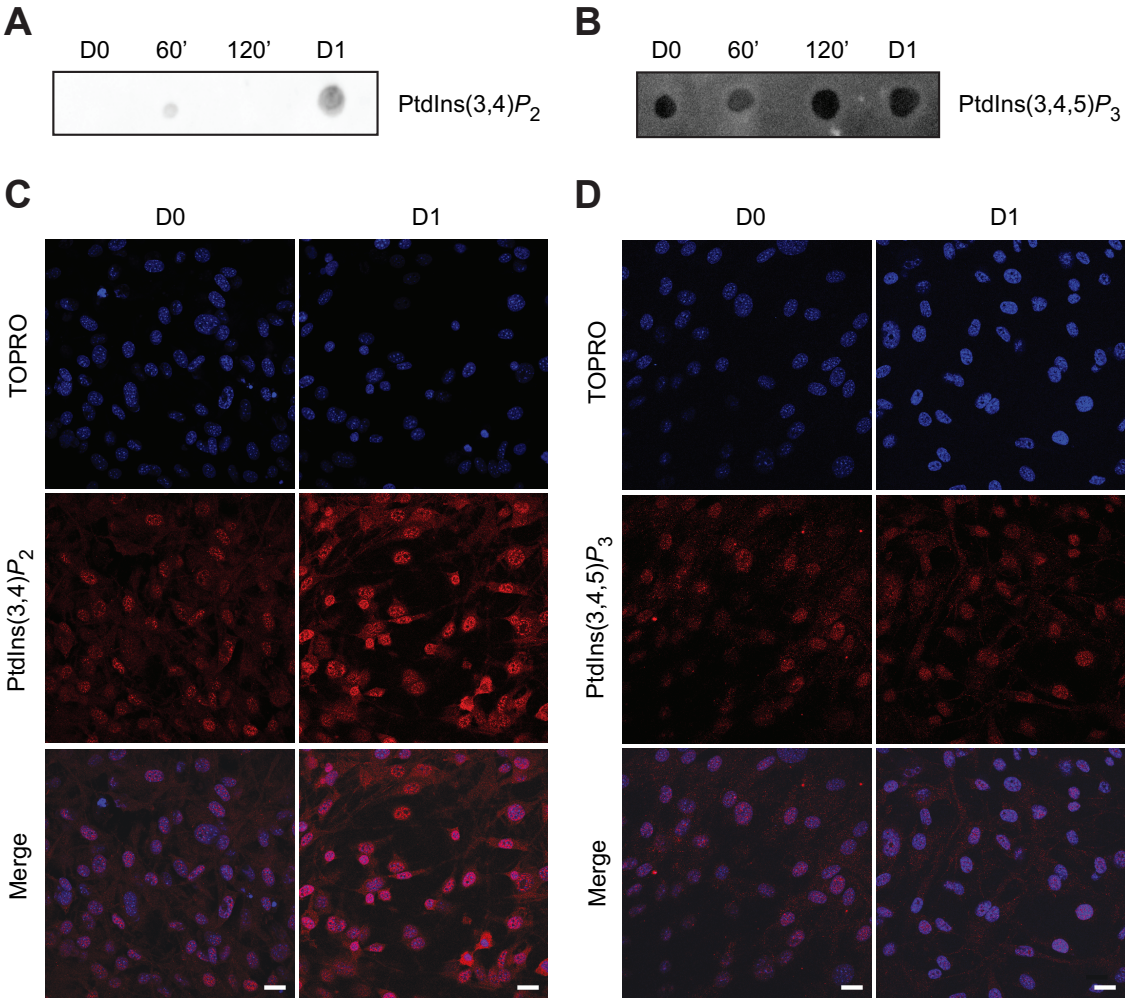
A
D0
60'
120'
D1
PtdIns(3,4)P_2
B
D0
60'
120'
D1
PtdIns(3,4,5)P_3
C
D0
D1
TOPRO
PtdIns(3,4)P_2
Merge
D
D0
D1
TOPRO
PtdIns(3,4,5)P_3
Merge

Figure 3

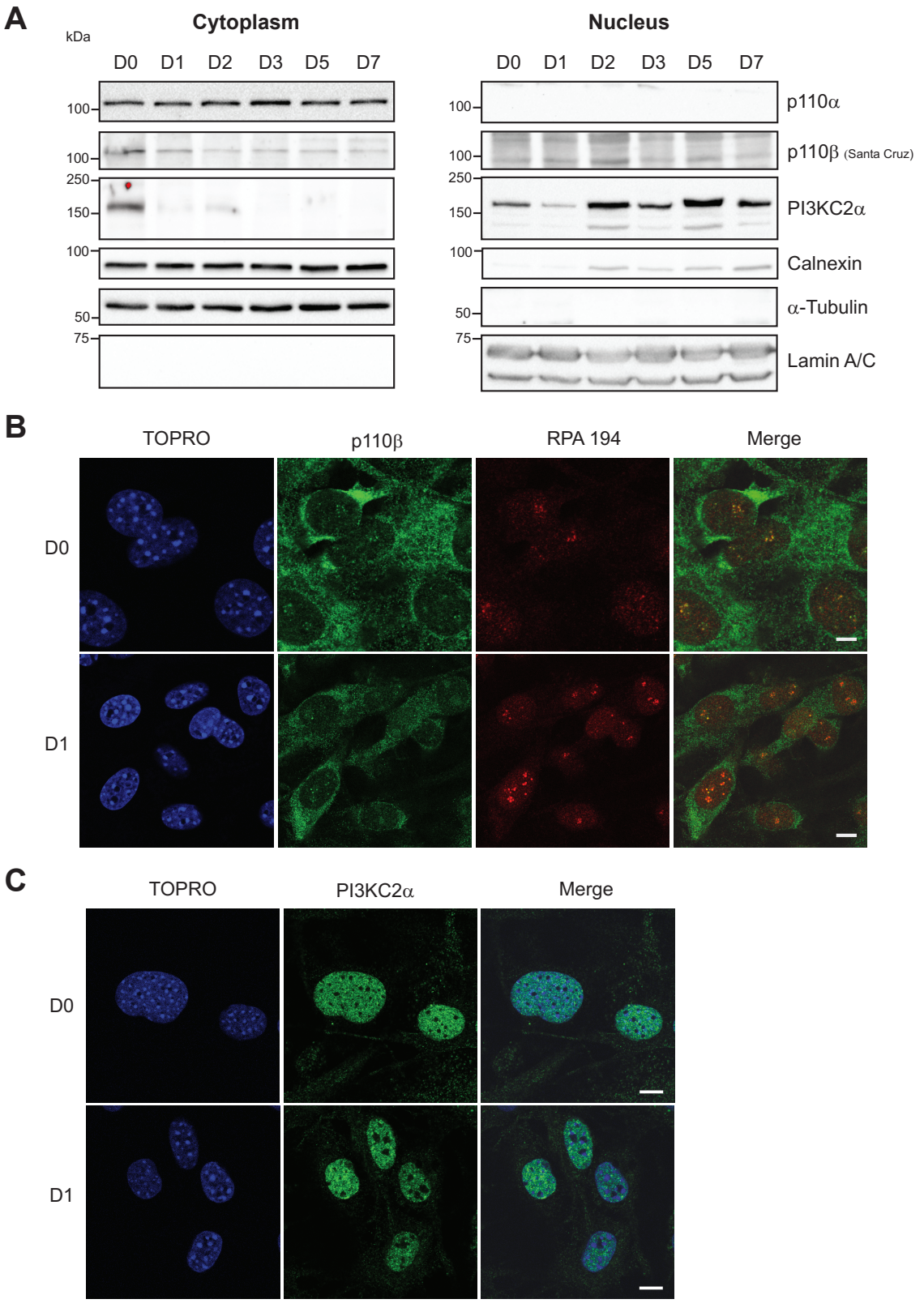
A
Cytoplasm
Nucleus
kDa
D0 D1 D2 D3 D5 D7
100
100
250
150
100
50
75
p110α
p110β (Santa Cruz)
PI3KC2α
Calnexin
α-Tubulin
Lamin A/C
B
TOPRO
p110β
RPA 194
Merge
D0
D1
C
TOPRO
PI3KC2α
Merge
D0
D1

Figure 4

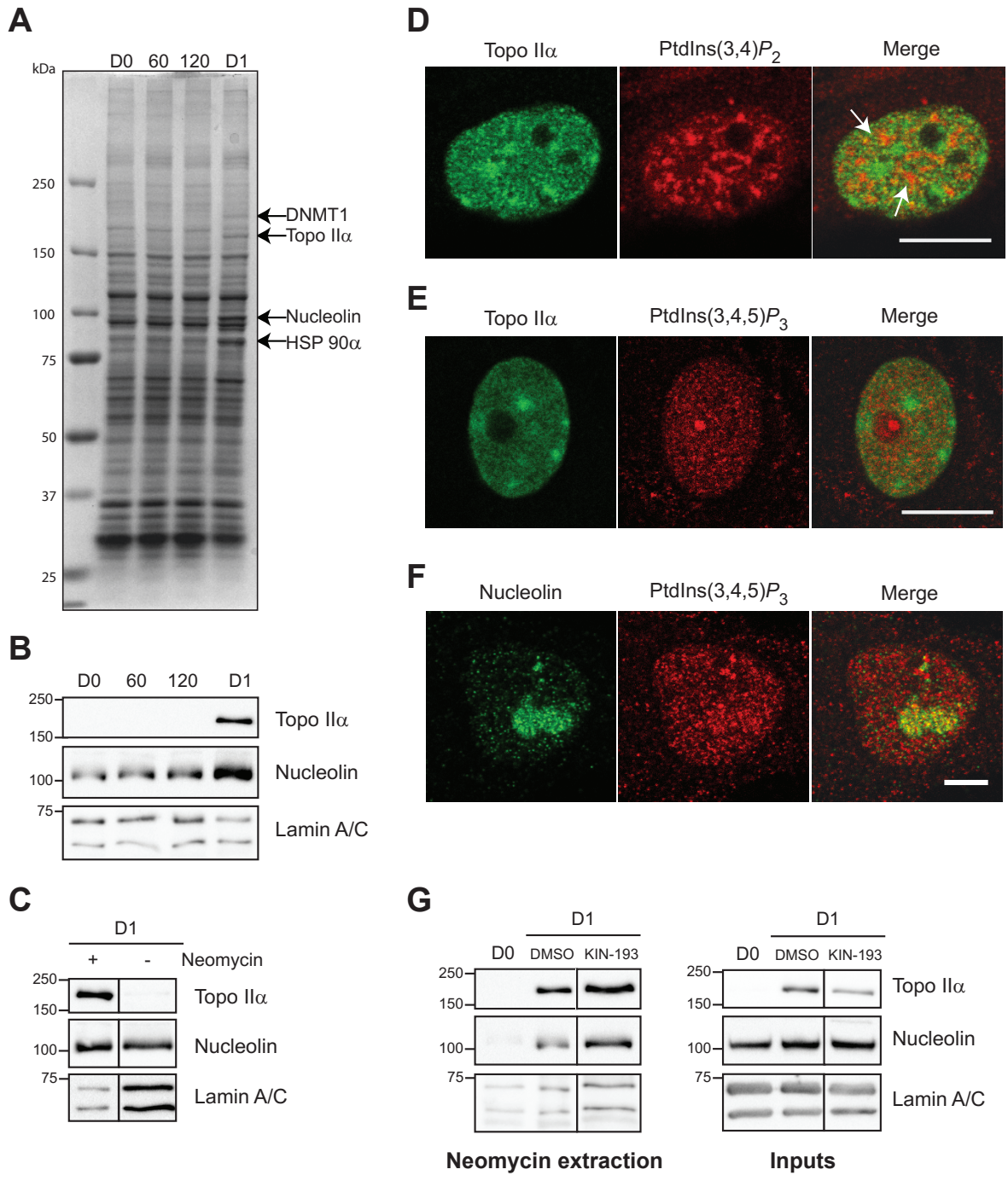
A
kDa
D0 60 120 D1
250
150
100
75
50
37
25
DNMT1
Topo IIα
Nucleolin
HSP 90α
B
D0 60 120 D1
250
150
100
75
Topo IIα
Nucleolin
Lamin A/C
C
D1
+ -
Neomycin
250
150
100
75
Topo IIα
Nucleolin
Lamin A/C
D
Topo IIα
PtdIns(3,4)P2
Merge
E
Topo IIα
PtdIns(3,4,5)P3
Merge
F
Nucleolin
PtdIns(3,4,5)P3
Merge
G
D1
D0 DMSO KIN-193
250
150
100
75
Topo IIα
Nucleolin
Lamin A/C
Neomycin extraction
Inputs

Supplementary data

Supplementary Table S1

List of antibodies used in Western immunoblotting and immunostaining

Name	Manufacturer	Cat. number	WB	Immunostaining
Akt	Cell Signaling	2920	1:2000	
p-S473-Akt	Cell Signaling	9271	1:1000	
Calnexin	Abcam	ab22595	1:1000	
Topo IIα	Abcam	Ab52934	1:5000	
GST-HRP	Abcam	ab3416	1:30,000 (lipid blot)	
Lamin A/C	Santa Cruz	sc-376248	1:10,000	
Nucleolin	Cell Signaling	14574	1:5000	1:1000
p110α	Cell Signaling	4249	1:1000 / 3000	
p110β (IgM)	Santa Cruz	Sc-376492	1:1000	
p110β	Abcam	151549		1:50
PI3KC2α	Santa Cruz	sc-67306	1:1000	
PtdIns(3,4)P_2	Echelon	Z-P034	1:2000	
PtdIns(3,4,5)P_3	Echelon	Z-P345b		
PPARγ	Invitrogen	419300	1:5000	
α-tubulin	Sigma	T5168	1:10,000 / 4000	
anti-rabbit-Alexa 488	Life Technologies	A11008		1:200
anti-mouse-Alexa 594	Life Technologies	A11005		1:200
anti-rabbit-HRP	Life Technologies	G21234	1:10,000	
anti-mouse-HRP	Life Technologies	G21040	1:10,000 (1:20,000 LE9)	
anti-mouse IgM HRP	Abcam	ab5930	1:10,000	

Supplementary Table S2

MALDI-TOF fingerprinting results

Uniprot ID	Gene name	Protein Name	Number of matches	Mascot score
P13864	DNMT1	DNA Methyltransferase 1	15	83
Q01320	TOP2A	DNA Topoisomerase IIα	14	87
P09405	NUCL	Nucleolin	12	89
P07901	HS90A	Heat shock protein HSP90-α	19	73

Supplementary figure legends

Figure S1. Validation of specificty of PtdIns(3,4)P_2 and PtdIns(3,4,5)P_3 probes by lipid overlay assays using PIP strips and arrays

A) PIP strip (left) and PIP array schemes from Echelon spotted with 100 picomol of different phospholipids (strip) or a gradiant of all phosphoinositides (array). **B-C)** PIP strip (left) and array (right) incubated with 1:2000 of anti-PtdIns(3,4)P_2 antibody (B) or 0.2 mg/mL (strip) or 0.5 mg/mL (array) of GST-GRP1-PH (C). **D)** PIP Array incubated with 1:10.000 of anti-PtdIns(3,4,5)P_3 antibody. Signal detection was carried out with anti-mouse IgG-HRP (1:10,000) for antibodies and anti-GST-HRP (1:50,000) followed by enhanced chemluminescence.

Figure S2. PtdIns(3,4)P_2 immunostaining

3T3-L1 cells grew confluent on cover slips. 2 days post-confluence, adipogenesis was induced by incubating the cells with a differentiation cocktail for 5, 30 and 60 min. The slips were incubated with antibody raised against PtdIns(3,4)P_2 and stained with DAPI before they were imaged by fluorescence microscopy at 40 x magnification, exposure time 445 ms, gain 2.7. Magnification of selected cells to demonstrate speckle-like localization of PtdIns(3,4)P_2. The images are representative of experiments performed three times.

Figure S3. PtdIns(3,4,5)P_3 immunostaining

3T3-L1 cells grew confluent on cover slips. 2 days post-confluence the cells were treated with a differentiation cocktail for 5, 30 and 60 min. The slips were incubated with antibody raised against PIP_3 and stained with DAPI before imaging by fluorescence microscopy at 40 x magnification, exposure time 589 ms, gain 4.5. Magnification of selected cells to demonstrate nucleolus-like staining. The images are representative for experiments performed three times.

Figure S4. Detection of p110β in cytoplasmic and nuclear fractions

3T3-L1 cells were induced to differentiate with a differentiation cocktail and fractionated at time-points indicated. Proteins were detected by Western-immunoblotting. α-Tubulin and Lamin A/C were used as loading and purity controls. Detection of the kinase p110β was done with an anti-p110β antibody from abcam (ab151549).

Figure S1

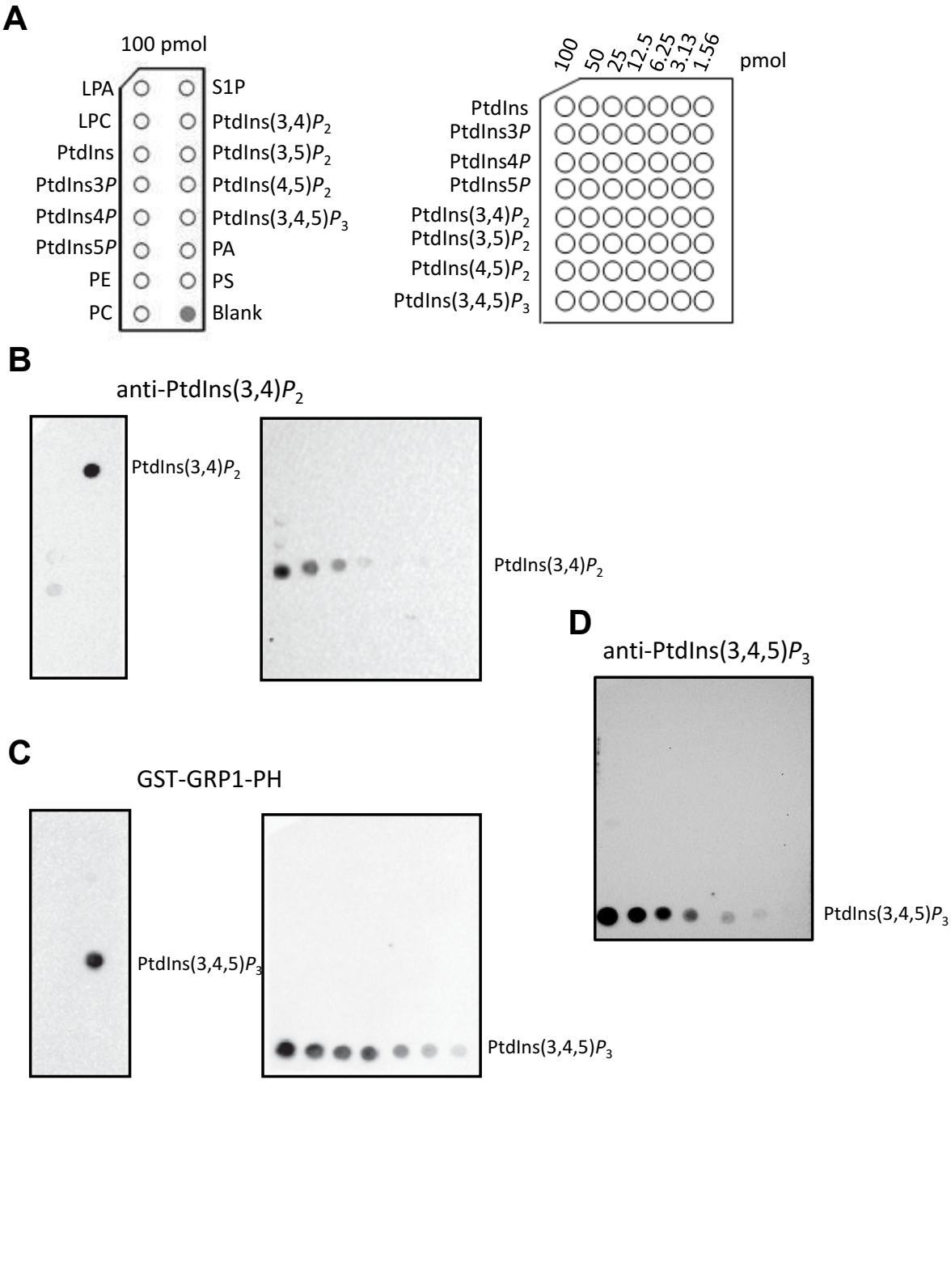
A
100 pmol
LPA
LPC
PtdIns
PtdIns3P
PtdIns4P
PtdIns5P
PE
PC
S1P
PtdIns(3,4)P2
PtdIns(3,5)P2
PtdIns(4,5)P2
PtdIns(3,4,5)P3
PA
PS
Blank
100
50
25
12.5
6.25
3.13
1.56
pmol
PtdIns
PtdIns3P
PtdIns4P
PtdIns5P
PtdIns(3,4)P2
PtdIns(3,5)P2
PtdIns(4,5)P2
PtdIns(3,4,5)P3
B
anti-PtdIns(3,4)P2
PtdIns(3,4)P2
PtdIns(3,4)P2
C
GST-GRP1-PH
PtdIns(3,4,5)P3
PtdIns(3,4,5)P3
D
anti-PtdIns(3,4,5)P3
PtdIns(3,4,5)P3

Figure S2

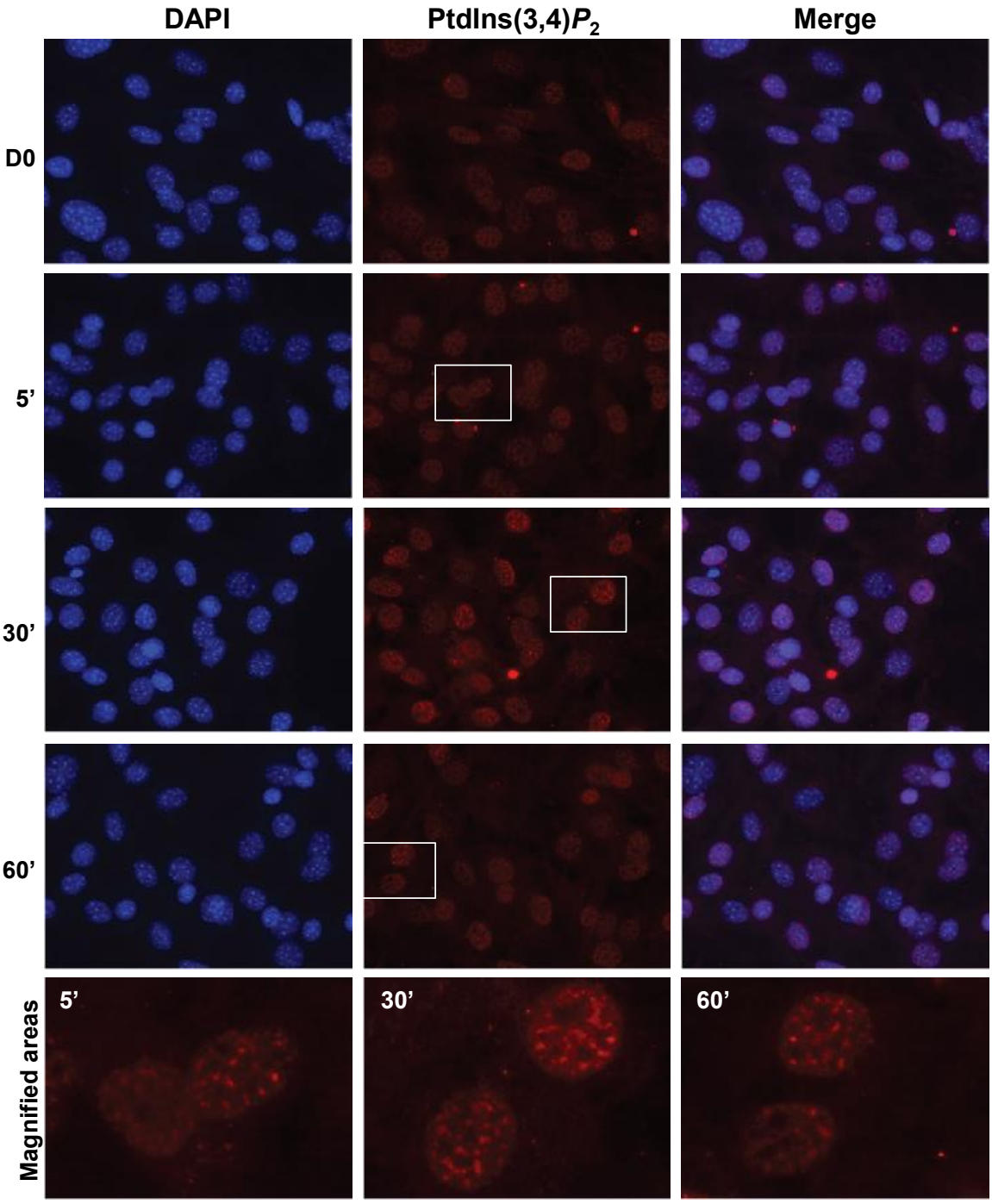

Figure S3

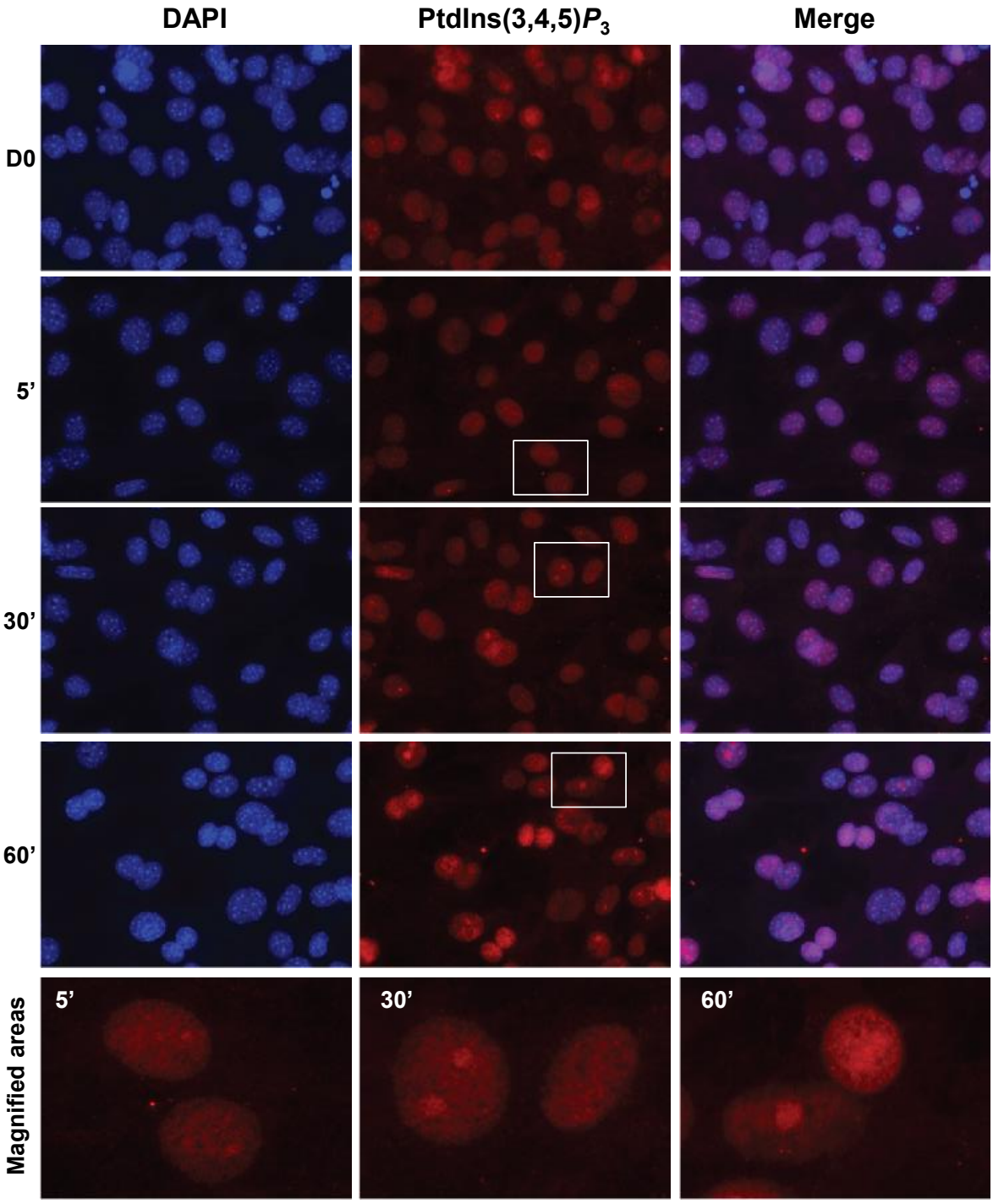

Figure S4

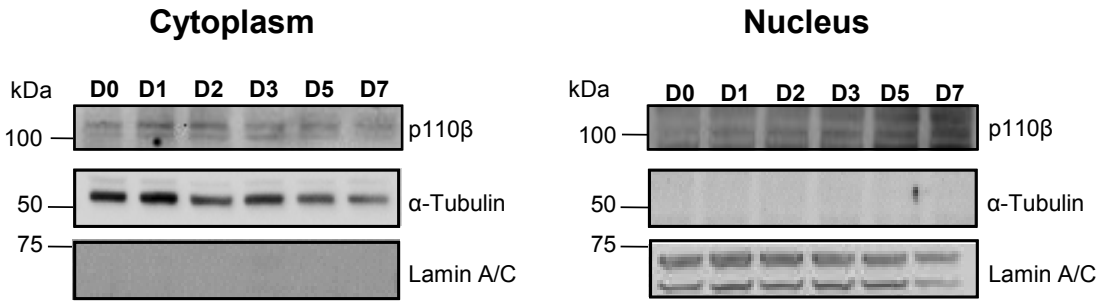
Cytoplasm
Nucleus
kDa
D0 D1 D2 D3 D5 D7
100
50
75
p110β
α-Tubulin
Lamin A/C

Graphic design: Communication Division, UiB / Print: Skipnes Kommunikasjon AS

uib.no

ISBN: 978-82-308-3866-2